New mixtures to be used in permeable reactive barrier for heavy-metals contaminated groundwater remediation : long-term removal efficiency and hydraulic behavior

Maria Grazia Madaffari

UNIVERSITÀ DEGLI STUDI *MEDITERRANEA* DI REGGIO CALABRIA

DOTTORATO DI RICERCA IN

INGEGNERIA GEOTECNICA E CHIMICA DEI MATERIALI
XXVII CICLO - S.S.D. ICAR/07
DIPARTIMENTO DI INGEGNERIA CIVILE, DELL'ENERGIA,

DELL'AMBIENTE E DEI MATERIALI (DICEAM)

ÉCOLE CENTRALE PARIS

ÉCOLE DOCTORALE« SCIENCES POUR L'INGÉNIEUR » ED287
SPÉCIALITÉ : GÉNIE CIVIL ET ENVIRONNEMENT
LABORATOIRE MÉCANIQUE DES SOLS,

STRUCTURES ET MATÉRIAUX (LMSSMAT)

NEW MIXTURES TO BE USED IN PERMEABLE REACTIVE BARRIER FOR HEAVY-METALS CONTAMINATED GROUNDWATER REMEDIATION: LONG-TERM REMOVAL EFFICIENCY AND HYDRAULIC BEHAVIOR

PH.D.CANDIDATE:

Maria Grazia MADAFFARI

SUPERVISORS:

Prof. Eng. Nicola MORACI

Prof. Eng. Arézou MODARESSI

CO-SUPERVISOR:

Eng. Paolo S. Calabrò

HEAD OF THE DOCTORAL SCHOOL:

Prof. Eng. Nicola MORACI

REGGIO CALABRIA, FEBRUARY 2015

CentraleSupélec

THÈSE

présentée par

Maria Grazia MADAFFARI

pour l'obtention du

GRADE DE DOCTEUR

Spécialité : Génie Civil et Environnement

Laboratoires d'accueil :
Ingegneria Geotecnica ; Dipartimento di Ingegneria Civile, dell'Energia, dell'Ambiente e dei Materiali
Mécanique des Sols,Structures et Matériaux de l'Ecole Centrale Paris

SUJET :NEW MIXTURES TO BE USED IN PERMEABLE REACTIVE BARRIER FOR HEAVY-METALS CONTAMINATED GROUNDWATER REMEDIATION: LONG-TERM REMOVAL EFFICIENCY AND HYDRAULIC BEHAVIOR

soutenue le : 23 Mars 2015

devant un jury composé de :

Mme MODARESSI Arézou	**Co-directrice de Thèse**
M. HICHER Pierre-Yves	**Rapporteur**
M. SIMONINI Paolo	**Rapporteur**
Mme PANTET Anne	**Examinatrice**
M. AVERSA Stefano	**Examinateur**
M. LANZO Giuseppe	**Examinateur**

No. 2015-00-25

Acknowledgments

It is no easy task to acknowledge all of the people I have been fortunate to meet and know in the three year course of my Ph.D. studies.
I am truly thankful to my Supervisors, Prof. Arézou Modaressi and Prof. Nicola Moraci.
I would also like to express my profound thanks to Prof. Moraci for having had confidence in me and for having guided me in this research work both with his masterful intellect and with his openness to innovative ideas.
I am really thankful to Prof. Arézou Modaressi for having offered me an exceptional opportunity to develop and for having welcomed and hosted me at the École Centrale Paris. The time that she has dedicated, her suggestions and her style will always remain as indelible lessons to me.

I have also really appreciated the precious support of Eng. Paolo S. Calabrò.
I would also like to acknowledge Prof. Fernando Lopez Caballero, Prof. Elsa Vennat and Prof. Barbara Malinowska for having always been available and helpful.

I would like to thank the members of the thesis committee: Prof. Pierre-Yves Hicher, Prof. Paolo Simonini, Prof. Anne Pantet, Prof. Stefano Aversa and Prof Giuseppe Lanzo, I am indebted to Prof. Pierre-Yves Hicher and Prof. Paolo Simonini for accepting my request to review the manuscript.

Special thanks also go to my friends and colleagues at the École Centrale Paris and the Mediterranean University in Reggio Calabria for having rendered this period of research and study both pleasant and fruitful.

Finally, I am deeply grateful to my parents and to my brother for having been an everlasting source of support and encouragement.

Index

List of Figures

List of Tables

1 Groundwater contamination and PRB remediation technology

1.1 Introduction

In this chapter a background representing the basis and the theme of the research activity will be described. Particular attention will be paid to the global challenge of sites pollution, focusing on the contaminants that most affect groundwater matrix. The state of the art of the innovative and well-accepted Permeable Reactive Barrier Groundwater Remediation Technology will be introduced, considering advantages and main issues concerning its long-term performance of its implementation at different scales. Finally, the choice of research subject, objectives and method will be presented.

1.2 Contaminated sites in Europe

Since 2000 the European Environmental Agency has drawn up six reports about the state of the art of contaminated sites in Europe. Similar data have been obtained in the data collections reported in the different versions. The Joint Research Centre of the European Commission published in May 2014 the last work of data collection exercises completed regarding the indicator CSI 015 "Progress in the management of Contaminated Sites in Europe" (Van Liedekerke et al., 2014). The European Soil Data Centre (ESDAC) of the European Commission has conducted a project to collect and manage the contaminated sites data collected through the European Environmental Information and Observation Network (EIONET). Precisely, EIONET includes 28 Member States of the European Union together with Iceland, Liechtenstein, Norway, Switzerland, Turkey, and the West Balkan cooperating countries: Albania, Bosnia, Herzegovina, the former Yugoslav Republic of Macedonia, Montenegro, and Serbia as well as Kosovo.

The data collection regarded management of contaminated sites, remediation targets and technologies, contribution of polluting activities to local soil contamination, environmental impacts and expenditure (http://www.eea.europa.eu/data-and-maps/indicators/progress-in-management-of-contaminated-sites-3/assessment).

Regarding the parameters on the number of sites, ESDAC has detailed the definition for each parameter. In a "contaminated site" (CS) the presence of the contamination must be confirmed and management measures should be decided on the basis of the potential risk, in a "potentially contaminated site" (PCS), an unacceptable contamination is suspected and investigations need to verify the risk, while "management of contaminated sites" is aimed at remediation. A distinction is made between "estimated" and "identified" sites.

The Figures 1-1 a) and b) provide data on identified numbers of PCS and CS and on estimated numbers of PCS and CS, represented respectively.

A key aspect for research and development of remediation, analyzed by Van Liedekerke et al. (2014) consists of the percentage of contaminants affecting soil and fluid matrices. A similar distribution of contaminants affecting soil and groundwater can be deduced from the analysis results reported in Figure 1-2. In particular, heavy metals represent the dominant contaminant category. The second category mainly found is that of mineral oil.

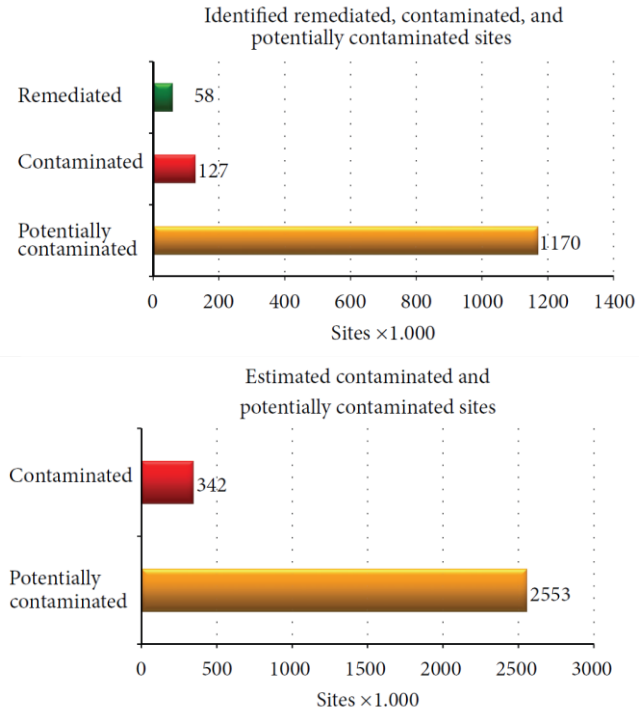

Figure 1-1 a) identified PCS, CS and RS; b) estimated PCS and CS (Panagos et al., 2013)

The EIONET-CSI data collection can be integrated with heavy metal data provided by other projects such as the European Pollutant Release and Transfer Register (E-

PRTR) and data about water and soil chemical characteristics available after the Land Use/Cover Area frame statistical Survey (LUCAS) soil survey, aimed at digital soil mapping to overcome the disadvantages due to the privacy issue in contaminated soil identification.

Regarding the activities that mostly contribute to soil contamination, waste disposal and treatment account for 38% of sources of local soil contamination over the total number of sources identified, industrial and commercial activities account for 34%, while the agricultural sites and waste water treatment facilities account for 8%. In particular, concerning the industrial and commercial activities, the production sector, including metal, chemical and oil industries and energy production, accounts for 60% of contamination, while the service sector, mainly gasoline stations, accounts for 33% (Panagos et al., 2013).

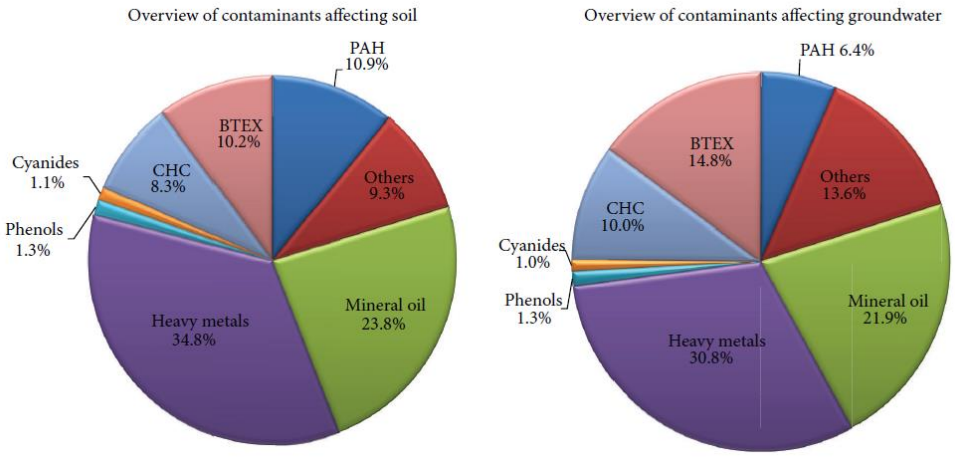

Figure 1-2 Distribution of contaminants affecting soil and groundwater in Europe (Panagos et al., 2013)

1.2.1 Water Framework Directive

The Water Framework Directive, of which the official title is Directive 2000/60/EC of the European Parliament and of the Council of 23 October 2000, introducing a framework for Community action in the field of water policy, established an innovative approach for water management based on river basins and a framework aiming to protect and keep water cleaner across Europe, promoting its sustainable use. The directive concerns inland surface waters, transitional waters, coastal waters and groundwater. The Directive also introduces the integrated management of groundwater and surface water, considered the exiting cycle linking them, and it

recognizes the importance of a good status of groundwater to protect the aquatic and terrestrial ecosystems.

Groundwater represents over 95% of the world's freshwater, excluding glaciers and ice caps and it supplies the steady flow of rivers and wetlands. Maintaining this source free from pollution is essential for surface water quality and ecosystems. Furthermore, groundwater represents in a few countries the main source of drinking water and the water systems used by three out of four Europeans, as well as for industrial cooling and agricultural irrigation.

The expected goals for 2015 consist of achieving a good quantity and chemical status of groundwater.

Regarding the first status, the long-term sustainable use required by the directive ensures that the extraction of water from groundwater does not exceed the rate at which freshwater replaces it. Good chemical status is achieved by complying with the quality standards set by each Member State on the basis of the 2006 directive on groundwater and the measures required by the Nitrates Directive (EU Directive on Nitrates from Agricultural Sources (91/676/EEC)).

However, other EU directives, such as the EU Waste Framework Directive (2008/98/EC), the EU Groundwater Directive (2006/118/EC) and the EU Integrated Pollution Prevention and Control Directive (2008/1/EC) are aimed at the prevention and clean-up of soil contamination and different resources supporting work on contaminated sites remediation (JRC, EUGRIS, NICOLE, EURODEMO).

In France, the basol database (http://basol.developpement-durable.gouv.fr) on contaminated soils and sites gathers their localization, the nature of pollutants and their impact on the environment as well as the technical situation of the site.

1.3 Groundwater remediation solutions

The most widely used technology to remediate contaminated groundwater has been the “Pump-and-Treat” (P&T) system, which consists in extraction of water from the ground and its treatment in a water remediation plant. This kind of technology requires removal of a large amount of groundwater for a long time, leading to a depletion of resources and high treatment costs. Furthermore its remediation

efficiency depends on the extraction of contaminants, some of which are highly linked to the aquifer solid matrix. For this reason, one of the main issues in research on groundwater remediation has been focused on the development of sustainable groundwater remediation technologies, during recent decades.

1.3.1 PRB definition and history

Permeable reactive barrier (PRB) is an *in-situ* technology for remediation of contaminated groundwater (Tratnyek, 2002; USEPA, 2002). It consists of a engineered zone of reactive material placed in an aquifer in order to intercept the contaminant plume perpendicularly and to remove the contamination from groundwater flowing through it (Rumar and Mitchell, 1995) (Figure 1-3).

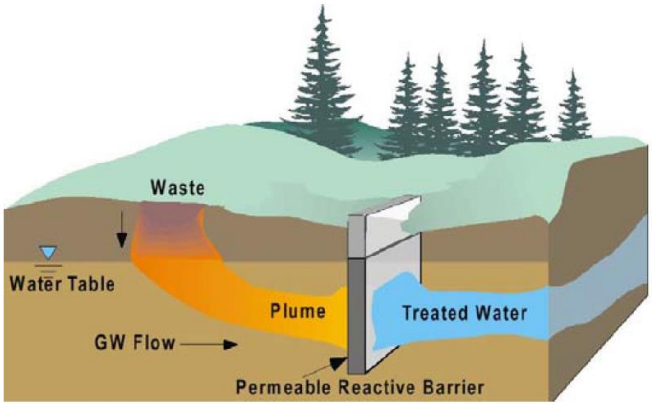

Figure 1-3 Example of permeable reactive barrier (USEPA, 1998)

This technology is based on the natural aquifer gradient to move the contaminated groundwater through the reactive zone. As the contaminants pass through the barrier, they react with the reactive media that either transform them into less harmful compounds or block them into the reactive zone (Powell et al., 1998; Carey et al., 2002; Skinner and Schutte, 2006). Different tested reactive materials have the ability to remove organic and inorganic contaminants from groundwater. Moreover, PRB reduces the exposure of workers to contaminants and allows for use of the land surface, developing the treatment underground.

This technology has been extensively investigated, obtaining results which make it a sustainable alternative to conventional P&T (Korte, 2001; Carey et al., 2002; Wilkin

and Puls, 2003; Puls, 2006; Skinner and Schutte, 2006; Henderson and Demond, 2007; Chen et al., 2011). However, the application in real scale of most of the successful laboratory-based investigations on PRB long-term performance and improvements in treating a broad spectrum of contaminants need to be validated by empirical evidence (Warner and Sorel, 2002).

Since the 1970s, limestone-based installations have been used for passive remediation of surface water or shallow groundwater contaminated by acid mine drainage (Pearson and McDonnell, 1975; Hedin et al. 1994).

At the University of Waterloo, Zero Valent Iron (ZVI) was discovered to be able to be used to remediate groundwater contaminated by halogenated organic solvent (Gillham and O'Hannesin, 1992). The first ZVI-PRB was built at the Canadian Forces Base at Borden, in Ontario in 1991. Since this time, the implementation of ZVI-PRB has been quickly developed and accepted.

1.3.2 Configurations

On the basis of a well-done contaminated site characterization, the appropriate configuration can be chosen among the different conventional and innovative solutions to optimize the PRB design.

Continuous PRB is the most common configuration that has minimal impact on the groundwater flow. It is completely filled with reactive material and it can be chosen when groundwater flow and plume geometry are well understood (Figure 1-4).

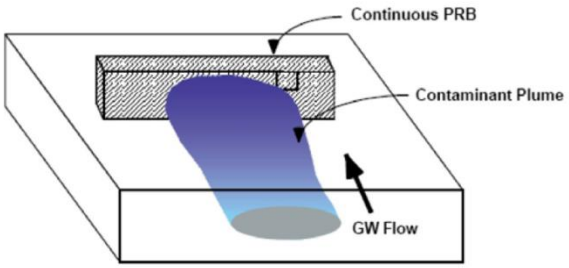

Figure 1-4 continuous PRB trench system (USEPA, 1998)

In Funnel-and-Gate configuration, the impermeable Funnels drive the contaminant plume to the reactive zone (Gate) (Figure 1-5). In the case of very large contamination or high aquifer heterogeneity , a multiple Funnel-and-Gate can be installed, while multiple reactive media layers can be designed to treat a number of contaminants.

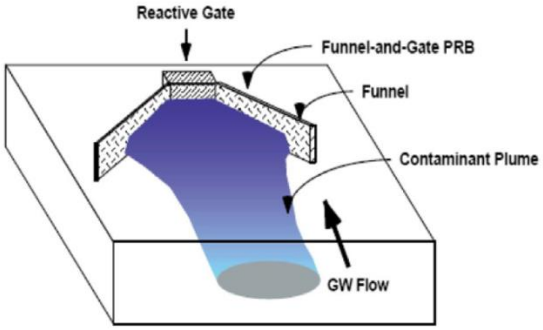

Figure 1-5 funnel-and-gate system (USEPA, 1998)

Reactive Vessels configuration is very similar to the Funnel-and-Gate. The difference is that the vessel can be extracted in order to replace the reactive material when it is exhausted and it enables investigation and fixing performance problems. An example is the panel-drain® process developed by Soletanche-Bachy Company (Figure 1-6).

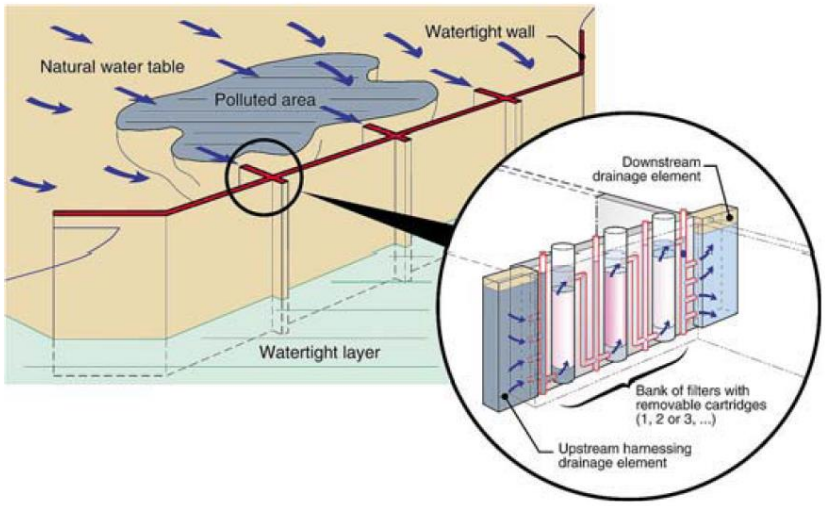

Figure 1-6 Panel-drain principle (Soletanche-Bachy's patent) (Courcelles et al., 2008)

Caissons PRB is similar to Funnel-and-Gate, consisting in low permeability sections that direct the flow to the reactive material contained in the caisson. The main characteristic is the upward flow of groundwater through the reactive zone.

GeoSiphon™ is a configuration patented by the Westinghouse Savannah River Company and it is based on a siphon effect to induce the upward flow of contaminant plume though the reactive zone to a discharge point of groundwater table (Figure 1-7).

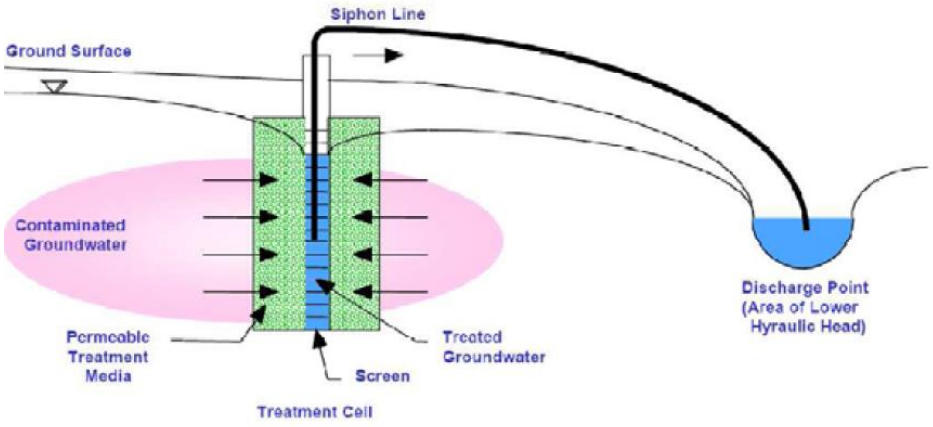

Figure 1-7 GeoSiphon™ configuration (Di Molfetta et al., 2005)

1.3.3 PRB construction techniques

The choice of the PRB installation method constitutes a critical issue for the success of PRB performance because of the influence of design and construction steps on barrier operation. Different aspects such as geotechnical and civil design, method of construction, waste material management, service and infrastructures availability and safety measures should be considered.

The groundwater table depth is one of the first site-characteristics to evaluate in construction method selection. For a shallow depth, excavation is the suitable technique, while for a deeper barrier, injection is more appropriate. This choice is a function of the contaminant present and disposal methods of generated soil, too. The heterogeneous nature of aquifer and aquitard as well as the contaminated site soil quality influence the type of excavation.

Excavation techniques, that are easier and that generate less spoil than injection, include five main construction methods.

Biopolymer trenching can be used to construct a barrier with a depth of up to 21 m. Using a standard backhoe 9 m depth can be reached, while using a modified one it is possible to excavate down to 25 m. (Gavaskar, 1999). This technique consists of pumping biopolymer slurry, e.g. guar gum, into the trench to make the trench wall stable (Day et al., 1999) (Figure 1-8). During excavation work and trench wall stabilization biopolymer remains in the trench and other kinds of support may not be necessary. After reactive material placement, enzymes can be used to degrade the biopolymer.

Figure 1-8 Biopolymer trenching (Naidu and Birke, 2015)

Continuous trenching is appropriate for treatment zones 11 m deep and 0.3-0.9 m wide. A thick wall can be obtained through an arrangement of parallel trenches (Naidu and Birke, 2015). This method consist in filling with reactive material and backfilling in not to leave the trench open at any time.

Figure 1-9 Sheet piles installation (Naidu and Birke, 2015)

A standard backhoe can be used for PRB construction also without side wall support, if the depth of the trench is less than 6 m and can remain about 4 h without caving in.

Otherwise, for a trench more than 6 m deep, the side walls can be supported by trench boxes and hydraulic shores.

Sheet piling can be used to construct a continuous barrier as well as a reactive zone and an impermeable zone in Funnel-and-Gate configuration. Usually, sheet piling is placed around the perimeter of the PRB during the trench excavation and is removed after the reactive material filling and the backfilling, allowing natural groundwater flow. To build the impermeable zone of Funnel-and-Gate, a crane with a vibrating hammer is normally used to install the sheet piles interconnected by interlocking edges (Figure 1-9). This is a suitable method where there is horizontally limited space to work and it does not generate much soil. It is appropriate for depths of about 15 m.

Slurry wall does not have the same limit in depth as the sheet pile. It is usually constructed for the impermeable zone of a Funnel-and-Gate barrier. The trench is excavated using a backhoe, a modified backhoe or a clamshell digger, in function of the design depth. The most common slurries is made of soil/bentonite, cement/bentonite or other composites (Meggyes, 2005). During the excavation, appropriate slurry, used to maintain trench stability, permeates the sides of excavation, forming a hydrated filter cake along the sides. A soil/bentonite backfill is put in place to fill the excavated space.

Injection techniques include hydraulic fracturing, jetting and soil mixing.

Hydraulic fracturing consists in installing a series of wells along the perimeter of the barrier under construction and creating a vertical fracture in them. A mixture made of iron/gel or slurry of soil/bentonite, soil/cement or composite slurry is injected into the well to create reactive zone or impermeable zone respectively. Enzyme can be used to degrade the gel. Attention should be paid to choose high quality and purity gel useful for the suspension and transport of iron, in order not to have impact on iron reactivity and permeability.

The practice of inject grouting to improve mechanical characteristics of soil has been recently proposed to be used for construction of the funnel.

Soil mixing techniques allow the attainment of more uniform PRB and a higher hydraulic conductivity than the jetting. This consists in creating a row of columns, using a hollow-stem auger with mixing paddles that rotate mixing the soil at the desired depth and injecting the reactive slurry.

1.3.4 EU-projects about PRB research

PRBs have not been fully and readily accepted and incentivized as new general remediation technologies in Europe, probably because (1) there is lack of reliable information on long-term performance, longevity and long-term effect, because of still missing long-lasting projects (Puls et al., 2000, Yoon et al., 2000, Rochmes, 2000, Sarr, 2001, Simon et al., 2002, Vidic, 2001), (2) all degradation pathways are not identified and precise mass balances cannot be determined, while the toxicity of intermediary or final products is also under discussion (Wienberg, 1997), (3) at present, insufficient information is available on the costs of PRBs, considering also the possibility of performance decreases over time and (4) knowledge regarding the applicability and longevity of combined contamination solutions, especially regarding heterogeneous and complex scenarios, is at an early stage (Rochmes, 2000, Scherer et al., 2000). For these reasons, some projects have been promoted and proposed in order to ease the research and application of groundwater remediation technologies, such as the Permeable Reactive Barrier.

PEREBAR is a European Project regarding "Long-term Performance of Permeable Reactive Barriers used for the Remediation of Contaminated Groundwater". It was a Research Project within the 5th Framework Programme of the European Union. The Universitaet Karlsruhe (Technische Hochschule) in Germany worked as coordinator while the Federal Institute For Material Research And Testing in Germany, G.U.T. Gruppe Umwelt & Technik Gmbh in Austria, the Ingenieursbuero Fader Umweltanalytik in Germany, Mecsekerc Koernyezetvedelmi Rt in Hungary, the Miskolc University in Hungary, the National Technical University of Athens in Greece and the University of Leeds in United Kingdom have taken part as participants.

The objective of the PEREBAR project was to assess and improve the long-term performance of permeable reactive barrier systems, focusing on systems based on sorption and precipitation of heavy metals and sorption and decomposition of organic compounds. The primary PEREBAR model site is an area in southern Hungary contaminated by uranium mining. (http://www.perebar.bam.de/).

ADVOCATE, a Marie Curie Initial Training Network, aims developing innovative *in-situ* remediation approaches for the sustainable management of contaminated land and groundwater, as required by the Water Framework Directive and at optimizing

resource investment in environmental restoration. The eight work packages representing the research themes regard socio-economic and sustainability aspects of *in situ* remediation, linking soil and vadose zone processes to *in-situ* remediation of groundwater, groundwater-surface water interaction and *in-situ* remediation, *in-situ* metal-contaminated sites remediation, developing *in-situ* treatment strategies for mixed contaminants using sequenced reactive biobarriers, enhancing bioremediation processes, performance assessment of natural attenuation at field-scale and network knowledge transfer and research dissemination (http://www.theadvocateproject.eu).
RUBIN, standing for (in German) "Reaktionswände und -barrieren im Netzwerkverbund" and in English meaning "reactive wall and barrier projects cooperating in a network/concerted action", initiated in 2000, was a four year program funded by the German Federal Ministry for Education and Research (BMBF). It consisted of a large-scale German Permeable Reactive Barrier (PRB) R&D network with the aim of planning, designing, implementing, monitoring and evaluating pilot and full-scale PRB projects in Germany, and applying novel innovative approaches.
In Germany, 9 pioneering PRB projects, full and pilot scale, have been implemented in Bernau (built 2001 cVOCs, iron filings, pilot scale), Bitterfeld (1999 CHC like chlorinated benzenes, PAH, microbiological degradation and palladium and iron plus activated carbon in different reactors, pilot scale with focus on R&D, specific reactor systems), Denkendorf (2000 cVOCs, activated carbon, full scale, drain and gate), Edenkoben (1998, 2001 cVOCs, iron filings, pilot scale, expanded to full scale since 2001, funnel and gate), Karlsruhe (2000 PAH, activated carbon, full scale, funnel and gate), Oberursel (2002 cVOCs, iron granules, full scale, funnel and gate), Reichenbach (2000 cVOCs, activated carbon, full scale, specific design), Rheine (1998 cVOCs, iron filings and iron sponge, pilot scale, continuous wall) and Tübingen (1998 cVOCs, granular iron, full scale, funnel and gate). (Birke, V. et al., 2007, http://www.rubin-online.de/)
SAFIRA, "Sanierungsforschung in regional kontaminierten Aquiferen", in English meaning "remedial research applied to regionally contaminated aquifers", an R&D network using specifically designed *in-situ* reactors in a semi-technical scale for testing different reactive materials, was the first initiative to study the potentials of PRBs in a broader scope (Weiß et al., 1999). The pilot plant treats groundwater

contaminated by a complex mixture of CHCs, i.e., mainly chlorobenzenes, and other pollutants at Bitterfeld, Federal State of Saxony-Anhalt.

AQUAREHAB was an EU financed large scale project which started 1st May 2009 and lasted for 56 months, until 2013. The project, coordinated by VITO involving a consortium of 19 partners, was aimed at developing innovative rehabilitation technologies for soil, groundwater and surface water contaminated by a number of contaminants. These technologies include activated riparian zone/wetland, open trench with smart biomass containing carriers, capping of sediment & stimulated biobarriers, multifunctional permeable reactive barriers and reactive zone with injectable Fe-based particles. Methods and tools to improve their design , to evaluate their effects on river basin as well as the development of a framework to evaluate and disseminate the research output in other river basins have been objectives of the research project too. (https://aquarehab.vito.be/home/Pages/home.aspx)

1.4 PRB for heavy metals

Different reactive materials have been tested for heavy metals contaminated groundwater remediation using PRB technology. In table 1-1, the reactive materials are reported in function of the kind of metal or metalloid and of the main mechanism employed to remove it.

Constituents	Mechanism	Media	Comments
Oxyanions (e.g., As, Se, V, Cr, Sb, Mo, SO_4)	Adsorption	ZVI Surfactant modified zeolites Basic oxygen furnace slag Amorphous ferric hydroxide Neutralized red mud Diatomaceous earth Ferrous sulfate (HFO) Activated	Neutral-to-acid pH is optimal Rare-earth or Fe-doping improves adsorption capacity High levels of sulfates may depress adsorption

		alumina Hybrid ion exchange resin Rare earth elements Kanchan™ arsenic filter Granulat Ferric Hydroxide™ Clays	
	Precipitation	ZVI Ferrous sulfate (Cr) Sodium dithionite (Cr) Organic carbon	Obtained by chemical reduction or as solid solution with Fe
Cations (e.g. Fe, Mn, Cd, Pb, Ni, Be, Ba, Tl)	Adsorption	ZVI Humasorb™ Ferrous sulfate (HFO) Zeolites Clays	Neutral-to-alkaline pH is optimal
	Precipitation	Phosphates Limestone ZVI Organic carbon Neutralized red mud Oxygen sparging	May include sulfides, sulfates, carbonates, oxides and hydroxides

Table 1-1 Main reactive materials used in PRB for heavy metals and metalloids contamination (EPRI, 2006)

In table 1-2 the characteristics of PRBs installed to treat heavy metal contaminated groundwater are reported.

Country	City and year of installation	Contaminants	Barriers and Reactive Materials	Reference
France	Brest (2002)	hydrocarbon+ phenols +heavy metals	Panel-drain Activated carbon	RECORD, 2004 - Courcelles, 2007 – Rai, 2012
Spain	Rio Agrio (2000)	Acid Mine Drainage (AMD) (pH, zinc, Cadmium)	Funnel and Gate Calcite, compost, iron	Gilbert, 2004 - Bolzicco, 2001
UK	Shilbottle, Northumberland (2002)	AMD (iron, manganese, pH)	Continuous PRB Purin, compost and limestone	Bowden Lawrence et al., 2005
Canada	Near Sudbury Ontario (1985)	AMD and sulfates	Continuous PRB Organic Carbon	Benner, 1999 - www.rtdf.org/public/permbarr/prbsumms/default.cfm ITRC, 2005
Canada	Ontario	As, B, Cr, Mo, Se, and V	Funnel and Gate, three cellules (ZVI, ion-exchange resin, zeolites)	EPRI, 2006
Canada	Vancouver, British Colombia (2000)	Dissolved metals and sulfates	Continuous PRB Organic carbon	Mountjoy and Blowes, 2002
USA	Monticello, UT (1999)	Uranium and Metals (As, Mn, Se, V)	Funnel and Gate ZVI	Morrison, 2001 - RTDF.org - EPRI, 2006 - FRTR, 2002, USEPA 2002
USA	Nesquehoning, Pennsylvania (1998)	Heavy metals (Pb, Cd, As, Zn, Cu)	Continuous PRB Limestone	www.rtdf.org/public/permbarr/prbsumms/default.cfm
USA	Carteret, New Jersey (1993)	Heavy metals (Cu, Ni, Zn, As, Cd, Pb, Sn)	Continuous PRB Dolomitic limestone and sodium carbonate	ITRC 2005 and Bronstein, 2005
USA	Wallace, Idao (2001)	Zinc, Plomb, Cadmium	Two cells PRB Apatite	ITRC 2005, Bronstein, 2005 and EPRI, 2006
USA	Richmond, California (2002)	AMD (pH, Fe, Hg, As, Cu Zn)	Continuous PRB Compost andt sulfate-reducing bacteria	ITRC 2005 and Bronstein, 2005
USA	Charleston, South Carolina (2002)	Arsenic, heavy metals and acidity	Continuous PRB Compost, iron and limestone	ITRC 2005 and Bronstein, 2005- EPRI,2006
USA	Durango, CO (1995)	Arsenic, Molybdenum, Selenium, Uranium, Vanadium, Zinc	Drains and continuous PRB ZVI, Copper and steel wool	www.rtdf.org/public/permbarr/prbsumms/default.cfm - PEREBAR, 2000

USA	Wallace, Idaho (2001)	AMD	Funnel and Gate, Two cellules Apatite	Bronstein, 2005 - EPRI, 2006
USA	Nesquehoning, PA (1998)	Pb, Cd, As, Zn, and Cu	Continuous PRB Limestone	EPRI, 2006
USA	Portland, OR	Chrome VI (+TCE)	Continuous PRB Zeolite	RTDF.org
USA	South Dakota	AMD (As, Cd, Co, Cu, Pb, Zn)	Continuous PRB Viromine™ Acid-B Extra™	Lee C. Fergusson, 2009
USA	Carteret, NJ (2000)	Copper, Nickel, Zinc	Continuous PRB Dolomitic limestone and sodium carbonate	Bronstein, 2005 - EPRI, 2006
USA	Newport, Delaware (2002)	Mn, Ba, Cd, Cu, Ni, Pb, and Zn	Continuous PRB Sand, sulfate of calcium, ZVI and carbonate of magnesium	Bronstein, 2005 - EPRI, 2006
USA	Granger, IN (1995)	Chrome VI, Cu et As	Technique mixed "BPR" and "P&T" Polysulfide of calcium	Bronstein, 2005 - EPRI, 2006
USA	Shiprock, New Mexico	Uranium, SO_4, NO_3, Sb, Cd	Organic material and bacteria	PEREBAR, 2000

Table 1-2 List (not exhaustive) of PRBs installed to treat heavy metal contaminated groundwater (adapted from RECORD, 2010)

1.5 ZVI-PRB: main issues

Some of main issues concerning PRB regard long-term removal efficiency, the hydraulic behavior and the release of contaminants. In fact, usually, when a PRB is designed, a sufficient reactive material is quantified to be placed in the barrier that is previewed as having a certain longevity.

When the barrier is built, it comes into contact with groundwater constituents and a number of reactions can take place, forming mineral precipitation and other products that might fill the pores of porous material and reduce hydraulic conductivity.

Concerning ZVI, the possible causes of hydraulic efficiency decrease are indicated in the expansive nature of iron corrosion products (Caré et al., 2008; Zhao et al., 2011), the gas formation (Henderson and Demond, 2011, Reardon, 1995, 2005, 2014), the biofilm formation (Gu et al., 1999), the secondary mineral precipitates accumulation (O'Hannesin and Gillham, 1998; Liang et al., 2000; Kamolpornwijit et al., 2003; Jeen et al., 2008) and the retention of fine particles derived from upstream soil in the pores (Moraci, et al., 2014).

The iron corrosion is developed through the reactions between ZVI and groundwater, including its constituents, involving Eh decrease and pH increase (Blowes et al., 2000; Geranio, 2007). This means that ZVI can react with water oxygen, magnesium, carbonates, calcium and sulfates dissolved inorganic constituents (Puls et al., 1999; Puls, 2006; Jeen et al., 2008).

Under anaerobic conditions, water is reduced and at high pH, ferrous hydroxide or green-rust minerals can be formed (Zolla et al., 2007, Wilkin et al., 2000), whereas under aerobic conditions, dissolved oxygen reacts as the oxidant and ferric oxides and oxy-hydroxides can precipitate (Wilkinet al., 2000).

Notwithstanding the fact that on the basis of a number of laboratory research studies, iron corrosion products can lead to hydraulic conductivity and removal efficiency decrease, in some field studies PRB performance has not declined. This means that the rate of decline can be different and that many PRBs are too new for gathering this kind of information. (Kouznetsova et al., 2007).

1.6 ZVI-PRB for heavy metals

The proposal of the research activity, of which results will be presented in the following chapters, deals with the remediation of heavy-metal contaminated groundwater using PRB made of granular ZVI mixed with other granular materials. The choice to treat heavy-metals contaminants was driven by the knowledge of high presence of this kind of pollutants in water matrix, e.g. as previously mentioned for EU countries (paragraph 1.2.2).

1.6.1 Nickel, Copper and Zinc removal using ZVI/granular material mixtures

Among the different heavy metal elements, the choice of the defined contaminants to study was on two main considerations.

The first concerns reactive materials. The main reactive material chosen to be used in the research has been ZVI, which is able to remove organic and inorganic contaminants. It is the most widely used in *in-situ* and pilot installations as well as in

a number of laboratory studies, focused on its behavior improvement, and it can be considered the most versatile and the most suitable reactive material for treating a complex contamination. It is, however, true that the choice of reactive material and its characteristics depends on different considerations on contamination and site configuration, so that it is not possible to take a decision a priori and evaluation is necessary, case by case.

Given ZVI/granular material mixtures as reactive material to be used, the possible heavy metals removal mechanisms involved using ZVI have been considered so as to optimize their representation and the possibility of studying them. ZVI can remove heavy metals by reduction, adsorption onto corrosion products or co-precipitation (Noubactep, 2008, 2009; Noubactep and Schöner, 2009; Cundy, et al., 2008; Rangsivek and Jekel, 2005; Moraci and Calabrò, 2010). Three heavy metals have been chosen for study in function of their different affinity to iron oxides and the different redox behaviors of the couples, each one made of one of the chosen heavy metals and ZVI. The proposed heavy metals are Nickel (Ni), Copper (Cu) and Zinc (Zn).

The difference of electrode potential (E^0) between the elements involved gives information about the different redox behaviors. Zinc, whose $E^0_{Zn(II)/Zn(0)}$ value is –0.763 V, cannot be reduced by ZVI, whose $E^0_{Fe(II)/Fe(0)}$ value is -0.44 V. Copper can be readily reduced by ZVI because its $E^0_{Cu(II)/Cu(0)}$ is +0.337 V. Nickel has a standard electrode potential close to that of ZVI. The value of $E^0_{Ni(II)/Ni(0)}$ is -0.25 V. This means that redox process is not sure and that the main Nickel removal process using ZVI is not redox. The metallic ions can be removed by four main mechanisms: co-precipitation with iron hydroxides, adsorption onto the (hydr)oxide surfaces, isomorphic substitution for Fe in the iron oxide structure, or adsorptive size-exclusion (Herbert, 1996, Wang and Qin, 2007, Vodyanitskii, 2010, Bilardi, et al., 2013). Reduction can be developed through different reaction paths: direct reduction on ZVI, reduction by aqueous Fe(II), reduction by adsorbed or structural Fe(II), reduction by molecular (H_2) or atomic (H) hydrogen (Noubactep and Schöner, 2009; Bilardi, et al., 2014). Furthermore, the removal of the three heavy metals has been tested in a number of batch and column tests using ZVI/Pumice mixtures (Moraci and Calabrò, 2010; Moraci et al., 2011; Calabrò et al., 2012; Bilardi et al., 2013a and 2013b; Moraci et al., 2014; Bilardi et al., 2014). The results represented the basis for development of part of program of research activity presented in this work. Using the

same ZVI/Pumice weight ratio mixture and monocontaminat solutions of Cu, Zn and Ni at initial concentration of 500 ppm, 50 ppm and 50 ppm respectively, in column tests performed with the same constant velocity rate, the removal sequence observed was Cu > Zn > Ni. Using a pluricontaminant solution of Cu, Zn and Ni at the same initial concentration above-reported, the removal efficiency is reduced for Ni and Zn only and in one particular case the removal sequence observed was Cu > Ni > Zn. This means that Copper mantains its affinity with iron surface, while Nickel and Zinc are more difficult to remove (Bilardi et al., 2013). Particularly, regarding the results of ZVI/Pumice mixtures, Nickel is the most difficult to remove if it is used in monocontaminant solution, whereas its removal is reduced not as much as happens for Zinc, if it is used in pluri-contaminant solution. For this reason, the research activity that will be introduced focuses mainly on Nickel contaminant.

The second consideration supporting the choice concerns the lists of priority substances previewed by different laws. More precisely, Nickel is among the 33 substances that are on the list of priority substances according to Annex II of Directive on Environmental Quality Standards of European Commission (Directive 2008/105/EC) as required by the Water Framework Directive (2000/60/EC). Nickel, Copper and Zinc are among the 129 Priority Pollutants selected and prioritized by EPA on the basis of the list of toxic pollutants, making this list more practical for testing and for regulation, as previewed by the Clean Water Act. This law, together with the Safe Drinking Water Act, the Resource Conservation and Recovery Act, and the Superfund Act, provides groundwater protection in the United States.

In France, Nickel constitutes 5.85% of the in-situ contaminants and is positioned at the 9th position according to basol database. Copper is the 5th (8.25%) and Zinc is the 8th (5.93%).

1.6.2 Hydraulic issue: mixtures

Different strategies have been evaluated to overcome the problem related to the permeability loss of ZVI-PRB. Moraci and Calabrò (2010) proposed mixing ZVI with Pumice at a different weight ratios in order to avoid the fast permeability reduction observed using ZVI under the same boundary conditions. The proposal applied to heavy-metal removal has led to good results in terms of long-term removal efficiency

and hydraulic behaviors. Different mixtures made of ZVI/sand, ZVI/Pumice, ZVI/gravel, ZVI/anthracite have been tested for TCE contaminated groundwater removal by O'Hannesin and Gillham (1998), Ruhl, et al. (2012) and Bi, et al. (2009) but these systems have been unefficient for this kind of contaminant.

Other suggestions to resolve the hydraulic issue were to increase the thickness of the barrier, distributing better the materials, to equalize the zones up- and down-gradient the barrier through addition of pea gravel, to place a pre-treatment zone up gradient, to adjust the pH, to utilize larger ZVI grains and mechanical mixing (Blowes et al., 2000; Li and Benson, 2010).

During the research activity, the choice in trying overcome the permeability issue has been to mix ZVI with a new granular material. The mixtures have been tested to study their long-term heavy-metals removal efficiency and hydraulic behaviors. ZVI has been mixed with granular Lapillus, which is a volcanic material characterized by a chemical composition and structure a little different from Pumice. Its characteristics will be further described in Chapter 2.

1.7 PRB design

The design of PRB requires well-done contaminated site characterization. On this basis, the suitable reactive material and its characteristics, PRB dimensions and configuration, and method of construction can be chosen. One of the first steps is to select the reactive material that should be reactive with respect to the contaminant to be removed, environmentally compatible, stable, easily available and cheap. The selection regarding the removal efficiency of the potential reactive material is based on the results of batch and column tests. The latter give information not only about the possible efficacy of contaminant removal, but also about the variables influencing long-term removal and hydraulic behavior, e.g. the available reactive surface, the residence time, the velocity rate and the concentration of contaminant.

However, different authors are working on the model development, to produce more complete or easier design tools. During the research activity, a model of the experimental tests carried out has been developed and this will be introduced in Chapters 6.

As mentioned above, one of the possible causes of hydraulic behavior decrease that can be avoided theoretically a priori regards the choice of grain size distribution, considering PRB as a geotechnical filter.

1.7.1 Filter criteria

The choice of the geotechnical characteristics of the granular reactive medium, namely grain size distribution, initial values and evolution ranges of porosity and permeability depend strictly on the proprieties of the aquifer. In fact the geotechnical characteristics of base soil, that are grain size distribution, porosity, internal stability and permeability, must be known and taken into account in PRB filter design. Moraci et al. (2014) pointed out the important geotechnical issue that has to be considered in the choice of reactive medium grain size distribution and this consists of satisfying filter design criteria towards the surrounding soil. There are the main design criteria for granular filter design in mono-dimensional flow conditions: internal stability, retention and permeability (Moraci et al., 2012a)

The internal stability criteria regards the ability of granular filter to prevent the loss of its own small particles due to disturbing forces (Kenney and Lau, 1985). Considering the PRB granular filter, it is important that it does not undergo significant variations in permeability and particle size distribution due to the dragging force of fluid. This stability depends on the grain size distribution, the soil relative density and the applied hydraulic gradient. To evaluate the influence of the first of these it is sufficient, in a first approach, to observe the grain size distribution. If it presents a concave upward curve, a gap-graded soil or a broadly graded soil can be considered to be internally unstable (Moraci et al., 2012b). The criteria proposed by Kezdi (1969) and Sherard (1979) based on classical retention criteria for granular soils and that introduced by Kenney and Lau (1985) on the basis of experimental and theoretical results, are commonly used to evaluate the internal instability of a granular soil that is subjected to seepage.

Moraci et al. (2012b) have developed a new theoretical method based on simulation of seepage through a granular soil represented by a sequence of parallel layers containing constrictions and spherical particles with different packing. The particle packing and the distance between two layers is a function of soil relative density. The

soil internal stability is evaluated by comparing particles contained in a layer to the constrictions of the next layer in the hydraulic flow direction.

The retention and permeability criteria deal properly with the function of the filter. When water flows through the soil, erosion can occur because of dragging of fine particles. The function of the filter is in fact to retain the soil particles and to avoid the increase of internal pore pressure at soil-filter interface at the same time. This means that the granular filter should be fine enough to retain loose soil particles and coarse enough to avoid the development of high internal pore pressure, without modifying the natural seepage flow (Giroud, 2010). A PRB filter can respect the permeability criteria, verifying the high internal pore pressure and flow rate requirements. In fact, on the one hand the hydraulic conductivity of the filter has to be higher than the surrounding soil to avoid the development of high internal pore pressure at soil-filter interface, and on the other hand the difference between the flow rate in the aquifer and that in the aquifer where PRB is placed should not be more than 10% (Moraci, 2010), to have an acceptable filter.

Geometric, physical, hydraulic, chemical and biological factors can affect the PRB hydraulic performance and the seepage and its evolution between the base soil and the granular filter (Caré et al., 2013). Among these factors, there are the shape of particles and the particle size distribution, the structure of the filter, including the pore constriction size and distribution, the particle surface roughness, the filter density, the particle specific density, the applied total head, the hydraulic gradient, the mass flow rate and changes in porosity of the filter in function of the water and soil chemistry and bacterial activity.

1.8 Conclusions

Considering the most used reactive material and its removal efficiency on the contaminants that most affect the groundwater matrix, at least in Europe, the research activity carried out has focused on the improvement of ZVI-PRB to remediate heavy metals contaminated groundwater.

In particular, ZVI has been tested mixed with Lapillus, considering that tested ZVI/Pumice and ZVI/sand mixtures have demonstrated a better hydraulic and heavy metal removal efficiency than pure ZVI. Filter criteria have been taken into account to prepare the mixtures.

Experimental results and model development will be introduced in the following chapters.

In Chapter 2 the reactive materials used in the research are introduced. Zero Valent Iron, Pumice and Lapillus were characterized by grain size analysis, pycnometer measurements, Scanning Electron Microscopic (SEM) observation and Mercury Intrusion Porosimeter analysis. In Chapter 3, the results of batch tests performed using Pumice, ZVI and ZVI:Pumice mixture put in contact with solutions of Nickel at different initial concentration at different solid to liquid ratio are considered to develop a Nickel removal model. In Chapter 4 the experimental data obtained from column tests performed using ZVI and ZVI:Pumice mixtures to remediate heavy-metal contaminated groundwater are reviewed in the light of the development of the column test model. In Chapter 5, the experimental results of column tests performed using Lapillus and ZVI:Lapillus mixtures are shown and discussed. In Chapter 6, a model to simulate the long-term removal efficiency of the previously tested mixtures is proposed. In Chapter 7, a comparison among ZVI:Pumice and ZVI:Lapillus mixtures tested under the same experimental conditions is described. In Chapter 8, release tests results and the evolution of Iron concentration compared to that of Nickel along the column length and during the time are reported.

2 Materials Characterization

2.1 Introduction

As introduced in Chapter 2, in this work an internally porous material, Lapillus, is mixed with ZVI to investigate the long-term removal efficiency and hydraulic behavior of ZVI:Lapillus mixtures. Furthermore, a model to simulate experimental data obtained by previous batch and column tests using ZVI:Pumice mixtures is developed. For this reason, Lapillus, Pumice and ZVI were characterized.

In this chapter, the materials used in the experimental activity will be described. These are reactive materials whose heavy metals removal efficiency and hydraulic behavior will be investigated, and the heavy metal contaminants used to prepare the synthetic contaminated solutions. The reactive materials used are Zero Valent Iron, Pumice and Lapillus. They have been characterized to know their physic-chemical and geotechnical properties and they have been observed using a scanning electronic microscope (SEM) to observe their shape and surface in order to obtain useful information for understanding the removal mechanisms and the processes leading to the reduction of hydraulic conductivity.

2.2 ZVI

The Zero Valent Iron used is of the FERBLAST RI 850/3.5 type, distributed by Pometon S.p.A., Mestre, Italy. The material is mainly made of iron (>99.74%) and the impurities include Mn (0.26%), O, S and C. (Bilardi et al., 2013). ZVI has been characterized by grain size analysis. Its grain size distribution is shown in Figure 2-5. The mean grain size (d_{50}) is about 0.5 mm and the coefficient of uniformity (U) is 2. The used ZVI microstructure was observed using Scanning Electron Microscopy (SEM). ZVI samples were prepared for SEM observation placing them on an appropriate support and fixing them on using silver varnish. Afterwards, they were conserved under vacuum conditions. Only before placing them into the instrument a plasma using a source of Gold-Palladium (Au-Pd) was used to put some atoms on the surface of the sample in order to create on the surface a layer capable of conducting the electrons for a clear observation.

2.2.1 SEM

Some pictures taken during the observation are shown in Figures 2-1, 2-2, 2-3 and 2-4. In the first (Figure 2-1 a), an overview of the sample can be seen. A small number of grains can be observed and one can be clearly seen. The others can be less easily distinguished from each other probably because of the plasma layer not being sufficient or of the varnish (Figure 2-1 b). Thus the observation focused on the grain clearly distinguishable whose size is representative of d_{50} of the grain size distribution (Figure 3-1 a). On the almost smooth surface of this ZVI particle, the are some small particles, that according to the analysis carried out by SEM-EDX seem to be iron oxides. These little particles that are compounds of Iron were observed using an enlargement of 500 X (Figure 2-3 a), 2000 X (Figure 2-3 b), 4000 X (Figure 2-4 a) and 7500 X (Figure 2-4 b). They increase the roughness and the specific surface of the ZVI particle. They seem to have different shapes (Figures 2-3) and can be either highly porous or not (Figures 2-4). Their surface can be smooth or highly rough (Figures 2-4 a), while for porous small particles, pores of 1 µm or less can be observed (Figures 2-4 b).

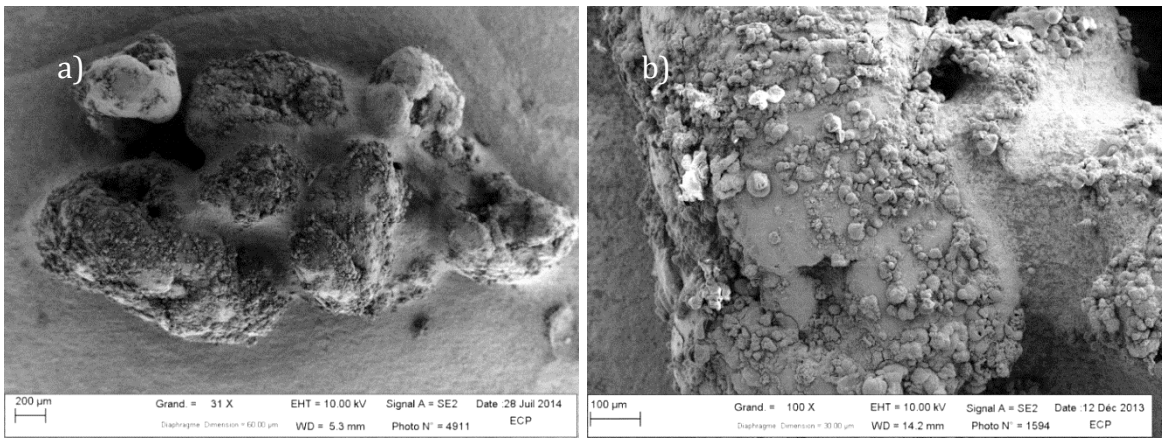

Figure 2-1 SEM pictures of ZVI samples using an enlargement of a) 31X and b) 100X

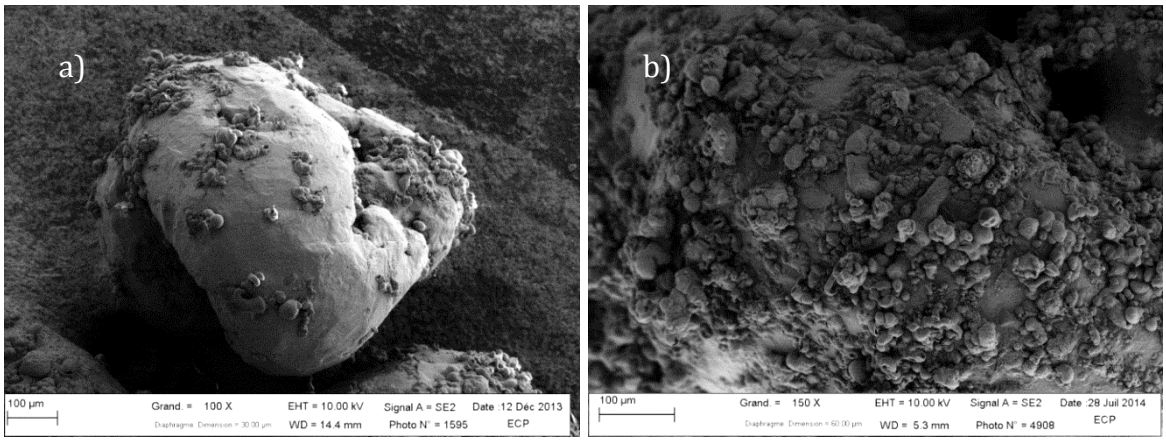

Figure 2-2 SEM pictures of ZVI samples using an enlargement of a) 100X and b) 150X

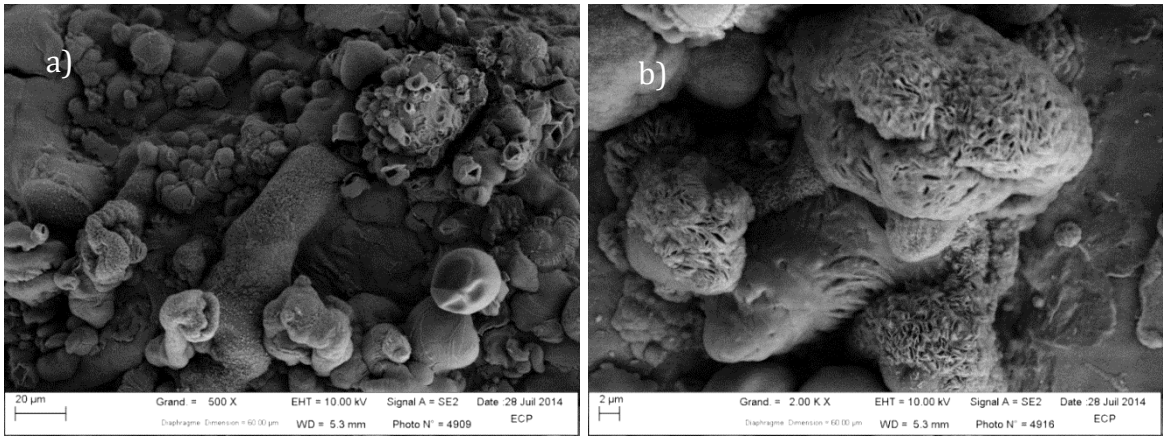

Figure 2-3 SEM pictures of ZVI samples using an enlargement of a) 500 X and b) 2k X

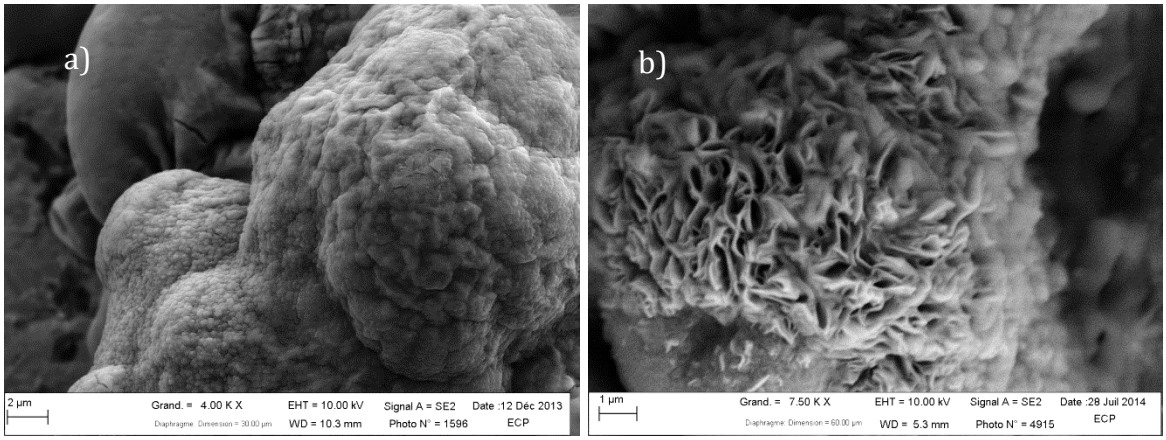

Figure 2-4 SEM pictures of ZVI samples using an enlargement of a) 4k X and b) 7.5k X

2.3 Pumice

Pumice is a product of explosive volcanic eruption and it is the main component of pyroclastic deposits. Fischer and Schmincke (1984) defined pumice as highly vesicular silicic to mafic glass foam, which will commonly float on water. Whitham and Sparks (1986) and Esposito and Guadagno (1997) have investigated the characteristics of pumice, presenting new measurements and analysis about physical geotechnical properties, internal surface area, connectedness of vesicles and their size distribution. They studied the behavior of pumice in contact with water, highlighting how the penetration of water into particle pores modify the weight-volume relationship. The experiments demonstrated a similar pattern in water adsorption of pumice samples characterized by different sizes, internal porosity and density. In fact, an initial rapid absorption, resulting in a significant part of pore space occupied by water, is followed by a slow steady absorption of water lasting weeks or months, until the sinking of pumice.

2.3.1 Chemical composition

The Pumice used in this research is classified as "2B" by the producer Pumex Spa. It originates from the Aeolian Island of Lipari, Sicily, Italy. In Table 2-1, its mineralogical composition of is shown. In addition it contains about 4% of structural water and traces of CaO, SO_3, MgO, TiO_2, FeO, MnO, P_2O_5 (Bilardi et al., 2013a).

Pumice mineralogical composition (gr/100 gr)	
SIO_2	71.75
Al_2O_3	12.33
Fe_2O_3	1.98
Na_2O	3.59
K_2O	4.47

Table 2-1 Pumice mineralogic composition

2.3.2 Grain size distribution

In Figure 2-5, the used Pumice grain size distribution is shown. The mean grain size (d_{50}) is about 0.3 mm and the coefficient of uniformity (U) is 1.4.

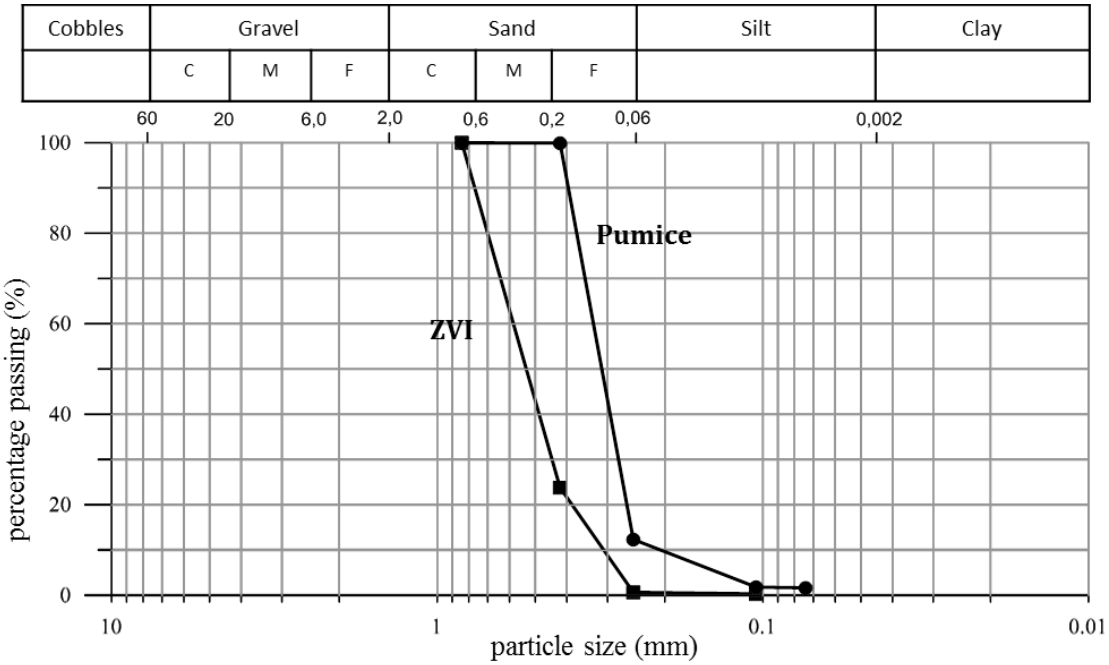

Figure 2-5 Pumice and ZVI grain size distributions

2.3.3 SEM

A Pumice sample was observed using SEM. The preparation was the same carried out for ZVI samples. The observation of the Pumice sample was carried out in order to know the structure of used Pumice, to characterize the material and to have useful information for interpretation of data from Mercury Intrusion Porosimetry (MIP) analysis. Two pictures taken during the observation are shown in Figures 2-6. The high internal porosity of Pumice and the large range of variation of pores size can be observed.

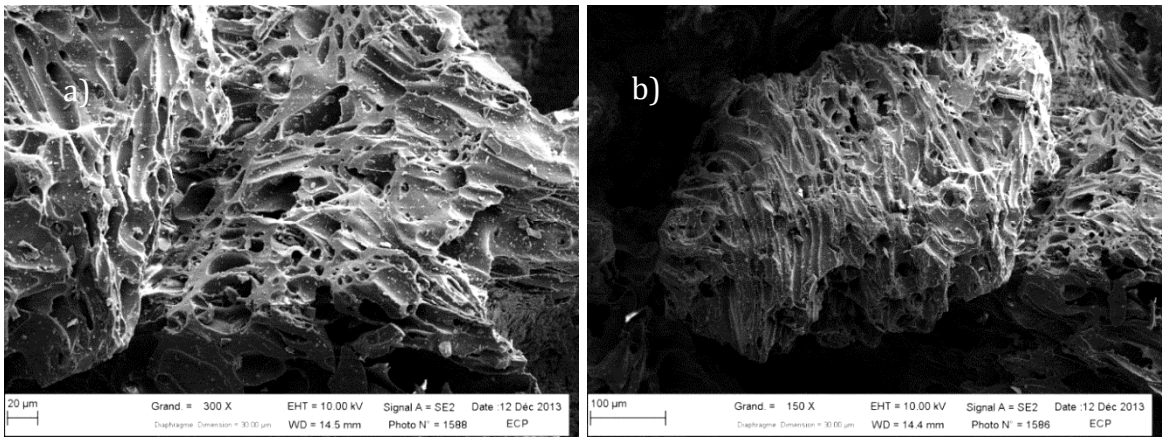

Figure 2-6 SEM pictures of Pumice samples using an enlargement of a) 300 X and b) 150 X

2.3.4 Mercury Intrusion Porosimetry (MIP)

The Mercury Intrusion Porosimetry analysis is based on the method described by Washburn in 1921 to determine the effective pore diameters in a coarsely granular sample using mercury as a non-wetting liquid to be forced into the pores at known pressures. The sample is placed into a sample cup that is first evacuated to remove all the gases adsorbed from the sample. Afterwards, pure mercury is pumped into the sample through a series of increasing pressures steps and the intruded volume is measured. Based on the equation of Young (1805) and Laplace (1806) that describes the equilibrium of the internal and external pressures for spherical surfaces, Washburn derived an equation directly applicable with mercury. This latter does not wet most of the substances and has to be forced to enter into the pores because it does not penetrate into them by capillary action. The method is based on the equation 2-1.

$$D = \frac{-4\gamma cos\theta}{P} \qquad (2-1)$$

where D is the pore diameter, P the applied pressure, γ the surface tension and θ the contact angle. In fact, there are three necessary physical parameters to be able to describe the intrusion of a liquid into a capillary. These are the surface tension, the contact angle and the geometry of the boundary line of contact among solid, liquid and vapor. The Washburn procedure is based on the hypothesis of cylindrical pores and the circular cross-section of the opening.

AutoPore IV of Micromeretrics (Model 9505/9500) was used to characterize Pumice. The specifications of instrument characteristics are reported in Table 2-2.

Characteristics	**Specifications**
Low Pressure	
Measurement	0 to 50 psia (345 kPa)
Resolution	0.01 psi (69 Pa)
Pore Diameter	360 to 3.6 µm
Transducer Accuracy	±1 of full scale
High Pressure	
Measurement	From atmospheric pressure to 33,000 psia (228 MPa)
Resolution	0.2 psi (1400 Pa) from 3,000 psia (21 MPa) to 33,000 psia (228 MPa) and 0.1 psi (689 Pa) from atmospheric pressure to 3,000 psia (21MPa)
Pore Diameter	6 to 0.005 µm
Transducer Accuracy	±1 of full scale

Table 2-2 Specificatio of AutoPore IV of Micromeretrics (Model 9505/9500)

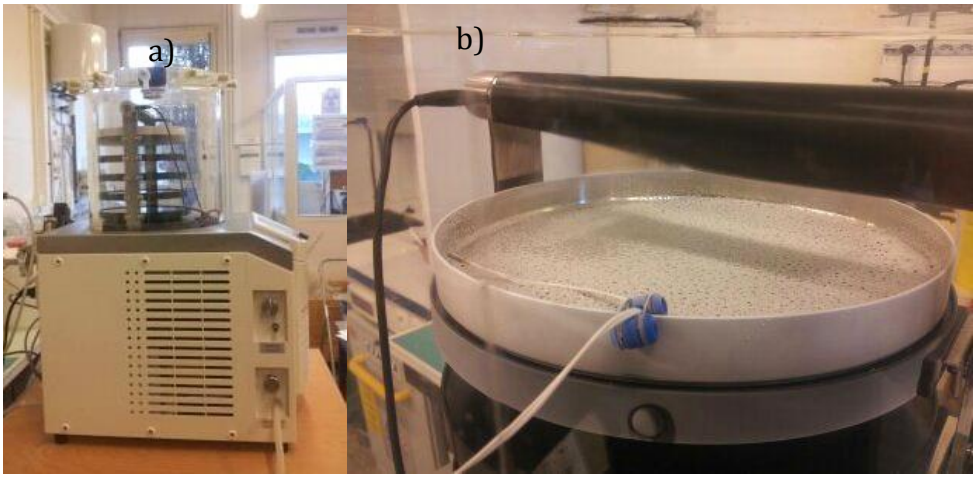

Figure 2-7 a) lyophilizer instrument and b) plate with sample in the lyophilizer

The Pumice samples were first dried using a lyophilizer (Figures 2-7). The used Pumice can be classified as a porous powder for this kind of application, therefore a penetrometer for powder was used (Figures 2-8 a and b).

Pumice quantity used was about 0.11 g for each tests to be able to use the available mercury volume of the penetrometer. Penetrometer type 14-0138 was used. Its characteristics are reported in Table 2-3.

Figure 2-8 a) used penetrometer and Pumice sample; b) sample chamber

Penetrometer Constant	11.117 µL/pF
Stem Volume	0.412 mL
Penetrometer Volume	3.2934 mL
Penetrometer Weight	56.9905 g
Maximum Head Pressure	0.030682 MPa
Assembly Weight	99.539 g

Table 2-3 used penetrometer characteristics

Four tests (A, B, C and D) were carried out to characterize the porosity of Pumice. The results are summarized in table 2-4.

Average sample quantity (g)	Average Max Diameter (µm)	Average Internal Volume (mL/g)
0.11	143-113	1.25-1.02

Table 2-4 Pumice characteristics obtained by four MIP tests

In Figures 2-9 – 2-11 some steps of analysis procedure are shown. In Figure 2-9 a) the chamber filled with Pumice sample is shown, in Figure 2-9 b) the penetrometer with greased ready be placed in the Low Pressure chamber is shown (Figure 2-10 and 2-11 a). First, the analysis in Low pressure chamber is performed (Figure 2-10 b), while the second step is developed in the High Pressure Chamber (Figure 2-11 b).

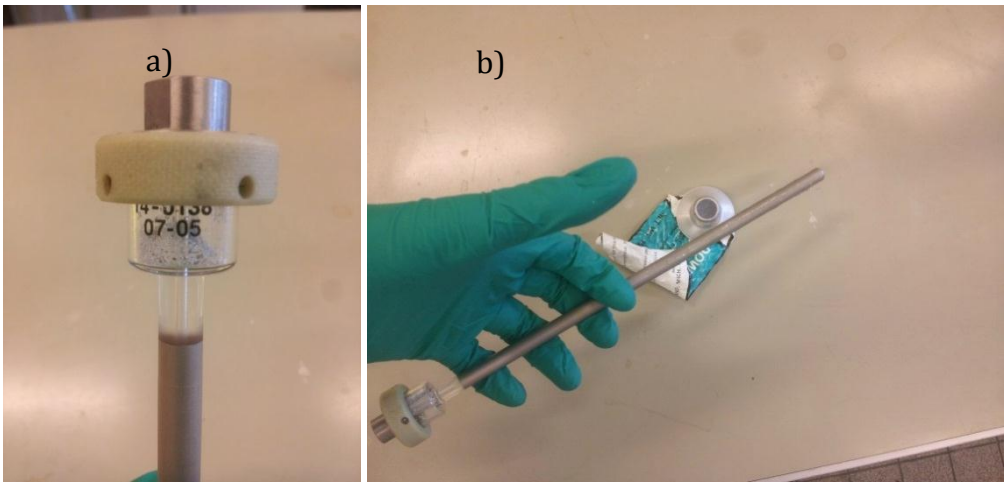

Figure 2-9 a) used penetrometer filled with Pumice sample; b) greasing step

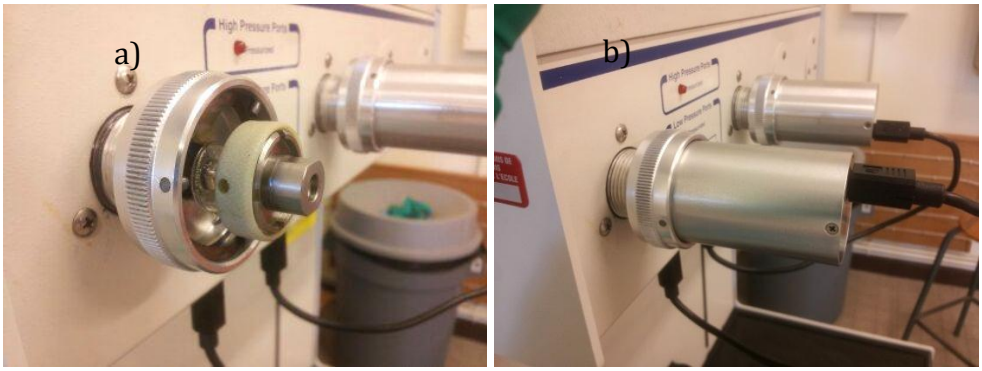

Figure 2-10 a) penetrometer placed into Low pressure chamber; b) Low Pressure Chamber on

Figure 2-11 a) Low pressure analysis before beginning; b) AutoPore IV of Micromeretrics (Model 9505/9500) Low Pressure and High Pressure Chambers

In Table 2-4, the maximum diameter identified by analyzing the results and the cumulative volume of pores per unit of Pumice mass are reported. In Figures 2-12, 2-15 the log differential intrusion, cumulative intrusion and incremental intrusion as function of Pore Diameter are reported for A, B, C and D tests respectively. Through a general overview, it seems that pumice does not have well-defined families of pores and a large range of pore sizes can be observed. The numbers reported on each graph concern the pore sizes corresponding to the picks.

The D test was the first one carried out and it was used in order to evaluate the steps of pressure to be used for the subsequent tests. For this reason, precise data about the first steps of pressure are not available. The maximum diameter and the different pore size families as found by Mercury Porosimetry data analysis can be validated by observation of the SEM images.

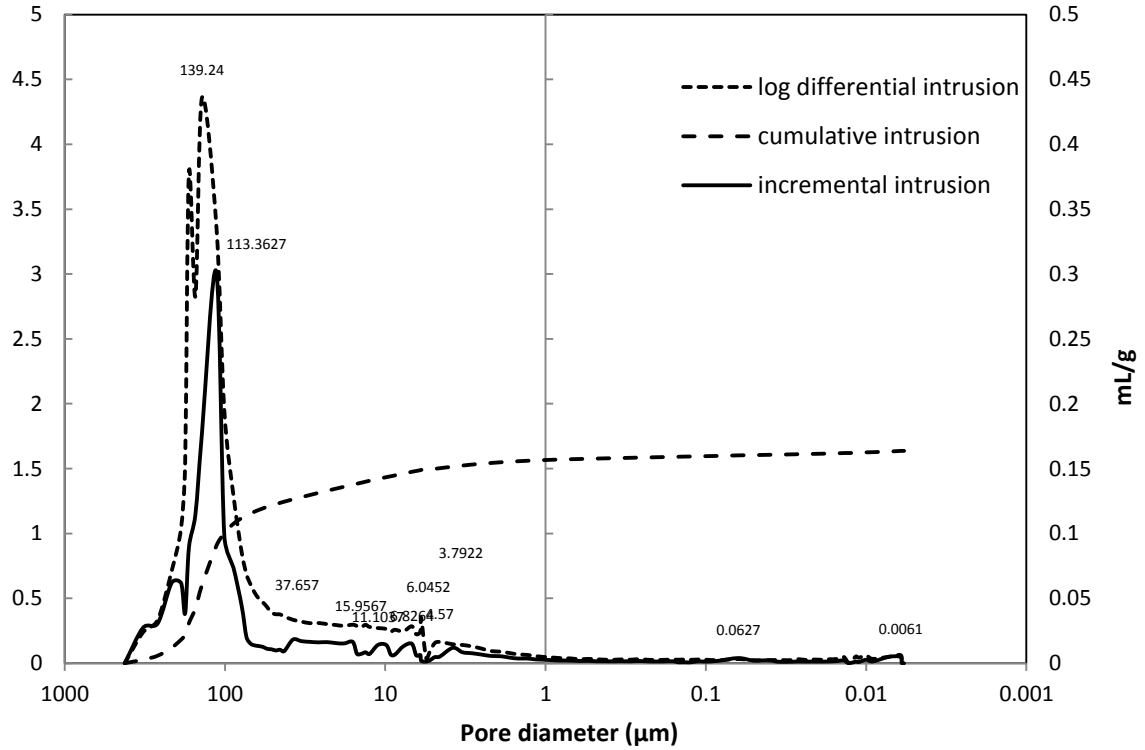

Figure 2-12 log differential intrusion, cumulative intrusion and incremental intrusion as function of pore diameter obtained for test A

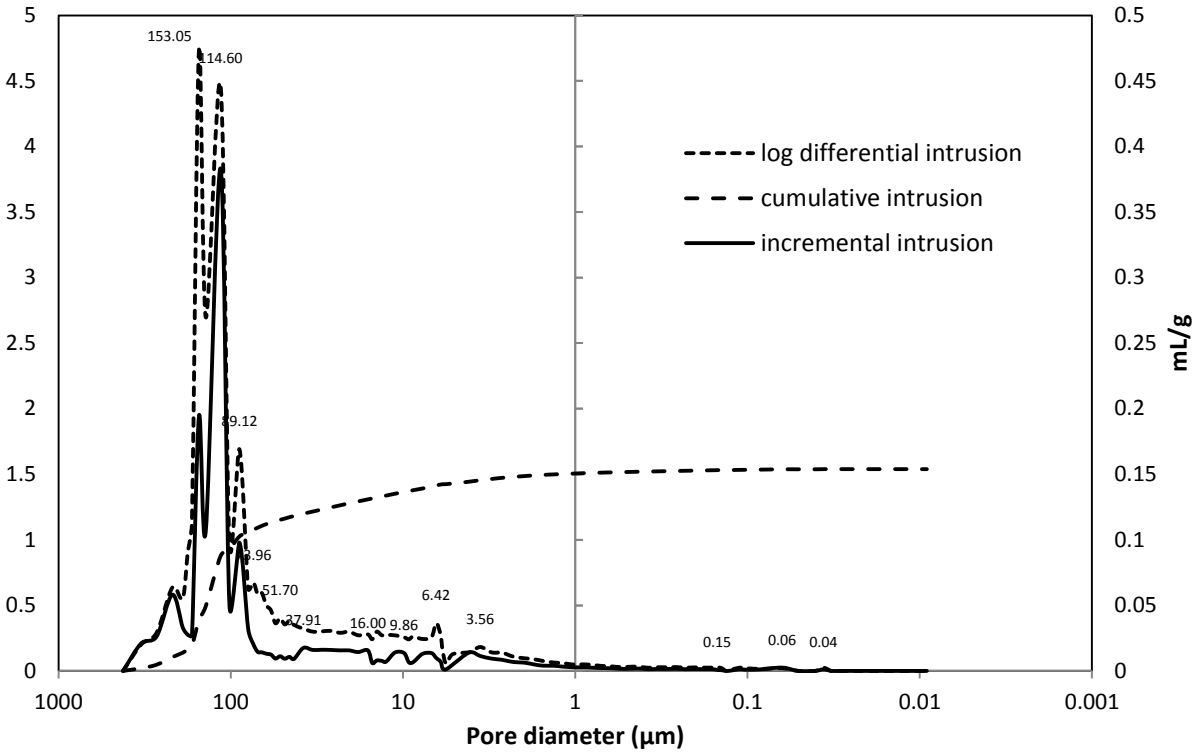

Figure 2-13 log differential intrusion, cumulative intrusion and incremental intrusion as function of pore diameter obtained for test B

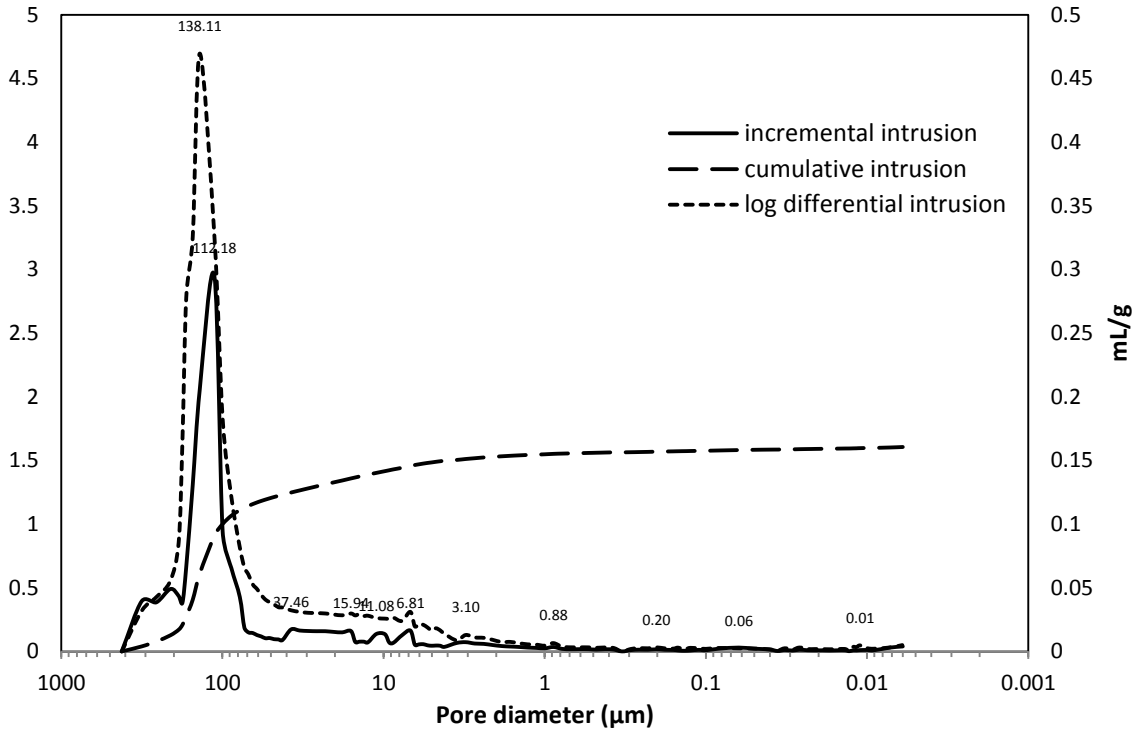

Figure 2-14 log differential intrusion, cumulative intrusion and incremental intrusion as function of pore diameter obtained for test C

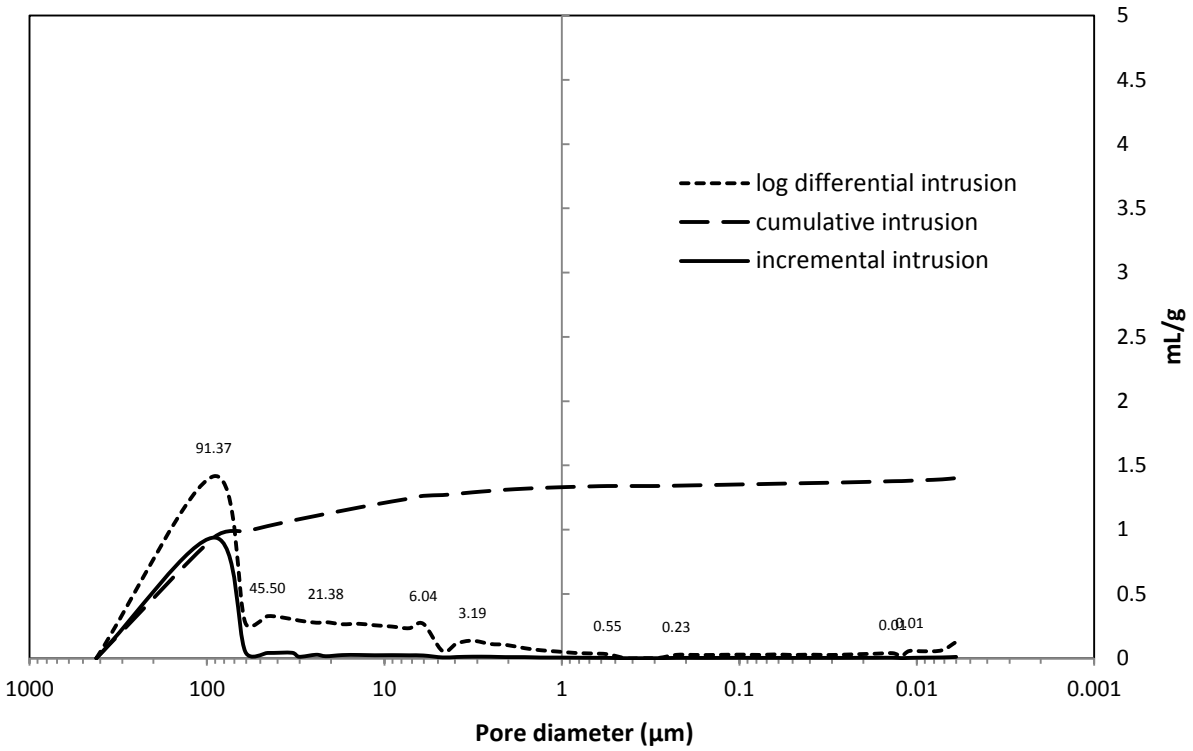

Figure 2-15 log differential intrusion, cumulative intrusion and incremental intrusion as function of pore diameter obtained for test D

In Figures 2-16 and 2-18 images taken during the Pumice samples observation using SEM are shown. An overview of the entire sample is reported in Figure 2-16 a) where some grains can be seen. In Figures 2-16 b) and 2-17 a) two particles are shown. In particular, it a correspondence was sought to the maximum value of pore sizes identified during SEM results analysis, to be able to distinguish between the Mercury volume that has intruded into intern pores and that has filled the inter-particles pores during MIP analysis. Pores of the same maximum size found in MIP results can be observed in SEM pictures. Figure 2.17 b) shows the large range of Pumice pores that can be observed and the preferential direction of pores in some particles. Figures 2-18 taken with an enlargement of 1000 and 2000 X respectively, show some little pores.

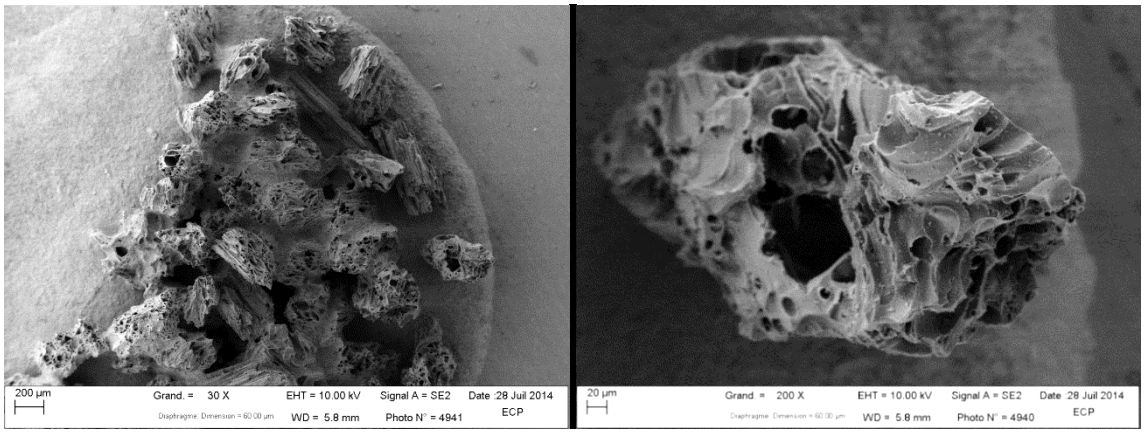

Figure 2-16 SEM pictures of Pumice samples using an enlargement of a) 30 X and b) 200 X

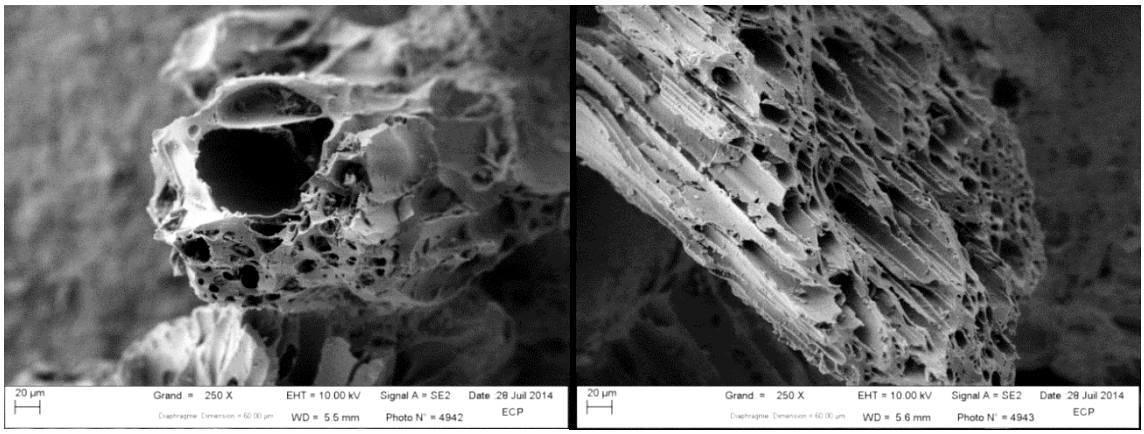

Figure 2-17 SEM pictures of Pumice samples using an enlargement of a) 250 X and b) 250 X

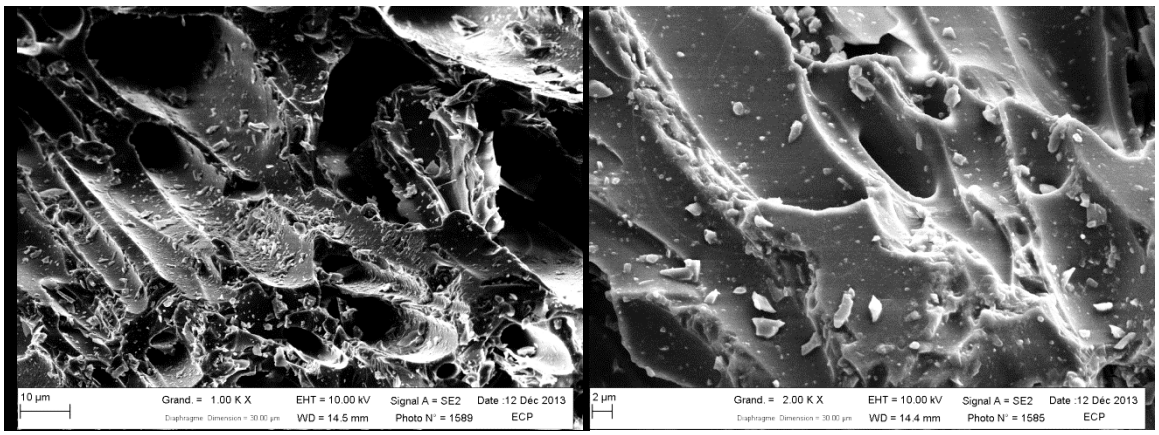

Figure 2-18 SEM pictures of Pumice samples using an enlargement of a) 1 k X and b) 2 k X

The volume of Mercury filling the penetrometer at the beginning of High Pressure chamber analysis V_m, after the vacuum is reached, is equal to the weight of mercury filling the penetrometer at the end of the Low Pressure step (0.2MPa) divided by the Y_m density of mercury. This can be expressed by the equation 2-2.

$$V_m = \frac{W_{psm} - W_s - W_p}{Y_m} \qquad (2-2)$$

where the weight of mercury is equal to the W_{psm} assembly weight minus the W_s sample weight minus the W_p empty penetrometer.

Knowing the volume of penetrometer V_p thanks to the previous calibrations and taking into account that part of the used stem volume has filled the inter-particles sample volume, after Low Pressure step, it is possible to calculate the bulk volume of Pumice particles V_b through equation 2-3.

$$V_b = V_p - V_m - V_{cum(>Dmaxpores)} \qquad (2-3)$$

The solid volume V_s can be calculated through equation 2-4.

$$V_s = V_b - V_{m,int} \qquad (2-4)$$

Where $V_{m,int}$ is the total internally intruded volume, the V_b the bulk volume. The $V_{m,int}$ total internally intruded volume is equal to the difference between $V_{cum(maxHP)}$ cumulative intrusion volume at the end of the measurement test and the inter-particle volume $V_{cum(>Dmaxpores)}$ (equation 2-5)

$$V_{m,int} = V_{cum(maxHP)} - V_{cum(>Dmaxpores)} \qquad (2-5)$$

Dividing the used pumice weight by the V_b bulk volume and the V_s solid volume, pumice apparent density ρ_{app} and real density ρ_s can be obtained respectively. The average value for ρ_{app} is 1.2 gr/cm^3 , while for ρ_s is 2.48 gr/cm^3. The φ_i internal porosity can be calculated by the equation 2- 6:

$$\varphi_i = 1 - \frac{\rho_{app}}{\rho_s} \qquad (2-6)$$

The calculated internal porosity was about 50%.

A quantity of information to characterize porous media can be deduced by analyzing Mercury Intrusion Porosimeter data, for example the number of pores and the material compressibility.

2.3.5 Pycnometer

The pumice density $\boldsymbol{\rho}$ measured using Pycnometer is about 2 gr/cm^3.

There are some differences among the density deduced by Pycnometer, the apparent density ρ_{app} and the real density ρ_s deduced by analyzing the Hg-porosimeter data. The sequence is $\rho_{app} < \boldsymbol{\rho} < \rho_s$. The difference can be searched on the wettability of pumice using different fluids (i.e. Hg and water) and in the capillarity phenomena that can be developed in the micro pores of pumice when it is put in contact with water. In fact, fast water sorption on pumice when it is put in the water, sinking experiments and long-time pore occupancy by water are reported in a number of studies (Whitham and Spark, 1986).

2.4 Lapillus

Lapillus is a sedimentary pyroclastic material. Sedimentary rocks result from consolidation of loose materials which were created from erosion and alteration of pre-existing rocks. Pyroclastic rocks are a particular group of sedimentary rocks and are formed after volcanic products deposition in conjunction with explosive eruptions (Scesi et al., 1997). The used lapillus is a natural material distributed by SEM "Società Estrattiva Monterosi s.r.l.", Viterbo, Italy. It has granular form and a red-maroon colour (Figure 2-19) and originated from explosive volcanic activity of the Sabatini Mountains.

Figure 2-19 Lapillus sample

2.4.1 Chemical composition

In table 2-20 the chemical composition provided by the Società Estrattiva Monterosi are shown. Other compounds as MnO, Na_2O are present in traces, while $CaCO_2$ is absent.

Lapillus mineralogical composition (gr/100 gr)	
SiO_2	47
Al_2O_3	15
Fe_2O_3 , FeO	7-8
MgO	5.5
CaO	11
K_2O	8
$CaCO_2$	absent

Figure 2-20 Lapillus chemical composition provided by SEM s.r.l.

2.4.2 Grain size distribution

The grain size distribution of Lapillus as received is reported in figure 2-21. The uniformity coefficient U (d_{60}/d_{10}) is equal to 10.4.

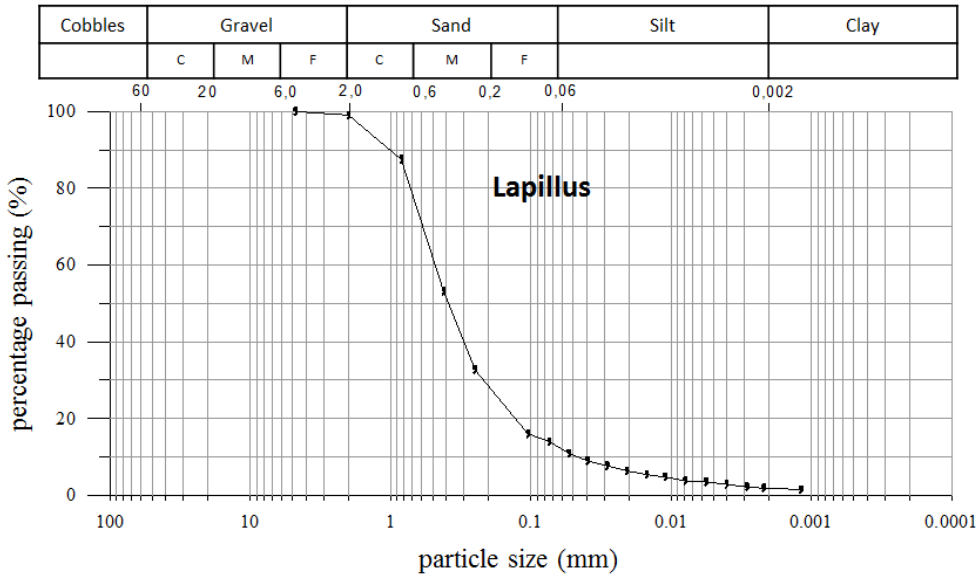

Figure 2-21 Lapillus grain size distribution (sample from quarry)

The grain size distribution of Lapillus samples used in column tests has been selected in function of that of zero valent iron and considering the internal stability filter design criteria (Moraci et al., 2012a). The Lapillus grains were washed, the retained grains on sieve No.20 (>0.84 mm) and the passing to the sieve No. 200 (<0.074 mm) were discarded in order to obtain a particle size distribution more similar to that of ZVI (Figure 2-22). The coefficient of uniformity U is about 3.2 and the mean grain size (d_{50}) is approximately 0.4 mm.

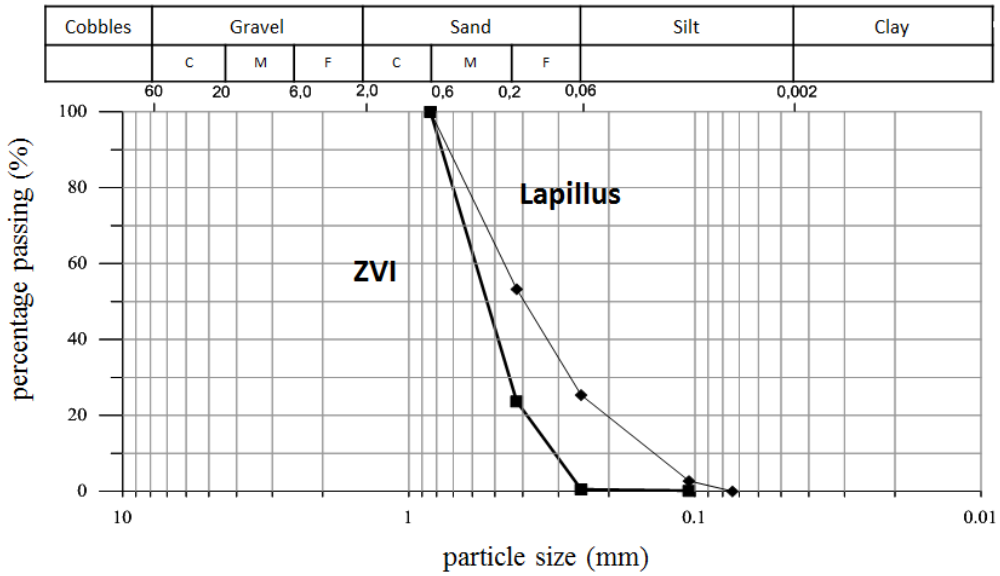

Figure 2-22 Lapillus and ZVI grain size distributions (as used in column tests)

2.4.3 SEM

Lapillus samples were observed by using SEM. The samples were treated for analysis as above-described for ZVI. Lapillus seems to be less porous than pumice. It has a more irregular and rougher surface than pumice. The pictures taken during SEM observation are reported. In Figure 2-23 a) a general view of lapillus sample is shown and it is evident that it has a lower porosity with respect to the pumice. Concerning the particle shown in Figure 2-23 b) larger pores than the ones observed in pumice samples are visible. Furthermore, a comparison between this particle and those shown in Figures 2-24 leads one to consider Lapillus porosity as not-homogeneous.

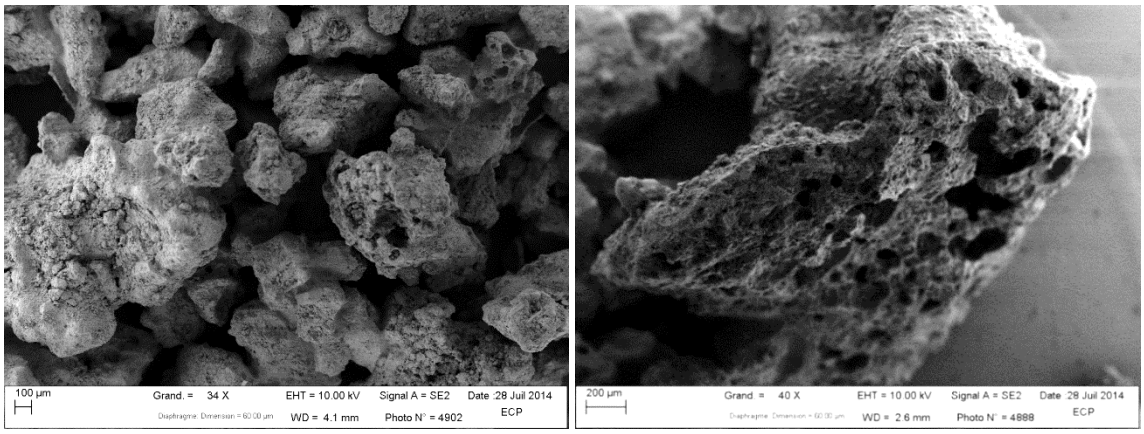

Figure 2-23 SEM pictures of Lapillus samples using an enlargement of a) 34 X and b) 40 k X

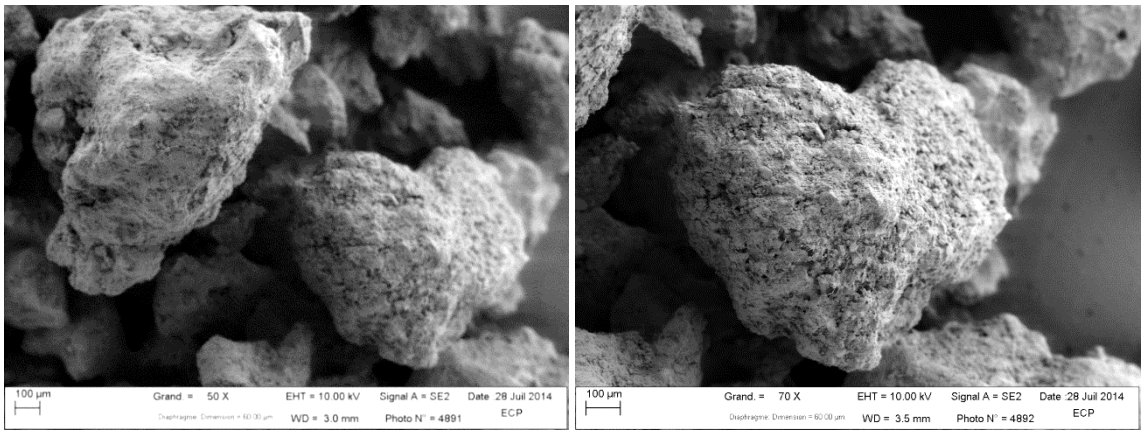

Figure 2-24 SEM pictures of Lapillus samples using an enlargement of a) 50 X and b) 70 X

The shape of Lapillus particles is really variable, as well as the porosity (Figures 2-24 and 2-25). Furthermore, the particle surface presents roughness at small scale also (Figure 2-26 and 2-27).

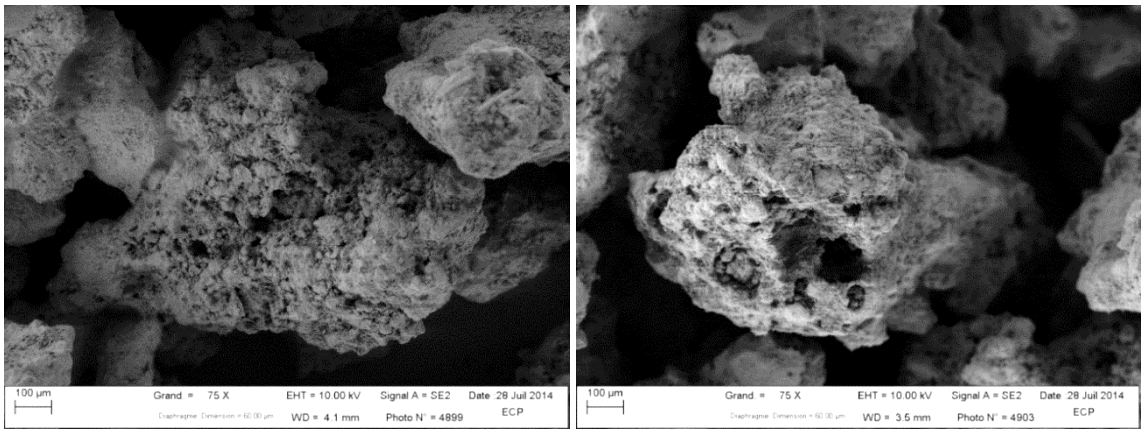

Figure 2-25 SEM pictures of Lapillus samples using an enlargement of a) 75 X and b) 75 k X

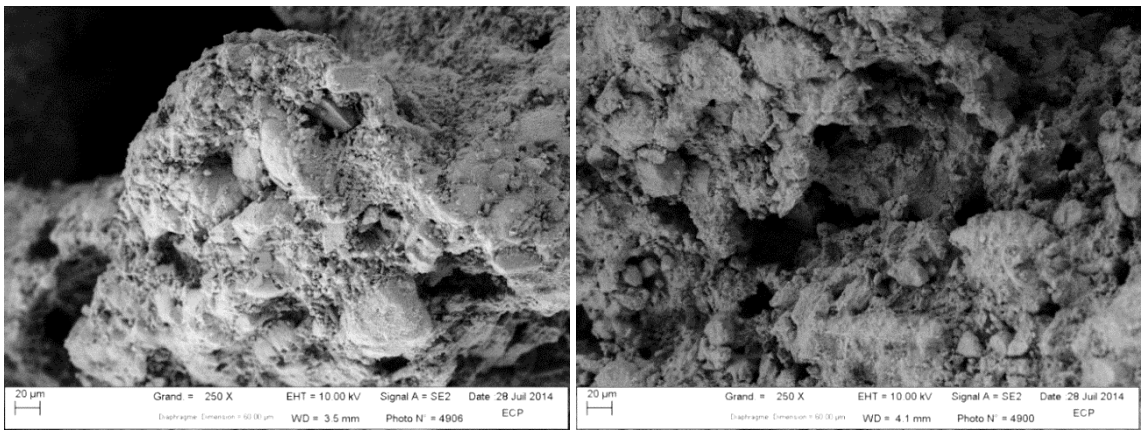

Figure 2-26 SEM pictures of Lapillus samples using an enlargement of a) 250 X and b) 250 X

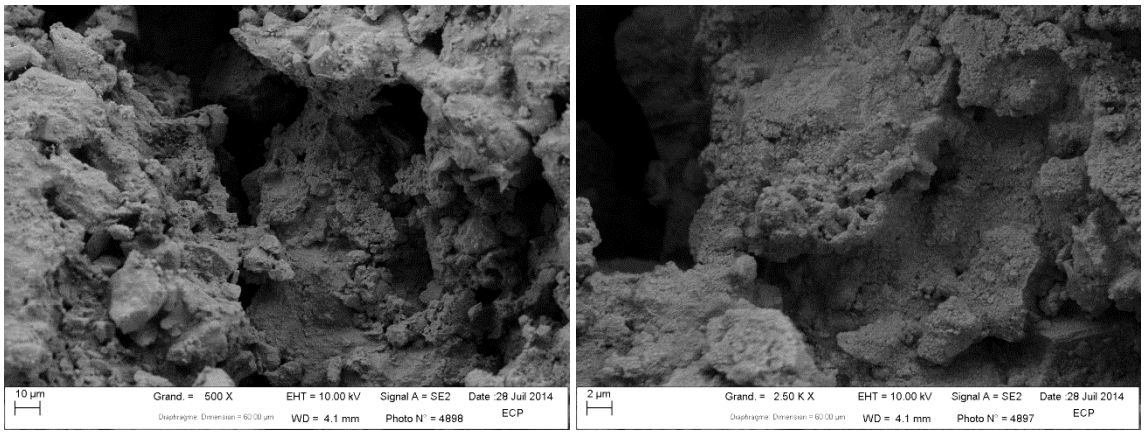

Figure 2-27 SEM pictures of Lapillus samples using an enlargement of a) 500 X and b) 10 k X

2.4.4 Mercury Intrusion Porosimetry (MIP)

As previously done for pumice, four tests (A, B, C and D) using lapillus were carried out using MIP. Log differential intrusion, cumulative intrusion and incremental intrusion variations are shown as function of the pore diameter for each test in the Figure 2-28 to 2-31.

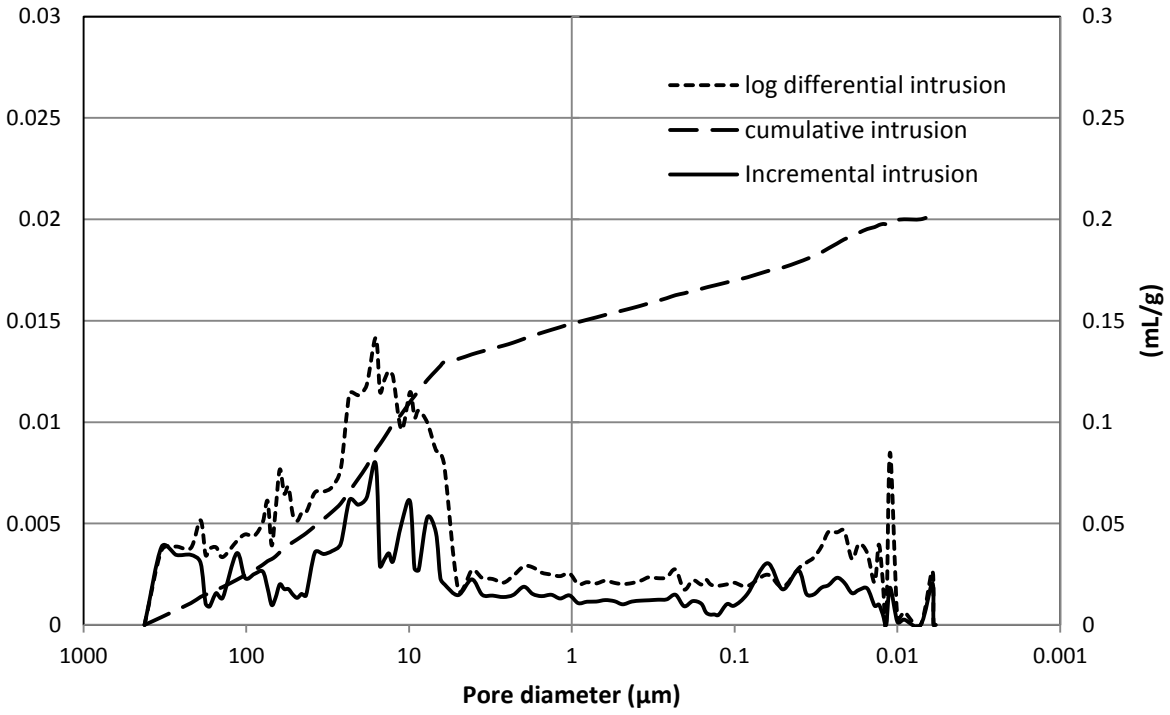

Figure 2-28 log differential intrusion, cumulative intrusion and incremental intrusion as function of pore diameter obtained for test A on Lapillus samples.

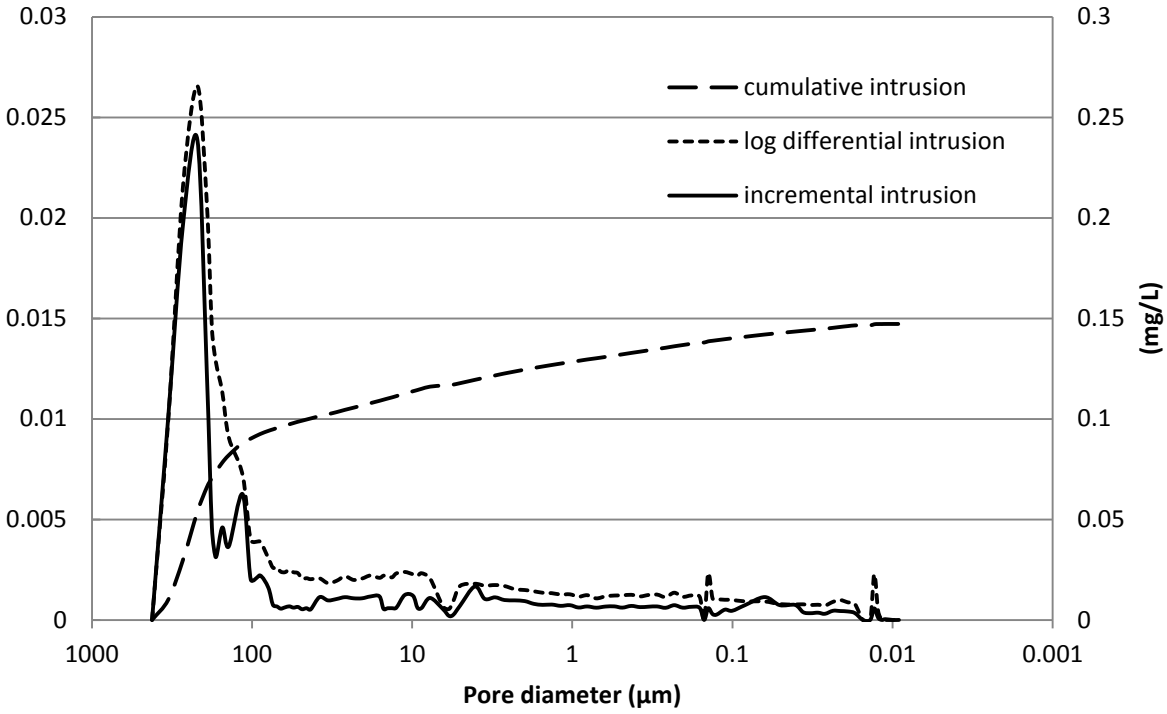

Figure 2-29 log differential intrusion, cumulative intrusion and incremental intrusion as function of pore diameter obtained for test B on Lapillus samples.

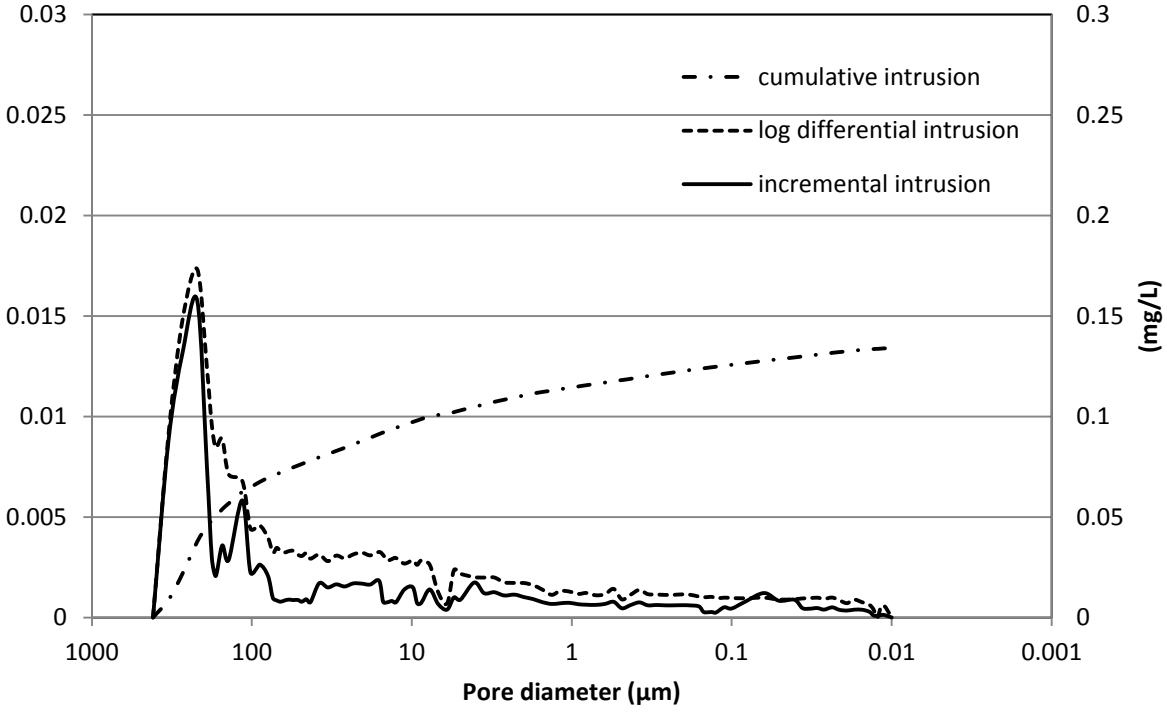

Figure 2-30 log differential intrusion, cumulative intrusion and incremental intrusion as function of pore diameter obtained for test C on Lapillus samples.

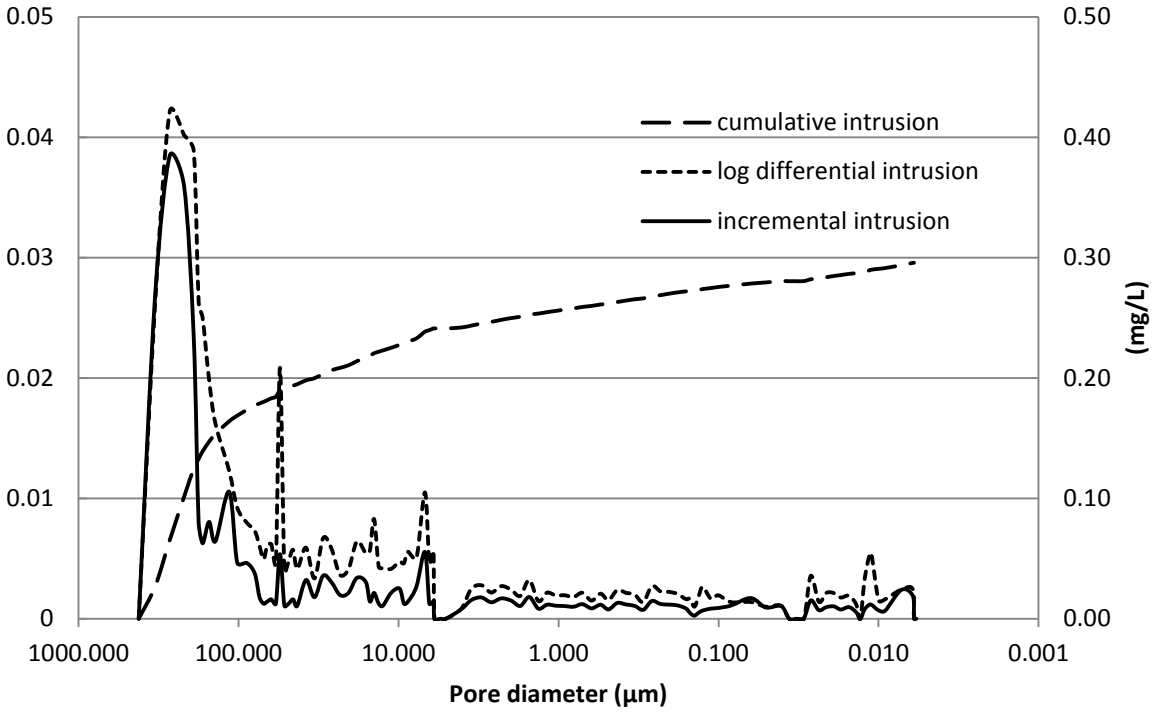

Figure 2-31 log differential intrusion, cumulative intrusion and incremental intrusion as function of pore diameter obtained for test A on Lapillus samples.

The results of MIP analysis are summarized in table 2-6.

Average sample quantity (g)	Average Max Diameter (µm)	Average Internal Volume (mL/g)
0.49	269-219	0.23 – 0.18

Table 2-5 Lapillus characteristics obtained by four MIP tests

Considering the same procedure used for pumice, the average apparent density ρ_{app} and the average real density ρ_s of lapillus were equal to 2.2 gr/cm^3 and 3 gr/cm^3 respectively. The calculated internal porosity φ_i was about 40%.

2.4.5 Pycnometer

The Lapillus density $\boldsymbol{\rho}$ measured using Pycnometer resulted about 2.8 gr/cm^3. As can be expected, the sequence $\boldsymbol{\rho_{app} < \rho < \rho_s}$ is respected.

2.5 Heavy-metal contaminated solutions

The chemical composition of the synthetic solution used in both tests is reported by Bilardi et al. (2012b). The Nickel contaminated solution was prepared diluting Nickel Nitrate (Nickel(II) nitrate hexahydrate, purity > 99 %; Sigma-Aldrich) in distilled water in order to obtain the preset Nickel concentrations (10, 50 and 100 mg/L).
The Zinc contaminated solution was prepared diluting Zinc Nitrate (Zinc(II) nitrate hexahydrate, purity 99; Sigma-Aldrich) in distilled water in order to obtain the preset Zinc concentration (50 mg/L). The Copper contaminated solution was prepared diluting Copper Nitrate (Copper(II) nitrate hydrate, purity > 99%; Sigma-Aldrich) in distilled water in order to obtain the preset Zinc concentration (500 mg/L).

2.6 Conclusions

The used Zero Valent Iron is of the type FERBLAST RI 850/3.5, distributed by Pometon S.p.A., Mestre in Italy. The material is mainly made of iron. The mean grain size (d_{50}) is about 0.5 mm and the coefficient of uniformity (U) is 2. By SEM analysis, ZVI particles seem to have an almost smooth surface, while some small particles, that have been observed on the surface, seem to be iron oxides. These letters seem to have different shapes and to be highly porous internally, with a surface smooth or highly rough. The Pumice used in this research is “Pumice 2B” provided by Pumex Spa. It originates from the Aeolian Island of Lipari, Sicily in Italy and it is mainly made of SiO_2 (71.75%) , Al_2O_3 (12.33%), Fe_2O_3 (1.98%), Na_2O (3.6%) and K_2O (4.5%). The mean grain size (d_{50}) is about 0.3 mm and the coefficient of uniformity (U) is 1.4.
Pumice was characterized by MIP. Its maximum average diameter is about 140-110 μm. The calculated internal porosity was about 50%. The Pumice ρ density measured using Pycnometer is about 2 gr/cm^3, the apparent density ρ_{app} is 1.2 gr/cm^3 and real density ρ_s is 2.48 gr/cm^3.
Lapillus is a sedimentary pyroclastic material. The Lapillus used is a natural material and it is distributed by SEM “Società Estrattiva Monterosi”s.r.l., Viterbo, Italy. It has granular form and a red-marron colour (Figure 2-19) and it originated from explosive

volcanic activity of the Sabatini Mountains. It is made of SiO_2 (47%), Al_2O_3 (15%), Fe_2O_3 and FeO (7-8%), MgO (5.5%)

The coefficient of uniformity U is about 3.2 and the mean grain size (d_{50}) is approximately 0.4 mm. Observing Lapillus using SEM, it seems to be less porous than Pumice and to have a more irregular and rougher surface than Pumice. The average apparent density ρ_{app} and the average real density ρ_s of Lapillus is equal to 2.2 gr/cm^3 and 3.86 gr/cm^3 respectively. The calculated internal porosity φ_i is about 40%. The Lapillus density ρ measured using Pycnometer resulted about 2.8 gr/cm^3.

In Chapter 3 the characterization results of Pumice samples are used to develop a model for the simulation of nickel removal efficiency observed in batch tests performed using pure Pumice by previous Ph.D. studens.

3 Modelling of Nickel removal efficiency in batch tests using pure double Porous Materials and ZVI

3.1 Introduction

In this chapter the experimental data of batch tests carried out using pumice, ZVI and their mixtures for nickel removal and performed during previous Ph.D. cycles will be re-analyzed to propose a general overview and interpretation. The aim of this work is to observe the Nickel removal efficiency of the reactive materials as they are able to develop in this kind of interaction test, to hypothesize the removal mechanisms involved and to develop a model to simulate the results. The results of MIP analysis, SEM observation, grain size distribution and pycnometric analysis of Pumice samples, as obtained in Chapter 2, are taken into account for analysis of experimental results of batch tests and the modelling development for their simulation.

3.2 Experimental results analysis using Pumice

Pumice removal efficiency has been tested through batch and column tests during the previous Ph.D. thesis at Mediterranea University of Reggio Calabria by Ph.D. students (Rigano, 2007; Suraci, 2011; Bilardi, 2012). Batch tests were carried out setting two different liquid-solid ratios (10mL:1g here called Low Mass (LM) and 4mL:1g here called High Mass(HM)) and three different initial concentrations of Nickel (5mg/L , 50 mg/L , 500 mg/l). In LM and HM tests 5.4 g and 8 g of reactive material were used respectively. First, Nickel contaminant removal efficiency observed in batch tests using pure pumice will be considered. Table 3-1 shows a summary of batch tests carried out with pure pumice and Nickel-contaminated synthetic solutions. It should be considered that Pumice has been tested in column tests as pure reactive material too (Moraci and Calabrò, 2010). The results collected by this test were considered and analyzed together with those of batch tests to have more information and in order to be able to hypothesize the possible Nickel removal mechanisms developed by using pumice only.

Tests	L:S (mL:g)	Ni C_0 5 mg/l	Ni C_0 50 mg/l	Ni C_0 500 mg/l
LM	10:1	x	x	
HM	4:1	x	x	x

Table 3-1 Batch tests carried out using pumice

3.2.1 Batch tests

Batch tests were performed preparing vials containing the reactive materials and the contaminated solution, putting them in rotation through an end over end rotating stirrer (Stuart Scientific Drive STR/4.1) and sampling the contaminant solution at different times. Reactive material and contaminant solution were placed in septum-capped vials with no head-space with a prefixed liquid to solid ratio. At each sampling time, the vial from which liquid samples was drawn was sacrificed.

The Figures 3-1 a) and b) show the results of batch tests carried out with pure Pumice and with low solid : liquid ratio (Low Mass – LM) and with high solid : liquid ratio (High Mass – HM) with different Nickel initial concentration. The star symbol refers to 5 mg/L of initial Nickel concentration, the circle to 50 mg/L and the rhombus to 500 mg/L.

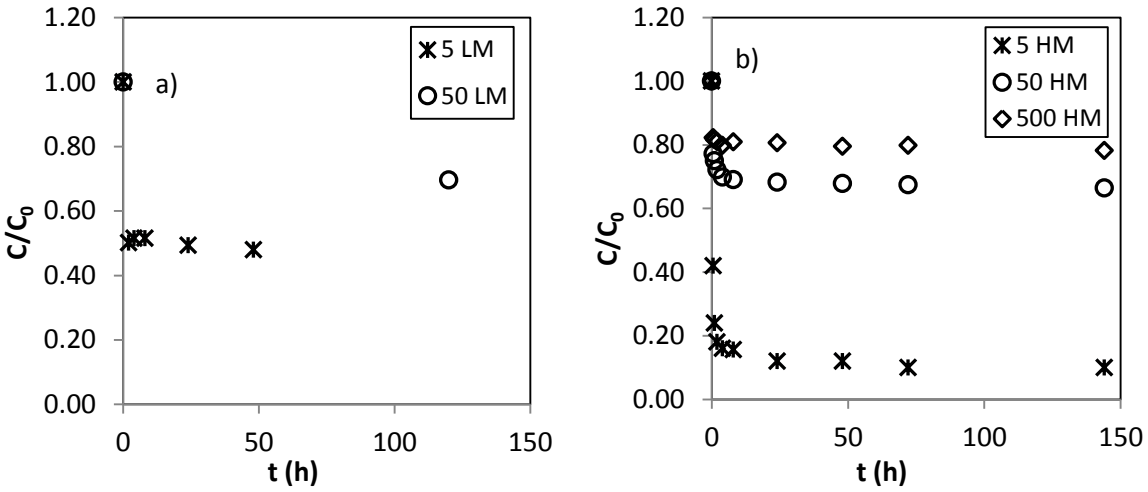

Figure 3-1 Batch tests results: variation of nickel normalized concentration over time for a) LM and b) HM tests

Pumice immediately reduces the initial nickel concentration of a certain percentage increasing with the solid : liquid ratio. It is possible to make some hypothesis. It is

observable that the main nickel removal by pumice is immediate and it reaches a certain percentage of initial concentration, after which pumice is almost not able to remove further quantities anymore, if not really slowly. In addition, the nickel mass quantity removed by pumice and the removal rate in pure Pumice tests depend on the solid : liquid ratio and the initial concentration. Looking at the same concentration, it seems that removed nickel mass and removal rate increase with the solid : liquid ratio. Considering the same solid : liquid ratio, the values of contaminant concentration are proportional to the nickel initial. In each test, a minimum concentration, called C_{min} , is reached and its value depends on the initial concentration C_0. Table 3-2 illustrates the minimum concentration C_{min} values reached in each batch test with pure Pumice and Figure 3-2 a) shows a linear relationship between C_{min} and C_0.

C_0 (mg/l)	C_{min} (mg/l)	
	HM	LM
5	0.42	2.5
50	32.43	35
500	350.3	

Table 3-2 C_{min} reached as function of C_0

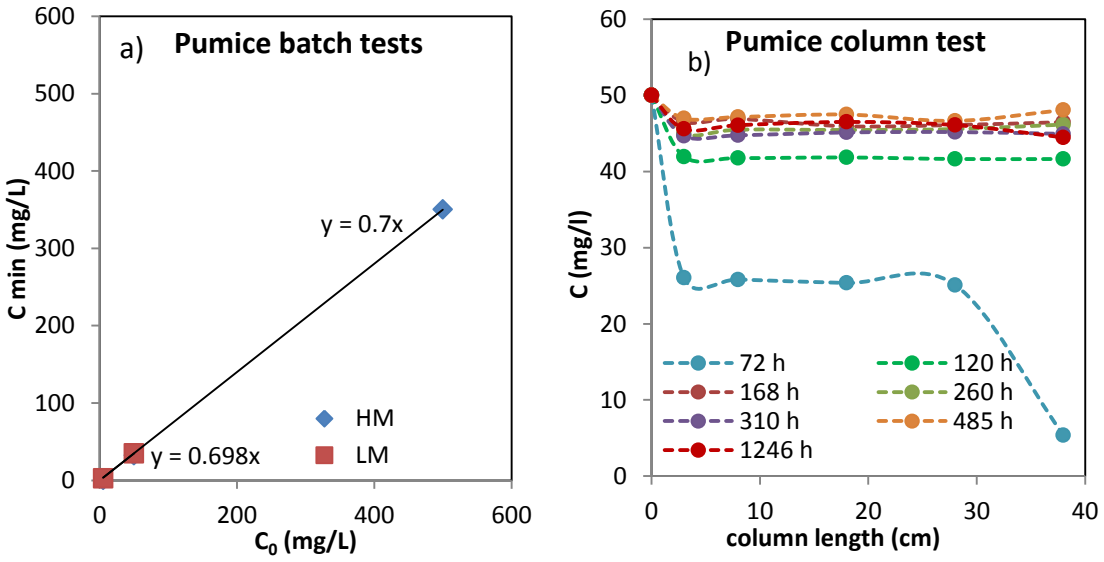

Figure 3-2 a) relationship between the C_{min} and C_0 in batch tests; b) Nickel concentration evolution as function of filter thickness for different sampling times in column test

In Figure 3-2 b) the results regarding a column test carried out with pumice and ZVI placed in series are shown. The data refer only to the first layer of pumice. The results show that at the beginning of the test, the concentration reduces by half and the removal efficiency reduces with time.

3.3 Ni removal efficiency using pure Pumice

Heavy metals removal by pumice can depend on the surface functional groups and on high internal porosity. Iron and aluminium oxides are very effective for heavy metal removal due to their high specific surface areas and reactive surface functional groups (Potter, 1999). The charge on these hydroxyl surface functional groups depends on pH value; at low pH, protonation favors the formation of positively charged groups while at high pH de-protonation leads to the formation of negative groups (Hohl et al., 1980). The pH at which the net surface charge is zero is termed the zero point of charge or pH_{zpc} (Parks and De Bruyn, 1962). Oxide minerals containing silica have a pH_{zPc} of about pH 2, Fe oxides about pH 7-8 and oxides around pH 9 (Kinniburgh et al., 1976; Schulthess and Huang, 1990). At pH value greater than pH_{zpc}, heavy metal cations will be tight to the reactive material surface through electrostatic attraction. Thanks to the chemical affinity of same surface groups for certain heavy metals, surface complexes formation is possible. The adsorption proceeds through the diffusion consisting of transfer of adsorbate from solution to adsorbent surface, the migration of adsorbate into pores and interaction with available sites on the interior surface of pores. The factors influencing the adsorption are surface area of adsorbent, contact time or residence time, particle size of adsorbent, solubility of substances, affinity of the solute for the adsorbent, size of the molecule with respect to the size of the pores, degree of ionization of the adsorbate molecule, pH and initial concentration.

3.4 Batch test model

To develop a model to simulate the nickel removal in batch tests carried out with pure Pumice, two main approaches can be followed: one is an approach to

representative elementary volume, while the second is a particle approach. In this chapter, both are developed, analyzing the differences.

A conceptual model representing the real test conditions is considered. In a certain volume, a fixed ratio of granular porous reactive mass and contaminant solution are put in contact. At the beginning, all of the mass of nickel is in solution at a certain initial concentration, defined as C_0, and all the reactive sites on the surface of the reactive material are available. Overtime, the concentration of nickel in solution, called C_{Ni}, decreases, while the nickel molecules are sorbed on the reactive material surface sites. Sorption terms include different phenomena: adsorption, chemisorption, absorption and ion exchange. Adsorption consists of solute clinging to the solid surface. Solute incorporation on a sediment, soil, rock surface by chemical reactions is defined as chemisorption. Absorption is a phenomenon that happens in porous materials, when the solute diffuses into the particle and is adsorbed onto the interior surface. Ion exchange occurs when a cation is exchanged with another of the same sign present on the solid surface (Fetter, 1999; Di Molfetta and Sethi, 2012).

3.4.1 Reversible linear kinetic sorption model

It can be hypothesized that the nickel removal processes on Pumice particles are sorption-based. This hypothesis can be validated by considering the chemical composition and the structure of Pumice. Hypothesizing that the rate of solute sorption is related to the amount that has already been sorbed, it is possible to consider a reversible sorption model. The model of batch tests is finalized to model batch tests and can be used for column tests. So it is important to consider the relation between the considered removal mechanism rate related to others possible and its rate in comparison to the flow rate in the column.

Of course, the term kinetic is considered by Fetter (1999) in view of the insertion of the representing equation in the advection-dispersion mono-dimensional equation. So it is necessary to compare the removal mechanism rate with the flow rate to choose the best model able to represent the relative rate.

A mechanism is defined as kinetic in that context as the opposite the of equilibrium process. The equilibrium models are based on the assumption that the rate of change in concentration due to sorption mechanisms is much greater than the change due to other processes and that the flow rate is low enough to make equilibrium achievement possible.

The phenomenon can be hypothesized as kinetic and reversible, considering that the sorption rate can be dependent on the already sorbed nickel, as can be observed in the experimental results, and the reaction time is comparable to the residence time in the column test, function of the flow rate. The first approach to model pure pumice batch tests is based on the equations 3-1 and 3-2:

$$\frac{\partial C_{Ni}}{\partial t} + \frac{\partial C^*_{Ni}}{\partial t} = 0 \qquad (3-1)$$

$$\frac{\partial C^*_{Ni}}{\partial t} = k_2 C_{Ni} - k_3 C^*_{Ni} \qquad (3-2)$$

where C_{Ni} and C_{Ni}^* are the present nickel concentration and the removed nickel mass divided by the solution volume respectively. The coefficients k_2 and k_3 can be easily found through batch tests experimental data. This approach can probably work also for batch tests with Lapillus, having a higher sorption capacity than Pumice.

3.4.2 Sorption and diffusion model

The second approach can be developed considering the pumice as an assembly of solid particles with a multi-scale structure. Therefore, the pumice is described as a spherical or cylindrical material of diameter D_p with cylindrical micro-pores of diameter d_p and length D_p (Figure 3-3).

When the material is placed in the solution, a diffusion mechanism due to the concentration gradient inside the micro pores takes place and the transport of the dissolved substance ceases when the concentration in the micro-pores is equalized. In this approach, in addition to the sorption mechanism related to the external surface of the particles, an internal sorption can be considered or not.

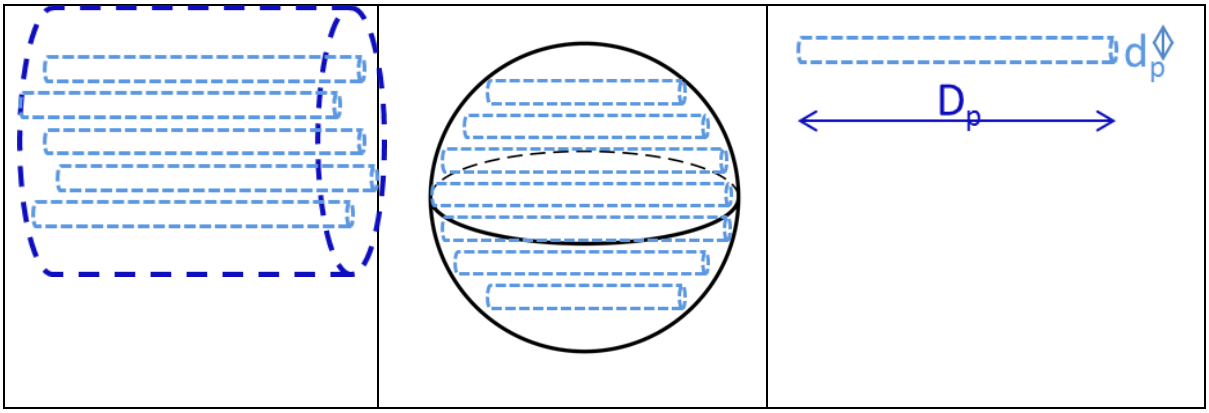

Figure 3-3 Schematic double scale structure of a pumice particle a) Cylindrical form assumption b) spherical form assumption c) geometry of an internal pore

Let us consider the partitioning of m_{Ni} mass of nickel dissolved in the external solution at initial time. Part of that mass is hypothesized instantaneously adsorbed onto the external surface of pumice particles and to be equal to $(m_{Ni})_e^s$. Some quantity noted as $(m_{Ni})_i$ will progressively diffuse into the internal pores and the remaining nickel mass in solution is represented by $(m_{Ni})_e$ term (equation 3-3).

$$m_{Ni} = (m_{Ni})_e + (m_{Ni})_e^s + (m_{Ni})_i \qquad (3-3)$$

Considering that identical phenomena occur in all inter-pores, the definition of concentration is introduced in each scale by:

$$C_e = \frac{(m_{Ni})_e}{Vol_{sol}} \qquad (3-4)$$

$$c_i = \frac{(m_{Ni})_i}{n \cdot V_{1pore}} \qquad (3-5)$$

where C_e is the concentration of nickel in external solution, c_i is the concentration of nickel in solution contained in the internal pores volume, Vol_{sol} is the volume of solution and V_{1pore} is the volume of one internal pore of pumice particle, corresponding to the one pore internal solution volume under hypothesis of totally saturation. n is the total number of internal pores defined as the number of pumice particles η times the average number of internal pores of each particle θ (equation 3-6).

$$n = \eta \cdot \theta \qquad (3-6)$$

As the experimental results have shown, the mechanisms involved depend not only on the concentration of the species but also on the mass of the reactive material; for example mechanisms where the surface interactions take place. Therefore, it will be useful to introduce normalized quantities with respect to the mass of pumice and unit surface for example. This will facilitate the generalization of the model to mixtures too.

Let us introduce a model parameter defined by the following equation 3-7:

$$M_p = \frac{m_p}{Vol_{sol}} \qquad (3-7)$$

M_p is a parameter equal to the ratio between the pumice mass m_p and the volume of solution Vol_{sol}. The pumice mass is equal to the sum of the mass of each particle or to the average mass of particles m_{p_i} multiplied by the number of pumice particles η (equation 3-8).

$$m_p = \sum m_{p_i} = \eta \cdot m_{p_i} \qquad (3-8)$$

Considering that the n number of particles of pumice can be deduced using an average diameter D_p equal to d_{50}, it can be calculated hypothesizing a spherical geometry (equation 3-9) or a cylindrical geometry (equation 3-10):

Spherical geometry:

$$n = \frac{m_p}{\rho_{app} \ \frac{4}{3}\pi \ \left(\frac{d_{50}}{2}\right)^3} \qquad (3-9)$$

Cylindrical geometry:

$$n = \frac{m_p}{\rho_{app} \ \frac{\pi}{4} \ (d_{50})^3} \qquad (3-10)$$

These relations show that there is a difference of 30% in the number of pores simply due to the assumption on the form of the grains.

3.4.2.1Sorption model

Considering the adsorbed nickel mass, it is possible to introduce the definition of S^* that is equal to the $(m_{Ni})_s$ mass of nickel adsorbed divided by the m_p pumice mass (equation 3-11).

$$S^* = \frac{(m_{Ni})_s}{m_p} \qquad (3-11)$$

To quantify S^* Langmuir (1915, 1918) equilibrium sorption isotherm can be used as given in equation 3-12:

$$S^* = \frac{\alpha\beta_0 C}{1+\alpha C} \qquad (3-12)$$

Where β_0 [-] defines the capacity of the absorbent and α [L^3M^{-1}] reflects the affinity between the absorbent and adsorbate. This model was chosen on the basis of observations of batch and column tests experimental results. S^*, contaminant adsorbed mass on reactive mass increasing with initial concentration C_0 , in

correspondence of an initial values range, and not depending on C_0 after the maximum S^* value is reached can be hypothesized. A certain removal limit, which is function of the initial concentration C_0, is in fact observed in each test. In particular, the maximum value of S^* , function of C_0 as defined in Langmuir model, is found analyzing the batch tests experimental results and considering the almost instantaneous removal effect of nickel onto the pumice external surface, developed during the first sampling time at half an hour from the start of the batch test.

Considering an instantaneous sorption on the external surface of pumice depending on the initial concentration of the solution can be taken into account using equation 3-13:

$$(S^*)_e = \frac{(m_{Ni})_e^s}{m_p} = \frac{\alpha\beta_0 C_0}{1 + \alpha C_0} \qquad (3-13)$$

To convert the $(S^*)_e$ quantity, representing the mass of nickel instantaneously sorbed on the external surface, into the correspondent concentration $(C_s)_e$, meaning the mass of nickel removed from the external solution volume by external surface of pumice, it is enough to multiply it by M_p (equation 3-14).

$$(C_s)_e = \frac{\alpha\beta_0 C_0}{1 + \alpha C_0} M_p \qquad (3-14)$$

where:

$$(C_s)_e = \frac{(m_{Ni})_s}{Vol_{sol}} \qquad (3-15)$$

The nickel concentration in the solution after this instantaneous sorption on the external surfaces becomes:

$$C_e = (C_e)_0 - (C_s)_e = C_0 - (C_s)_e \qquad (3-16)$$

To develop a model that can take into account the sorption on internal surface it is necessary to introduce the model parameters as function of unit surface. The

Langmuir equilibrium sorption isotherm is therefore represented by the following equation:

$$S^* = \frac{\alpha\beta_{S_0} S_{sur}\, C_0}{1 + \alpha C_0} \qquad (3-17)$$

where S_{sur} is the specific surface per unit mass of absorbent and β_{S_0} is defined by the equation 3-18:

$$\beta_{S_0} = \frac{\beta_0}{(S_{sur})_e} \qquad (3-18)$$

If the sorption isotherm for the external surface is aimed, it designates the external surface A_{ext} per unit mass, referred to $(S_{sur})_e$, given by equation 3-19.

$$(S_{sur})_e = \frac{A_{ext}}{\rho_{app} V_{ext}} \qquad (3-19)$$

Hypothesizing a spherical geometry, the external surface A_{ext}, the external volume V_{ext} and the specific external surface per unit mass $(S_{sur})_e$ of pumice are given by equations 3-20, 3-21 and 3-22 respectively.

$$A_{ext} = \pi\left(D_p\right)^2 \qquad (3-20)$$

$$V_{ext} = \frac{\pi}{6}\left(D_p\right)^3 \qquad (3-21)$$

$$(S_{sur})_e = \frac{6}{\rho_{app}\, D_p} \qquad (3-22)$$

For cylindrical geometry, they can be calculated using equations 3-23, 3-24 and 3-25.

$$A_{ext} = \frac{3\pi}{2}\left(D_p\right)^2 \qquad (3-23)$$

$$V_{ext} = \frac{\pi}{4}(D_p)^3 \qquad (3-24)$$

$$(S_{sur})_e = \frac{6}{\rho_{app}\, D_p} \qquad (3-25)$$

It should be noted that the specific surface is independent of the mass or the number of pumice grains in the solution.

To convert the $(S^*)_e$ quantity in the correspondent concentration, meaning the mass of nickel removed from the external solution volume by external surface of pumice per unit of external solution volume $(C_s)_e$, it is sufficient to multiply it by M_p (equation 3-26).

$$(C_s)_e = (S^*)_e M_p = \frac{\alpha\, \beta_{S_0} (S_{sur})_e\ C_0}{1 + \alpha C_0} M_p \qquad (3-26)$$

To evaluate the sorption on the surfaces of internal pores, the surface of those pores for a unit mass of pumice designated by $(s_{sur})_i$ should be considered. Therefore:

$$(s_{sur})_i = \frac{A_{1pore}}{\rho_{app} V_{ext}} \qquad (3-27)$$

If A_{1pore}designates the internal surface of one pore, it can be calculated by equation 3-28:

$$A_{1pore} = \pi d_p D_p \qquad (3-28)$$

Hypothesizing a spherical geometry, the internal specific surface of one pore per unit mass of one pumice particle is defined by equation 3-29.

$$(S_{sur})_i = \frac{6\, d_p}{\rho_{app}(D_p)^2} \qquad (3-29)$$

For cylindrical geometry, equation 3-30 can be used.

$$(S_{sur})_i = \frac{4d_p}{\rho_{app}(D_p)^2} \qquad (3-30)$$

Therefore, the mass of nickel absorbed by internal pores surface per unit mass of pumice $(c^*)_i$ is defined by equation 3-31:

$$(c^*)_i = \frac{\alpha\, \beta_{S_0} (S_{sur})_i\, c_i}{1+\alpha c_i} = \frac{\alpha\, \beta_0 \frac{A_{1pore}}{A_{ext}}\, c_i}{1+\alpha c_i} \qquad (3-31)$$

The corresponding concentration $(c_s)_i$, meaning the mass of nickel absorbed by internal pore surface of one pore per unit volume of one pore, is given by equation 3-32.

$$(c_s)_i = \frac{\alpha\, \beta_{S_0} (S_{sur})_i\, c_i}{1+\alpha c_i} \frac{m_{p_i}}{V_{1pore}} = \frac{\alpha\, \beta_{S_0} \frac{A_{1pore}}{V_{1pore}}\, c_i}{1+\alpha c_i} \qquad (3-32)$$

where the volume of one pore V_{1pore} is defined by equation 3-33.

$$V_{1pore} = \frac{\pi}{4}(d_p)^2 D_p \qquad (3-33)$$

The internal surface and the volume of one pore ratio is given by equation 3-34.

$$\frac{A_{1pore}}{V_{1pore}} = \frac{4}{d_p} \qquad (3-34)$$

Although the sorption term on one internal pore seems to be small, it could become non negligible according to the number of pores per grain.

3.4.2.2Internal diffusion model and external sorption

The variation of nickel concentration in space and time in the internal pores volume of pumice neglecting the sorption at internal pore scale is described by the Fick's lwas on molecular diffusion (Fick, 1855) 3-35:

$$\frac{\partial c_i}{\partial t} - D\frac{\partial^2 c_i}{\partial x^2} \quad = 0 \qquad (3-35)$$

Where D is the diffusion coefficient in one internal pore and c_i is the concentration of Ni at the pore scale where the diffusion takes place (Crank, 1975).
The boundary condition of this 1D problem is imposed by the concentration in the external solution. Therefore:

$$c_i(x=0,t) = c_i\big(x=D_p,t\big) = \ C_e\ (t) \qquad (3-36)$$

Where

$$C_e = C_0 - (C_s)_e - \frac{(m_{Ni})_i}{Vol_{sol}} \qquad (3-37)$$

$(C_s)_e$ is nickel mass adsorbed by pumice on its external surfaces per unit of external solution volume. The mass of nickel internally diffused $(m_{Ni})_i$ is equal to:

$$(m_{Ni})_i = V_{1pore}\frac{\int c_i\,dx}{D_p}n \qquad (3-38)$$

Where c_i is the solution of equation (3-35).
Therefore at each instant the concentration in the solution can be evaluated using equation 3-39.

$$C_e = C_0 - (C_s)_e - C_d \qquad (3-39)$$

Where the concentration C_d is defined by equation 3-40.

$$C_d = \frac{(m_{Ni})_i}{Vol_{sol}} = \frac{V_{1pore}.n.\int c_i\,dx}{Vol_{sol}.D_p} \qquad (3-40)$$

On the basis of analysis data of Mercury Intrusion Porosimetry (MIP) tests carried out on pumice samples, the number of pores contained in unit mass of pumice n_{pore} can be deduced:

$$n_{pore} = \frac{n}{m_p} \qquad (3-41)$$

Multiplying it for the mass of pumice per unit volume of external solution M_p, the number of pores per one solution volume N is obtained:

$$N = \frac{n}{Vol_{sol}} = n_{pore}\,M_p \qquad (3-42)$$

Considering that the V_{1pore} volume of one pore can be considered equal to the D_p length of the grain times the transversal section A_m, the concentration of nickel diffused into the pores can be calculated by the following equation:

$$C_d = NA_m \int c_i\,dx \qquad (3-43)$$

The number of pores per unit mass of pumice n_{pore} can be calculated using the equation 3-44.

$$n_{pore} = \frac{1}{D_p}\sum_i \frac{V_{inc.intrus.,i}}{A_i} \qquad (3-44)$$

where $V_{inc.intrus.,i}$ is the value of the incremental intrusion volume per unit mass of pumice, a data derived by MIP analysis, and A_i is the transversal area of the pore corresponding to the mean value of diameter of the range i. The transversal section A_m can be calculated by equation 3-45

$$A_m = \frac{\sum_i \frac{V_{inc.intrus.,i}}{D_p}}{n_{pore}} = \frac{\sum_i S_i * n_i}{n_{pore}} \qquad (3-45)$$

The pore transversal section A can be calculated as average value considering the total intrusion volume, as sum of $V_{pore,i}$ volume of each pore and dividing it for the product of n number of pores and D_p length of grain (equation 3-46).

$$A = \frac{\sum_n V_{pore,i}}{n\, D_p} \qquad (3-46)$$

3.4.2.3 Multiscale sorption model with internal diffusion

In the case where sorption can take place on the internal surfaces, the mass conservation equation in one pore becomes:

$$\frac{\partial c_i^s}{\partial t} - D\frac{\partial^2 c_i^s}{\partial x^2} + \frac{\partial (S)_i}{\partial t} = 0 \qquad (3-47)$$

Where c_i^s designates the concentration in the pore in presence of sorption. It varies with time due to diffusion mechanism into internal pores of pumice particles and the sorption on internal surfaces. Introducing equation (3-32) into the above equation, we obtain:

$$(1 + \frac{\alpha\, \beta_{S_0} \frac{A_{1pore}}{V_{1pore}}}{(1+\alpha c_i^s)^2})\frac{\partial c_i^s}{\partial t} - D\frac{\partial^2 c_i^s}{\partial x^2} = 0 \qquad (3-48)$$

The boundary conditions remain unchanged with respect to the case without internal sorption, though the value of C_e has implicitly changed now as the diffusion process is retarded:

$$c_i^s(x=0,t) = c_i^s\left(x=D_p,t\right) = C_e\,(t) \qquad (3-49)$$

where the nickel concentration in external solution volume C_e depends on the nickel mass adsorbed by external surface per unit of external solution volume $(C_s)_e$ and the mass diffused in the internal pores and absorbed by internal pores surface to pores per unit of external solution volume C_d^s (equation 3-50).

$$C_e = C_0 - (C_s)_e - C_d^s \qquad (3-50)$$

C_d^s can be calculated by the following equation:

$$C_d^s = NA_m \int c_i^s\, dx \qquad (3-51)$$

Same considerations can be done to apply that model to nickel removal efficiency using pure Lapillus. Of course having different structure and chemical composition the relative weight of the two main removal mechanisms, sorption and diffusion, will be different.

3.4.3 Model implementation

The model has been implemented using the values reported in Table 3-3 for the different parameters:

C_0	5 – 50 – 500 [mg/L]	Initial concentration
Dm	5e-3[mm^2/h]	Effective Diffusion Coefficient
d	0.3[mm]	Particle diameter
Mp	0.1 – 0.25 [g/mL]	LM and HM mass : volume ratio
α_0	0.6e4[-]	coefficient
α	A_p/Mp	Langmuir coefficient
β_0	66 [mg/kg]	Langmuir coefficient
β	β_0 Mp	
Npores_g	1e11 [1/g]	number of pores per unit of pumice mass
N	Npores_g*Mp	number of pores per unit of volume solution
Sm	1*(10^-6)[mm^2]	Average pore transversal section

Table 3-3 values of parameters used for model implementation

The variables used were:

$$C_s = \frac{\alpha\beta_0 C_0}{1 + \alpha C_0} M_p \qquad (3-52)$$

$$C_e = C_0 - C_s - N \cdot S_m \int_0^{D_p} c_i \, dx \qquad (3-53)$$

The geometry was defined as a one dimension domain having three points (x=0, x=d/2, x=d), introducing d equal to the d_{50} of studied pumice.

The initial condition was set as follows:

$$c_i = 0[\frac{mg}{L}] \qquad (3-54)$$

The Dirichlet Boundary Condition were set as follows:

$$c_i(x = 0) = c_i(x = d) = C_e \qquad (3 - 55)$$

3.4.3.1 Coefficients evaluation

The used values for number of pores, average pores sections and Langmuir coefficients were evaluated as will be explained.

3.4.3.1.1 Number of pores and average pores sections

The numbers of pores and average pore section obtained as defined in the model pumice description are calculated using MIP data and considering that the maximum pore diameter is about 113μm, the second is relative to the maximum pore diameter equal to 138 μm.

3.4.3.1.2 Langmuir coefficients evaluation

The evaluation of Langmuir coefficients is based on the analysis of batch tests results and experimental conditions. The latter are summarized in Table 3-6.

Tests	Reactive medium (mg)	Solution Volume (L)	initial contaminant mass (mg)		
			C_0 5 mg/L	C_0 50 mg/L	C_0 500 mg/L
LM	5400	0.054	0.27	2.7	
HM	8000	0.032	0.16	1.6	16

Table 3-4 Batch tests experimental conditions

In Table 3-4, data from batch tests carried out with Low Mass and High Mass and three different concentrations (5 mg/L, 50 mg/L, 500 mg/L) are reported.

LM			HM			
T(h)	**C(mg/L)**		**T(h)**	**C(mg/L)**		
0	5	50	**0**	5	50	500
2	2.506		**0.5**	2.1	38.6	411.1
4	2.578		**1**	1.2	37.5	408.2
8	2.578		**2**	0.9	36.1	405.1
24	2.465		**4**	0.8	34.94	398.9
48	2.395		**8**	0.78	34.5	404.7
96			**24**	0.6	34.12	403.2
120		34.82	**48**	0.6	33.92	397.3
			72	0.5	33.74	399
			144	0.5	33.22	391.1
			312	0.42	32.43	398

Table 3-5 Concentration measured during batch tests

Observing the experimental data, it is possible to make some hypotheses about removal mechanisms.

Figures 3-4 a) show the variation of nickel normalized concentration with time for all tests during the entire experimental period. Figures 3-4 b) and 3-5 and 3-6 a) and b) show the variation of concentration for each test during the first fifty hours.

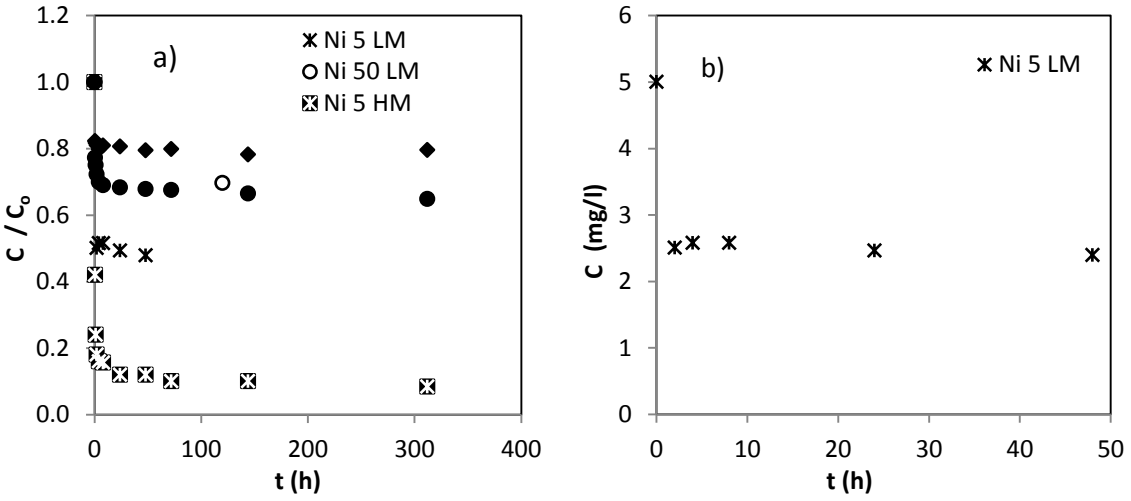

Figure 3-4 a) Nickel normalized concentration evolution for all tests and the entire duration time b) nickel concentration for batch test at LM liquid:solid ratio and 5 mg/L nickel initial concentration until 50 h

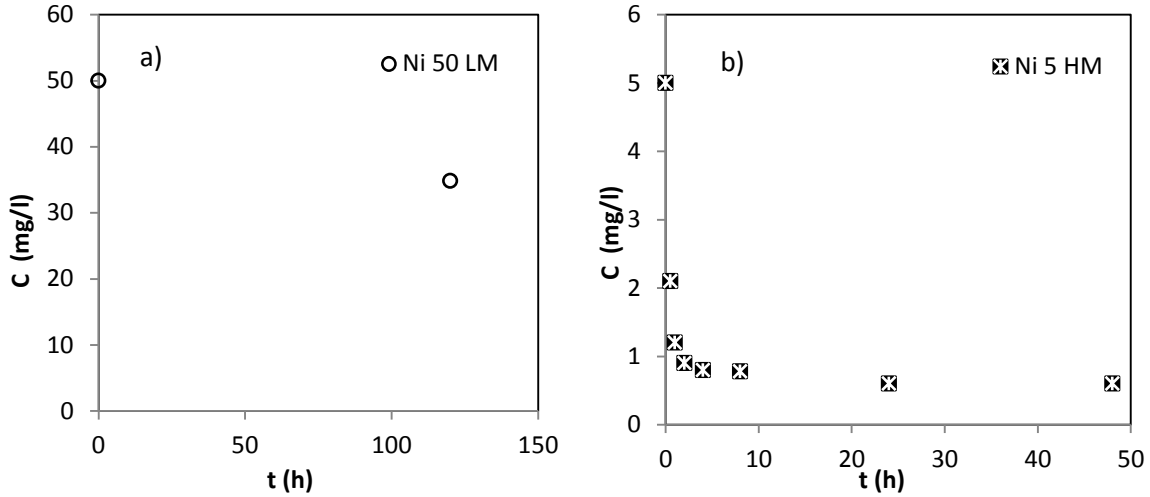

Figure 3-5 Nickel concentration for batch tests a) at LM liquid:solid ratio and 50 mg/L nickel initial concentration until 150 h and b) at HM liquid:solid ratio and 5 mg/L nickel initial concentration until 50 h

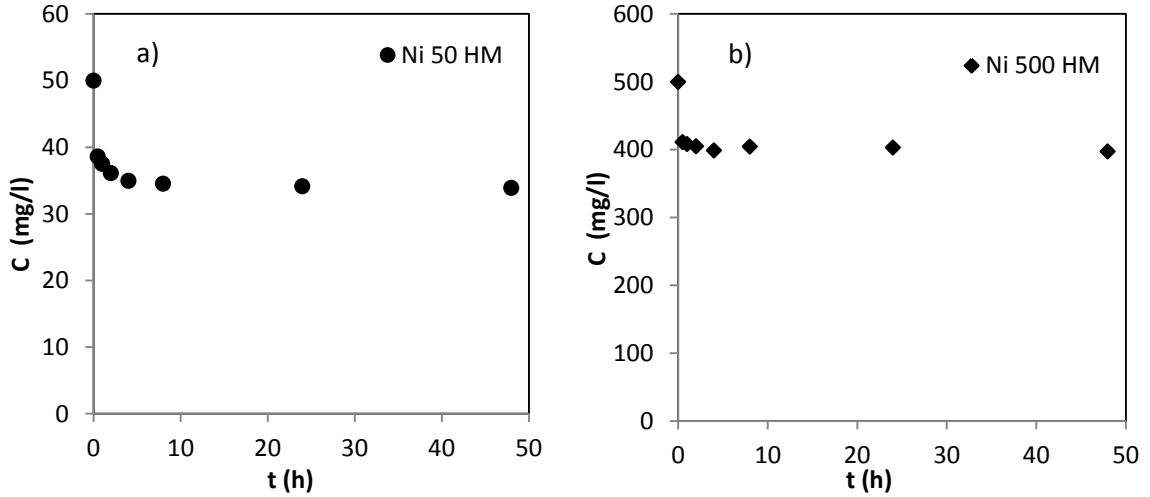

Figure 3-6 Nickel concentration for batch tests a) at LM liquid:solid ratio and 50 mg/L nickel initial concentration and b) at HM liquid:solid ratio and 5 mg/L nickel initial concentration until 50 h

It is possible to suppose that most removal effects are developed during the first eight or ten hours. In particular, an immediate mechanism and a time-dependent one can be clearly distinguished. The first one can be hypothesized as a sorption removal mechanism on external surface, considering the chemical structure and compositions of pumice. The second can be related to the high internal porosity of pumice particles and internal diffusion phenomena.

For sorption mechanisms, under this hypothesis mentioned above, the concentration values of the first time sampling for each tests need to be taken into account. Among the different relationships representing equilibrium surface reactions, that

considered to be able to model nickel sorption behavior on pumice is the Langmuir Sorption Isotherm. That relationship is described in the following equation:

$$C^* = \frac{\alpha\beta C}{1 + \alpha C} \qquad (3-56)$$

where C* is the mass of solute sorbed per dry unit weight of solid, expressed in (mg/Kg), α is an absorption constant related to the binding energy, expressed in (L/mg), β is the maximum amount of solute that can be absorbed by the solid, expressed in (mg/Kg) and C is the concentration of solute in solution.

To define the appropriate values of α and β coefficients, it is possible to consider and analyze different hypotheses, in order to establish the best one that allows the better representation of experimental results.

Since sorption is an equilibrium and instantaneous process, it is necessary to find an isotherm relationship using the residual concentration values measured at the first sampling time. To evaluate α and β coefficients for Langmuir relationship, nickel removed mass over reactive mass ratio for each solid to liquid ratio and initial concentration should be calculated and reported in a graph. The objective is in fact to find one α coefficient and one β coefficient valid for sorption mechanism between solution of nickel and pumice. The above-described model provides for the variation and influence of solid to liquid ratio, introducing a representative parameter, called M_p, as follows:

$$C_s = \frac{\alpha\beta_0 C_0}{1 + \alpha C_0} M_p \qquad (3-57)$$

M_p is equal to the solid to liquid ratio and useful to convert the C^* quantity in the correspondent concentration, meaning the nickel removed mass from the solution volume by external surface of pumice, called C_s.

Three hypothesis are the most immediate for α and β coefficients evaluation. The first is to find them graphically using the first time sampling C* values for all the tests (or without 500 mg/L initial concentration test) and in that way it is necessary to consider the error due to the different first time sampling: for LM, it is 2 hours for 5

mg/L of initial concentration and 120 hours for 50 mg/L of initial concentration; for HM, it is half an hour for all tests. The second one is to set the maximum amount of solute that can be absorbed by the solid to define β first. The third one is to find the best values of α and β to be able to better interpolate all the experimental tests (considering or not the value of 500 mg/L initial concentration test).

To evaluate the coefficients α and β_0, batch test results analysis was carried out. A maximum value of nickel mass removed to pumice mass ratio is hypothesized considering and comparing the results of batch tests with different solid to liquid ratio equal to 1mg:10 ml and 1mg:4ml.

β_0 in the Langmuir equation has the meaning of maximum contaminant mass to reactive media mass ratio. The Figure 3-7 shows the results of the batch tests carried out in terms of ratio between nickel mass removed and pumice mass as function of time. Results of four tests are reported. It is possible to hypothesize an immediate removal efficiency due to sorption and diffusion mechanisms effects time-depending for each tests.

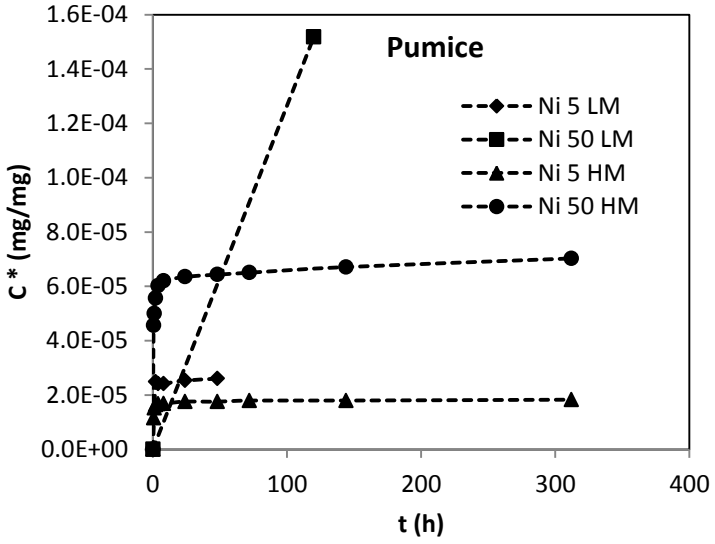

Figure 3-7 Nickel mass removed to pumice mass ratio as function of time

In Table 3-6 the values of nickel mass removed per unit of solution volume for all the tests at the first sampling time (reported) are summarized.

Cs (mg/L)			
C_0 (mg/L)	**5**	**50**	**500**
LM	2.5 (2h)	15.2 (120h)	
HM	2.9 (0.5h)	11.4 (0.5h)	88.9 (0.5h)

Table 3-6 Nickel mass removed for each bath test at the first sampling time (with time)

To evaluate the Langmuir relationship coefficients, the C* values have to be considered for all the tests. Table 3-7 reports the values of nickel removed mass to pumice mass ratio for each batch test at the defined times.

C*(mg/Kg)			
C_0 (mg/L)	**5**	**50**	**500**
LM	24.9 (2h)	151.8 (120h)	
HM	11.6 (0.5h)	45.6 (0.5h)	355.6 (0.5h)

Table 3-7Nickel removed mass and Pumice mass ratio for each batch test at the first sampling time

Let us consider the Langmuir coefficients as introduced in the model. The definition regarding them needs to be introduced. In particular, the α value used is defined as α_0 value, equal for all the tests carried out with solution of nickel and pumice and expressed in (L/mg) multiplied by M_p solid : liquid ratio (g/mL). β introduced in the model is β_0 that as defined above represent the maximum amount of solute that can be absorbed by the solid and this is expressed in (mg/Kg).

The calculated values to be used for definition by graphic methods are reported in the following table:

C_0/C^*(Kg/L)			
C_0 (mg/L)	**5**	**50**	**500**
LM	0.200	0.329	
HM	0.431	1.096	1.406

Table 3-8 values used to evaluate Langmuir coefficient

The Figures 3-8 a) and b) and 3-9 report the data as it should be plotted to find the Langmuir coefficients for the LM tests and for HM tests considering two or three initial concentrations.

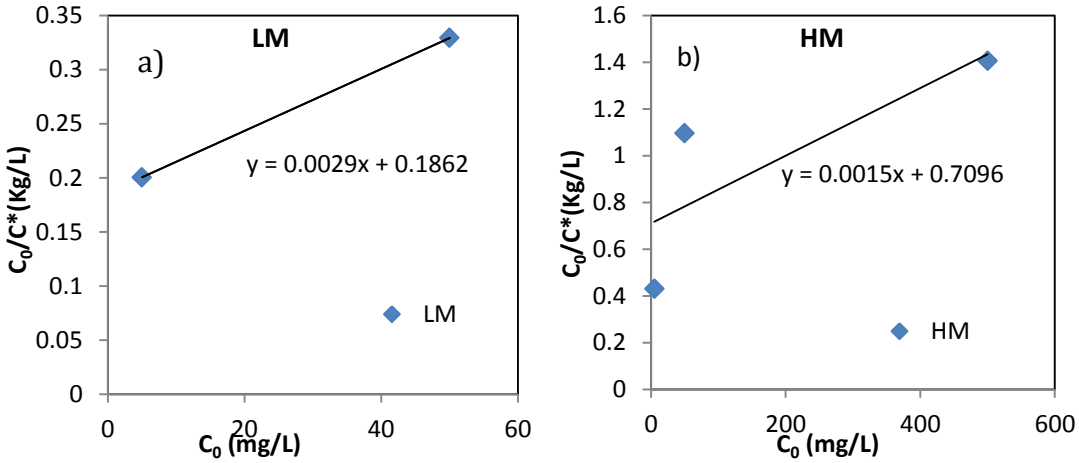

Figure 3-8 C_0/C^* as function of C_0 for a) LM tests and b) HM tests

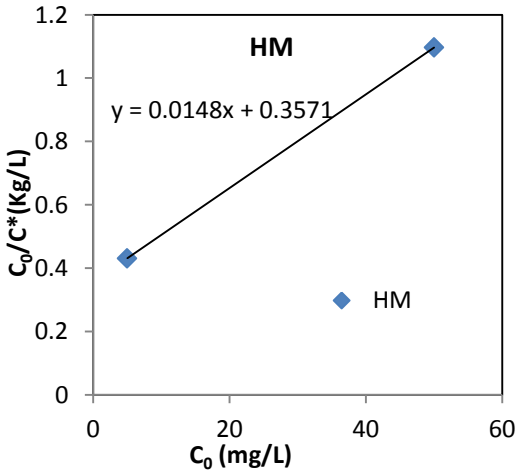

Figure 3-9 C_0/C^* as function of C_0 for HM tests considering tests with nickel at 5 and 50 mg/L initial concentration

Table 3-9 reports the values of α and β coefficients as calculated under the three above-mentioned hypotheses.

Hypoth.	α_0	β (mg/kg)	comments
1st	1E+03	3.45E-04	based on LM tests
	5E+02	6.67E-04	based on HM test (5 and 50 ppm init. Conc.)
	1E+04	6.76E-05	based on HM test (all init. Conc. tests)
	1E+03	5.06E-04	average related to tests with 5 and 50 ppm init.conc. LM and HM both)
	4E+04	3.60E-04	average related to all the tests (5, 50 and 500 ppm init.conc, LM and HM both)
2nd	3E+04	1.16E-05	β defined on the base of C* related to 5 HM test
	6E+04		
3th	5.9E+03	2.06E-04	optimization

Table 3-9 Langmuir coefficients used for the simulation

The combination of Langmuir coefficient values that better represent the experimental data of each test, concerning the first sampling time, is reported in figure 3-10 and corresponds to that reported in table 3-9 as second (α_0=5E+02 and β =6.67E-4 mg/Kg)

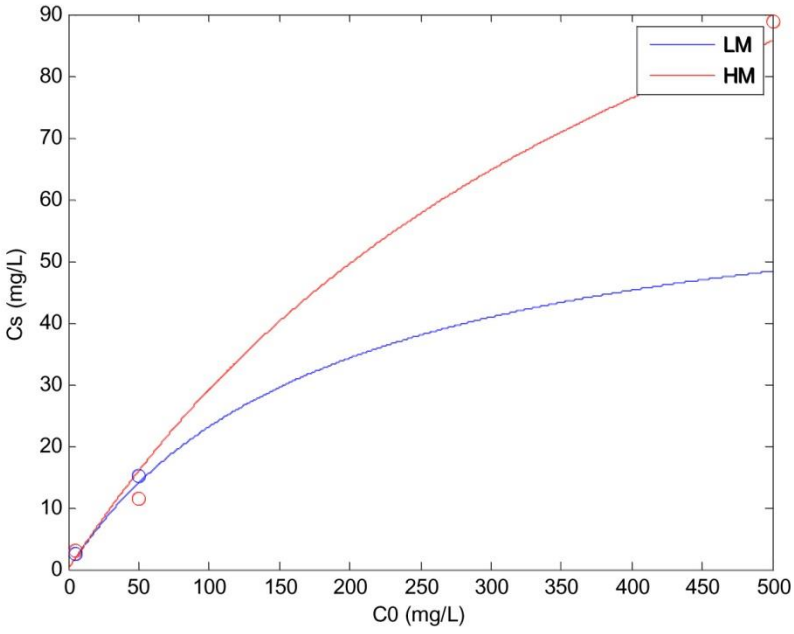

Figure 3-10 C_s as function of C_0 using Langmuir model

3.4.4 Sensitivity analysis

A global sensitivity analysis of model output was carried out to study the global importance of each input factor of the model to the output of the model. The method utilized was based on the Hybrid Random Balance Design – Fourier Amplitude Sensitivity Test (Hybrid RDB-FAST or HRF) (Saltelli et al. 1999, Tarantola et al. 2006). The value of coefficient of variance given as input for the analysis was for each input factor equal to 0.5. For Dm, d=D_p, β_0, α_0, Npores_g, Sm (A_m) the average value used is the same as the model input.

In Figures 3-11 to 3-16 the output of sensitivity analysis of the model are shown for each condition of batch tests carried out. As can be observed, the Sm parameter seems to influence the most the results if LM conditions with solution of nickel at 5 mg/L of initial concentration are used. For the other two initial concentrations (50 and 500 mg/L) of nickel, Npores_g, d and Sm have the highest influence in both LM and HM conditions.

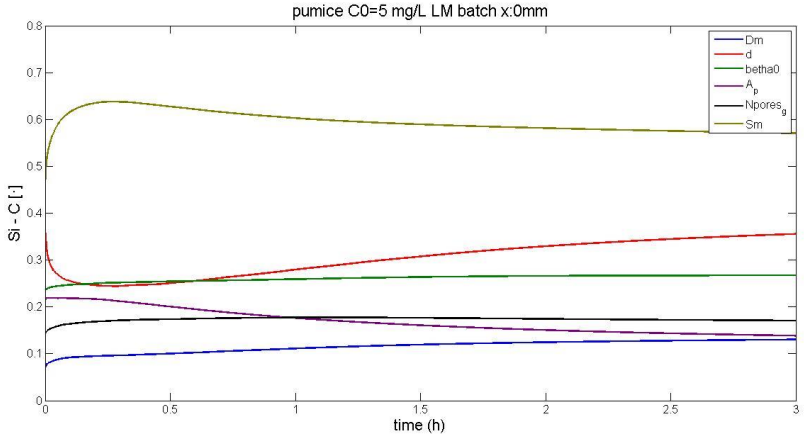

Figure 3-11 sensitivity analysis output for LM batch test model using solution of nickel at 5 mg/L C_0

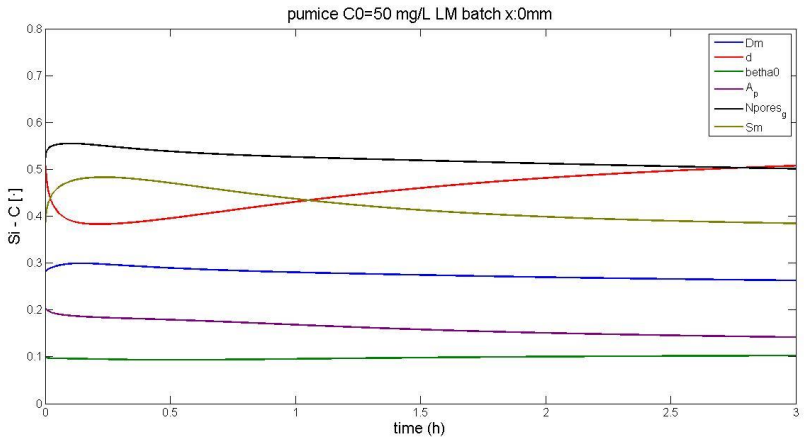

Figure 3-12 sensitivity analysis output for LM batch test model using solution of nickel at 50 mg/L C_0

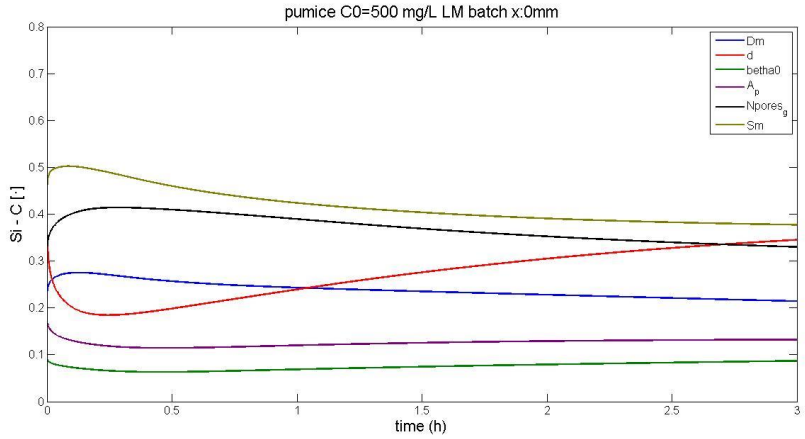

Figure 3-13 sensitivity analysis output for LM batch test model using solution of nickel at 500 mg/L C_0

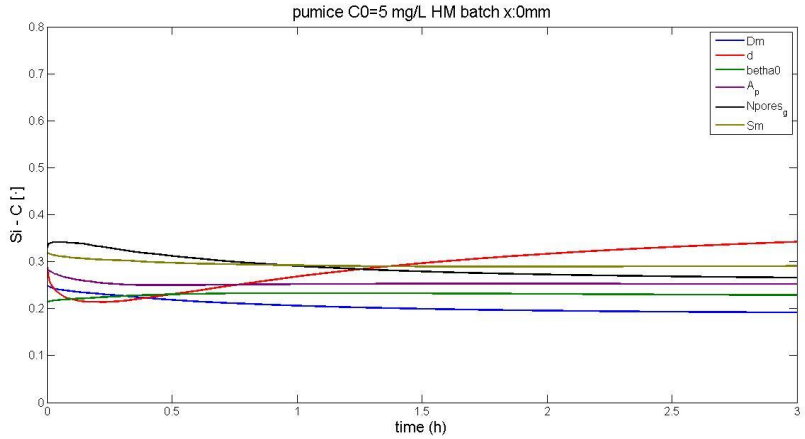

Figure 3-14 sensitivity analysis output for HM batch test model using solution of nickel at 5 mg/L C_0

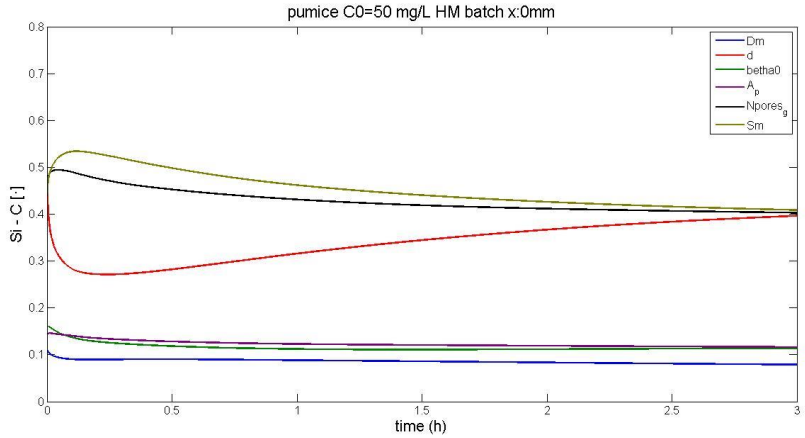

Figure 3-15 sensitivity analysis output for HM batch test model using solution of nickel at 50 mg/L C_0

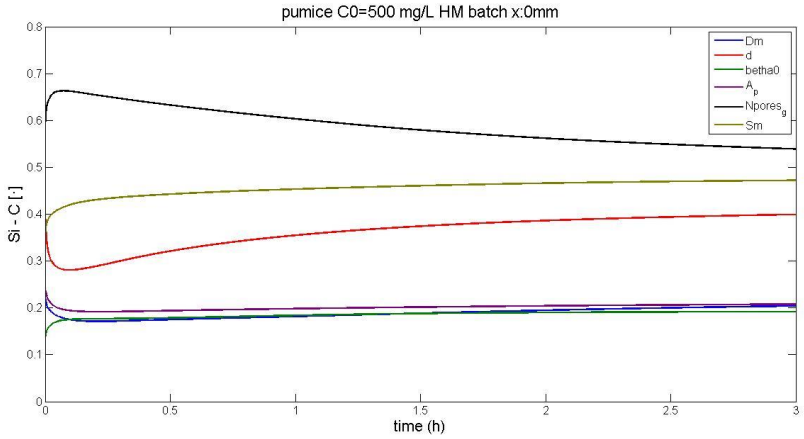

Figure 3-16 sensitivity analysis output for HM batch test model using solution of nickel at 500 mg/L C_0

3.4.5 Contribution to column test modelling using double porous materials

To develop a model to simulate nickel removal by pumice, two different choices can be made. It is possible to use a multi-scale model introducing the particle approach model into the column conceptual model or a representative elementary volume approach can be developed on the basis of that of the batch tests and considering the experimental results.

Equation 3-58 represents the 1D mass balance equation (Bear, 1979). for Ni in its general form applied at the external pore scale:

$$\frac{\partial C}{\partial t} - \frac{\partial}{\partial x}\left(D_L \frac{\partial C}{\partial x}\right) + \frac{\partial (v \cdot C)}{\partial x} + \sum_k \dot{R}_k = 0 \qquad (3\text{-}58)$$

D_L and v are the longitudinal dispersion coefficient and the velocity respectively. R_k represents the rate of mass change due to mechanism k.

On the basis of the consideration about batch and column tests experimental results, it is possible to hypothesize what Ni removal mechanisms take place. During the first interaction time, the immediate removal mechanism is probably attributable mostly to sorption process onto the external Pumice surface (k=1).

After the flow of several pore volumes have flowed, the pumice reactive sites onto surface seem completely occupied and the input constant concentration C_0 cannot be reduced anymore. It is possible to observe effects of a non-equilibrium removal mechanism, too, leading to a further decrease of the residual concentration. This second process could be attributable to the Ni concentration gradient between the inter-grains flowing water and internal pore stagnant water. It can take place after water has occupied at least part of the internal pores. The concentration gradient becomes the driving force of the molecular diffusion of nickel between the water outside and inside the pumice pores. It is possible to observe that at each of the considered column lengths, the concentration values tend to an equilibrium concentration value C_{eq}, that may vary slowly with time.

It is possible to identify a zone where the residual concentration rate decreases towards a steady-state zone which implies:

$$\frac{\partial C}{\partial t} + \sum_k \dot{R}_k = 0 \qquad (3-59)$$

Considering that only one retention mechanism is active at this stage, it is possible to introduce the equation 3-60:

$$\dot{R}_2 = -\alpha(C - C_e) \qquad (3-60)$$

where C_e is the equilibrium concentration which may change during the process. For C_e evaluation it is possible to refer to the observation about batch tests results where $C_e=0.7C_0$ relation has been found. Of course, this variable is function of the water occupying the internal pore and of the external concentration, so it increases progressively.

3.5 Modelling of nickel removal efficiency using pure ZVI

To model the Nickel removal efficiency of pure ZVI observed in batch tests, a representative elementary volume approach was used. On the basis of the literature studies about heavy-metal removal using ZVI and the experimental results of batch

tests and column tests performed with pure ZVI, a reversible kinetic sorption model was tested to simulate the experimental results.

3.5.1 Batch tests model

The batch conceptual model is the same used for batch tests based on pure pumice use, considering the variation of solid to liquid ratio and the nickel initial concentration. This approach to model the nickel removal efficiency observed in pure ZVI batch tests is based on the equations 3-1 and 3-2

The coefficients are easily deduced by experimental batch tests results analysis.

The results of simulation and the experimental data are reported in the figures 3-18, 3-19, 3-20 and 3-21.

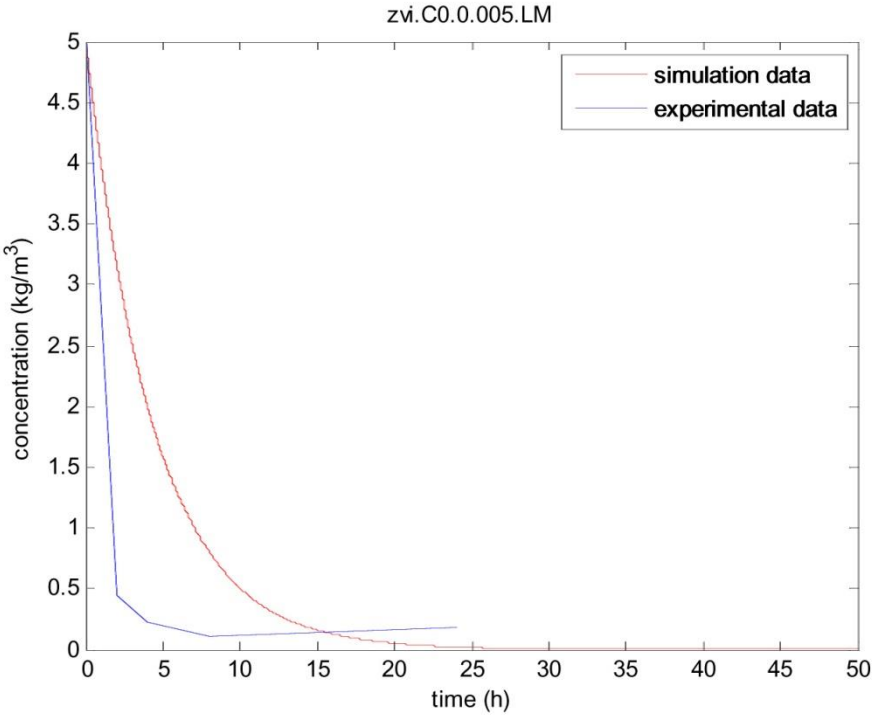

Figure 3-17 Experimental data and simulation output for LM batch test using pure ZVI and solution of nickel at 5 mg/L initial concentration

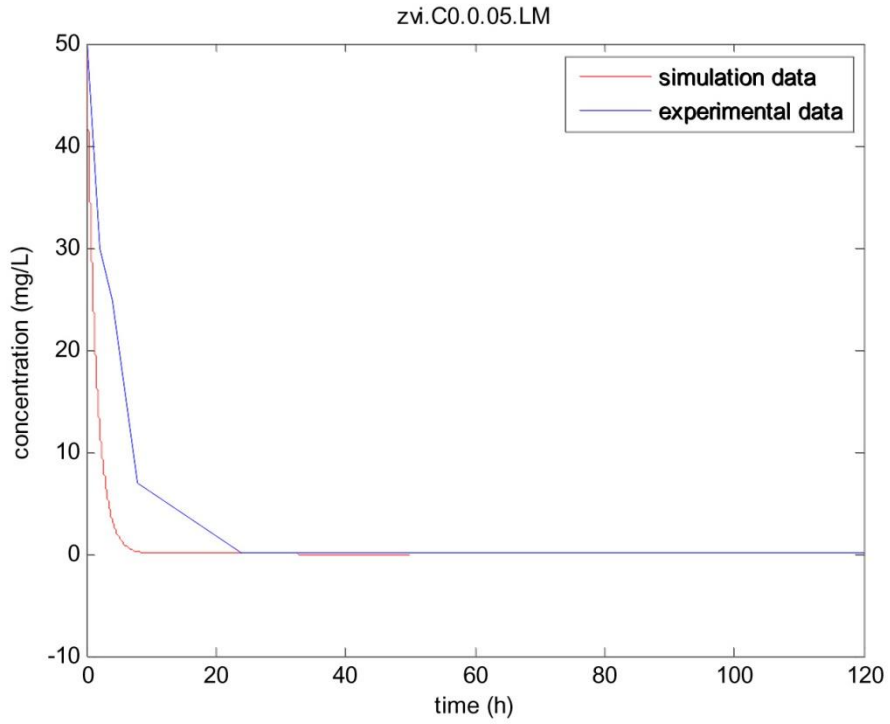

Figure 3-18 Experimental data and simulation output for LM batch test using pure ZVI and solution of nickel at 50 mg/L initial concentration

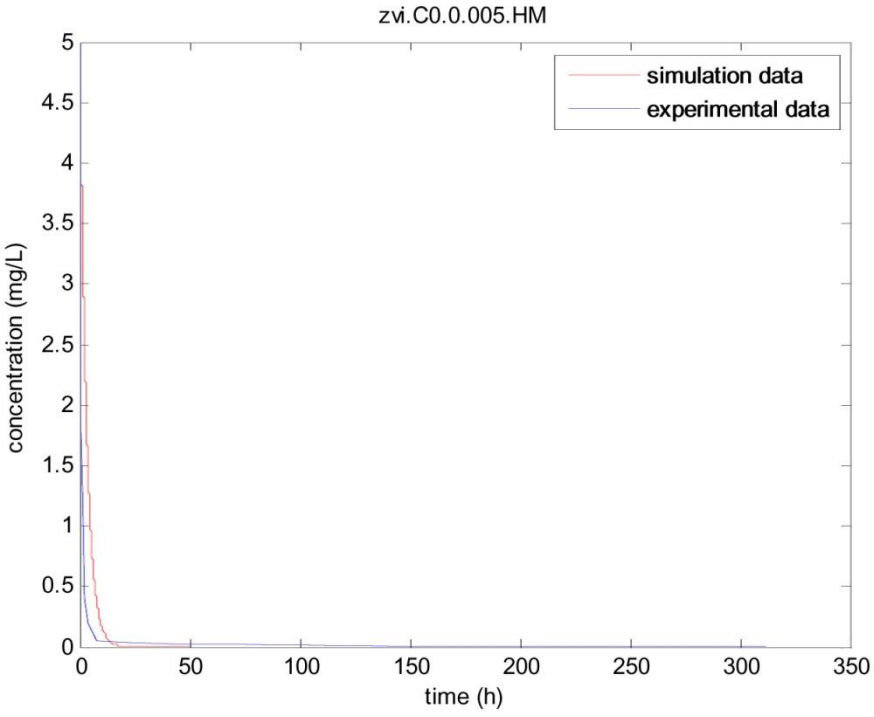

Figure 3-19 Experimental data and simulation output for HM batch test using pure ZVI and solution of nickel at 5 mg/L initial concentration

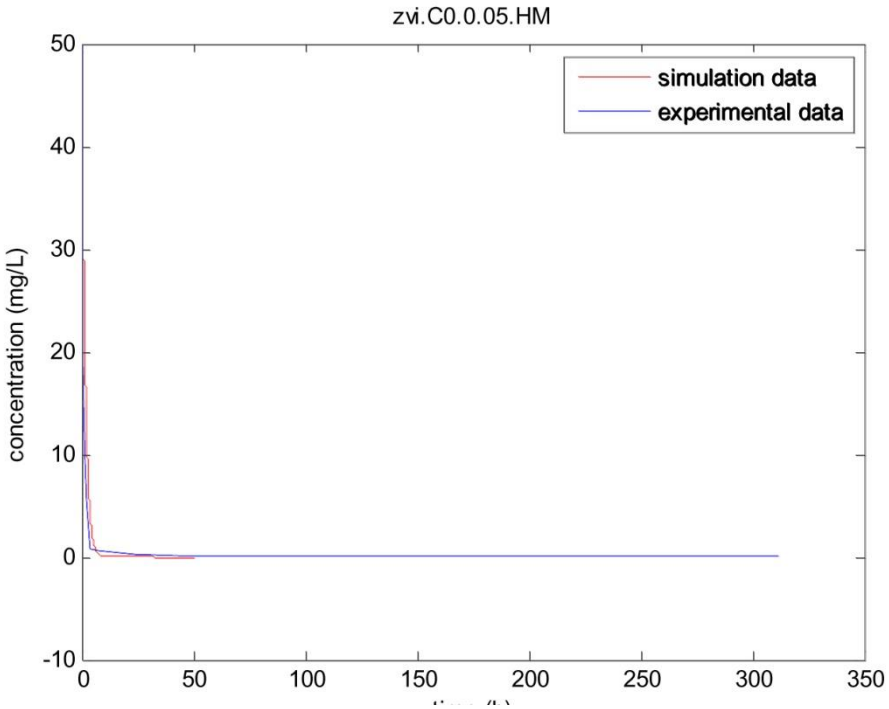

Figure 3-20 Experimental data and simulation output for HM batch test using pure ZVI and solution of nickel at 50 mg/L initial concentration

3.5.2 Contribution to column tests modelling using pure ZVI

The column test model is based on the 1D mass balance equation for nickel in its general form introducing as reaction term the reversible kinetic sorption term. While in pure pumice or lapillus column tests no permeability variation with time has been observed, in the other column tests carried out with ZVI : Pumice (or Lapillus) mixtures and, especially, pure ZVI, it is an issue. For this reason, a coupled model considering nickel removal efficiency and hydraulic behavior was developed. The two phenomena, in fact, influence each other. Really schematically, the physic-chemical reactions, that can take place in the column, can decrease the void volume available for the contaminant solution flow. This can mean a decrease in porosity and consequently of permeability. The nickel removal efficiency, as with the removal efficiency for the other heavy metals, can change in the same time as that of the hydraulic behavior because firstly the physic-chemical phenomena that determine the void reduction for fluid phase lead to a first main use of removal capacity, but also it can be influenced by the consequent residence time decrease and pore water pressure increase. For all these reasons, a chemical-hydraulic coupled model has

been developed. That for pure Pumice (or Lapillus) column tests can be considered as a particularization of the general model, considering that in these tests no permeability change has been measured. Not changing the external porosity, the residence time does not change. To have a more complete model considering all the possible mechanisms, the internal porosity is taken into account at the beginning. It can be a factor of removal mechanisms in double porous materials. Of course this issue is not relevant for permeability, so the hydraulic model is not influenced by it in pure pumice column test simulation. In mixtures column tests the internal porosity can play a role, probably minimal, of partial storage of iron corrosion products and precipitation.

For the column tests realized with ZVI, the permeability variation is a really important issue. However, the introduction of that model consists of a particularization of the more general ZVI : Pumice mixtures column model.

3.6 Modelling of batch tests using ZVI : Pumice (or Lapillus) mixtures

The model of nickel removal efficiency of ZVI : Pumice (or Lapillus) mixtures is based on the combination of the two models simulating the nickel removal efficiency using pure ZVI and pure Pumice, introducing each effect as a proportion of the considered weight ratio. In this case, two different possibilities can be chosen. It is possible to simulate that kind of batch test using for Pumice the reversible kinetic sorption model or the sorption-internal diffusion model. To introduce the ZVI influence on nickel removal efficiency the model based on reversible kinetic sorption was used, as for pure ZVI tests.

3.7 Conclusions

In this chapter, nickel contaminant removal efficiency observed in batch tests using pure Pumice, pure ZVI and ZVI:Pumice were considered and modelled.

To simulate the nickel removal in batch tests carried out with pure Pumice, two main approaches were followed: one is an approach to representative elementary volume, while the second is a particle approach.

For the first one, a conceptual model consisted on considering in a certain volume, a fixed ratio of granular porous reactive mass to contaminant solution put in contact. The nickel concentration at the beginning of test C_0 decreased with time, while the nickel molecules were sorbed on the reactive material surface sites. A reversible linear kinetic sorption model was used, considering the sorption-based removal process as studied in the literature. The second approach was developed considering the pumice as an assembly of solid particles with a multi-scale structure. Therefore, the pumice is described as a spherical or cylindrical material of diameter D_p with cylindrical micro-pores of diameter d_p and length D_p.

When the material is placed in the solution, a diffusion mechanism due to the concentration gradient inside the micro pores takes place and the transport of the dissolved substance ceases when the concentration in the micro-pores is equalized. In this approach, in addition to the sorption mechanism related to the external surface of the particles, an internal sorption can be considered or not.

To model the nickel removal efficiency of pure ZVI observed in batch tests, a representative elementary volume approach was used. Considering the literature studies on heavy-metal removal using ZVI and the experimental results of batch tests and column tests realized with pure ZVI, a reversible kinetic sorption model was tested to simulate the experimental results.

The model based on reversible linear kinetic sorption seemed to be able to represent more appropriately the experimental results obtained from tests on pure ZVI than those on pure pumice. These letters are better modelled considering external sorption and internal diffusion.

A first step of modelling the mixtures was performed and it should be study in depth. However, it seemed that a simple combination or addition of the models developed for each pure reactive material is not appropriate to simulate the experimental

results obtained from tests on mixtures. If it is true, it could mean that the effects of removal processes developed by each reactive material of the mixture are not overlapping.

It was In Chapter 4, the results of some column tests performed using ZVI:Pumice mixtures and pure ZVI, performed by previous Ph.D. student are taken into account and re-analyzed, to introduce the experimental results in view of the development of column test modelling.

4 Long-term removal efficiency and hydraulic behaviour of ZVI:Pumice granular mixtures: general review and modelling

4.1 Introduction

In this chapter, an analysis of the results of column tests using ZVI and ZVI:Pumice mixtures to remediate heavy-metal contaminated groundwater, carried out by the previous Ph.D. students (Rigano, 2007; Suraci, 2010; Bilardi, 2011), is proposed in order to collect useful information for the development of a coupled removal-hydraulic model. In fact, as studied in Chapter 3, a non-equilibrium sorption model can be used to simulate batch tests performed using pure ZVI and pure Pumice.

The dissertation is focused on the tests carried out using synthetic solutions contaminated by nickel, because for this element the availability of column tests and, consequently, of studies on the influence control variables is greater. For each column test, nickel concentration, pH, Eh, temperature and permeability values are available for different sampling times and ports.

Furthermore, one column test was performed during this Ph.D. course to test the Zinc removal efficiency of 50:50 ZVI:Pumice w.r. mixture and to compare it to the previously tested 30:70 ZVI:Pumice w.r. mixture performance.

4.2 Pure Pumice, Pure ZVI and ZVI:Pumice granular mixtures column tests general review

Considering that nickel concentration values are known for different distances of column length and for different times, it is possible to calculate the nickel mass retained by the reactive material placed between two sections of the column length. To calculate the nickel mass that has been retained or removed by the reactive medium, a mass balance equation was used. It can be defined as the point placed x_i along the column, where index i varies between zero and the n total number of the sampling ports, and t_j time, where index j is for the progressive number of sampling times. nickel mass retained in a column sector placed between x_i and x_{i+1}, during the interval between t_j and t_{j+1}, under the hypothesis of homogeneous distribution of

nickel mass retained in the transversal section S, can be calculated by the following equation (4-1) :

$$M_{r\,j-j_{+1}} = M_{in\,j-j_{+1}} - M_{out\,j-j_{+1}} \tag{4-1}$$

where the M_r is the retained mass between times j and j+1, M_{in} is the mass input through x_i section between times j and j+1 and M_{out} is the mass in output from the x_{i+1} section between times j and j+1. The equation (4-1) is more appropriate as the considered time is longer, because the possible contaminant mass in solution becomes negligible compared to that retained or removed by the reactive material.
The nickel mass flowing through the transversal section x_i during a Δt_j interval can be calculated by the following equation (4-2):

$$M_{x_i,\Delta t_j} = \frac{\left(C_{x_i,t_j} + C_{x_i,t_{j-1}}\right)}{2} \cdot \left(t_j - t_{j-1}\right) \cdot v \cdot S_{x_i} \tag{4-2}$$

where $C_{xi,\,tj}$ is the concentration measured at x_i, the i^{-th} point along the filter length and t_j, the j^{-th} time, v is the flow velocity and S_{xi} the transversal section corresponding to the i^{-th} point along the filter length. The nickel mass retained by the reactive material contained in Δx_i column sector during a Δt_j interval can be calculated through the following equation (4-3):

$$M_{r,\Delta x_i,\Delta t_j} = M_{x_{i-1},\Delta t_j} - M_{x_i,\Delta t_j} \tag{4-3}$$

The cumulative nickel mass retained by the Δx_i column sector until t_j time can be calculated as the following equation (4-4):

$$M_{r,\Delta x_i,t_j} = \sum_j M_{r,\Delta x_i,\Delta t_j} \tag{4-4}$$

The total mass retained by the entire filter length during time is given by equation (4-5):

$$M_{r,t_j} = \sum_i^n \sum_j M_{r,\Delta x_i,\Delta t_j} \tag{4-5}$$

The mass of nickel retained by unit of reactive material mass is calculated by dividing it by the mass of reactive material contained in the correspondent filter length.

4.2.1 Pure ZVI column tests

Column tests using pure ZVI and carried out by the previous Ph.D. students (Rigano, 2008; Suraci, 2010; Bilardi, 2011) are reported in table 4-1. Mass of reactive material, filter thickness, initial contaminant concentration, flow velocity, porosity, residence time and test duration are defined for each test. The φ porosity was calculated through equation (4-6):

$$\varphi = 1 - \frac{\frac{W_{ZVI}}{\rho_{ZVI}}}{V_{ic}} \qquad (4\text{-}6)$$

where the W_{ZVI} is the mass of Zero Valent Iron, ρ_{ZVI} is the ZVI density and V_{ic} is the internal volume of the column. The initial value of residence time was calculated by using the following equation (4-7):

$$\mathrm{T_{res}} = \frac{\mathrm{PV}}{\mathrm{v \cdot S}} \qquad (4\text{-}7)$$

where v is the flow velocity, S is the transversal section and PV is the initial value of Pore Volume calculated through equation (4-8):

$$PV = \varphi \cdot V_{ic} \qquad (4\text{-}8)$$

Reactive media	Mass (gr) and filter thickness (cm)	Initial contaminant concentration (mg/L)	Flow velocity (mm/min)	Porosity φ(%)	Residence time
Fe^0 (1)	240 (-3)	Ni 50	0.276	44	0.8
Fe^0 (2)	1680 – 19.25	Ni 40	0.055	48	32
Fe^0 (2)	1680 – 22.3	Ni 40	1.382	48	1.3
Fe^0 (2)	1680 – 22.3	Ni 8	1.382*	48	1.3
Fe^0 (2)	1680 – 22.3	Ni 8	0.055	48	32
Fe^0 (2)	1680-22.25	Ni 95	1.382	48	1.3
Fe^0 (2)	240 - 3	distilled water	0.276	44	0.8

Table 4-1 pure ZVI column tests carried out by the previous Ph.D. students

(1) Suraci (2010), (2) Bilardi (2011)

*test interrupted because of column clogging

Two column tests using pure ZVI and a contaminant solution of nickel at initial contaminant concentration of 40 mg/L were carried out using two flow velocities: one of 0.055 mm/min and one of 1.382 mm/min. The distribution of nickel removed along the filter with time, pH, Eh values and permeability evolution were considered. In Figure 4-1 – 4-3 a) and b), the nickel removed mass by ZVI unit mass are reported for different sectors of filter lengths at different times corresponding to the same input mass for both flow rate tests.

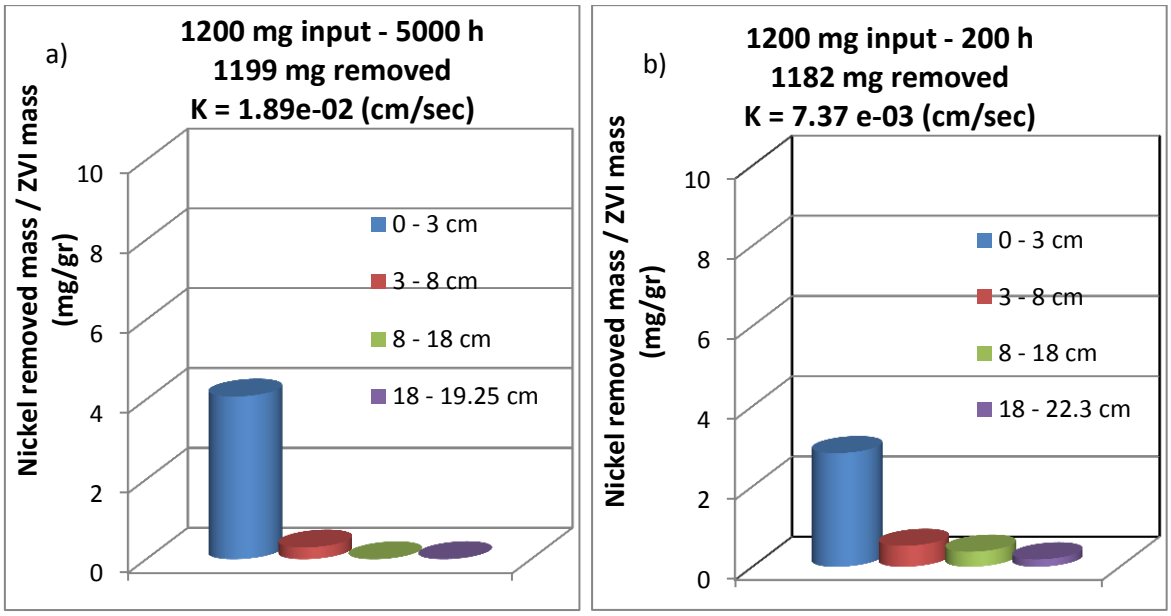

Figure 4-1 Nickel removed mass by ZVI a) in 0.055 mm/min test after 5000 h and b) in 1.382 mm/min test after 200 h

The two column tests were carried out with the same ZVI mass and almost the same filter length - they allow different initial residence time: for the slowest test it is about 22 hours, for the fastest it is about 1 hour. This means that to compare results relative to the same residence time, data obtained at the outlet of the fastest test and results relative to 1 cm from the bottom of the slowest test have to be taken into account.

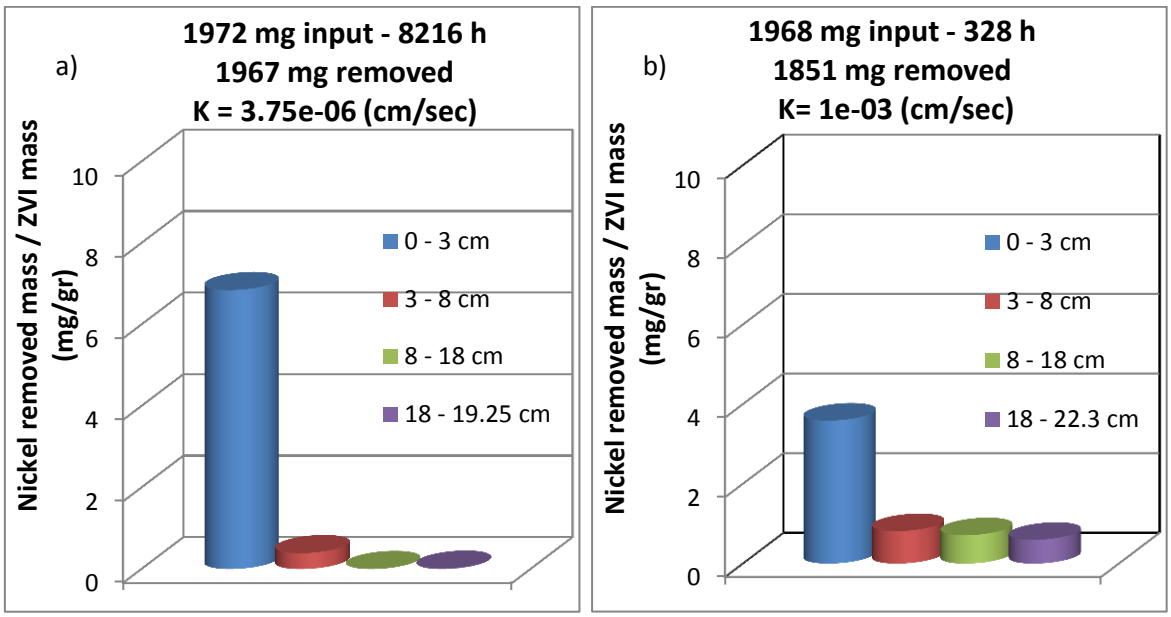

Figure 4-2 Nickel removed mass by ZVI a) in 0.055 mm/min test after 8216 h and b) in 1.382 mm/min test after 328 h

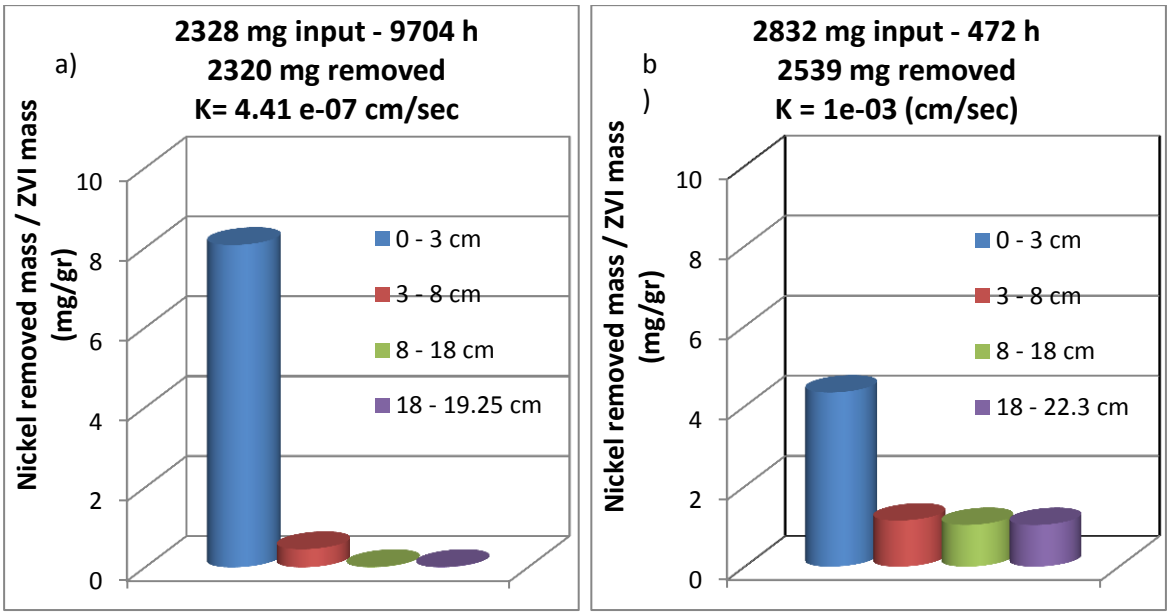

Figure 4-3 Nickel removed mass by ZVI a) in 0.055 mm/min test after 9704 h and b) in 1.382 mm/min test after 472 h

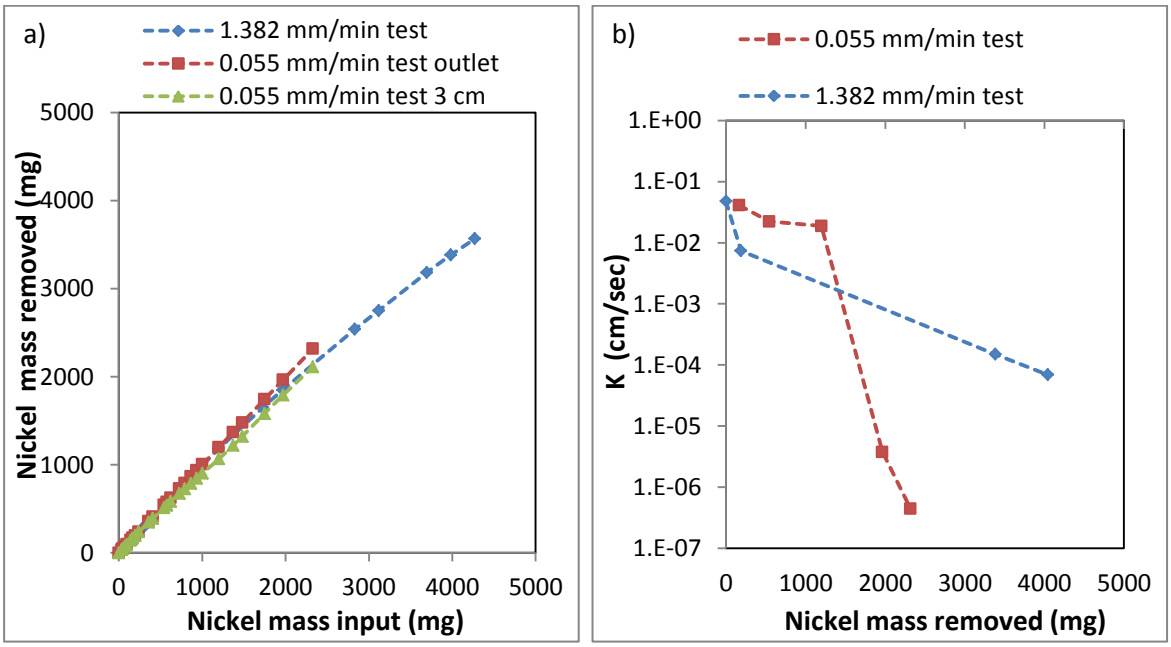

Figure 4-4 a) Nickel mass removed in function of nickel mass input; b) hydraulic conductivity as function of nickel mass removed

In fact, the evolution of the nickel removed mass as function of nickel input mass in the entire length of the column test performed with the highest velocity, and that removed in 3 cm of the slowest are comparable, as can be observed in Figure 4-4 a) (3 cm is the shortest filter length for which data are available for the slowest test). Furthermore the greater part of the removal capacity is performed by the first 3

centimetres in the slowest test, consequently if the total removed mass is calculated, the trend of removed mass at outlet is overlapped with that of three centimetres.
In term of hydraulic behaviour, a difference can be observed. Permeability evolution is reported as function of the nickel removed mass in Figure 4-4 b). A light permeability loss can be observed for the fastest, while no significant changes are observed for the slowest test until around to 1000 mg of nickel mass removed. After this, the permeability evolution slope is higher for the slowest test than that of the fastest one. As can be deduced from observation of Figure 4-1, the contact time for nickel removal seems to be an important parameter, considering that in the slowest test almost all the input mass is removed within 3 centimetres, while for the fastest test the total filter length is not enough to remove entirely the input mass, after a certain time.

4.2.2 ZVI-Pumice column tests

In Table 4-2 the characteristics of column tests performed using ZVI:Pumice mixtures to investigate their long-term nickel removal efficiency and hydraulic behaviour are reported. ZVI:Pumice weight ratio, flow velocity and nickel(Ni) initial concentration ere varied to study their influence. They were carried out by the previous Ph.D. students (Rigano, 2007; Suraci,2011; Bilardi,2012).

Reactive media	Fe^0 and Pumice mass(gr)	Contaminant and initial concentration (mg/L)	Flow velocity (mm/min)	Initial porosity n (%)	Residence time
Fe^0 – Pum. 10:90 w.r. (1)	153 - 1374	Ni 50	0.276	36	21.5
Fe^0 – Pum. 30:70 w.r. (1)	244 - 570	Ni 50	0.276	44	13.3
Fe^0 – Pum. 50:50 w.r. (1)	530 - 530	Ni 50	0.276	44	13.1
Fe^0 – Pum. 30:70 w.r. (2)	240-560	Ni 40	0.055	44	71.4
Fe^0 – Pum. 30:70 w.r. (2)	240-560	Ni 8	1.382	44	2.9
Fe^0 – Pum. 30:70 w.r. (2)	240-560	Ni 8	0.276	46	14.8
Fe^0 – Pum. 30:70 w.r. (2)	240-560	Ni 8	0.055	45	71.4
Fe^0 – Pum. 30:70 w.r. (2)	240-560	Ni 40	1.382	45	2.9
Fe^0 – Pum. 30:70 w.r. (2)	240-560	Ni 95	1.382	45	3
Fe^0 – Pum. 30:70 w.r. (2)	240-560	Ni 95	0.055	46	73

Table 4-2Characteristics of column tests performed using ZVI:Pumice mixtures

(1) Suraci (2010), (2) Bilardi (2011)

4.2.2.1Consideration about weight ratio influence

Three column tests were carried out by the previous Ph.D. student, Paolo Suraci, to investigate the influence of the weight ratio on the nickel removal efficiency of ZVI-Pumice mixtures (Calabrò et al., 2012). Results are here re-proposed and reviewed to finalize the observations and analysis to develop the results modelling step. In Figures 4-5 – 4-7, results of 10:90, 30:70 and 50;50 weight ratios are reported respectively. In the a) figures represent the results relative to the interaction time from the beginning to about 1440 hours after, the b) figures represent the time afterwards until the end of the tests. The three tests were realized under a constant

flow rate input of the contaminant solution equal to 0.276 mm/min. The column used to test the 10:90 weight ratio was 100 cm in height and it had a 5 cm diameter. The columns used to test the 30:70 and the 50:50 weight ratios were 50 cm in height and they had a 5 cm diameter.

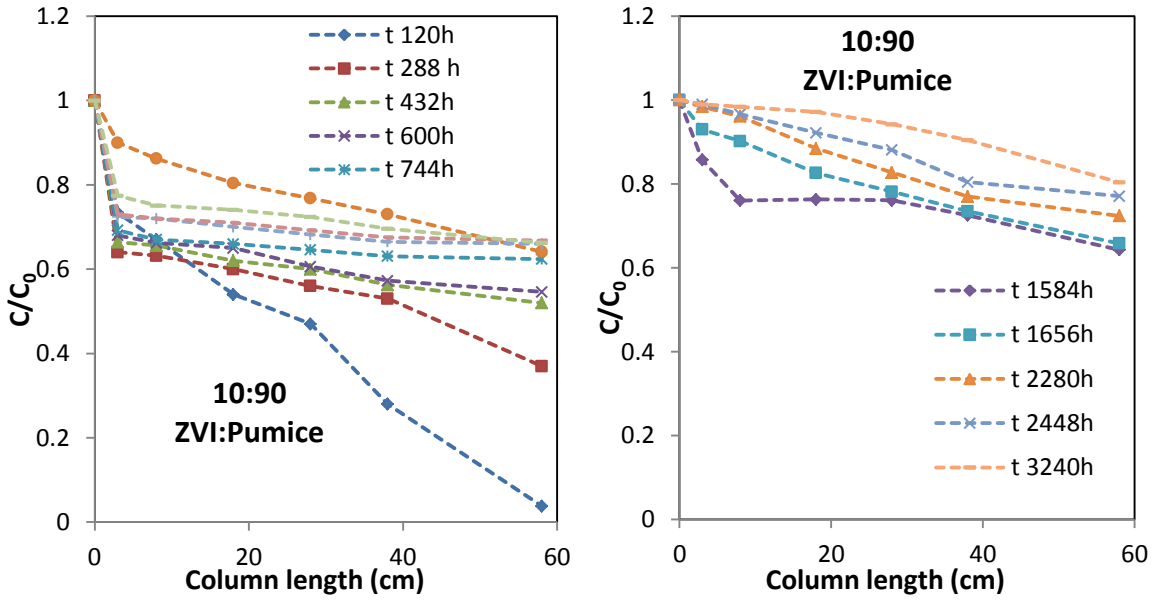

Figure 4-5 normalized concentration of nickel in 10:90 w.r. ZVI:Pumice, C0=50ppm, f.r=

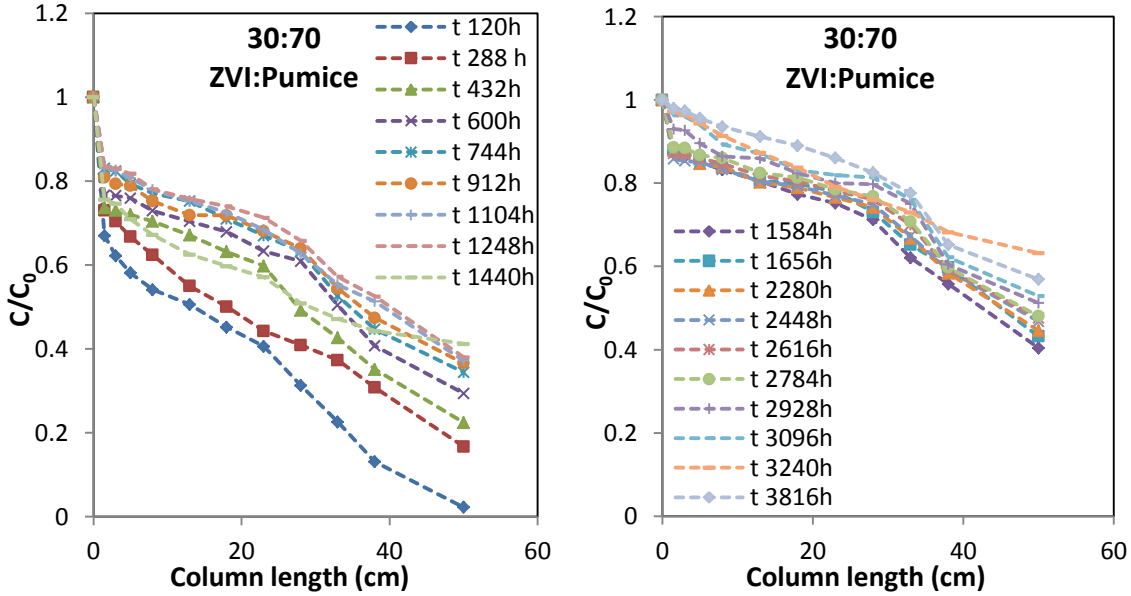

Figure 4-6 normalized concentration of nickel in 30:70 w.r. ZVI:Pumice, C0=50ppm, f.r.= column test

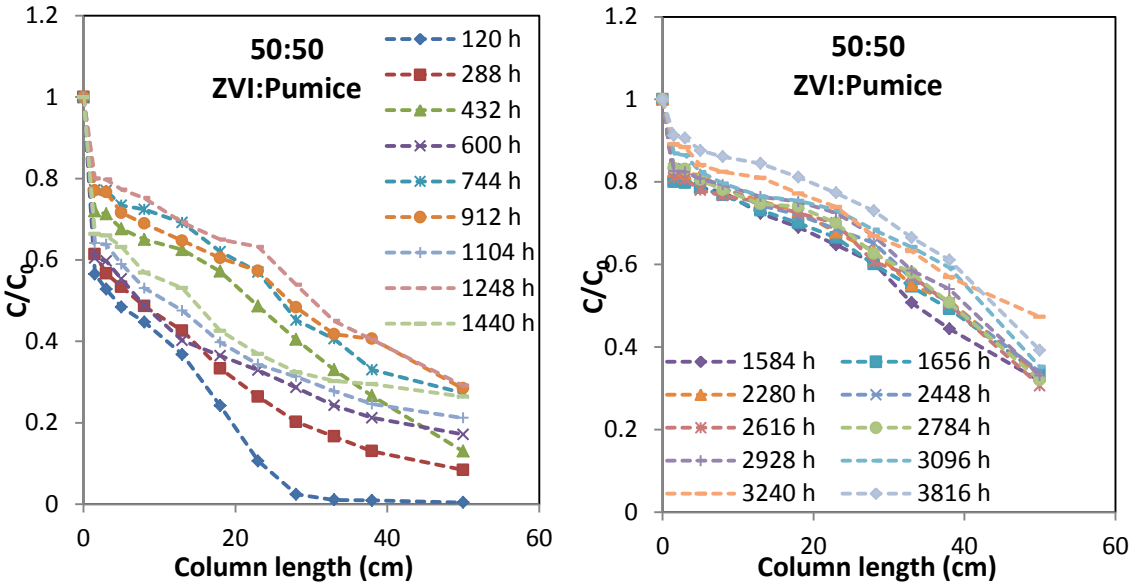

Figure 4-7 normalized concentration of nickel in 50:50 w.r. ZVI:Pumice, C0=50ppm, f.r. = column test

Moraci and Calabrò (2010) studied the removal efficiency of the three considered weight ratios. As can be observed, the 50:50 weight ratio seems to have the best behaviour in terms of removal capacity and this is due to the different ZVI content: 153 gr in 1 metre of filter made of 10:90 w.r., 244 gr and 530 gr in 50 cm of 30:70 w.r. and 50:50 w.r. respectively. Considering the evolution of the relative concentration, two main consideratios can be made. Firstly, using 10:90 and 30:70 weight ratios, the considered column lengths, 58 cm for 10:90 w.r. and 50 cm for 30:70 w.r. , are almost sufficient efficiently to reduce the nickel concentration until 120 hours after the interaction test start. In particular, 0.04 and 0.02 are the relative concentrations measured in that point. Using 50:50 weight ratio, 28 cm are enough to reduce the relative concentration to arount to the same above-mentioned value after 120 h.

The second consideration regards the general form of distribution of the experimental data. In all three tests, a different removal efficiency can be observed between the reactive materials placed in the first centimetres from the bottom of the column and that placed afterwards. This is more evident for the test containing a greater ZVI quantity. In fact, at the first sampling time, or rather 120 h, the relative concentration is 0.73, 0.67 and 0.56 in 10:90 w.r., 30:70 w.r. and 50:50 w.r. tests respectively. This value tends to increase more rapidly as lesser is the ZVI content. However, after 1656 hours of interaction, the relative concentration at 1.5 centimetres is about 0.93, 0.88, 0.8 for 10:90 w.r., 30:70 w.r. and 50:50 w.r. tests

respectively, while at the end of the tests, that is, after 3816 hours, the relative concentration at 1.5 centimetres is about 0.99, 0.97, 0.89 for 10:90 w.r., 30:70 w.r. and 50:50 w.r. tests respectively. In the 10:90 test, the value of 0.99 is already reached at 2448 hours. Looking at the end of the less efficient part of filter length, corresponding to the outlet of the 30:70 and 50:50 w.r. and to 58 cm of 10:90 w.r. filters, the final relative concentration is around 0.8, 0.63 and 0.47 for 10:90, 30:70 and 50:50 w.r column tests respectively.

This can suggests that the reaction between ZVI and nickel is immediate, considering the contact time ensured by the constant flow rate under which these tests have been realized. Under almost the same contact time, the higher the ZVI content the higher the removal efficiency. The calculated residence times are 21 h for 10:90 w.r. column test (considering 1 meter length) and 13 h for 30:70 and 50:50 column tests, considering the entire column length used. On the other hand, the contaminant flow needs about 20 minutes to pass through 1.5 centimenters of reactive filter, that are the most reactive.

The observed difference in terms of removal efficiency between the first 1.5 or 3 centimetres and the rest of the column can be researched for different reasons, e.g. the deactivation of ZVI because of the high content in silice of Pumice (Moraci and Calabrò, 2010), the competition of nickel removal mechanisms with others that need more contact time than that ensured in the first centimetres in the experimental conditions used, the ZVI corrosion that can be more favoured in the second part of the column than the first and that implies a decrease in removal efficiency, a non-homogeneous distribution of the two components of the mixtures due to the large difference in specific weight.

The nickel retained mass in each sector divided by the length of the sector will be introduced in Chapter 7.

4.2.2.2 Considerations about flow velocity and nickel initial concentration influences

In this section, some column tests performed varying the flow velocity and the nickel initial concentration are re-presented. In Figures 4-10, the nickel normalized concentration evolution is shown for tests performed using 30:70 ZVI:Pumice mixture with a solution of nickel at 50 mg/L of initial concentration and a flow velocity equal to 1.382 mm/min.

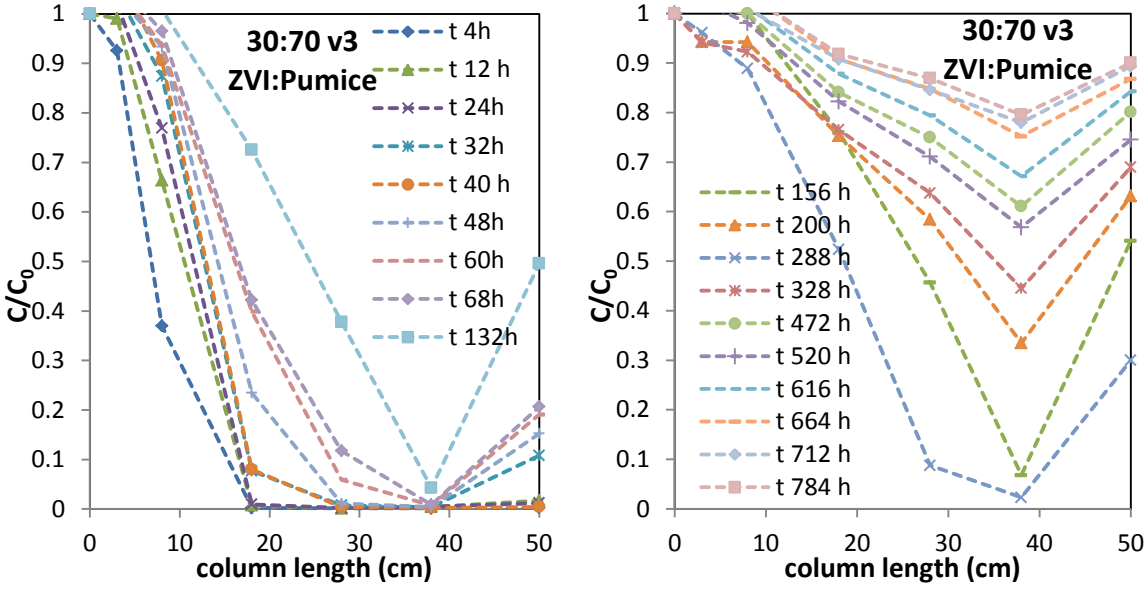

Figure 4-8 normalized concentration of nickel in 30:70 w.r. ZVI:Pumice test using solution of nickel at 50 mg/l of initial concentration and v3 flow velocity a) until 132 h and b) 784 h.

In Figures 4-11 a) the nickel normalized concentration evolution is shown for tests performed using 30:70 ZVI:Pumice mixture with a solution of nickel at 40 mg/L of initial concentration and a flow velocity equal to 0.055 mm/min , while in Figures 4-11 b) the nickel normalized concentration evolution is shown for tests performed using 30:70 ZVI:Pumice mixture with a solution of nickel at 8 mg/L of initial concentration and a flow velocity equal to 0.276 mm/min

The influence of flow velocity and nickel initial concentration were investigated in depth by Bilardi (2011), Bilardi et al. 2013.

Here the data about concentratio are re-proposed in view of the modelling development, that is the objective of Chapter 6.

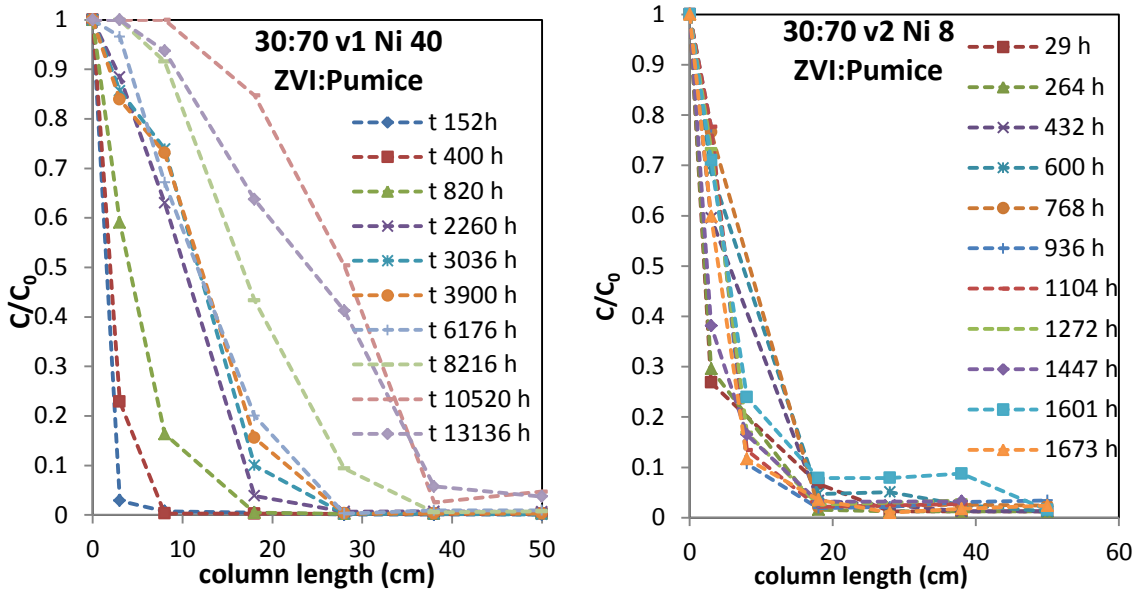

Figure 4-9 normalized concentration of nickel in 30:70 w.r. ZVI:Pumice tests a) using solution of nickel at 40 mg/l of initial concentration and v1 flow velocity and b) using solution of nickel at 8 mg/l of initial concentration and v2 flow velocity

4.3 ZVI:Pumice mixtures to remediate Zinc-contaminated solutions

In this section, the results for ZVI:Pumice mixtures tested to remmediate Zinc-contaminated water are presented. During this Ph.D. course, a column test using a 50:50 ZVI:Pumice w.r. mixture was performed. The obtained results are compared with those of the previously tests carried out using a 30:70 ZVI:Pumice w.r. mixture. For both tests a solution of Zinc at 50 mg/L intial concentration and a constant flow velocity of 0.276 mm/min were used. In table 4-2 the characteristics of considered column tests are reported.

React. Mat.	Weig. ratio	Initial cont. conc. (mg/ L)	React. thick. (cm)	React. area (cm^2)	React. Vol. (cm^3)	Fe^0 (gr)	Pum. (g)	n (%)	Flow veloc. (mm/ min)	PV (cm^3)	Tres (h)
Fe^0/ Pum	50:50	Zn 50	50	18.09	904.3	481	481	49	0.276	442.2 9	14.7
Fe^0/ Pum	30:70	Zn 50	50	18.09	904.3	229	534	45	0.276	104	3.5

Table 4-3 Characteristics of column tests performed using ZVI:Pumice mixtures and Zinc-contaminated solutions

In Figure 4-14 a) the evolution of Zinc concentration normalized by the initial value at outlet is shown for the two tests. It seems that the breakthrough is reached at the same time, altough the subsequent Zinc concentration increase is slower in the 50:50 ZVI:Pumice w.r. mixture test. In Figure 4-14 b) the hydraulic performance evolution as function of time is shown for both tests. The hydraulic conductivity stays constant for both tests.

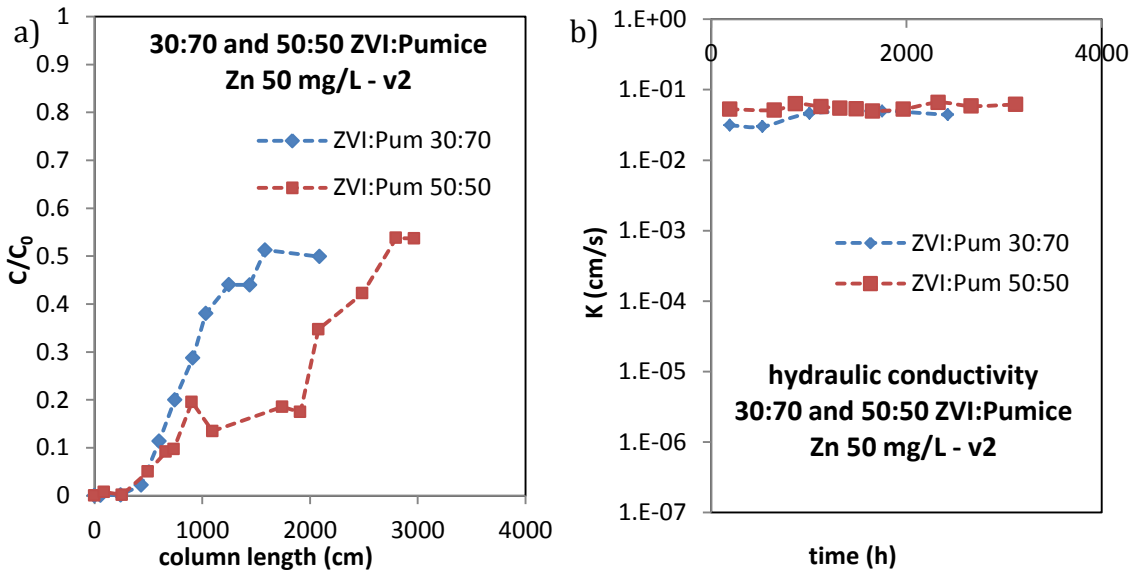

Figure 4-10 a) Evolution of Zinc normalized concentration with time and b) hydraulic conductivity evolution for 30:70 and 50:50 ZVI:Pumice mixtures tested with solution of Zinc at 50 mg/L initial concentration and 0.276 mm/min constant flow velocity

4.4 Conclusions

Two column tests using pure ZVI and a contaminant solution of nickel at initial contaminant concentration of 40 mg/L performed one at 0.055 mm/min and the other at 1.382 mm/min flow velocities were considered. The distribution of nickel removed along the filter with time showed as nickel is mainly retained in the three first centimetres in both cases.

Concerning the ZVI:Pumice mixtures, three different weight ratio (10:90, 30:70 and 50:50) were considered and compared. As already discussed, this study highlighted the highest nickel removal efficiency of mixture containing the highest ZVI mass.

During this Ph.D. course, a column test using a 50:50 w.r. ZVI:Pumice mixture and zinc contaminated solution was performed in order to compare its performance to the column test already carried out using a 30:70 w.r. ZVI:Pumice mixture. It seems

that the breakthrough is reached at the same time, altough the subsequent Zinc concentration increase is slower in the 50:50 ZVI:Pumice w.r. mixture test, while the hydraulic conductivity stays constant for both tests.

In Chapter 5, an analysis of column tests performed using ZVI:Lapillus mixtures is proposed. The influence of different factors, as contaminant initial concentration, flow velocity, weight ratio and filter thickness, on long-term removal efficiency and hydrualic behavior is investigated.

5 Lapillus column tests

5.1 Introduction

As observed in Chapter 4, different factor can influence the long-term removal efficiency and hydraulic behaviour of pure ZVI and ZVI:Pumice filters. They are considered in this work, to investigate whether and how the performance of ZVI:Lapillus mixtures can be influenced by the same factors.

One of the steps in the research activity has been developed through experimental tests at laboratory scale. The objective of the experimentation was to study and evaluate the heavy-metals removal efficiency of a new support, the Lapillus, to be mixed with ZVI and used as a reactive medium in PRB. ZVI/Lapillus mixtures was tested to investigate mono and pluri-contaminated solutions remediation.

Different ZVI/Lapillus weight ratio mixtures were tested to study the long-term heavy-metal removal efficiency and the hydraulic performance. Four parameters were varied to study their influence on nickel removal and the hydraulic behaviour: weight ratio, flow velocity, contaminant initial concentration and filter thickness. Column tests at the same boundary conditions were carried out using zinc contaminated solutions. As for Copper contaminant the easily remediation observed by previous studies using pure ZVI and ZVI/Pumice mixtures was taken into account in the program drafting (Moraci et al., 2011). Pluri-contaminated by nickel, zinc and copper was used to study the effect of simultaneous removal of the three contaminants on the long-term removal efficiency and hydraulic behaviour of ZVI/Lapillus mixtures.

5.2 Methodology

Different sets of column tests were planned in order to study the influence of some boundary and experimental conditions. These were performed following the same procedure with regards to column test assembling, performance monitoring, exhausted reactive media extraction, release tests and dismantling. The entire procedure, including the description of the experimental apparatus and the instruments used for performance monitoring will here be introduced.

Once the experimental data on contaminant concentration evolution with time and filter thickness and on hydraulic conductivity evolution with time were known, an attempt was made to observe, interpret and explain the long-term removal performance and hydraulic behaviour, looking also at physical and chemical parameters (pH, Eh and temperature). The scheme shown in Figure 5-1 summarizes the procedure followed for the interpretation of available experimental data for the i-th column test. Comparing the output of this procedure for each column test involved in a set of experiments performed varying one parameter, it was possible to study its influence. In the red and green squares the output and the intermediate processing steps are reported respectively.

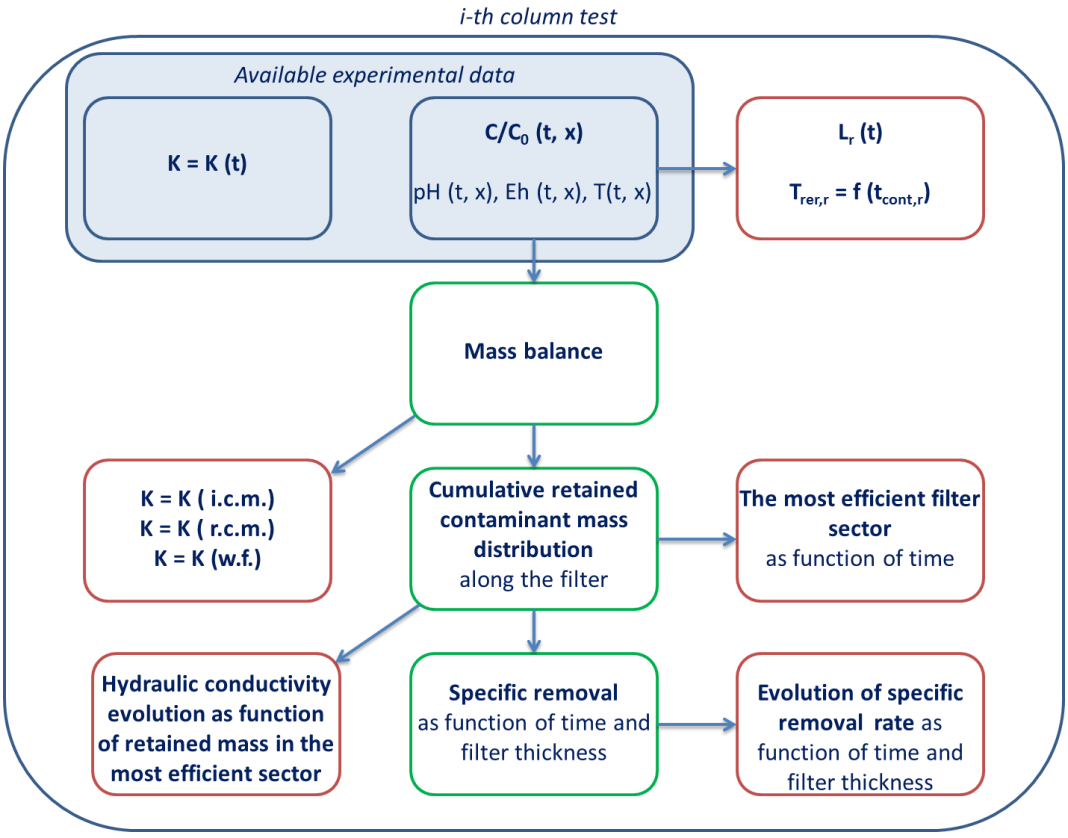

Figure 5-1interpretation procedure of experimental data available for the i-th column test

Considering the available data on evolutions of contaminant concentration, pH, Eh and temperature (T) as functions of time and filter thickness, the minimum filter thickness necessary for an efficient contaminant removal can be identified, for the i-th column test corresponding to certain boundary and experimental conditions. This length (L_r) assures a certain minimum residence time ($T_{res,r}$) function of the minimum

contact time ($t_{cont,r}$) necessary for remediation processes. It is then possible to obtain information about hydraulic and removal efficiency performance by a contaminant mass balance (i.e. the evolution of hydraulic conductivity as function of the input contaminant mass (i.c.m.), the cumulated retained contaminant mass (r.c.m.) distribution along the filter, the water flowed (f.w.)). This allows identification of the most efficient filter sector, that can vary with time, and the hydraulic conductivity evolution as function of the contaminant mass retained in the most efficient filter sector. Finally, the calculation of removal kinetics permits observation of the evolution of removal kinetics as a function of time in different filter thickness sectors.

5.3 Contribution of laboratory tests to PRB design

The contribution of laboratory tests to PRB design consists of simulating the flow of contaminant plume through the barrier. The column transversal section represents the elemental transversal section of the PRB, while its length corresponds to the PRB thickness. The inlet of the column test corresponds to the up-gradient side of the PRB, while the output represents the down-gradient side. This conceptual model of the column would be representative of the real removal process scheme if the same input contaminant mass to unit transversal area ratio were taken into account under the same boundary (C_0 initial concentration) and experimental conditions (v flow velocity). Thus, a criterion proposed to reproduce the *in-situ* hydraulic conditions consists of choosing the experimental flow velocity and Peclet number as similar as possible to the real values (Crittenden et al., 1991). The values used in this research were chosen on the basis of the range of the flow velocity registered for a number of PRBs *in situ* varying in 0.015-5.7 m/d range (Henderson and Demond, 2007).

On the geotechnical side, it would be an appropriate model if the geotechnical characteristics of the base soil were taken into account and the granular filter design criteria respected (Moraci et al, 2012a,b and 2014).

The limits of a similar model regard the differences between the laboratory and real scales and physical-chemical initial condition and its evolution.

5.4 Experimental apparatus and procedure

Column tests were carried out filling a 50 cm (or 100 cm) high and 5 cm large column with reactive material, pure Lapillus or ZVI/Lapillus mixtures at different weight ratio (Figure 5-2 a), to study their removal efficiency and hydraulic behavior, under a constant velocity rate of contaminant solution. Columns experiments were carried out using polymethyl methacrylate (PMMA-Plexiglas™) columns, equipped with sampling ports located at different distances from the inlet (Figure 5-3 a).

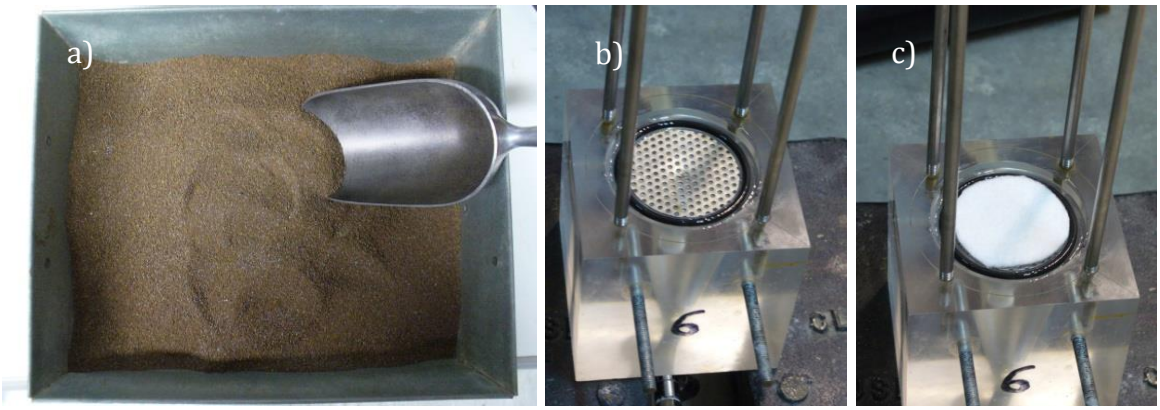

Figure 5-2 a) ZVI:Lapillus mixture; b) bottom of column with o-ring and inox grid; c) and with geotextile filter

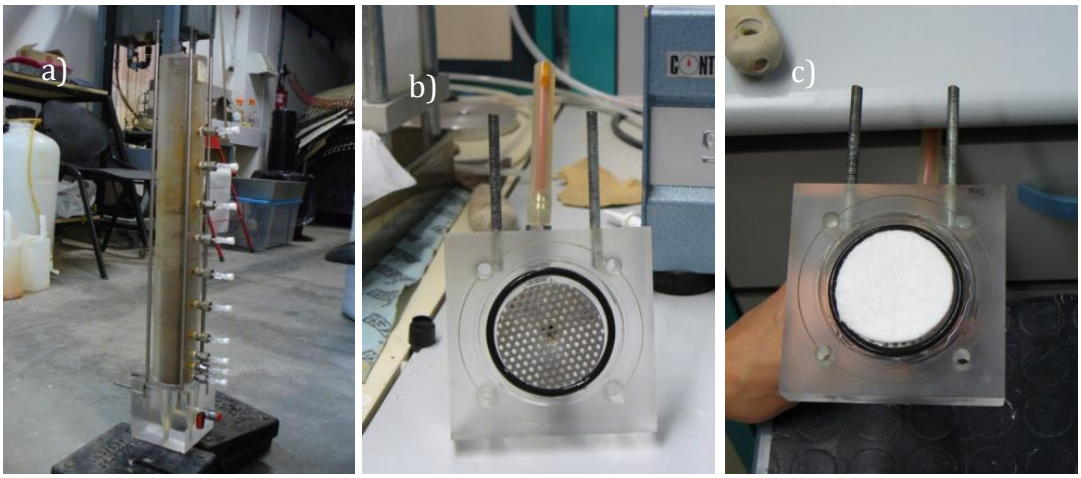

Figure 5-3 a) column assembly; b) top of column with o-ring and inox grid; c) and with geotextile filter

Sampling ports are located at a distance of 1.5, 3, 5, 8, 13, 18, 23, 28, 33, 38, 53.3 cm from inlet in a 50 cm in height column. They are at 3, 8, 18, 28, 38, 58, 78, 100 cm from inlet in a 100 cm in height column.

In Figure 5-2 b and c the bottom of the column is shown with O-ring, inox grid and geotextile filter placed on the intern side, before the assembling column . In the same way, the top of the column is shown in Figure 5-3 b and c.

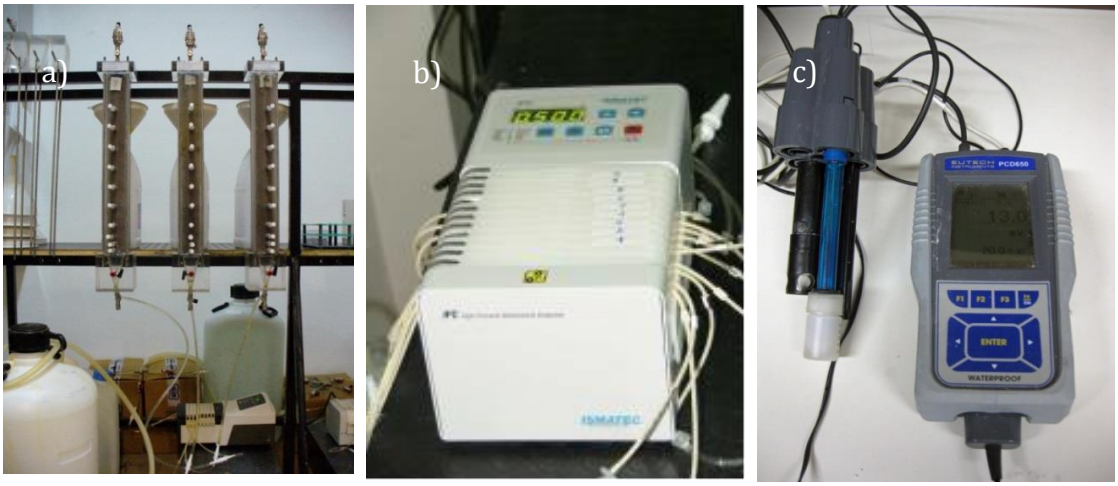

Figure 5-4 a) set of column; b) peristaltic pump; c) multi-parameter

A Watson Marlow 205S or Ismatec ISM930 (Figure 5-4 b) peristaltic pumps were used to feed the columns, under constant upward velocity, from one PE bottle (Figure 5-4 a).

The contaminated aqueous solution was prepared by dissolving nickel(II) Nitrate hexahydrate (purity>99.999) or Copper(II) Nitrate hydrate (purity>99.999) or Zinc(II) Nitrate hexahydrate (purity>99.0) obtained from Sigma-Aldrich, or a combination of them, in distilled water in order to prepare solution at set initial contaminant concentration. At fixed times samples of solution were collected from the sampling ports placed along the column. pH and Eh values were directly measured using a multi-parameter (WTW GmbH, Inolab pH/Cond 720) (Figure 5-4 c). The contaminant concentrations in the samples collected were measured using instruments based on different analytical techniques: in the firsts tests carried out by Atomic Absorption Spectrophotometry (AAS - Shimadzu AA – 6701F) then by Optical Emission Spectrometer with inductively couples plasma (ICP/OES) using conventional Standard Methods (APHA 2005).

AAS (Figure 5-5 a) is used for the quantitative determination of a particular element in the sample using the absorption of optical radiation by free atoms in a gaseous

state. Radiation is directed at the sample, the atoms of which absorb light at the specific wavelengths of the element. A detector measures the change in radiation after it has passed through the sample. Based on the Beer-Lambert Law and known concentrations of standards reference solutions, it allows one to know the amount of the concentration in the sample that is proportional to the absorbed light.

The Optical Emission Spectrometer with inductively couples plasma (ICP/OES) (Figure 5-5 b) is based on the emission spectroscopy used for the detection of trace metals. It is able to analyze for multiple elements at the same time. The samples introduced into the instrument as aerosol pass through the plasma and become ionized. A detector measures the intensity and wavelengths corresponding to the emission due to the coming back of excited atoms to ground state. Comparing to known standards, they are elaborated to obtain the concentration of the investigated elements.

Figure 5-5 Figure 0 5 a) AAS and b) ICP/OS

During the column tests, performed at room temperature (21 ± 4 °C), hydraulic conductivity was determined by using the falling-head (k < 10_6 m/s) or constant-head (k > 10_6 m/s) permeability methods (Head and Keeton, 2008) at given times to assess the permeability of the systems. To determine the hydraulic conductivity, the column test was interrupted and a tank or a burette, filled with the same contaminated solution used during the test, was connected to the column in order to perform the procedure. This latter lasted a limited time in order to re-establish the operational flow in the column, without causing an unacceptable disturbance to the system.

After some column tests, a sample of exhausted reactive material was withdrawn, as shown in Figure 5-6 a, and kept in an appropriate box to be analyzed. Release tests were performed after the some column tests. This step was carried out using distilled water which flows upward into the column at the same flow velocity used during the test and sampling the solution at different sampling times. This procedure allows evaluation of the possible release of the contaminants removed by the reactive medium.

Finally, the column was dismantled, as the images in Figures 5-6 b and c show.

Figure 5-6 a) reactive material sampling, b) and c) two steps of column tests disassembling

5.5 Experimental program and research objectives

The experimental program aimed at studying the long-term removal efficiency and hydraulic behaviour of new reactive media to be used in permeable reactive barrier Technology, is shown in Table 5-1. The column tests, using solution contaminated by nickel, were carried out in order to evaluate the influence of the following parameters:

1) ZVI/Lapillus weight ratio
2) Flow velocity
3) Contaminant initial concentration
4) Filter thickness

Further column tests were carried out using zinc-contaminated solution and pluri-contaminated solution of nickel, zinc and copper.

The investigation is focused on identifying also the most important parameters influencing the removal mechanisms of contaminants and the long term hydraulic

behaviour, and to find similar conditions, if they exist, and the best compromise to optimize ZVI use.

One column test was performed using pure Lapillus put in contact with a solution of nickel at an initial concentration of 50 mg/L using a 0.276 mm/min average constant flow velocity. The objective of the experiment was to investigate whether this material has a certain removal capacity, how much contaminant mass it is able to retain in the experimental conditions and the possible removal mechanisms involved. It was also useful to represent a benchmark for column tests carried out using ZVI/Lapillus mixtures.

Three tests were realized varying the weight ratio of each of the mixtures. In particular, 10:90, 30:70, 50:50 ZVI/Lapillus weight ratios were tested to observe the influence of ZVI quantity and the role of Lapillus in terms of removal efficiency and hydraulic behaviour, in order to establish the weight ratio corresponding to the best compromise between removal and preservation of hydraulic behaviour.

Tests varying the initial concentration of Nickel and the flow velocity were carried out.

Three column tests using solution of nickel at 10, 50 and 100 mg/L of initial concentration and three tests using constant flow velocity equal to 0.055, 0.276 and 1.382 mm/min were carried out.

All the column tests were carried out using 50 cm columns. One test only was performed in a 100 cm long column in order to investigate the influence of filter thickness. In particular, 30:70 weight ratio ZVI/Lapillus granular mixture was tested in this study with a solution contaminated by nickel at 50 mg/L initial concentration flowing at a constant mean flow velocity equal to 0.276 mm/min.

Reac Mat	W.r.	Init. cont. conc (mg/ L)	Reach eig. (cm)	Reac area (cm)	Reac Vol. (cm^3)	Fe^0 (gr)	Lap. or Pum. (gr)	n (%)	Flow vel (mm/ min)	PV (cm^3)	Tres (h)
Lap.		Ni 50	50	18.09	904.3		1289	35	0.276	318.5	10.6
Fe^0/ Lap.	10:90	Ni 50	50	18.09	904.3	138	1242	36	0.276	322.2	10.7
Fe^0/ Lap.	30:70	Ni 50	50	18.09	904.3	480	1120	37	0.276	334.3	11.1
Fe^0/ Lap.	50:50	Ni 50	50	18.09	904.3	970	970	38	0.276	340.1	11.3
Fe^0		Ni 50	3	18.09	54.26	240		44	0.276	23.76	0.8
Fe^0/ Lap.	30:70	Ni 50	100	18.09	1808	1098	2562	34	0.276	607	20.2
Fe^0/ Lap.	30:70	Ni 50	50	18.09	904.3	473	1104	37	0.055	336.7	56.1
Fe^0/ Lap.	30:70	Ni 50	50	18.09	904.3	468	1093	38	1.382	348.1	2.3
Fe^0/ Lap.	30:70	Ni 100	50	18.09	904.3	477	1113	37	0.276	337.5	11.3
Fe^0/ Lap.	30:70	Ni 10	50	18.09	904.3	480	1120	38	0.276	341.3	11.4
Fe^0/ Pum.	50:50	Zn 50	50	18.09	904.3	481	481	49	0.276	442.2	14.7
Fe^0/ Lap.	50:50	Zn 50	50	18.09	904.3	970	970	38	0.276	340.1	11.3
Fe^0/ Lap.	50:50	Ni 50, Cu 500, Zn 50	50	18.09	904.3	963	963	38	0.276	344.5	11.5
Fe^0/ Lap.	30:70	Ni 50, Cu 500, Zn 50	50	18.09	904.3	480	1120	37	0.276	334.2	11.1

Table 5-1Column tests program to study long-term removal efficiency and hydraulic behavior of ZVI:Lapillus mixtures

The Zinc efficiency removal was investigated using 50:50 ZVI/Pumice and ZVI/Lapillus weight ratios mixtures, using Zinc contaminant solution at 50 mg/L initial concentration flowing at 0.276 mm/min constant flow velocity.

Two column tests using tri-contaminant solution containing nickel, copper and zinc at 50, 500 and 50 mg/L initial concentrations respectively flowing at 0.276 mm/min constant flow velocity were carried out.

5.6 Results of column tests carried out with nickel-contaminated solutions

5.6.1 Lapillus

The performed column test using pure lapillus demonstrated a certain capacity of the volcanic material to reduce the nickel concentration in the above mentioned experimental conditions. 1289 gr of lapillus were used in the column test which lasted 2800 hours (116 days).

The experimental results are represented in Figures 5-7 a), b) and c) as function of time. In Figures 5-7 a), b) and c) the evolution of the nickel normalized residual concentration (C/C_0) of nickel, of pH and Eh values related to the three sampling ports located at a distance of 1.5, 18 and 50 cm from the column inlet are reported respectively. A correspondence among nickel residual concentration and pH and Eh values can be observed. Concerning the sampling ports where a high nickel concentration is observed, the pH is similar to input solution (6.5) and the Eh is positive and equal to about 30 or 40 mV. Two different time intervals can be identified in the test duration. The first one starts at the beginning of the test and goes on until 500 hours. During the first interval, an increase in nickel residual concentration, an increase in Eh value, from 15 to 40mV and a decrease in pH value, from almost 6.5 to 6 are observed for the sampling ports located at 3 and 18 cm from the column inlet. During the same time, low values of nickel concentration are measured at the outlet, while pH stays constant (around to 7) and Eh seems to decrease, (however its values are less than that of the first sampling port). After 500 hours of interaction testing, a new decrease of nickel concentration can be observed at the first ports, a pH increase up to 7 and Eh decrease down to 0 or negative values. At the outlet, an increase of nickel concentration is observed and in the same time pH decreases to around 6 and Eh increases to 40.

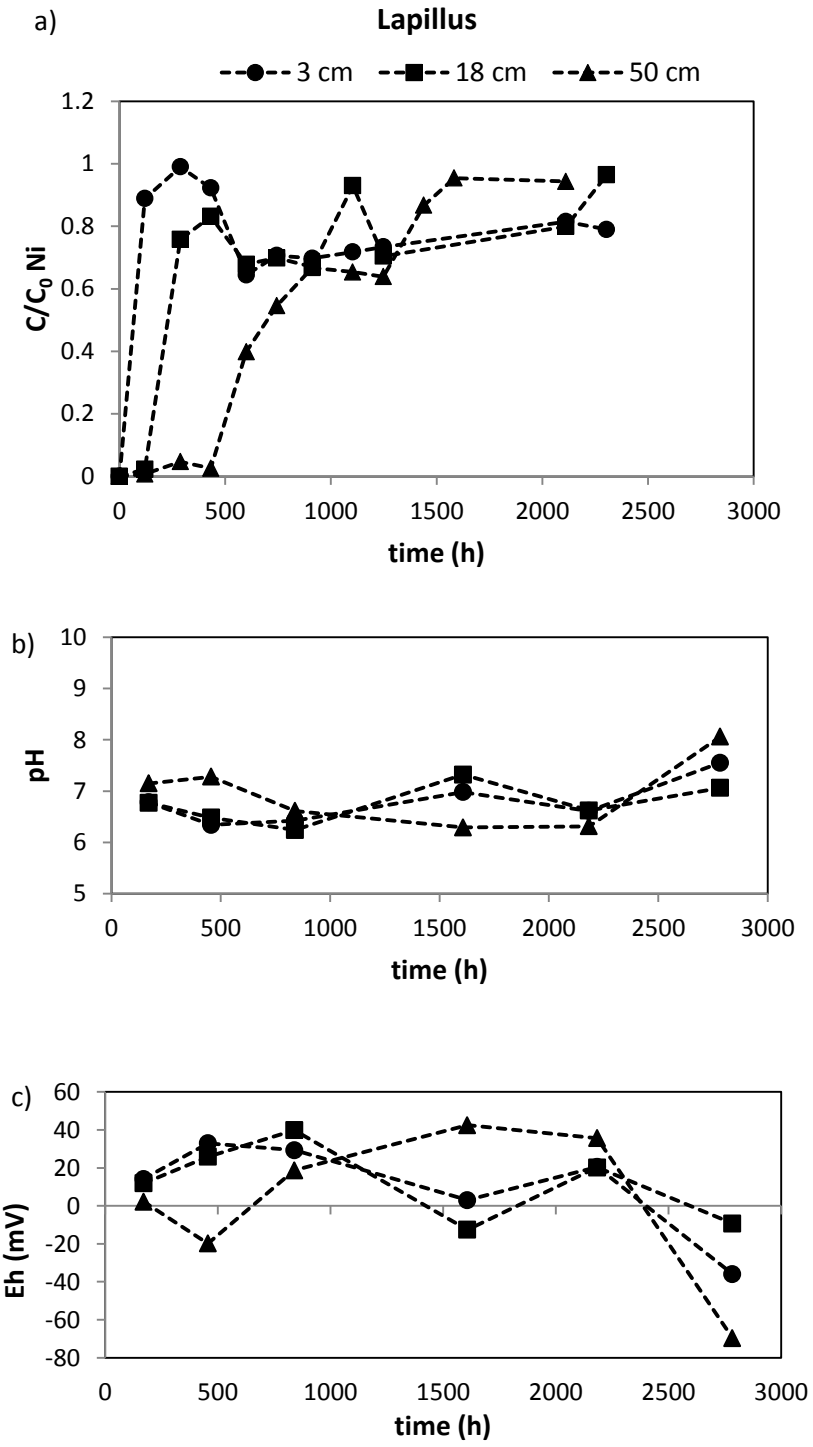

Figure 5-7 Variation of a) nickel normalized concentration ,b) pH and c) Eh (mV) over time for the pure Lapillus column test

The nickel normalized residual concentration as well as the pH and Eh values are reported as function of the filter thickness for the first part of the time (0-500 hours) in Figures 5-8 a), c) and e) and for the second part in Figure 5-8 b), d) and f).

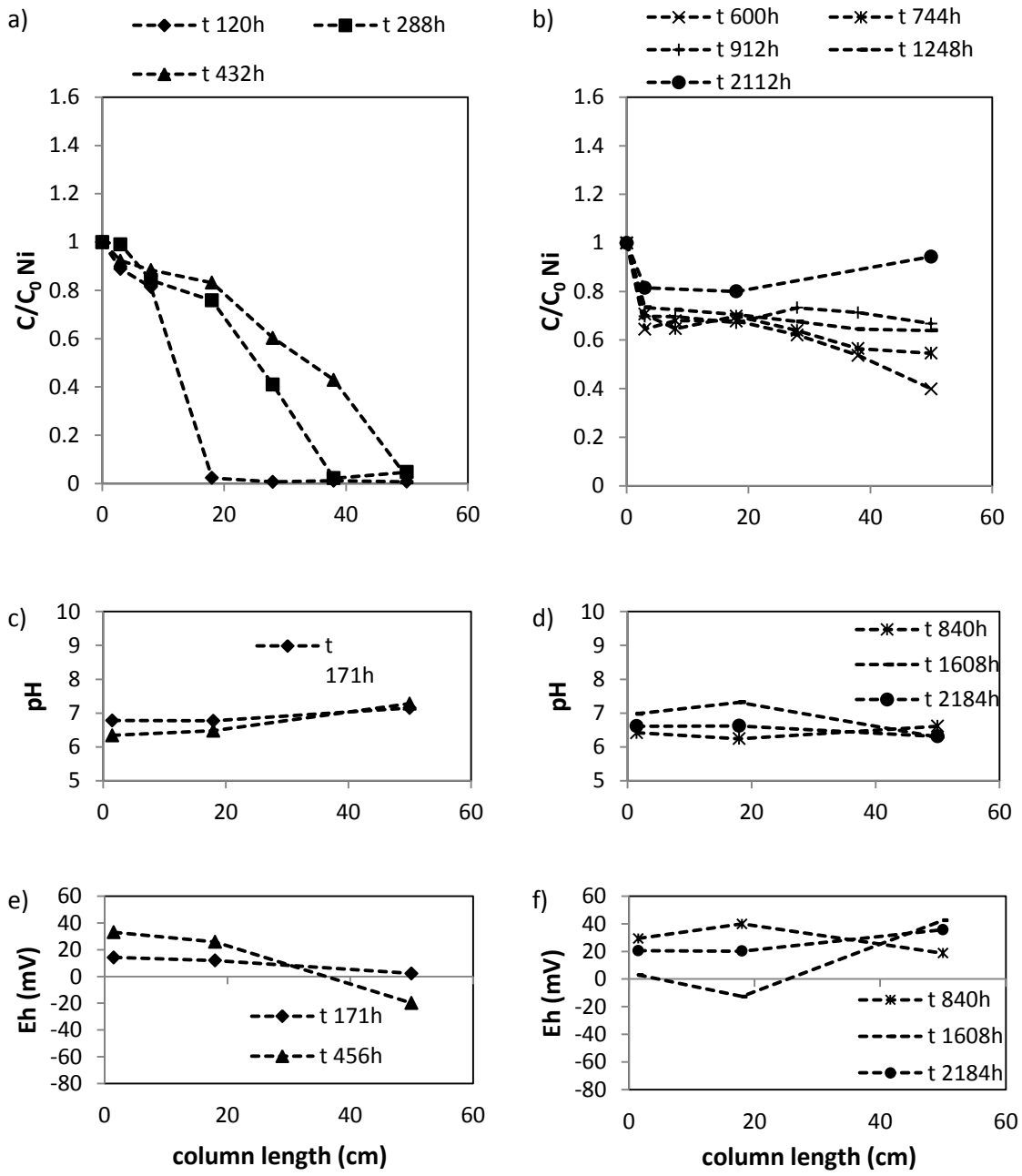

Figure 5-8 Pure Lapillus column test a) nickel normalized concentration ,b) pH and c) Eh (mV) variations with time

During the first time when nickel concentration is most reduced within 40 cm of the filter length, in the first half length of the filter, pH is about 6.5 and it seems to decrease with time, while at the outlet its value is around 7. The Eh in the first ports is positive and it seems to increase with time, while at the outlet it is negative or less than that corresponding to the first ports, at least. During the second time (starting after 500 hours), an increase of pH over time is observed for the first ports, while its values are lower than those of the first time to the outlet. A specular behaviour of Eh

can be observed. Therefore, pH decrease and Eh increase seem to be related to a first reduction in removal efficiency as it has been developed at each port.

Considering a removal efficiency defined as η_{rem} by the equation 5-1.

$$\eta_{rem} = \frac{C_0 - C_m}{C_0} \qquad (5-1)$$

where C_0 is the initial concentration and C_m is the measured concentration, it is possible to evaluate the removal efficiency of different double porous filter lengths as function of the input mass, as shown in Figure 5-9 a).

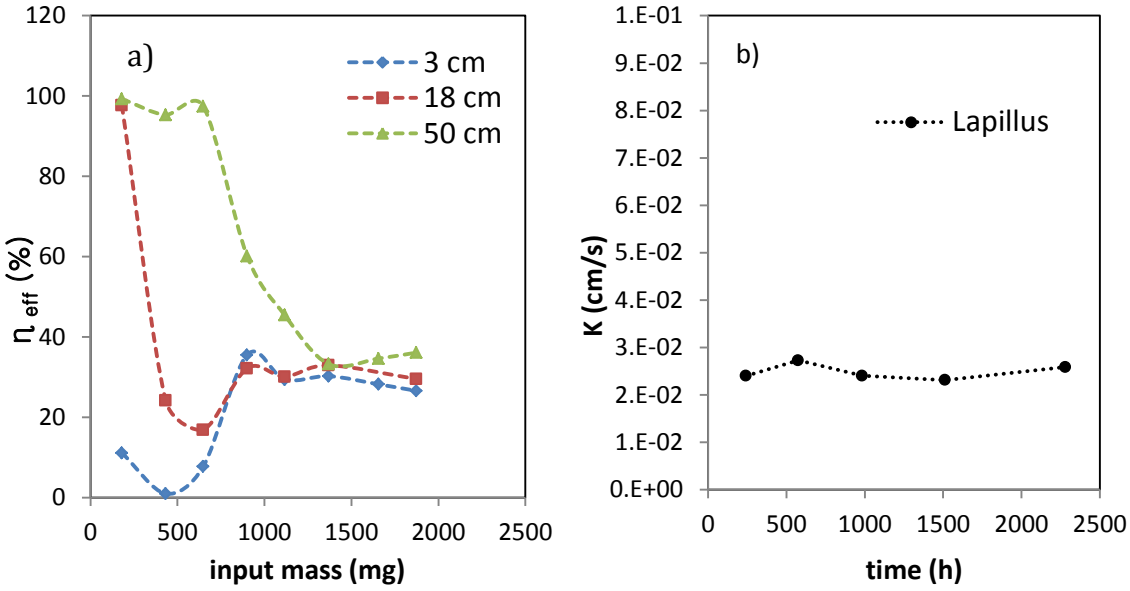

Figure 5-9 a) Nickel removal efficiency as function of the input mass for different lengths of pure Lapillus filter; b) hydraulic conductivity profile over time

Evolution of hydraulic conductivity is reported as function of time in Figure 5-9 b). The hydraulic behaviour does not change during the test.

Lapillus is an internally porous material. If no porosity change is hypothesized, and under the hypothesis of homogeneous molecular diffusion into the internal Lapillus pores, retained mass can be calculated using the equations 1-5. In Figure 5-10 a) cumulative nickel retained mass per unit of lapillus mass (mg/gr) is reported as function of the nickel input mass into the column for the first 3 cm and for the total filter length. The first centimetres of the filter do not have negligible capacity to retain nickel and it seems to be the most efficient part of the column. In Figure 5-10 b) the specific removal rate of lapillus column, related to the experimental conditions, are

shown for each column sector. Specific removal rates represent the quantity of nickel mass retained by unit of lapillus mass in the unit of time. They were calculated for each sector of filter length, considering the sampling time intervals. Their evolution in time and their difference among the sectors can let the conclusion be drawn that the highest removal specific removal rates have been developed in the first centimetres.

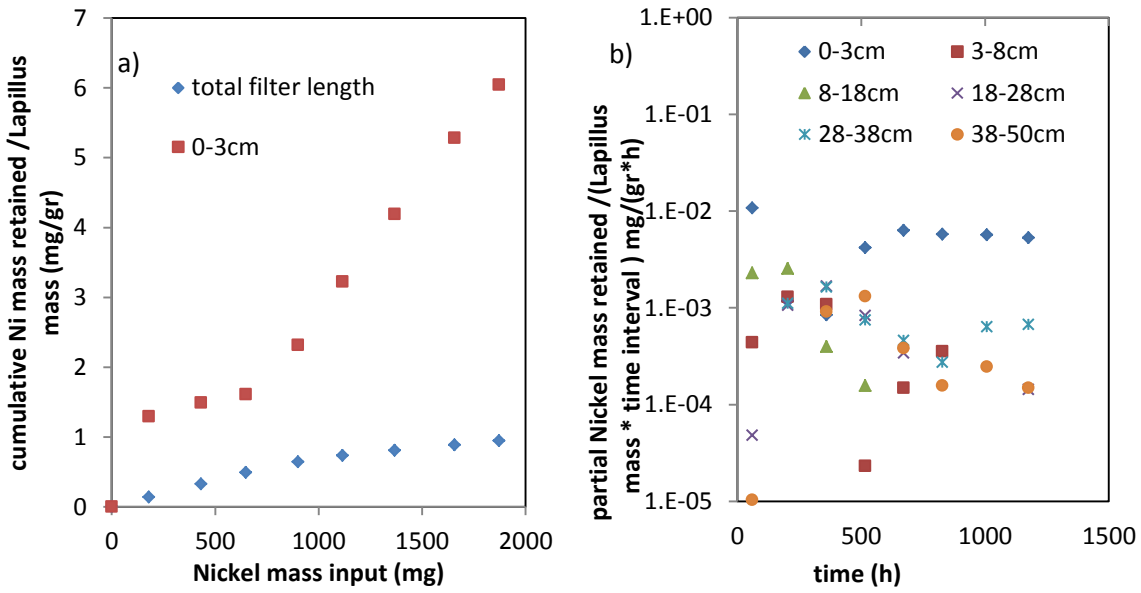

Figure 5-10 a) cumulative nickel mass retained per unit Lapillus mass (mg/gr) as function of nickel mass input; b) nickel mass retained by unit mass of Lapillus per unit time for each column sector (mg/(gr*h))

5.6.2 Weight ratio influence

In this paragraph an analysis of results of column tests carried out with different ZVI/Lapillus weight ratios will be proposed. The 10:90 ZVI/Lapillus column test has been performed using 138 gr of ZVI and 1242 gr of lapillus, the one with 30:70 ZVI/Lapillus weight ratio was prepared using 480 gr of ZVI and 1120 gr of Lapillus while for the 50:50

ZVI/Lapillus weight ratio test 970 gr of both reactive materials needed.

The three columns tests have been carried out under the same experimental conditions of flow velocity (0.276 mm/min) and nickel initial concentration (C_0=50 mg/L).

5.6.2.1Removal efficiency

In Figures 5-11a) and b) and 5-12 a), the nickel normalized concentration is shown as function of time for different sampling ports for 10:90 , 30:70 and 50:50 ZVI/Lapillus mixtures respectively. As can be observed, the less efficient mixture is the 10:90 w.r., while the most efficient is the 50:50 w.r. In fact, after 1500 hours of interaction, the 10:90 filter is no longer able to reduce the nickel concentration efficiently and nickel breakthrough occurs . The same phenomena can be observed after 2300 hours for the 30:70 w.r. column test, while after 4000 hours the 50:50 w.r. column test is still highly efficient.

Furthermore, some considerations concerning how the reactive material exhaustion occurs can be made. As ZVI weight content increases, breakthrough occurs at increasingly high times at the different ports, especially up to 38 cm. Then, for the subsequent ports, breakthrough is more rapid. In fact ZVI reacts not only with heavy metals but also with nitrates and water. Thus, its removal capacity is not intact when the reactive zone for heavy metals removal moves upward the column.

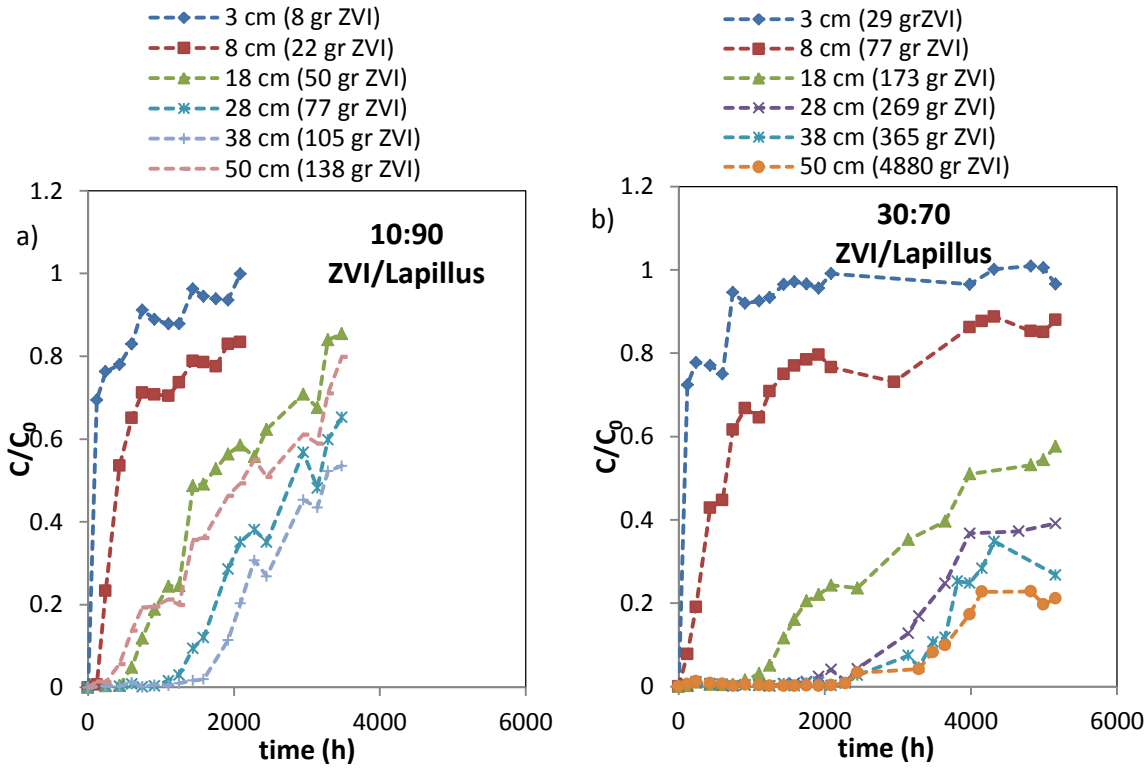

Figure 5-11 Nickel normalized concentration evolution for different sampling ports with time for a) 10:90 and b) 30:70 weight ratios ZVI/Lapillus column tests

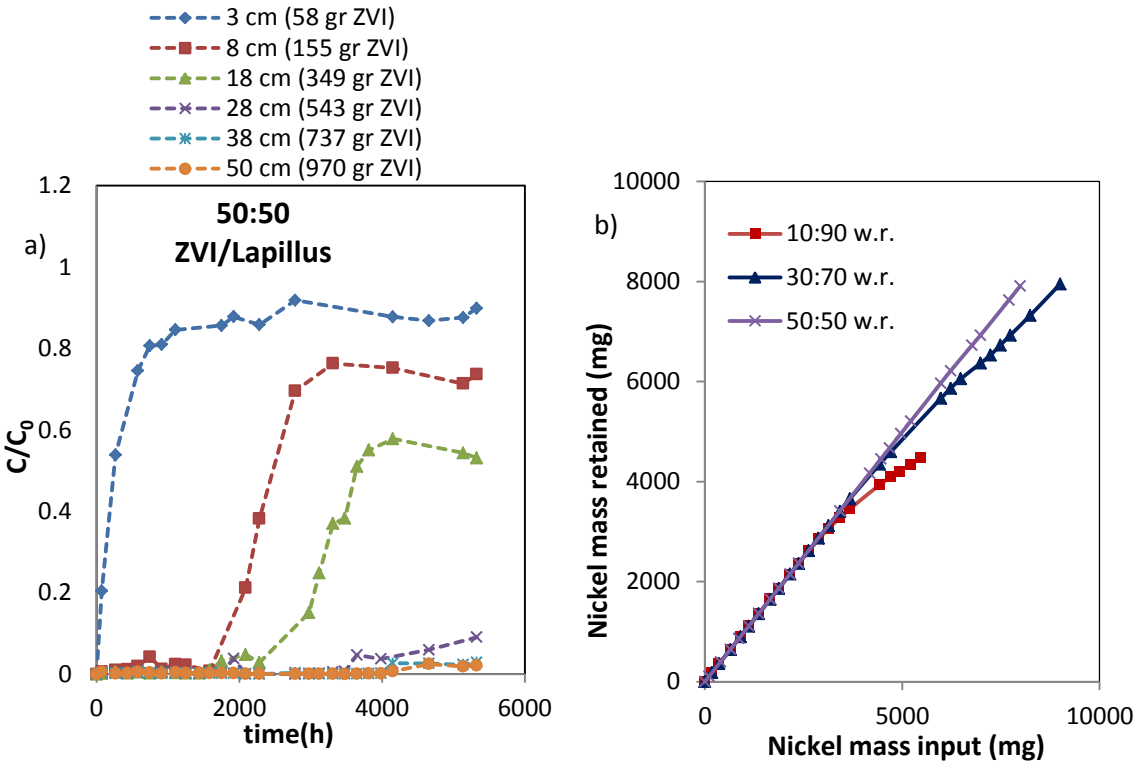

Figure 5-12 a) Nickel normalized concentration evolution for different sampling ports with time for a) 50:50 weight ratio ZVI/Lapillus column tests and b) nickel mass retained in function of nickel mass input for the three w.r. column tests

In Figure 5-12 b), the nickel cumulative retained mass as function of the Nickel mass input for each column test is shown. The efficiency after about 3600 hours of interaction, during which about 5500 mg of nickel have been flowed into the column, is about 82%, 99.5% and 99.8% for 10:90, 30:70 and 50:50 weight ratio tests respectively. The total retained contaminant is distributed differently into each column sector as will be shown later.

To better understand the removal mechanisms and their evolution, the results of each column are re-proposed divided into two or three graphs in function of the variation of measured pH and Eh values and of the form of the curves connecting the relative concentration experimental data points. In Figure 5-13, the nickel normalized concentration values for the column with 10:90 ZVI/Lapillus weight ratio from the beginning of the test to abound 912 hours of interaction (Figure 5-13 a) and from this time to the end of the test (Figure 5-13 b) are shown. In Table 5-2, the values of pH and Eh measured at 1.5 cm, 18 cm and 50 cm from the column inlet at different sampling times are reported.

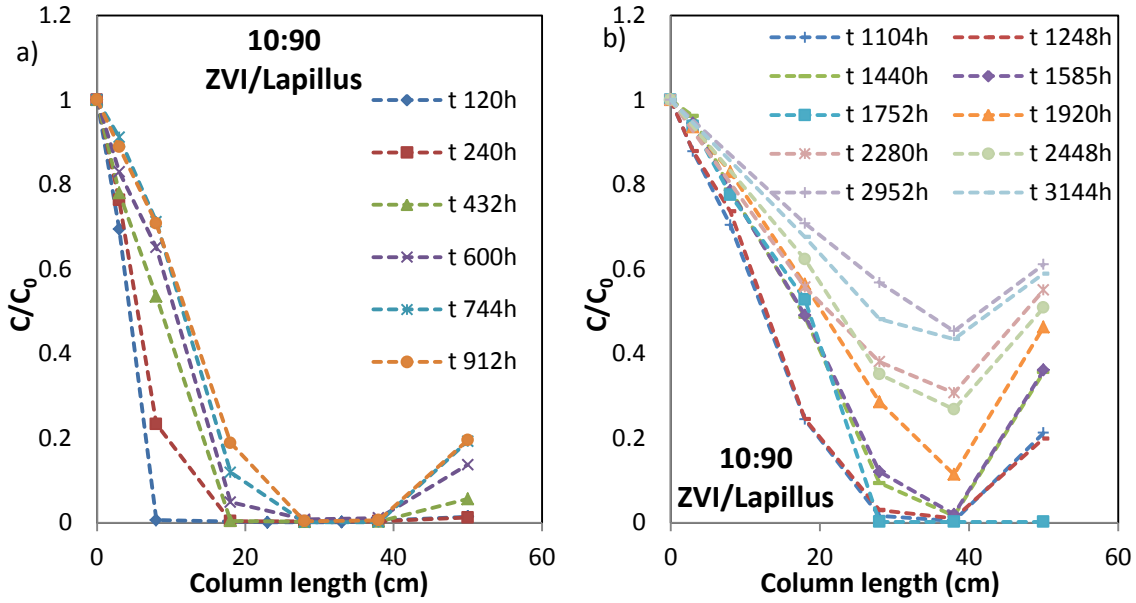

Figure 5-13 Nickel normalized concentration for 10:90 w.r. ZVI/Lapillus column test

t(h)\ dist (cm)	1.5		18		50		t(h)\ dist (cm)	1.5		18		50	
	pH	Eh (mV)	pH	Eh (mV)	pH	Eh (mV)		pH	Eh (mV)	pH	Eh (mV)	pH	Eh (mV)
151	6.18	54.2	8.11	-52	7.3	-3.5	1296	6.2	37.6	6.99	21	7.6	-20.6
440	6.52	30.2	7.96	-56.2	7.92	-54.6	1680	6.2	35.3	6.26	38	7.1	7.3
672	6.47	29.4	7.29	-9.8	7.31	-4.1	2424	6.1	42.6	6.5	29	7.1	8.4
960	6.53	26.9	6.8	21.6	7.04	14	3024	6.5	33	6.68	18	6.3	37.7

Table 5-2 pH and Eh(mv) measured values for 10:90 ZVI/Lapillus weight ratio column test

Noubactep (2007, 2008, 2010a, 2010b, 2011) showed as metal ions can be removed from the aqueous phase in packed ZVI beds by adsorption, co-precipitation, and adsorptive size-exclusion when the pH >4.5 (Bilardi et al., 2013a).

Looking at the evolution of nickel normalized concentration with time and the corresponding pH and Eh values for 10:90 w.r. ZVI/Lapillus mixture tested, it is possible to observe that for pH values more than 7 and Eh negative values, very low values of nickel concentration are measured. At 1.5 cm a certain nickel concentration is always measured, as pH is about 6.5 and Eh is around 30 mV. At 18 cm, low values of nickel concentration are measured until the pH remains around 8 and Eh is about -50 mV. As pH decreases and Eh increases, nickel measured concentration increases and nickel breakthrough occurs.

An 18 cm filter length is enough to reduce significantly the nickel concentration as input until 432 hours (650 mg nickel mass input). 18 cm of 10:90 w.r. ZVI/Lapillus mixtures in the carried out column test correspond to about 4 hours of residence time of solution in reactive filter, 50 gr of ZVI and 450 gr of lapillus. After this time, 28 cm of filter length are necessary to remediate efficiently until around to 1248 hours (1880 mg nickel mass input). This length corresponds to 6 hours residence time, 77 gr of ZVI and 695 gr of lapillus.

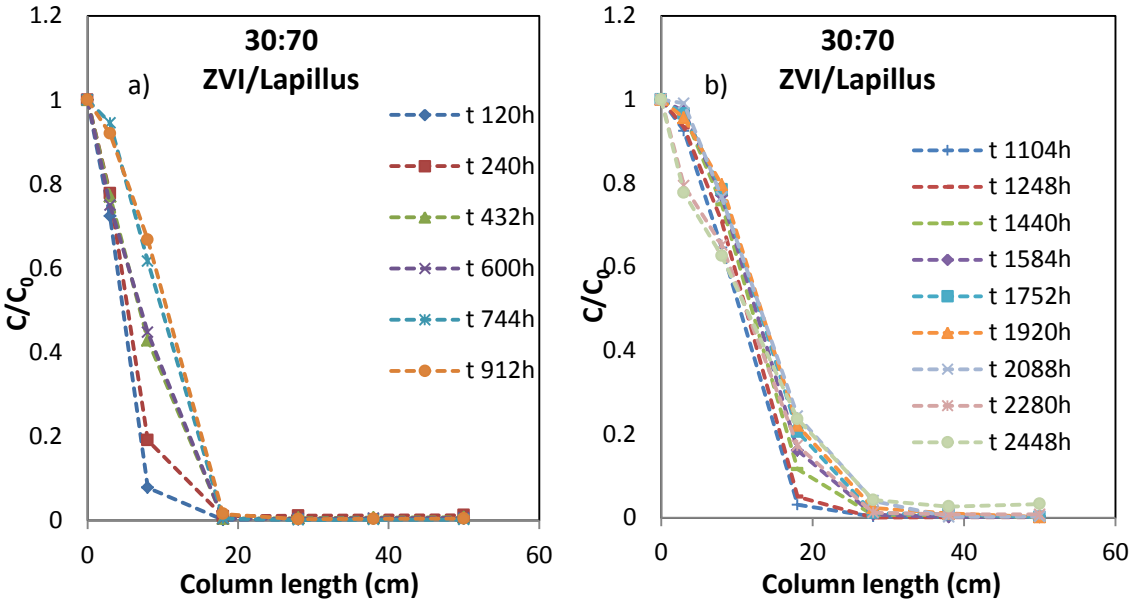

Figure 5-14 Nickel normalized concentration for 30:70 w.r. ZVI:Lapillus column tests until 2448 h

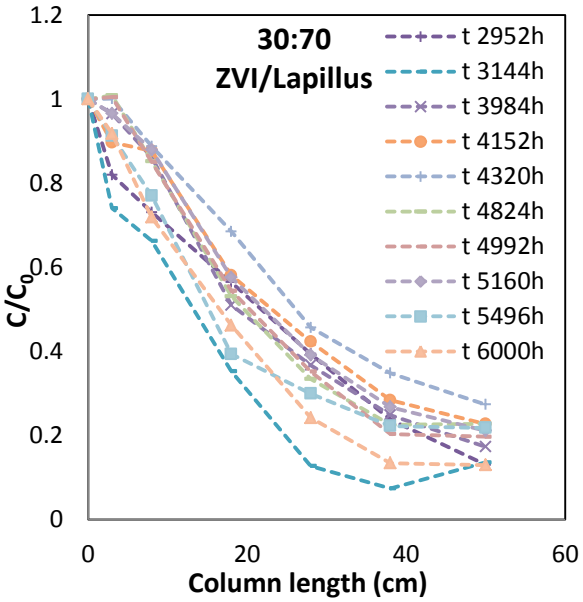

Figure 5-15 Nickel normalized concentration for 30:70 ZVI/Lapillus until the test end;

t(h)\ dist (cm)	1.5		18		50		t(h)\ dist (cm)	1.5		18		50	
	pH	Eh (mV)	pH	Eh (mV)	pH	Eh (mV)		pH	Eh (mV)	pH	Eh (mV)	pH	Eh (mV)
151	6.41	41.8	8.38	-67.5	8.81	-90	2424	6.41	30.	6.44	29.5	8.3	-63
672	6.52	26.2	8.48	-94	9.03	-110	3024	6.49	31	6.48	28.5	6.8	16
1296	6.19	41.6	6.23	41.2	9.02	-113	4176	6.55	20	6.12	45.4	6	50
1680	6.39	30.9	6.32	37.9	8.81	-108	4632	6.55	20	6.53	23.3	5.8	70

Table 5-3 pH and Eh(mv) values for 30:70 w.r. ZVI/Lapillus

In Figures 5-14 a) and b) and 5 -15 a), the nickel normalized concentration evolution along the 30:70 w.r. column is represented. pH and Eh (mV) values are reported in Table 5-3. The experimental data on nickel relative concentration evolution are divided into three different intervals. In the first figure, data related to the interval between the test beginning and 912 hours are represented. During this period, 18 cm of filter length are enough for remediation. pH is about 8 and Eh is negative at 18 and 50 cm, while pH is about 6.5 and Eh is positive at 1.5 cm; 18 cm filter length correspond in this test to 4 hours of residence time, 173 gr of ZVI and 403 gr of Lapillus. After this period, 28 cm filter length, corresponding to around 6 hours of residence time and 269 gr of ZVI and 627 gr of Lapillus, are needed to reduce the nickel input concentration until 2448 hours (3680 mg nickel mass input). After this time, the filter length from 28 to 50 cm seems to not have the same removal efficiency of the previous part of the column. A filter length greater than about 28 cm from column inlet has not the same removal efficiency observed in the filter zone closer to the inlet. Probably, this is due to the involvement of the ZVI in the farther filter zones from the inlet in other kinds of reactions, e.g. corrosion, during the time when nickel does not get to, leading to a decrease of its own nickel removal efficiency. This phenomenon is more evident in the 10:90 ZVI/Lapillus column.

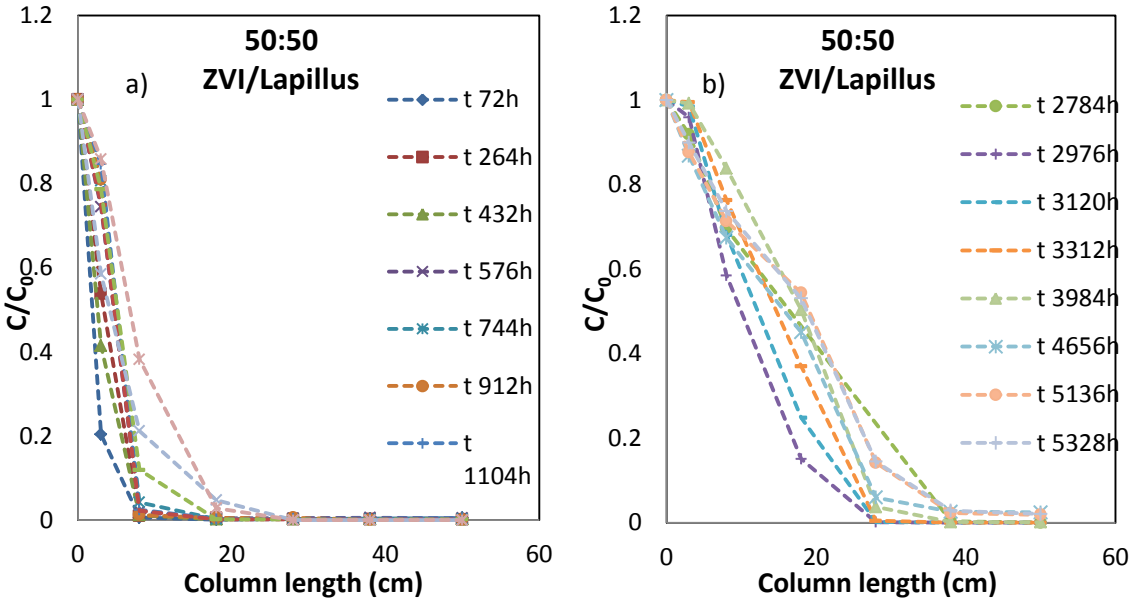

Figure 5-16 Nickel normalized concentration for 50:50 w.r. ZVI/Lapillus column test

t(h)\ dist (cm)	1.5		18		50		t(h)\ dist (cm)	1.5		18		50	
	pH	Eh (mV)	pH	Eh (mV)	pH	Eh (mV)		pH	Eh (mV)	pH	Eh (mV)	pH	Eh (mV)
272	6.88	23.4	8.8	-69.9	9.9	-144.9	2856	6.64	26.7	7.4	-1	7.6	-32
504	6.68	13.8	8.73	-103	9.26	-130.6	3456	6.82	5.3	7.2	-28.3	8.2	-74
1128	6.53	23.5	8.54	-90	9.14	-122.4	4176	6.8	6	6.1	59.7	6.6	56
1512	6.3	36	7.23	18.7	9.02	-115.5	4632	6.79	8.4	6.9	8.8	6.2	69

Table 5-4 pH and Eh(mv) values for 50:50 w.r. ZVI/Lapillus

In Figures 5-16 a) and b), the evolution of nickel normalized concentration for 50:50 w.r. column is shown. During a first interval (from the test beginning to about 2280 hours), the remediation occurs within 18 cm (Figure 5-16 a), in a second interval a filter thickness of 28 cm and afterwards 38cm (Figure 5-16 b) are enough for reducing of nickel concentration. In Table 5-4, the pH and Eh measured values for different sampling times are reported. During this time, the nickel relative concentration at 1.5 cm is lower than that in the previously analyzed tests. pH is higher, about 6.8, and the Eh is lower than tet ones at 1.5 cm in 10:90 and 30:70 tests. This is probably due to higher ZVI content. However, an 8 cm long reactive filter of ZVI/Lapillus mixture with 50:50 weight ratio, corresponding to 2 hours of residence time and 155 gr of ZVI, is enough to remediate nickel contaminated water until 1248

hours (1880 mg nickel mass input). At 18 cm, pH decreases from 8.8 to around 7.4 and Eh increases remaining in the negative values range, while at 50 cm pH decreases from 9.9 to 9 and Eh increases from -144 mV to -115 mV, during the first considered interval.

On the other hand, an 18 cm long filter , corresponding to 4 hours residence time and 350 gr of ZVI, is enough to remediate nickel contaminated water until 2280 hours (3420 mg nickel mass input).

The next interval, the second one, goes by until 5328 h. During this time, at 1.5 cm., pH is about 6.8 and Eh is about 10 mV, at 18 cm., pH decreases from 7.5 to 6.9 and Eh increases from negative to around 10 mV, while at the outlet pH decreases to 6.6 value and Eh becomes positive and equal to 56 mV, limited nickel concentration is detected at the outlet. However, 28 cm of 50:50 ZVI/Lapillus reactive filter, containing 543 gr of ZVI and corresponding to 6 hours of residence time, are enough to remediate nickel-contaminated water until 3312 hours (4980 mg nickel mass input). Subsequently, a 38 cm long filter is necessary, assuring a residence time of 8.6 hours and containing 1474 gr of ZVI, to reduce significantly the nickel concentration, until 3984 hours (6000 mg nickel mass input).

To better understand how nickel removal efficiency is developed and if and how it can influence the permeability, different histograms will be proposed to analyze in which sector the mass of nickel is mainly retained and how this changes with time.

In Figures 5-17 a) and b) and 5-18, the cumulative mass of nickel retained in each sector divided by the length of the sector is reported for different times, namely 432, 1440 and 2088 hours for 10:90 w.r. ZVI/Lapillus. It can be observed that the nickel mass input to the column is mainly retained by the first sector (from 0 to 3 cm from column inlet). The nickel retained in the first sector increases with time like that retained on the following sectors. However, the cumulative contaminant mass retained by each sector decreases as the distance from the inlet increases.

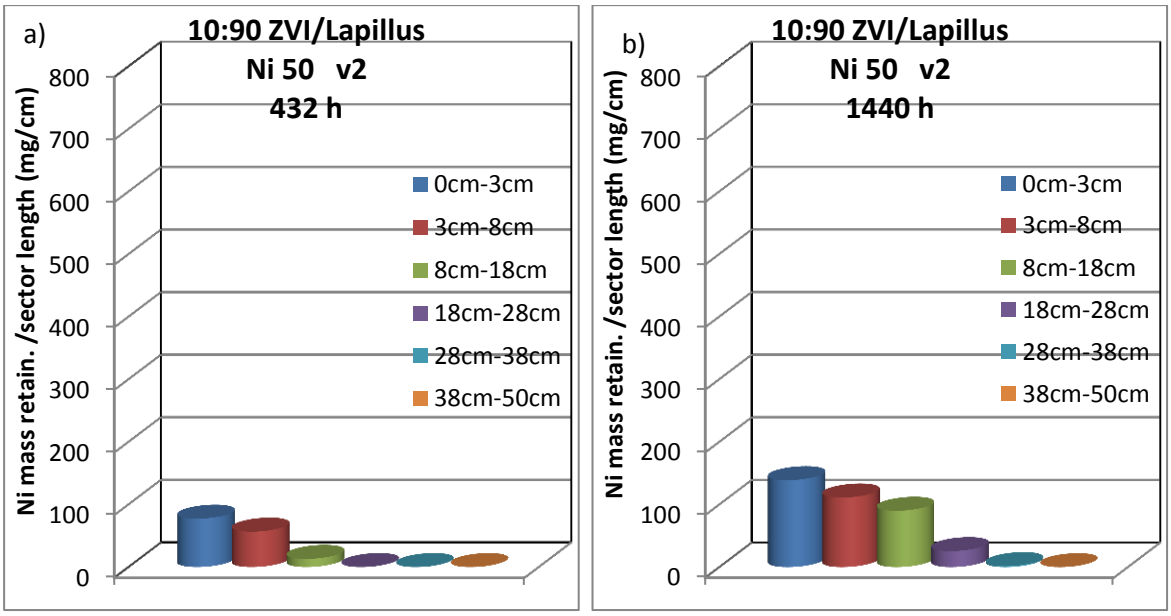

Figure 5-17 Nickel mass retained in each sector divided by the length of the sector in 10:90 w.r. ZVI/Lapillus column test at a) 432 hours and b) 1440 hours

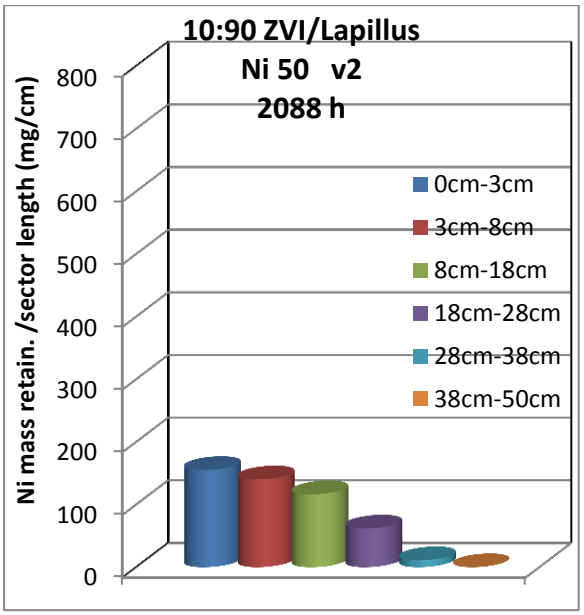

Figure 5-18 Nickel mass retained in each sector divided by the length of the sector in 10:90 w.r. ZVI/Lapillus column test at 2088 hours

In Figures 5-19, 5-20 and 5-21 cumulative Nickel mass retained in each sectors divided by the sector length for 30:70 w.r. ZVI/Lapillus is reported for 432 , 1440, 2088, 3144 and 5496 hours. Looking at the progressive variation in distribution of cumulative nickel mass retained by transversal section in each sector, it is possible to observe that the first three sectors, corresponding to distances from 0 cm to 18 cm from the column inlet seem to be the most efficient in the long term.

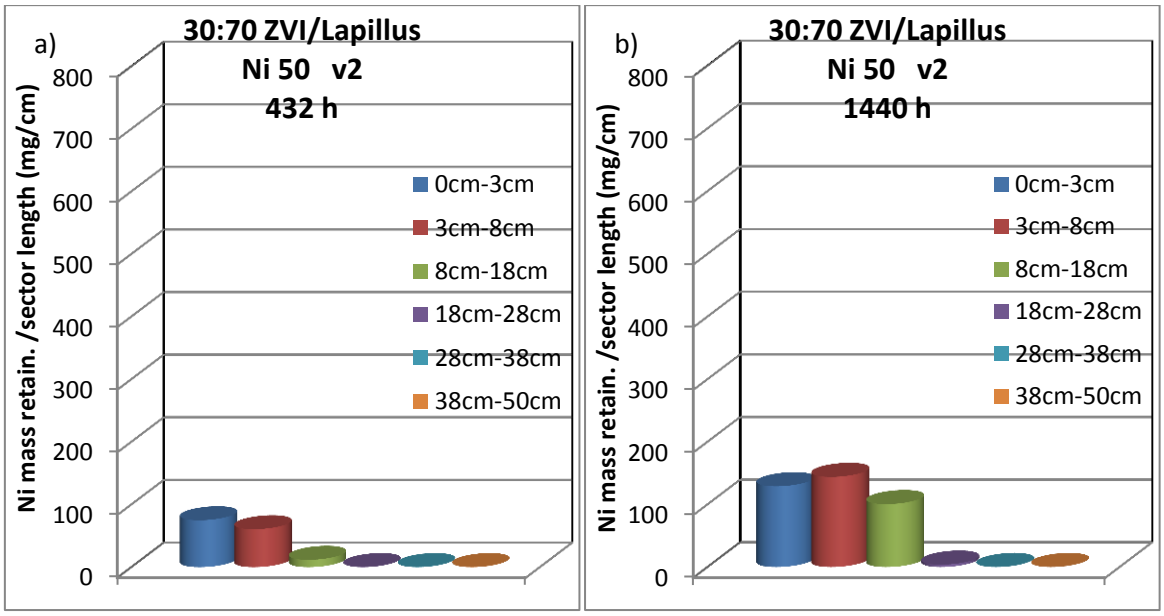

Figure 5-19 Nickel mass retained in each sector divided by the length of the sector in 30:70 w.r. ZVI/Lapillus column test at a) 432 hours and b) 1440 hours

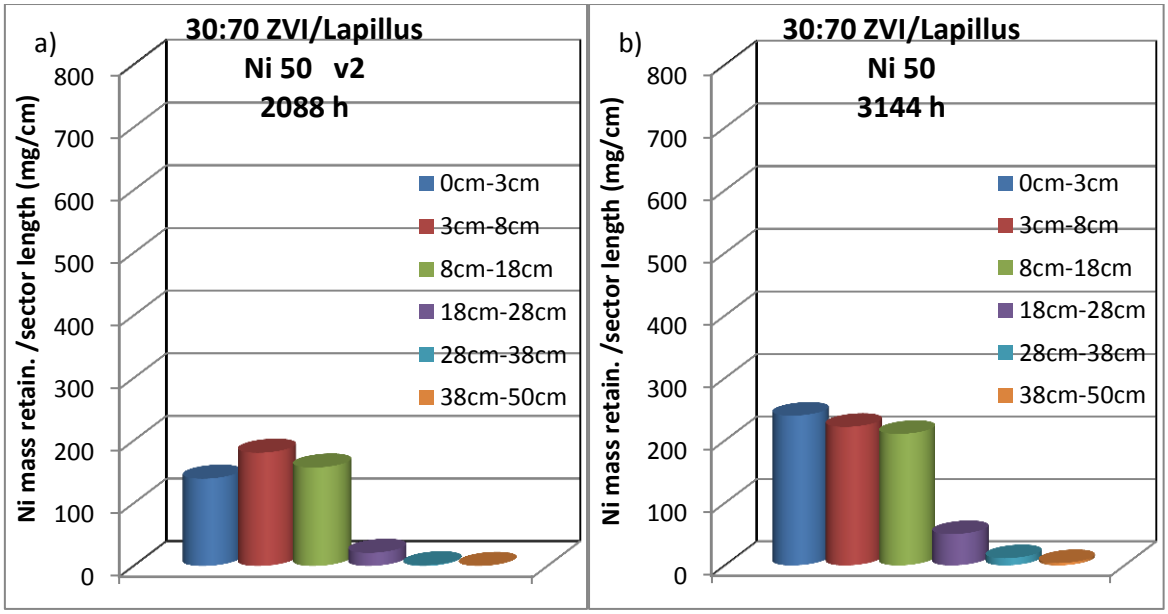

Figure 5-20 Nickel mass retained in each sector divided by the length of the sector in 30:70 w.r ZVI/Lapillus column test at a) 2088 hours and b) 3144 hours

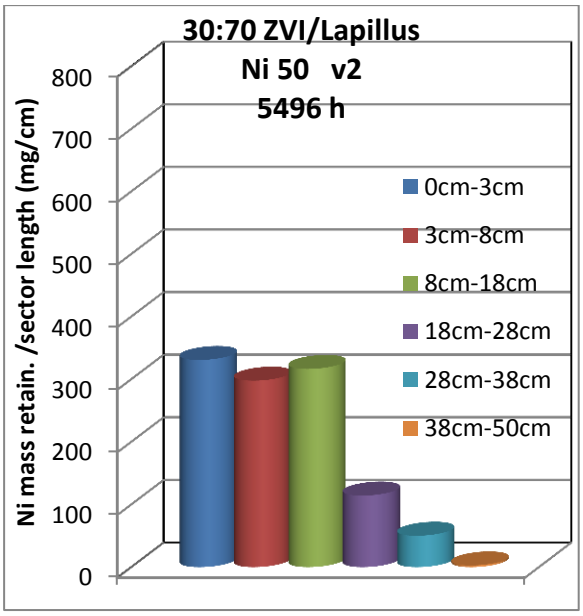

Figure 5-21 Nickel mass retained in each sector divided by the length of the sector in 30:70 w.r. ZVI/Lapillus column test at 5496 hours

In 50:50 w.r. ZVI:Lapillus, as is shown in Figures 5-22, 5-23 and 5-24 a), the nickel mass retained by section in the 3cm-8cm sector is always higher than that of the other sectors.

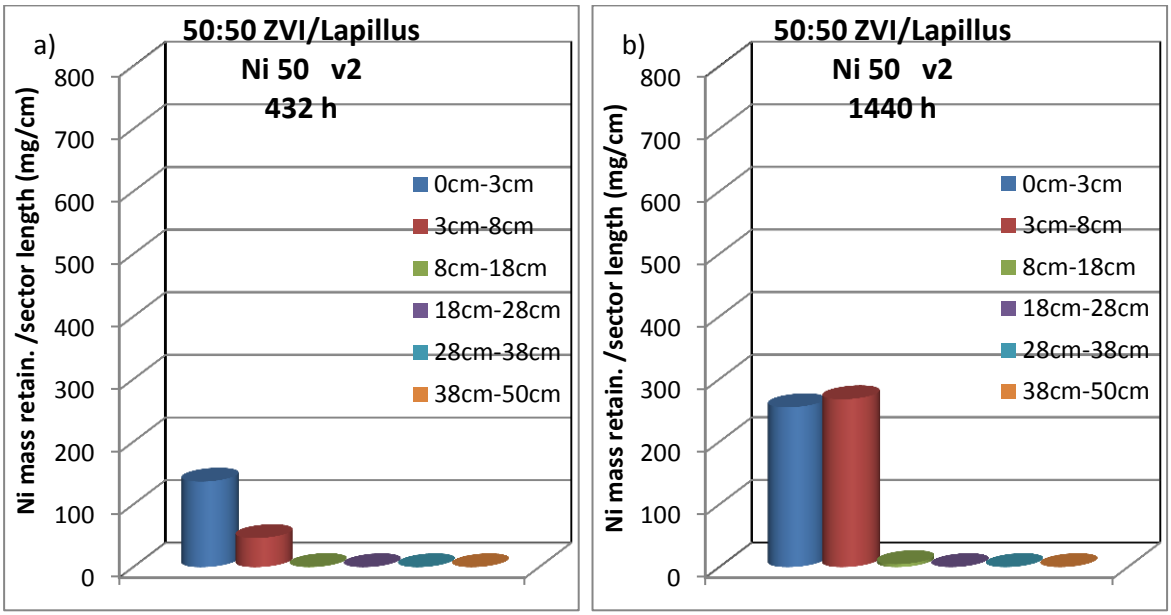

Figure 5-22 Nickel mass retained in each sector divided by the length of the sector in 50:50 w.r ZVI/Lapillus column test at a) 432 hours and b) 1440 hours

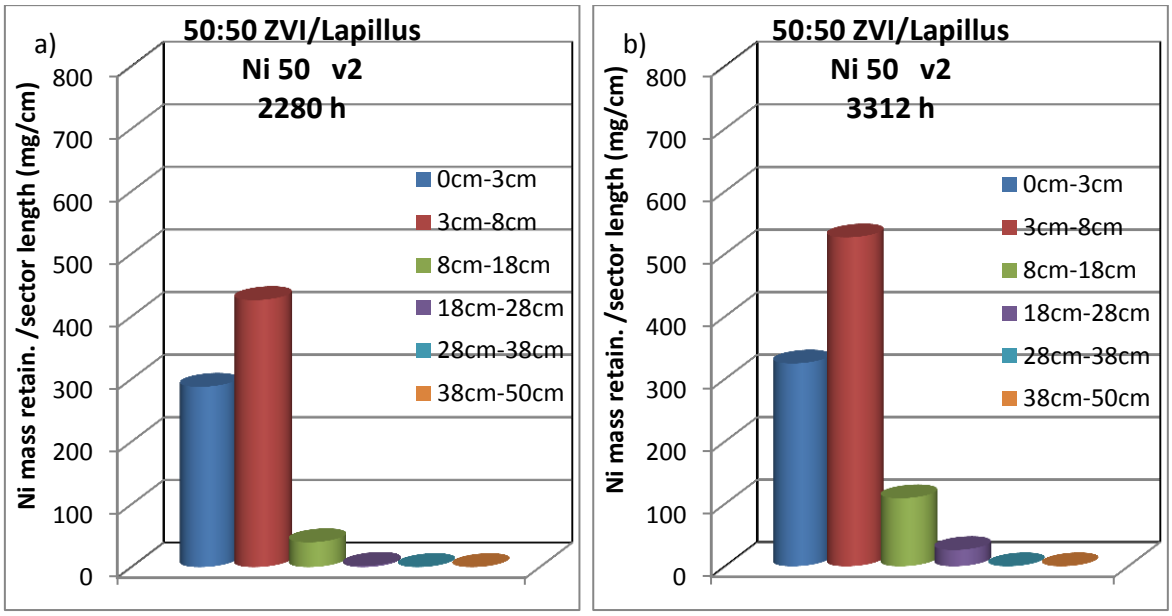

Figure 5-23 Nickel mass retained in each sector divided by the length of the sector in 50:50 w.r. ZVI/Lapillus column test at a) 2280 hours and b) 3312 hours

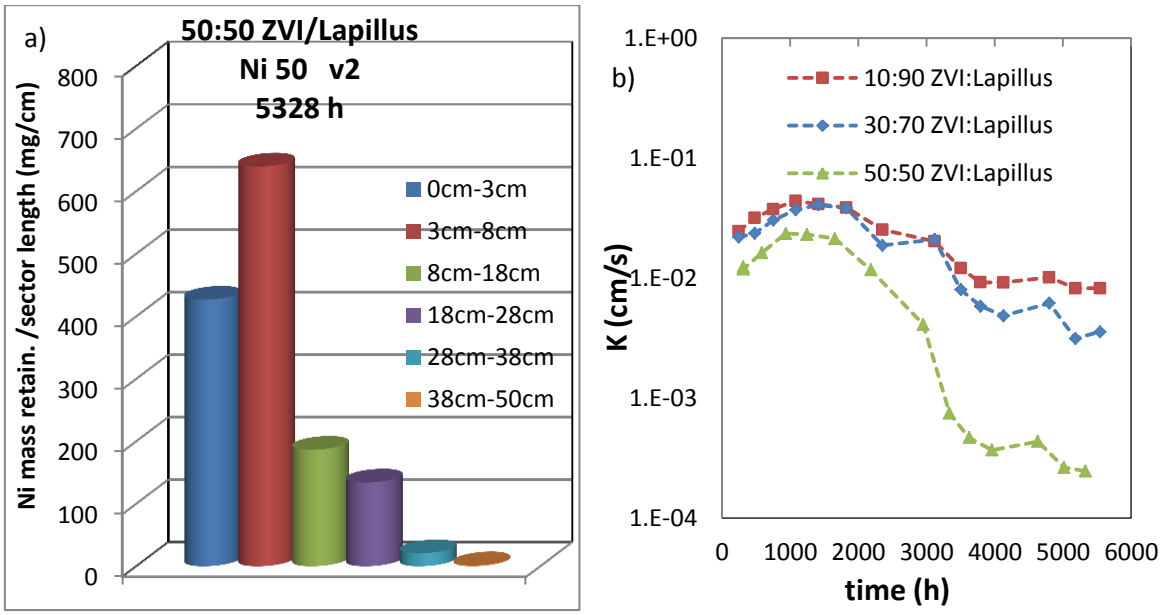

Figure 5-24 Nickel mass retained in each sector divided by the length of the sector in 50:50 w.r. ZVI/Lapillus column test at 5328 hours and b) hydraulic conductivity evolution as function of time

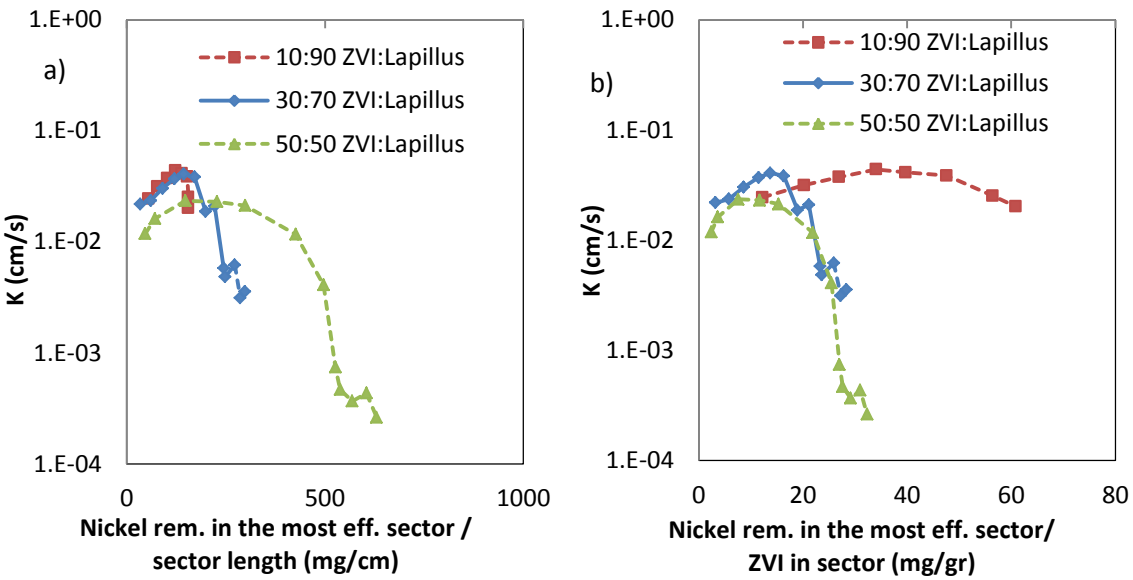

Figure 5-25 a) hydraulic conductivity as function of the nickel mass removed in the most efficient sector divided by the sector length and b) as function of the nickel mass removed in the most efficient sector divided by the ZVI mass content in the considered sector b

5.6.2.2 Hydraulic behavior

The hydraulic conductivity evolution with time for the three mixtures ZVI/Lapillus is shown in Figure 5-24 b). The highest reduction of hydraulic conductivity was observed in the mixture 50:50, while the best hydraulic behavior was observed for the mixture 10:90 w.r. This can be due mainly to higher quantity of ZVI corrosion products and gas formation (Caré et al., 2013). Furthermore the nickel retained and mineral precipitation can play a role. The effects of these factors can be localized in different filter zones. For example, the nickel retained mass would be more concentrated in the shorter filter zone close to the inlet, as the ZVI quantity is higher.

Regarding the corrosion effects, although it is not easy to individuate where the most quantity of the most expansive products are localized, some information can be gathered by considering the pH and Eh values.

Comparing the evolution of pH and Eh values with the hydraulic behavior it is possible to observe some correspondences between the data measured at the outlet (but also at 18 cm form inlet) and the time when the most permeability loss occurs. In fact, hydraulic conductivity reduction is slower as the ZVI content is smaller and this occurs after a certain interaction time. Considering the pH and Eh values evolution in

the three weight ratio tests, pH and Eh values ranges are larger in 50:50 w.r., than in the other tests, while the final pH and Eh values are almost the same. It means that 50:50 w.r. column passes through more different chemical conditions, but the values to which pH and Eh tends are similar for the three test. This is more evident if values at outlet are mainly taken into account. In fact, the most hydraulic conductivity loss seems to occur when the pH is decreasing at the outlet. Because the initial pH is higher in 50:50, the difference to be covered to have stable conditions is also higher. In particular, when the pH decreases from 9 at 1500 hours, permeability loss seems to star too.

In Figures 5-24a), hydraulic conductivity evolution is reported as function of the nickel mass retained by section in the most efficient sector as individuated for each weight ratios tested (Figure 5-25a) and as function of nickel mass retained in the most efficient sector divided by ZVI mass contained in the considered sector (Figure 5-25b).

Looking at the permeability evolution with time, the more rapid and higher loss of permeability is observed for higher ZVI content. There being more ZVI particles number in a section as ZVI content increases in weight ratio, after a certain time void volume is more reduced because of ZVI particle expansion, precipitates formation or other factors due to ZVI presence.

As was observed in the previous paragraph, not all the sections are equally interested by contaminant retention. In fact in the 10:90 w.r. column test, the sections comprised between 0 and 3 cm are those which contain the most cumulative quantity of nickel retained per section. The same thing is evident for the sector comprised between 3 and 8 cm of 50:50 ZVI/Lapillus w.r. column test. An intermediate phenomena, not allowing one to establish in the same evident way what column sector is more efficient, happens for 30:70 ZVI/Lapillus w.r. column test. However for this test, the sector between 3 and 8 cm can be considered the most efficient during the time. On the basis of these considerations, permeability evolution has been represented as a function of nickel mass retained by section located in the most efficient sector for each column test, in order to investigate whether the average mass of contaminant retained by the most efficient sections can be considered as cause of permeability loss. Except for the same hydraulic behaviour in the three tests

until a certain time (200 h), no correspondence between nickel retained in the most efficient section and permeability loss can be found.
However if the permeability evolution is represented in function of contaminant mass retained in the most efficient section divided by ZVI quantity contained in the section, a certain correspondence can be observed between permeability loss in 30:70 and 50:50 w.r.. The different hydraulic behaviour of 10:90 w.r. filter in this case can be due to the low ZVI content, that does not entail important permeability loss, and to the high Lapillus quantity that can be an important factor of nickel retention and that avoids high permeability loss.

5.6.2.3 Specific removal rate

The three tested ZVI/Lapillus mixtures with different weight ratios have been characterized by different rates of nickel retention and different maximum quantity of nickel that can be retained in each transversal section. This is mainly due to the different composition of the mixtures and different proportion between ZVI and Lapillus particles in the transversal section and along the filter among the three tests at different weight ratios.
To investigate how the specific removal rate can vary along the column, with time and for each ZVI/Lapillus tested mixture, the partial mass of nickel retained by each column sector at different intervals of time was calculated and divided by the mass of ZVI or by the total mass of reactive materials contained in each sector. These values are shown in normal and semi-logarithmic scale for 10:90 w.r. test, in figures 5-26 and 5-27, for 30:70 w.r. test in figure 5-28 and 5-29 and for 50:50 w.r. test in figure 5-30 and 5-31 respectively.
Looking at the graphs the influence is evident of advection phenomenon, representing an important factor of contaminant transport through the porous reactive material under the experimental conditions of the tests carried out. As can be observed in the semi-logarithmic graphs, the specific removal rate for each sector tend to a certain value. This is more evident for 10:90 w.r. where a faster removal efficiency exhaustion occurs, due to the lower ZVI content. In the tests where ZVI content is higher, the dispersion of specific removal rate is higher. It should be related to the faster removal efficiency exhaustion in tests with less ZVI content.

Looking at the graphs in natural scale, different information can be drawn up. In particular, the variation of nickel removal capacity of each sector is more evident and the presence of sectors more efficient than others. In correspondence to the reactive media placed in the first sector (0-3cm) the highest specific removal rate was developed. It happens at the beginning of the tests. Afterwards, in the 10:90 w.r. test the specific removal rate decreases for the first sector, while it increases for the next sectors, never exceeding the value relative to the first sector at the considered time (except for the 8-18 cm sector). This does not happen in the other w.r. tests. In fact, in 30:70 w.r. when the coefficient relative to the first sector decreases with time, that obtained for 3-8 cm and 8-18 cm sectors increases going beyond the first. For a certain time the specific removal rate of the 8-18 cm sector is higher than that of the 3-8 cm sector. The same thing happens for 50:50 w.r. tests where after about 500 hours the specific removal rate related to the 3-8 cm sector is always the highest.

The specific removal rate obtained for the column sectors included from 18 to 50 cm have generally lower values than those relative to 0 – 18 cm of column. Some factors of this behaviour can be found in the lower contaminant concentration that arrives at the higher filter length, if a retention capacity function of the contaminant concentration is assumed, or in the lower removal efficiency observed at the higher filter length.

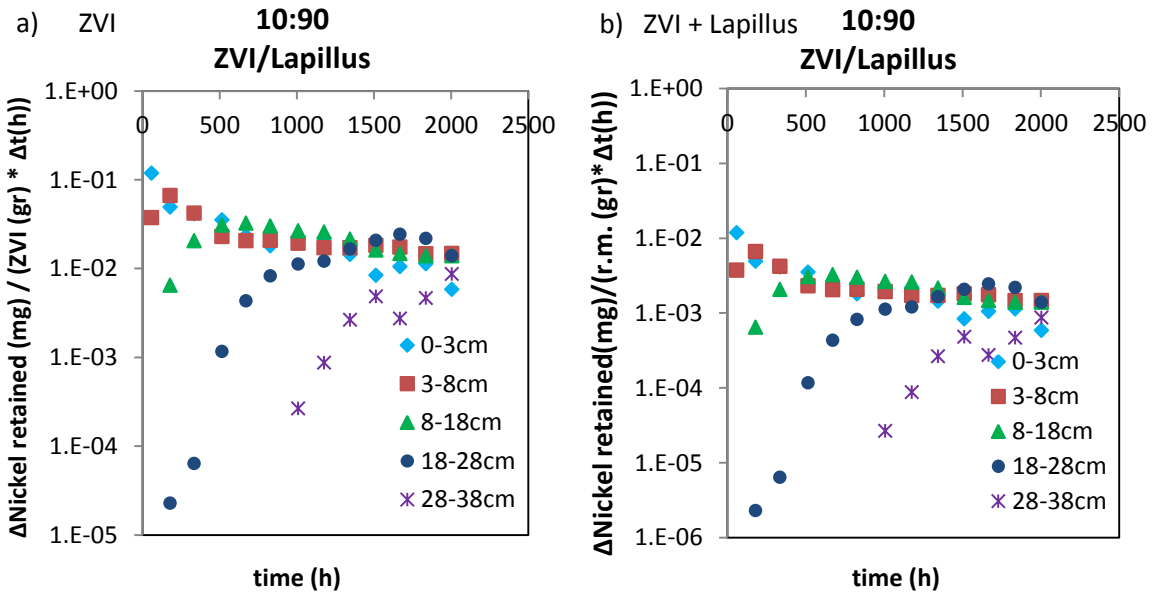

Figure 5-26 a) Partial Nickel mass retained in each column sector during each interval divided by the ZVI mass contained in the sector per unit time (semilog scale); b) Partial Nickel mass retained in each column sector during each interval divided by the reactive material mass contained in the sector per unit time (semilog scale) in 10:90 w.r. column test

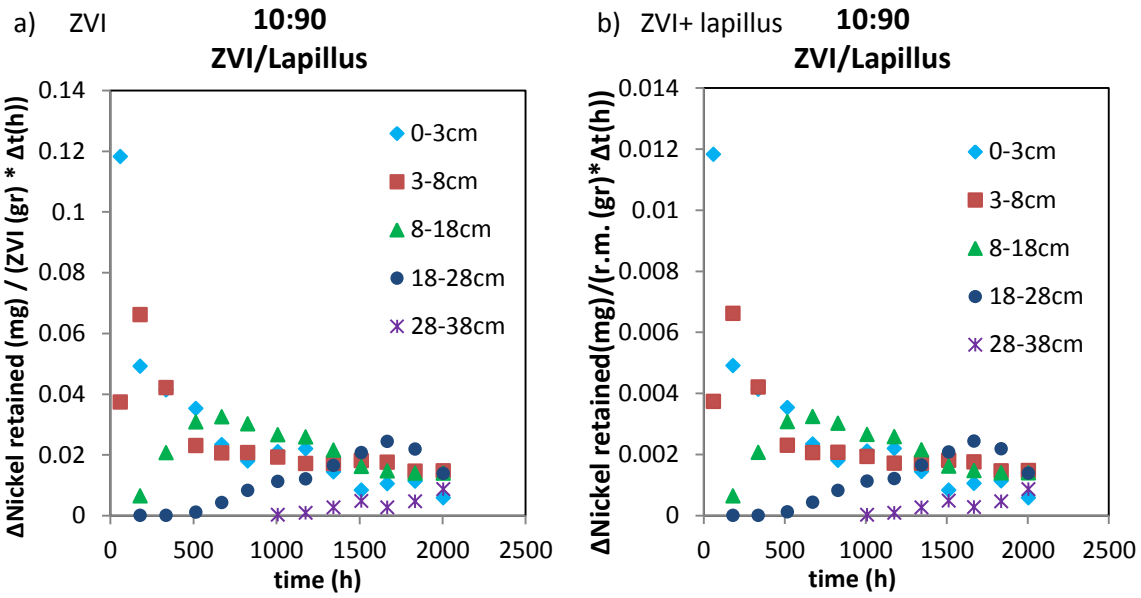

Figure 5-27 a) Partial Nickel mass retained in each column sector during each interval divided by the ZVI mass contained in the sector per unit time; b) Partial Nickel mass retained in each column sector during each interval divided by the reactive material mass contained in the sector per unit time in 10:90 w.r. column test

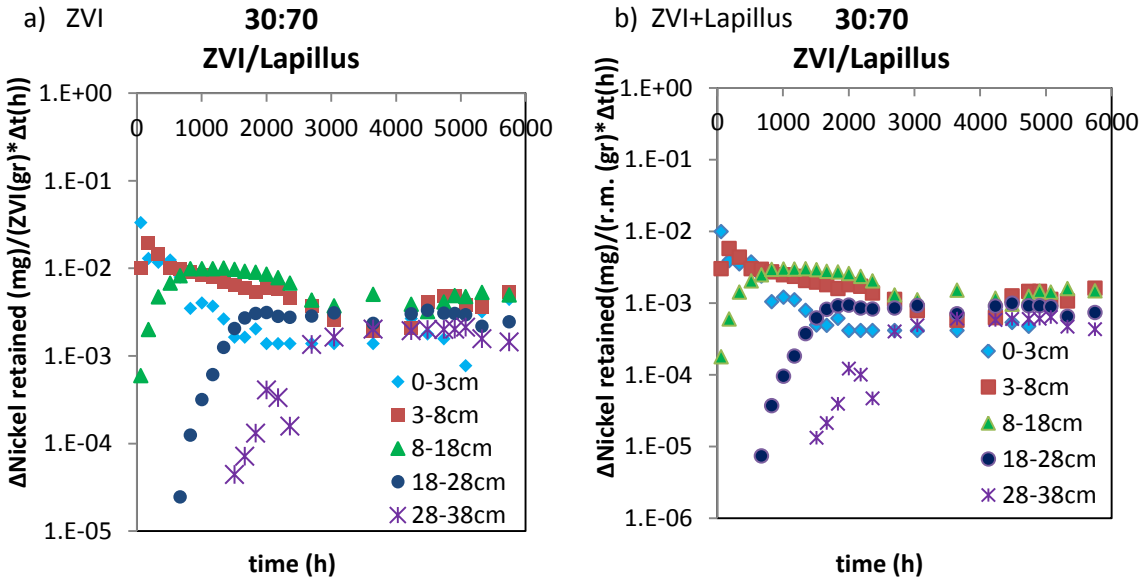

Figure 5-28 a) Partial Nickel mass retained in each column sector during each interval divided by the ZVI mass contained in the sector per unit time (semilog scale); b) Partial Nickel mass retained in each column sector during each interval divided by the reactive material mass contained in the sector per unit time (semilog scale) in 30:70 w.r. column test

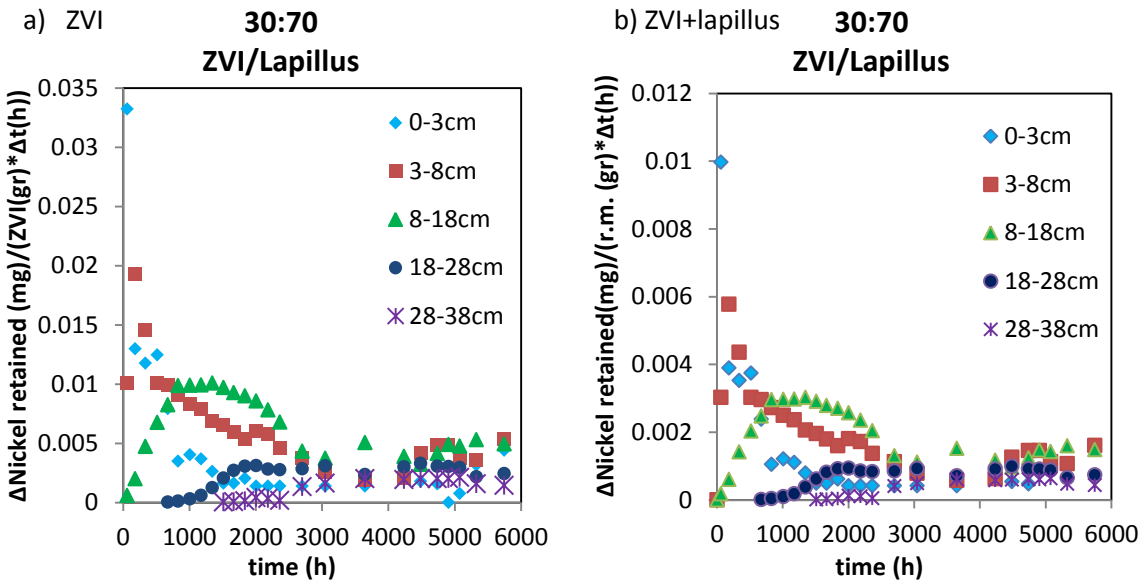

Figure 5-29 a) Partial Nickel mass retained in each column sector during each interval divided by the ZVI mass contained in the sector per unit time; b) Partial Nickel mass retained in each column sector during each interval divided by the reactive material mass contained in the sector per unit time in 30:70 w.r. column test

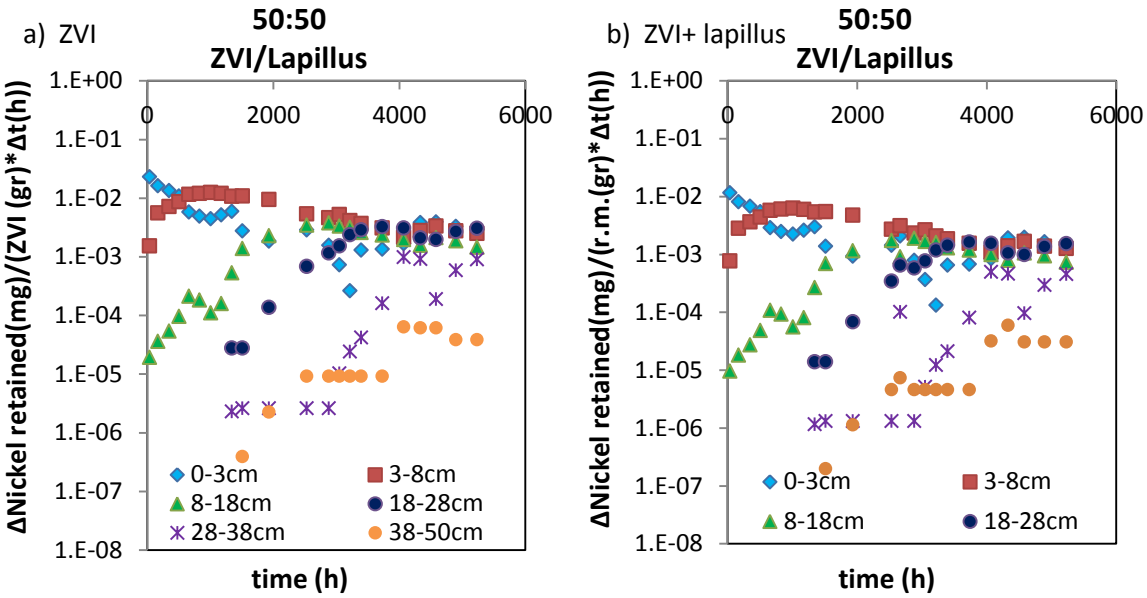

Figure 5-30 a) Partial Nickel mass retained in each column sector during each interval divided by the ZVI mass contained in the sector per unit time (semilog scale); b) Partial Nickel mass retained in each column sector during each interval divided by the reactive material mass contained in the sector per unit time (semilog scale) in 50:50 w.r. column test

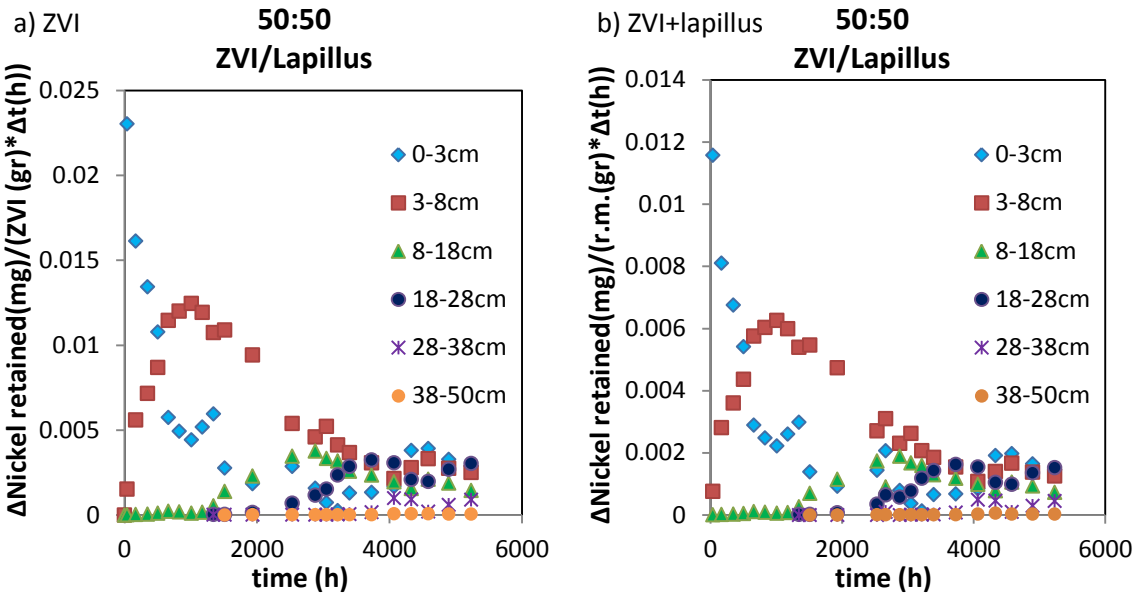

Figure 5-31 a) Partial Nickel mass retained in each column sector during each interval divided by the ZVI mass contained in the sector per unit time; b) Partial Nickel mass retained in each column sector during each interval divided by the reactive material mass contained in the sector per unit time in 50:50 w.r. column test

5.6.2.4 Comparison among the granular mixtures ZVI/lapillus at different w.r. based on the same ZVI content

Different comparisons can be made among the three tested weight ratios based on the same ZVI content. In Table 5-5 different filter thickness with the corresponding ZVI mass and residence time is reported. The residence time is calculated using the initial porosity. The ratio between ZVI and Lapillus particles numbers was calculated considering the d_{50} of each component of mixtures.

ZVI content (gr)	22	28	77	77	50	58	365	349
w.r. filter length (cm)	10:90 8 cm	30:70 3 cm	10:90 28 cm	30:70 8 cm	10:90 18 cm	50:50 3 cm	30:70 38 cm	50:50 18 cm
T res (h)	1.7	0.66	6	1.8	3.86	0.68	8.5	4
ZVI: Lapillus particles number	1:63	1:16	1:63	1:16	1:63	1:7	1:16	1:7

Table 5-5 characteristics of column tests considered in comparison based on the same ZVI content

The first comparison can be made considering the 8 cm of 10:90 w.r. test (22 gr of ZVI) and 3 cm of 30:70 w.r. test (28 gr of ZVI).

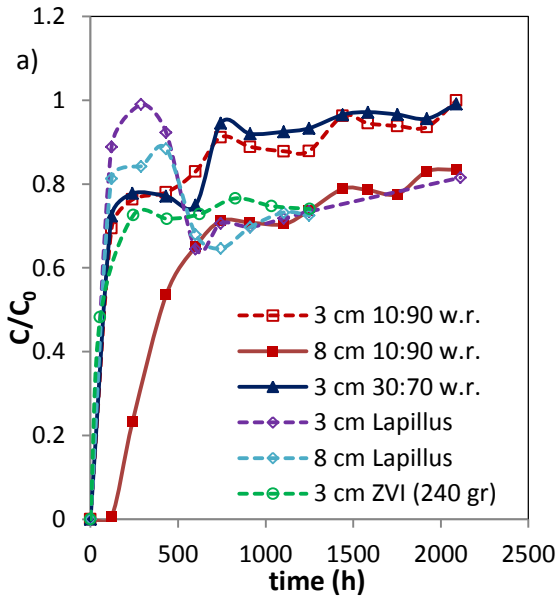

Figure 5-32 a) Nickel normalized concentration evolution determined over time at 3 cm of 30:70 w.r. column test and at 8 cm of 10:90 w.r. column test and at other benchmark

In Figure 5-32 a) the Nickel normalized concentration evolution measured at 3 cm of 30:70 w.r. ZVI/Lapillus column test and that at 8 cm of 10:90 w.r. ZVI/Lapillus column test are shown using continuous lines. As it is possible to observe, 8 cm of 10:90 w.r. filter seems to be more efficient than 3 cm of 30:70 ZVI/Lapillus w.r. mixture. Its Nickel removal efficiency loss proceeds more slowly and the residual efficiency remains higher during the time than that of the 3 cm long filter of 30:70 w.r. ZVI/Lapillus that contains the same ZVI weight and less Lapillus quantity.

At 120 hours the relative concentration is equal to 0.7 for 30:70 w.r and 0.006 for 10:90 w.r. After 600 hours, it is about 0.9 for 30:70 w.r. and 0.7 for 10:90w.r. After 2000 hours of interaction, it is around 0.99 for 30:70 w.r. column tests and about 0.8 for 10:90 w.r. There are different variables that can play a role in this behaviour: advection, diffusion, dispersion and reaction term. Both columns were carried out under the same flow velocity. This means that the advection term is the same and that the contaminant front should take the same time to reach a certain filter length, under the same experimental conditions.

The other three terms that can influence the interaction between contaminant flow and reactive material are dispersion, diffusion and reaction terms. Probably, diffusion plays a minor role with respect to the effects of the other phenomena, considering the number of Peclet and the relative higher importance of advection and dispersion terms. However, diffusion effect should be almost the same along the column and in both tests, considering that the grain size distribution is almost the same, as tortuosity. Dispersion effects on contaminant concentration evolution can be more evident as the considered point is longer from the input in the main flow direction, corresponding to different times from test beginning. To investigate whether diffusion and dispersion have influence on contaminant concentration evolution with time and along the column, it is possible to compare the 3 cm and 8 cm of column length of the pure Lapillus test. This comparison shows a light influence of these two phenomena on the contaminant concentration evolution.

To investigate the relative influence of each phenomenon on contaminant concentration evolution with time, a comparison can be made between the results related to 8 cm long pure Lapillus filter and those of 8 cm long 10:90 w.r. filter. The difference between the two considered cases during the first 600 hours of interaction suggests the influence of the presence of ZVI on Nickel removal represented by the reaction term. In fact, the higher removal efficiency of 10:90 w.r. 8 cm long filter compared to that of the pure Lapillus filter of the same length that can be observed during the first 600 hours of interaction can be due to the ZVI removal efficiency. Furthermore, the superposed experimental data of both tests during the subsequent time can suggest that contaminant retention on Lapillus can be the main removal phenomena after 600 hours for the mixture test and that a second time characterized by a lower Nickel removal efficiency of ZVI has been developed.

However, the role of ZVI and especially its distribution along the column seem to be really important for Nickel removal, related to the residence time too. Nickel normalized concentration evolution with time is reported for 3 cm length of 10:90 and 30:70 ZVI:Lapillus weight ratios filters and for 8 cm of 10:90 w.r. columns in Figure 5-32 a). 8 cm of the first and 3 cm of the latter filter correspond to the same ZVI content. In the same Figure 5-32 a) normalized concentration for 3 cm of pure ZVI column length, containing 240 g of ZVI, and that for 3 cm and 8 cm of pure Lapillus column lengths are reported too.

The evolution of Nickel concentration at 3 cm of 30:70 w.r. column length is almost the same as that at 3 cm of 10:90 w.r. filter length. This can suggest that the optimized ZVI content in 3 cm of column is that of the 10:90 w.r, because it maximizes the Nickel removal efficiency. This means also that in the first 3 cm of 30:70 w.r. column, the ZVI content can be in excess in relation to the Nickel removal efficiency that can be developed in 3 cm of column length, in the considered interaction interval. This is more evident compering the results above-considered to that measured at 3 cm of pure ZVI column. The experimental data relative to 3 cm length of the three considered tests are overlapped until 600 hours of interaction, suggesting that the optimal ZVI content for certain filter length and time exists. Considering the three tests carried out, the best ZVI content for the 3 cm column length and the assured residence time is that of the 10:90 w.r. test. This is true until 600 hours, after this time pure ZVI 3 cm long filter has a higher residual removal efficiency than the other tests. 600 hours correspond to 900 mg of input Nickel mass. 3 cm and 8 cm of the carried out column tests lengths mean about 0.66 and 1.7 hours of residence time respectively.

The evolution of the relative concentration corresponding to 8 cm of 10:90 w.r. column and 3 cm of 30:70 w.r. column, as with that at 3 cm of pure ZVI column, shows the ability of lapillus to optimize the removal efficiency of the ZVI and the influence of residence time compared to the ZVI content, for certain contaminant initial concentration and constant velocity. In fact, Lapillus plays an important role, because it is able to reduce the Nickel normalized concentration to 0.7 value if it is used as pure reactive material. The importance of residence time for Ni removal was highlighted also for ZVI/Pumice mixtures (Moraci and Calabrò, 2010; Calabrò et al. 2012; Bilardi et al. 2013a; Moraci et al. 2014)

In Figures 5-33 a) and b), some comparisons of Nickel removal efficiency using the mixtures at different weight ratios are shown. In Figures 5-33 a), the evolution of Nickel normalized concentration measured at 18 cm of 10:90 ZVI/Lapillus w.r. filter and at 3 cm of 50:50 ZVI:Lapillus w.r. filter corresponding to 50 and 58 g of ZVI content respectively are reported. As the benchmark tests, 3 cm of pure ZVI column test and18 cm of pure Lapillus column test, are considered too. A higher removal efficiency is observed for 18 cm long 10:90 w.r. filter.

The same length of pure Lapillus filter does not have the same removal efficiency but its behaviour is similar to that of 3 cm pure ZVI filter and 3 cm of 50:50 w.r. filter. In 5-32 b), Nickel relative concentration is reported for 8 cm of 30:70 ZVI/Lapillus w.r. filter and for 28 cm of 10:90 ZVI/Lapillus w.r. each one containing 77 g of ZVI.

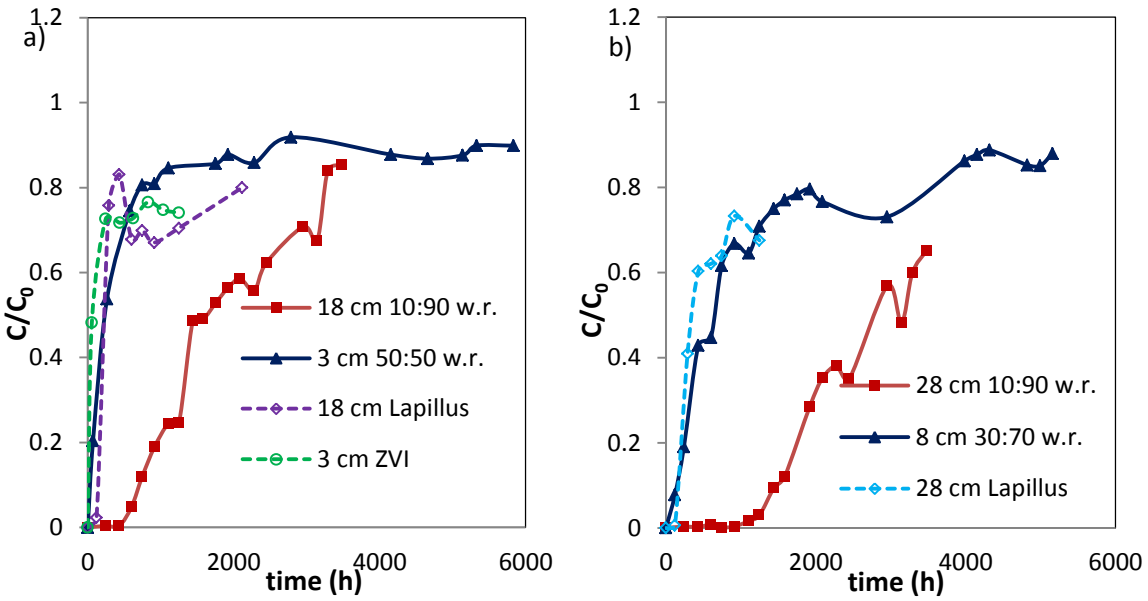

Figure 5-33 a) Nickel normalized concentration evolution determined over time at a) 18 cm of 10:90 w.r. and 3 cm of 50:50 w.r. column tests, 18 cm of lapillus and 3 cm of ZVI and at b) 28 cm of 10:90 w.r., 8 cm of 30:70 w.r. and 28 cm of lapillus.

The benchmark is represented using a dashed line and it is referred to 28 cm of pure Lapillus filter thickness. It is possible to observe that the Nickel removal behaviour is similar using a thickness of 28 cm and 8 cm of Lapillus and 30:70 ZVI/Lapillus w.r. filters respectively. Furthermore, it is possible to hypothesize that the high difference in terms of removal between the 28 cm of pure Lapillus filter and the same length of 10:90 ZVI/Lapillus w.r. filter should be due only to the presence of the ZVI. The difference observed between the efficiency of 28 cm long 10:90 w.r. and 8 cm long 30:70 w.r. filters can be due to the higher residence time

In Figure 5-34a) Nickel normalized concentration evolution at 38 cm of 30:70 ZVI:Lapillus w.r. column test and at 18 cm of 50:50 ZVI/Lapillus w.r. column test is shown (Table 5.5). The first considered length corresponds to 365 gr of ZVI and 8.5 hours of residence time. The second one length contains 349 g of ZVI and the corresponding residence time is 4 hours. Both considered thicknesses are highly

efficient until about 2000 hours. Afterwards the 18 cm long filter of 50:50 w.r. starts to reduce Nickel removal efficiency before the 38 cm long filter of 30:70 w.r. mixture. This can probably be due to Lapillus residual removal efficiency, considering its higher quantity, and to the higher residence time ensured by the most efficient test . Another comparison can be made to better understand the parameters mostly influencing the Nickel removal efficiency using ZVI/Lapillus mixtures. The previous couples of filters lengths at different weight ratio selected in order to have the same ZVI content can be compared to see how much ZVI mass and column length, as the residence time, influence Nickel removal.

In Figure 5-34 b) the Nickel mass retained is shown as function of the Nickel mass input for 8 cm long 10:90 w.r. filter and 3 cm long 30:70 w.r. filter containing each one about 22 g of ZVI. In the same graph, data related to 28 cm long 10:90 w.r. filter and to 8 cm long 30:70 w.r. filter are reported too. Each one of these two tests contains about 77 g of ZVI. The less efficient is the considered 3 cm long filter test corresponding to 0.66 hours of residence time, the most efficient is that which is 28 cm long that needs 6 hours to be passed through. Furthermore, both tests, where a thickness of 8 cm is considered, have the same removal efficiency, although one contains a mass of ZVI almost four times greater than the other. This is surely true until 3000 mg of Nickel mass input. The residence time corresponding to 8 cm filter length in this case about 1.8 hours.

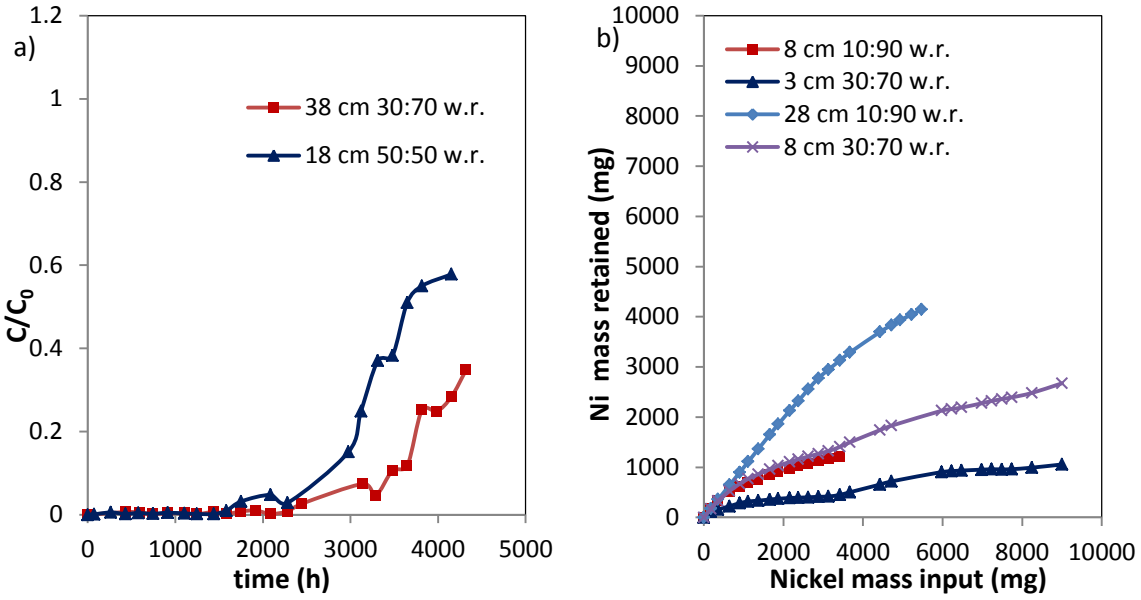

Figure 5-34 a) Nickel normalized concentration evolution determined along time at 38 cm of 30:70 w.r. and 18 cm of 5 0:50 w.r. column tests and b) Nickel retained mass as function of Nickel mass input at 8 cm of 10:90 w.r., 3 cm of 30:70 w.r., 28 cm of 10:90 w.r. and 8 cm of 30:70 w.r. column tests.

In Figure 5-35 a) Nickel mass retained is shown as function of the Nickel mass input for 8 cm long 10:90 w.r. filter and 3 cm long 30:70 w.r. filter, containing each one about 22 gr of ZVI, and for 18 cm long 10:90 w.r. filter and 3 cm long 50:50 w.r. filter, containing about 50 g of ZVI. It can be observed that the most efficient test is the 18 cm long filter of 10:90 w.r. mixture, while the 8 cm long filter of 10:90 w.r. mixture and the 3 cm long filter of 50:50 w.r. mixture have almost the same Nickel removal efficiency, although the 8 cm long filter of 10:90 w.r. mixture is slightly more efficient and it contains less than half ZVI content of the 3 cm long filter of 50:50 w.r. mixture. The residence time corresponding to 8 cm long filter is about 1.8 hours, while that relative to 3 cm is about 0.68 hours.

In Figure 5-35 b) Nickel retained mass is shown as function of Nickel mass input for the 38 cm long filter of 30:70 w.r. mixture, the 18 cm long filter of 50:50 w.r mixture, containing each one about 350 g of ZVI, and for the 18 cm long filter of 10:90 w.r. mixture and the 3 cm long filter of 50:50 w.r. mixture, containing both about 50 g of ZVI. It can be observed that the Nickel removal efficiency is almost the same up to 2000 mg of Nickel in input for both 18 cm long filters and for 38 cm long filters. However, until 5000 mg of Nickel input, the removal efficiency of the 38 cm long filter of 30:70 w.r. mixture and 18 cm long filter of 50:50 w.r. mixture is the same and the ZVI is the same in both tests.

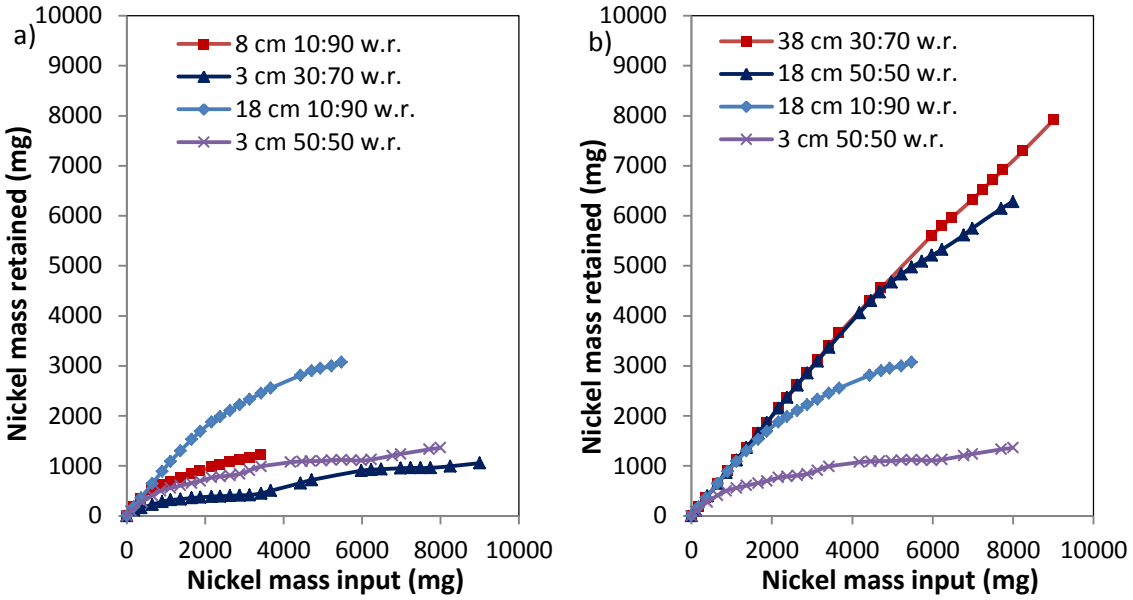

Figure 5-35 a) Nickel mass retained mass as function of Nickel input mass at 8 cm of 10:90 w.r., 3 cm of 30:70 w.r., 18 cm of 10:90 w.r. and 8 cm of 50:50 w.r. column tests and b) at 38 cm of 30:70 w.r., 18 cm of 50:50 w.r., 18 cm of 10:90 w.r. and 3 cm of 50:50 w.r. column tests.

However, from this time to the end of the tests, the 38 cm long filter is the most efficient as can be expected considering the higher Lapillus content and residence time than the 50:50 w.r. mixture 18 cm long filter.

A comparison of the experimental results obtained by the three ZVI/Lapillus weight ratio column tests can be made considering the same residence time or the same filter thickness.

In each of the following graphs, reported in Figure 5-36, 5-37 and 5-38, the Nickel mass retained is represented for each test for a certain filter length in function of the Nickel mass input. The Nickel mass retained in 3 cm of 10:90 w.r. and 30:70 w.r filter tests is almost the same and less than that removed in 3 cm of 50:50 w.r. filter (Figure 5-36 a). However the Nickel removal efficiency of the 3 cm long filter is limited and that of 50:50 w.r. tests after 8000 mg of Nickel input is around 15% (Figure 5-36 b).

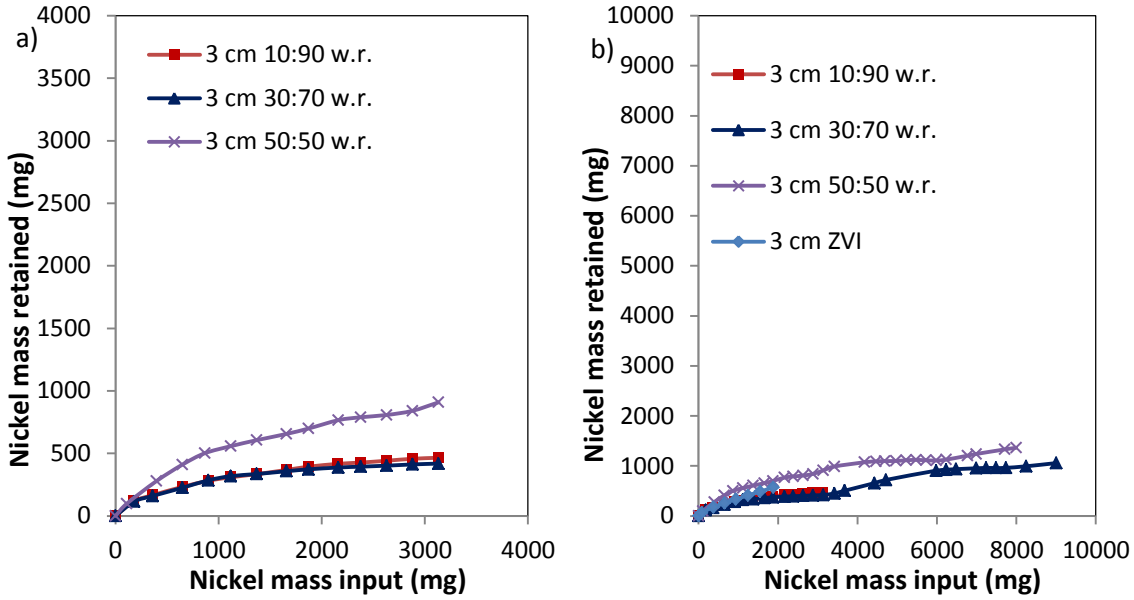

Figure 5-36 a) Nickel mass retained as function of Nickel mass input in 3 cm filter length of the three tested weight ratios until 300 mg of Nickel mass input and b) until 8000 mg of Nickel mass input

Considering a filter thickness of 8 cm for the three weight ratio mixtures, as shown in Figure 5-37 a), the efficiency of 10:90 w.r. and 30:70 w.r. filters is similar, while the same length of 50:50 w.r. filter has a much efficiency. However after 3000 mg of Nickel input mass, the removal efficiency of the 8 cm long filter of 50:50 w.r. mixture is about 50% only.

Considering the thickness of 18 cm for the three tests, the removal efficiency is almost the same for all the tests until 2000 mg of Nickel input, as can be observed in Figure 5-37 b). After this time, the removal efficiency decreases more quickly as the ZVI mass contained in the mixture is less. The residence time corresponding to 18 cm of filter length is about 3.8 hours. At the end of the test, the 18 cm of 50:50 w.r. filter has a removal efficiency equal to 78%.

As can be observed in Figure 5-38 a) and b), where 28 and 38 cm of filter thickness are compared respectively, the difference in removal efficiency among the three ZVI:Lapillus weight ratio tests decreases as the length of the considered filter increases. In fact, Nickel removal efficiency is the same for the three tests until 3000 mg and until 4000 mg of Nickel in input, considering 28 and 38 cm filter lengths respectively. After this value of Nickel mass input, a difference in removal efficiency can be observed. However, the 50:50 w.r. test is the most efficient and has a removal

efficiency equal to 95.8% and 98.8%, if 28 and 38 cm are considered respectively, after 8000 mg of Nickel mass in input.

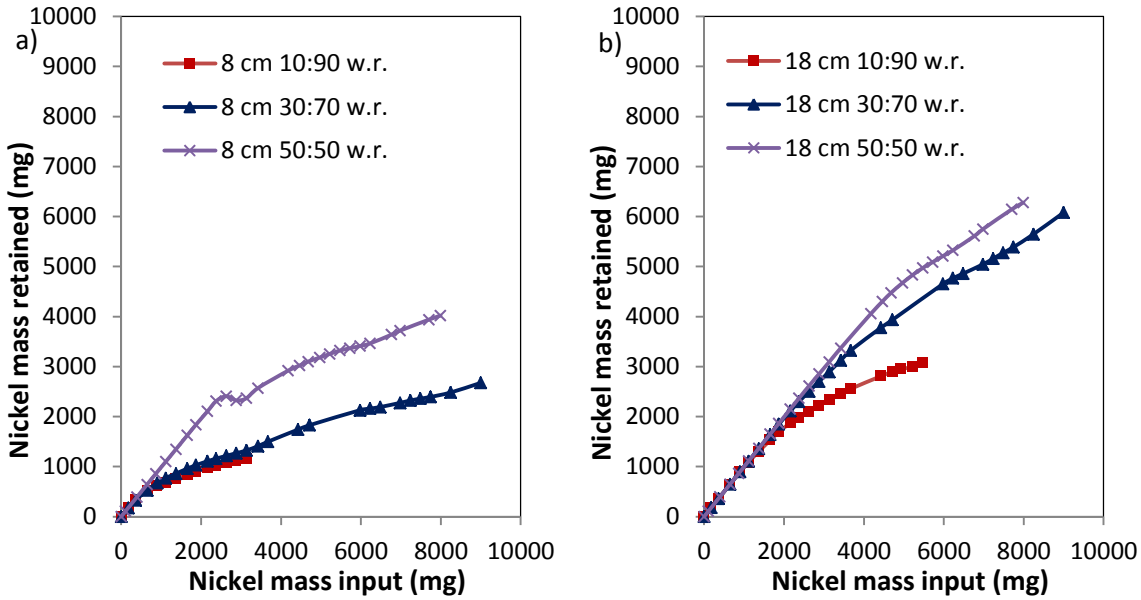

Figure 5-37 a) Nickel mass retained as function of Nickel mass input in 8 cm filter length and b) 18 cm filter length of the three tested weight ratios

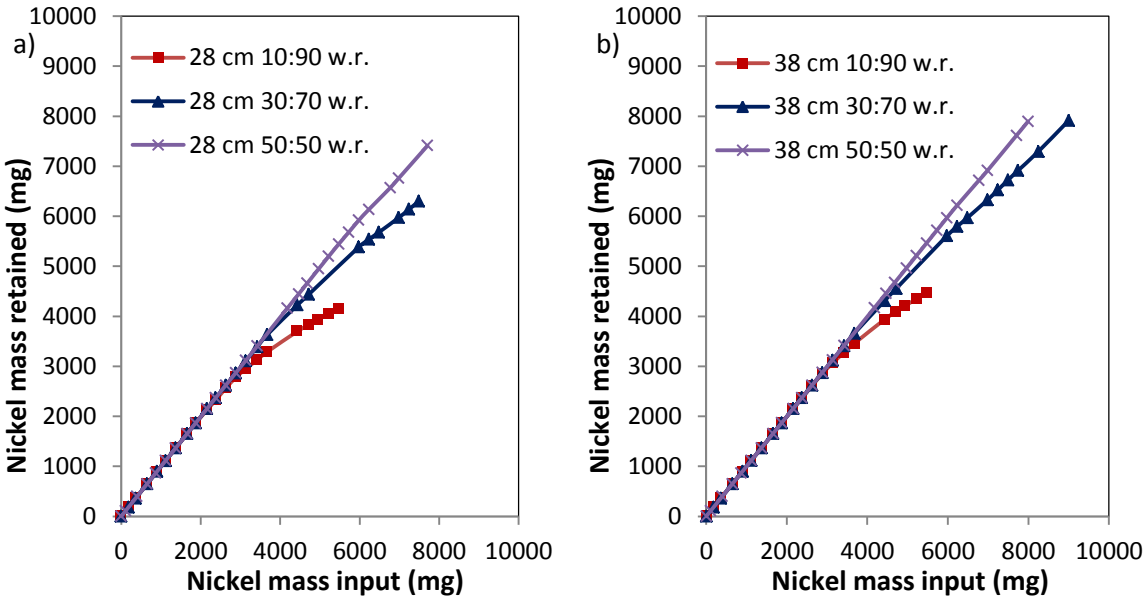

Figure 5-38 a) Nickel mass retained as function of Nickel mass input in 28 cm filter length and b) 38 cm filter length of the three tested weight ratios

5.6.3 Flow velocity influence

Similarly to what has been already done with ZVI/Pumice mixtures (Bilardi et al. 2012c), three column tests varying the flow velocity were carried out in order to study the influence of flow velocity on long-term Nickel removal efficiency and hydraulic behaviour. The characteristics of the columns are summarized in Table 5-6. The used weight ratio ZVI:Lapillus was 30:70, while the Nickel initial concentration was 50 mg/L. This means that only the residence time varies significantly among the three tests. For the test performed using a constant average flow velocity v_1 equal to 0.055 mm/min (9.2e-07 m/s and 0.079 m/d), the initial residence time was about 56 hours, for that using v_2 equal to 0.276 mm/min (4.6e-06 m/s and 0.4 m/d), it was about 11 hours, while for the test carried out with v_3 equal to 1.382 mm/min (2.3 e-05 m/s and 1.9 m/d) flow velocity, the initial residence time was about 2 hours.

In Figure 5-39 a) and b) the Nickel normalized concentration evolution at each sampling time as function of filter thickness and at each sampling port as function of time is shown respectively for column test carried out at v_1 constant average flow velocity.

In Figure 5-40 a) and b) the Nickel normalized concentration evolution is represented for column tests carried out using v_3 constant average flow velocity.

React. Mat.	Weig. ratio	Initial cont. conc. (mg/L)	React. Thick. (cm)	React. area (cm)	React. Vol. (cm^3)	Fe^0 (gr)	Lapil. (gr)	n (%)	Flow velocity (mm/min)	PV (cm^3)	Tres (h)
Fe^0/ Lap	30:70	Ni 50	50	18.09	904.3	473	1104	37	0.055	336.8	56.1
Fe^0/ Lap	30:70	Ni 50	50	18.09	904.3	480	1120	37	0.276	334.3	11.1
Fe^0/ Lap	30:70	Ni 50	50	18.09	904.3	468	1093	38	1.382	348.1	2.3
Fe^0	-	Ni 40	19.25	18.09	348.2	1680	-	48	0.055	167.1	27.9
Fe^0	-	Ni 50	3	18.09	54.26	240	-	44	0.276	23.76	0.8
Fe^0	-	Ni 40	22.3	18.09	403.3	1680	-	48	1.382	193.6	1.3

Table 5-6 Characteristics of carried out column tests to study the flow rate influence

In Table 5-7, pH and Eh values measured at 1.5, 18 and 50 cm from inlet for different sampling times are reported for tests using v_1.
In Table 5-8, the values shown for pH and Eh are related to the column test carried out using v_3.
The duration of the test performed at v_1 velocity is 15000 hours (it is still in progress), corresponding to 4500 mg of Nickel in input, the test using v_2 was for 6000 hours with 9000 mg of Nickel in input, while the duration of the test using v_3 was 859 hours and the Nickel mass in input was 6442 mg.

5.6.3.1 Influence of flow velocity on the removal efficiency

To analyse the Nickel removal efficiency of the test performed at v_1 the interpretation of contaminant concentration and pH and Eh evolutions together can offer some useful information.
Firstly, regarding this test it is important to highlight that in Figure 5-39 b) only the sampling ports where Nickel concentration was above detection level have been taken into account. As can be observed in Figure 5-39 a), Nickel concentration was efficiently reduced by 28 cm long filter considering a mass in input equal to 4500 mg . 3 cm long filter is able to significantly remove Nickel concentration until about 300 hours (900 mg of Nickel mass input). At about 170 hours, in fact, the pH value at 1.5 cm from the inlet is about 7.11 and the Eh is positive. As can be observed for the above-analysed column tests, in this chemical condition a breakthrough occurred or is ready to occur. In the other sampling ports corresponding to higher distances from inlet, pH is about 9 or more, while the Eh is negative and equal to 100 mV in absolute value.

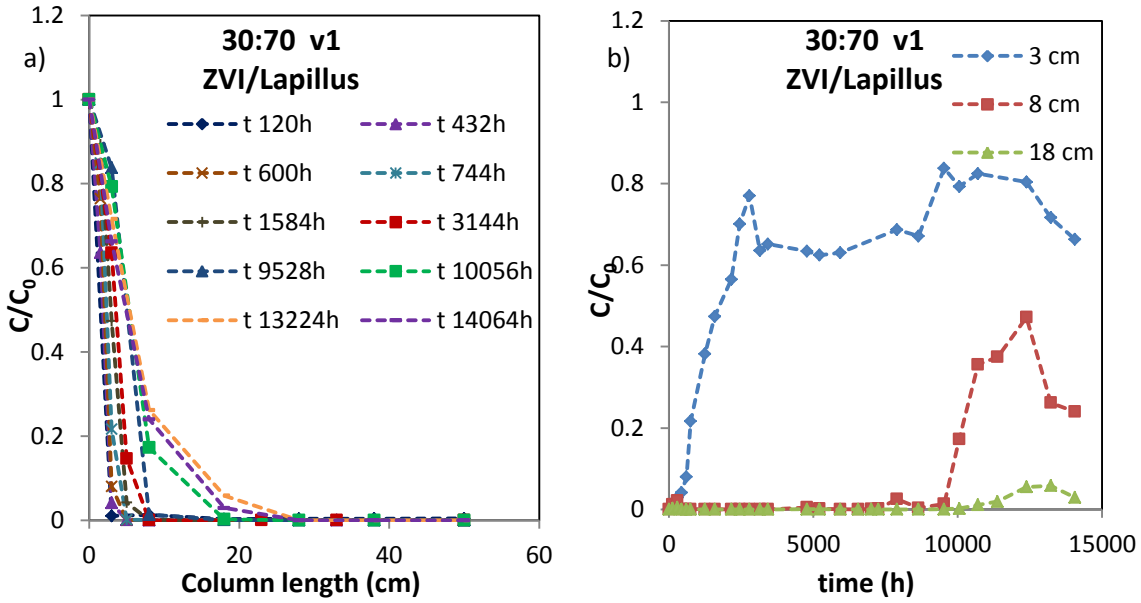

Figure 5-39 Evolution of Nickel normalized concentration a) along the column at different sampling time and b) at each sampling port during the time for 30:70 ZVI/Lapillus column test carried out under 0.055 mm/min constant flow velocity

t(h)\ dist (cm)	1.5		18		50	
	pH	Eh (mV)	pH	Eh (mV)	pH	Eh (mV)
171	7.11	16	8.95	-107.2	7.44	-38.4
528	6.48	32.8	9.47	-143	9.64	-154.5
840	6.5	34.3	8.66	-103.3	9.71	-145.6
1608	6.85	11.6	9.21	-126	9.42	-134.6
2184	6.45	29.3	9.12	-127.6	9.1	-124
9576	6.83	16.2	8.4	-73.2	8.9	-115.4
14856	5.9	22.3	6.38	5.2	8.6	-111.6

Table 5-7 pH and Eh values at different filter length and different sampling times for 30:70 ZVI:Lapillus column test carried out under v1

For about 10000 hours (3000 mg of Nickel mass input), 8 cm long filters are able to reduce the Nickel concentration under detection limit. At this time, at 18 cm pH has decreased to 8.4 (from 9.2 at 1600 h) and Eh has increased to -70 mV (from -126 mV at 1600 h), while at the outlet pH has decreased to 8.9 (from 9.6 at 528 h) and Eh has increased to -115 mV (from -154 mV minimum measured value at 528 h). Simultaneously, at the sampling port placed at 8 cm from the inlet, Nickel measured concentration is about 20 mg/L, while at the sampling port at 18 cm from the inlet Nickel concentration starts to increase (up to 1-2 mg/L, maximum valued measured until the end of the test).

In Figure 5-40 a) the Nickel normalized concentration evolution with filter thickness for each sampling time for v_3 test is shown. In Figure 5-39 b) its evolution at each sampling port with time is depicted.

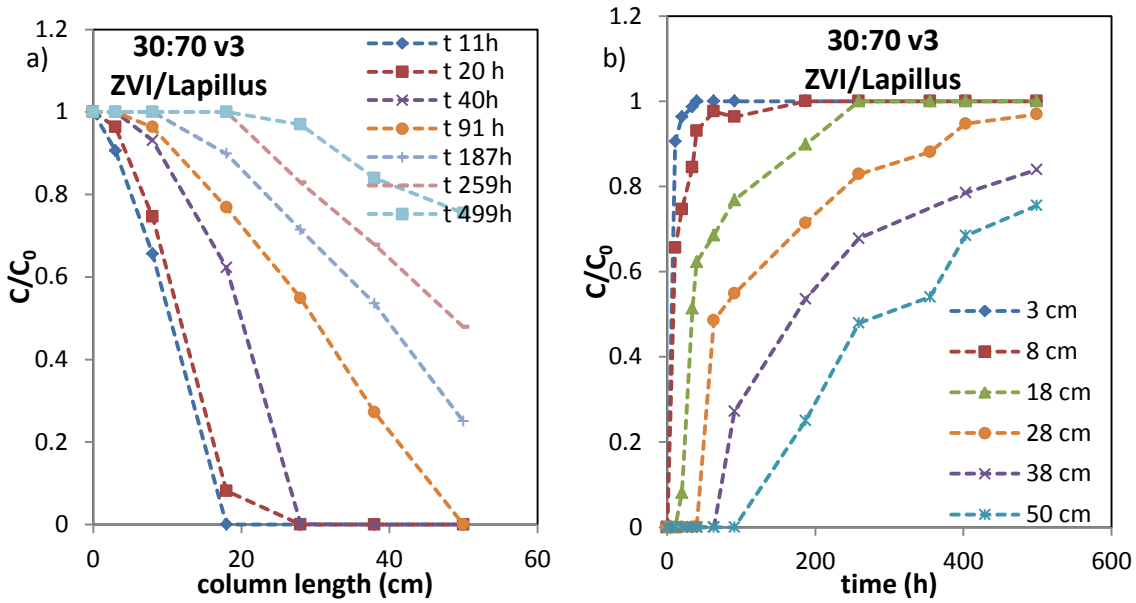

Figure 5-40 Evolution of Nickel normalized concentration a) along the column at different sampling time and b) at each sampling port during the time for 30:70 ZVI/Lapillus column test carried out under 1.382 mm/min constant flow rate

Removal efficiency is scarce: a breakthrough is observed at the outlet after 91 hours (680 mg of Nickel mass input) of interaction.

t(h)\ dist (cm)	1.5		18		50	
	pH	Eh (mV)	pH	Eh (mV)	pH	Eh (mV)
4	6.2	46.1	6.15	46.8	6.5	17.7
78	6.23	46.6	6.12	47.2	6.55	17
379	6.24	44.9	6.2	47.2	5.98	62.4
595	6.33	39.3	6.27	41.5	6.11	59.2
739	6.25	43.4	6.19	40.1	6.46	45.7

Table 5-8 pH and Eh values at different filter length and different sampling times for 30:70 ZVI:Lapillus column test carried out under v3

With regard to the pH and Eh evolution, information about the processes that have developed in the three columns can be gathered. Two things can be brought to light: one is related to the ranges of the values, the second regards their variation over time.

In fact, pH keeps about 6-6.5 and Eh is about 40-5 mV for all the test duration at each sampling port in column tests carried out at v_3. In tests performed at v_1 and v_2 they vary in different ranges: pH range is 9.7 – 6 in v_1 and 8.8 – 6 in v_2 tests, while Eh range is -154 – 30 mV in v_1 and -113 – 60 mV in v_2 tests.

Moreover, in the column test performed with v_2 the maximum value of pH and the minimum value of Eh were measured mainly at the outlet in the first sampling time, while in the test performed at v_1 the pH increases more slowly and decreases after a certain time, reaching the maximum value after a long interaction time. This behaviour is observed at sampling ports at 18 cm and 50 cm from the inlet in v_1 test.

The results suggest that in v_3 column tests there is not enough contact time for iron corrosion and nickel removal. In the other two tests, a certain contact time is assured for their development, higher in the v_1 test than in the v_2 one. This parameter together with the chemical condition that the Lapillus support allows can influence the formation process of products, their structure, density and order. Probably in opportune hydraulic conditions for corrosion, the higher contact time may assure products more well-done, with an ordered structure and higher density than in faster development processes.

It should be highlighted that in v_2 after about 1300 hours the pH is already about 6 and Eh positive and the same phenomenon is observed at the outlet after about 3000 hours. pH is always higher than 8.6 and Eh smaller than -110 mV at the outlet of v_1 test for all the test duration. Almost the same thing happens at the sampling port at 18 cm from the inlet. If the products that cause pore clogging can be formed in chemical conditions of 6 pH and positive Eh reached after previous corrosion processes, the v_2 is already subject to hydraulic issue, while v_1 is not yet so.

In Figure 5-41 a) the Nickel cumulative retained mass by the three tests carried out at three different constant flow velocities is shown. Until 1500 mg of Nickel in input the removal efficiency is high for all the tests. As this quantity increases, the removal efficiency of v_3 test decreases until 60% corresponding to 4000 mg of Nickel in input, while that relative to the other two tests stays at high values (about 99%) until 6000 mg of Nickel input mass.

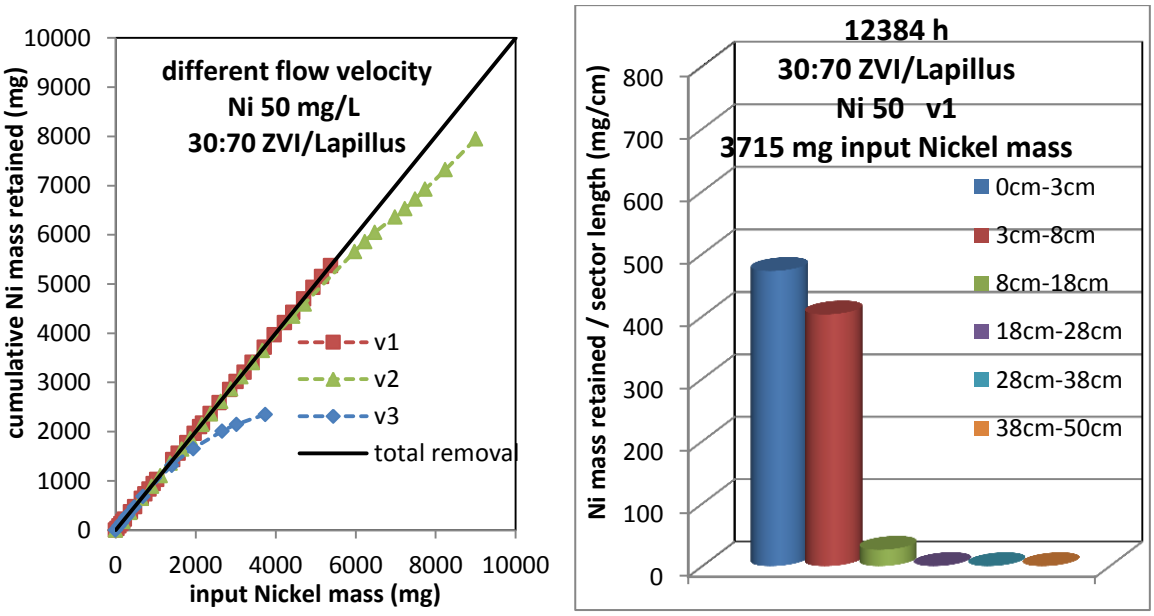

Figure 5-41 a) cumulative nickel mass retained as function of Nickel mass Input for v1, v2 and v3 tests; b) nickel mass retained per unit of sector length for each filter sector for v1 test at 12384 hours.

The distribution of Nickel retained mass among the different filter length sectors is shown in Figure 5-41 b), Figure 5-42 a) and b) for v_1, v_2 and v_3 tests respectively for a fixed Nickel input mass. In particular, the Nickel retained mass is represented per unit of filter length, representing the average Nickel mass retained per unit of length in each sector.

As can be expected, taking into account the previous consideration about the importance of residence time for removal efficiency, the greater Nickel mass is retained in the first 8 cm of the filter tested using v_1. It is equally distributed in the first 18 cm of filter thickness in column test carried out at v_2. Whereas the entire filter is involved in Nickel removal efficiency in the v_3 test and the Nickel retained mass is concentrated in the filter length included between the sampling port at 18 cm from the inlet and the outlet.

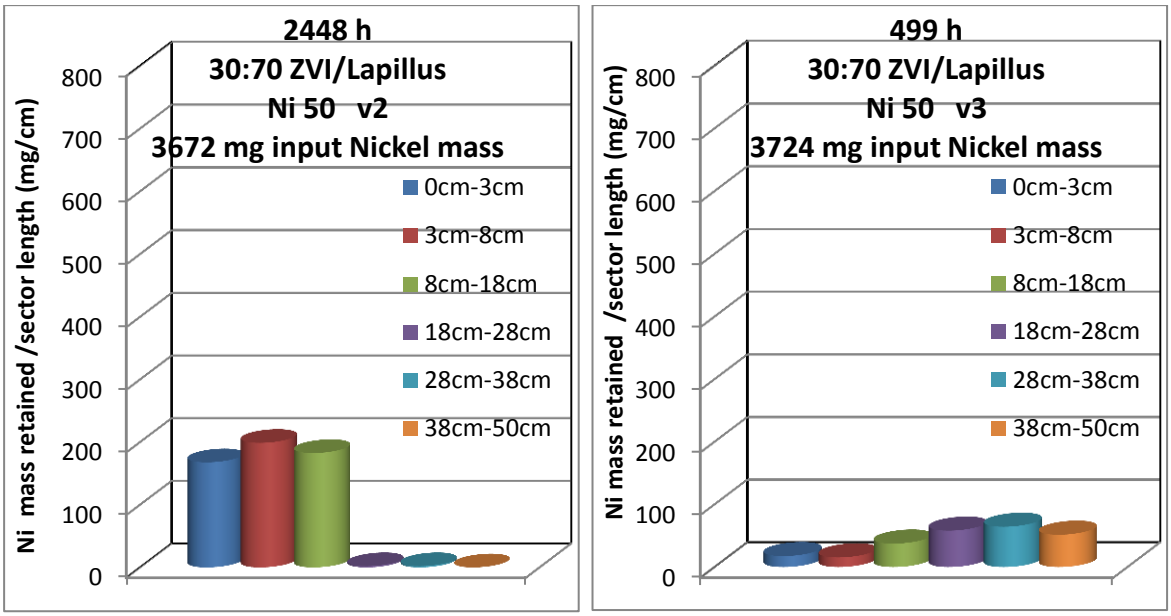

Figure 5-42 a) Nickel mass retained per unit of sector length for each filter sector for v2 test at 2448 hours and b) for v3 test at 499 hours.

5.6.3.2 Influence of flow velocity on hydraulic behavior

In order to investigate the hydraulic behaviour, the evolution of the hydraulic conductivity for the column tests carried out at different flow velocities has been analysed as function of different parameters. This study aims to investigate the conditions that mainly influence the hydraulic behaviour of the reactive mixtures .

In Figures 5-43 a) and b) 5-44 a) and b) and 5-45, the hydraulic conductivity evolution is shown as function of time, of Nickel mass input, of water input, of cumulative Nickel retained mass and of Nickel retained mass in the most efficient filter length per unit of ZVI mass.

Looking at Figure 5-43a, a light hydraulic conductivity increase is observed for each test at the beginning. Subsequently, its values for v_1 and v_3 tests stay constant, while they are reduced by one order of magnitude at the end of the v_2 test.

Moreover, looking at the other graphs as function of the other considered parameters, none of them seems to individuate an element able to explain the hydraulic behaviour evolution of the three column tests.

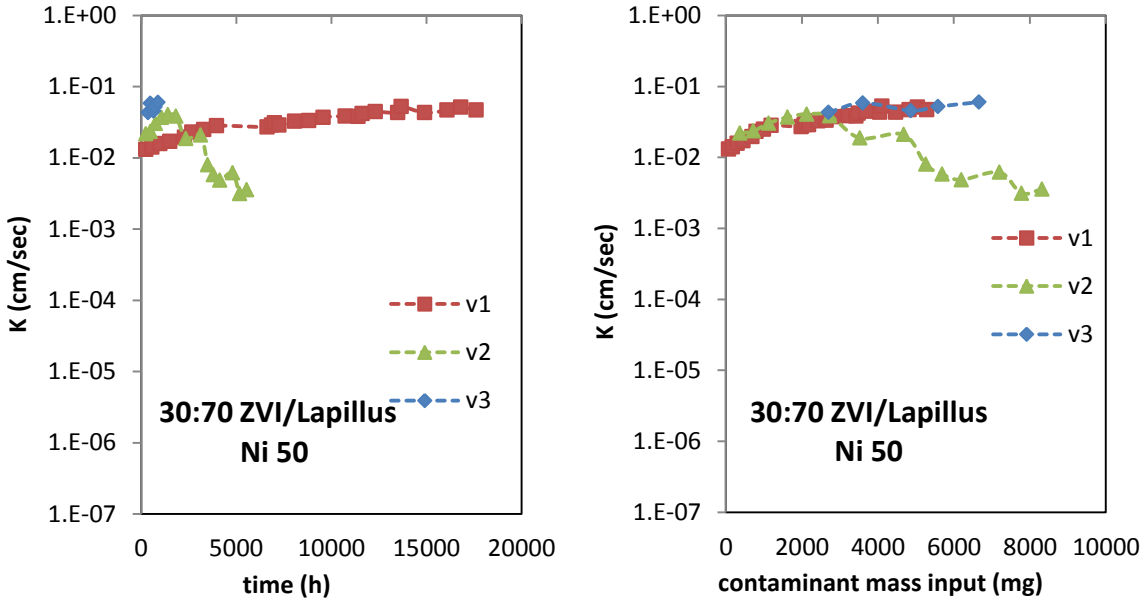

Figure 5-43 Hydraulic conductivity evolution a) as function of time and b) as function of input contaminant mass

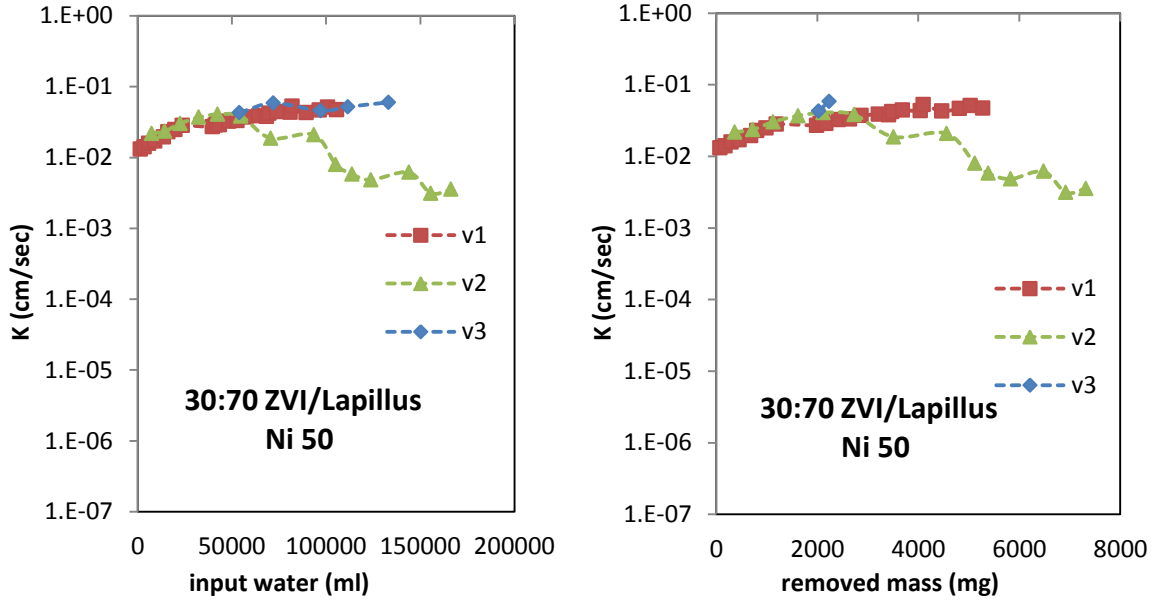

Figure 5-44 Hydraulic conductivity evolution a) as function of input water and b) as function of removed contaminant mass

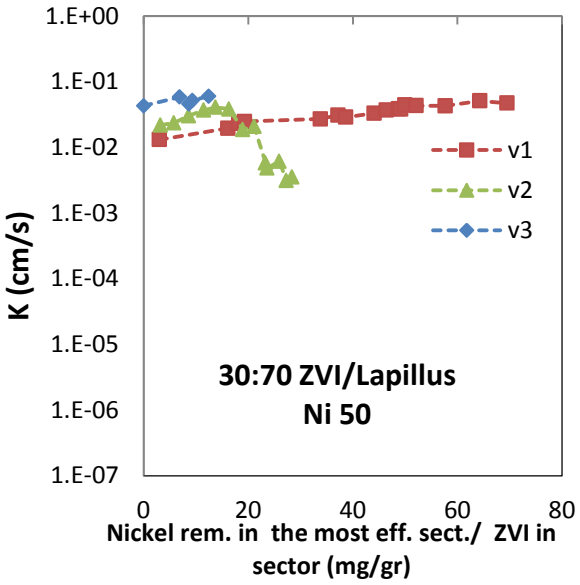

Figure 5-45 Hydraulic conductivity evolution as function of retained contaminant mass in the most efficient filter sector per unit of ZVI mass

5.6.3.3 Influence of flow velocity on specific removal rate

Concerning the specific removal rates representing the mass of contaminant retained by unit of reactive materials mass per unit of time, three main considerations can be made. The specific removal rate evolution with time for each sector is illustrated in Figure 5-46 a) and b) and Figure 5-47 for v_1, v_2 and v_3 tests respectively. The value related to the first sector at the test beginning increases as the constant flow velocity does. Furthermore, the main value calculated for the most efficient sectors is higher and the flow velocity is also higher.

For the v_1 test, the highest specific removal rate is related to the first 8 cm of the filter and its value seems to be stabilized after about 2000 hours of interaction around 0.001 mg/(gr*h) average value. This situation changes after 14000 hours. The evolution of specific removal rate coefficients, as calculated for the v_2 test, shows a variation of removal efficiency of each sector with time probably more affected by advection term than the previous test. Each highly efficient sector is characterized by a similar evolution of specific removal rate coefficients, decreasing after the maximum value has been reached. Looking at the graph of the v_3 test, it can be observed that the highest values are related to the second half length of the filter.

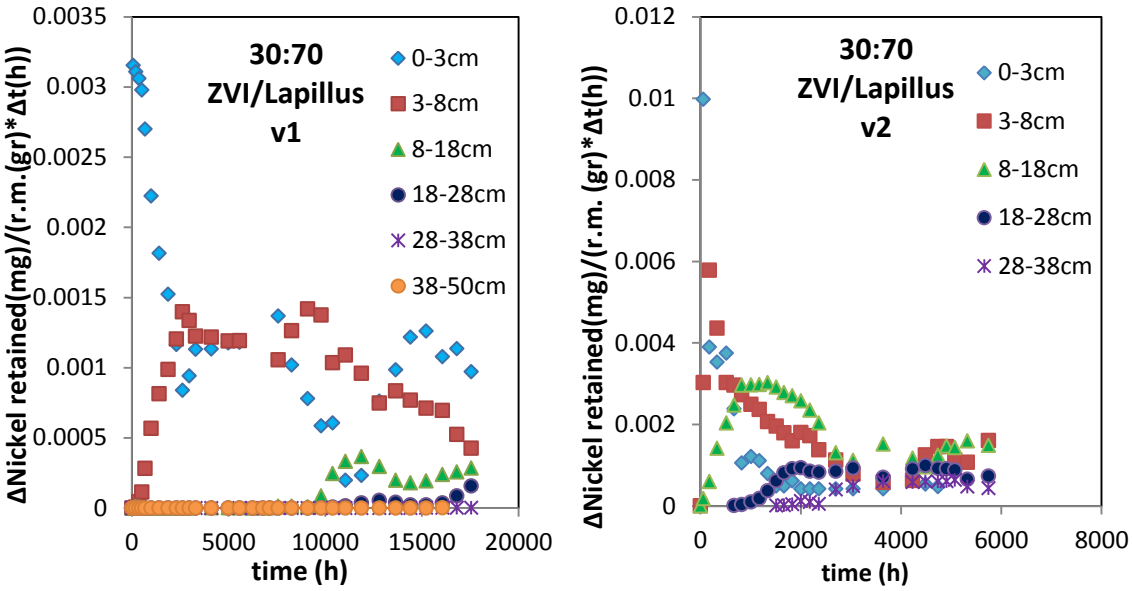

Figure 5-46 specific removal rate evolution with time for each filter sector a) for v1 test and b) for v2 test.

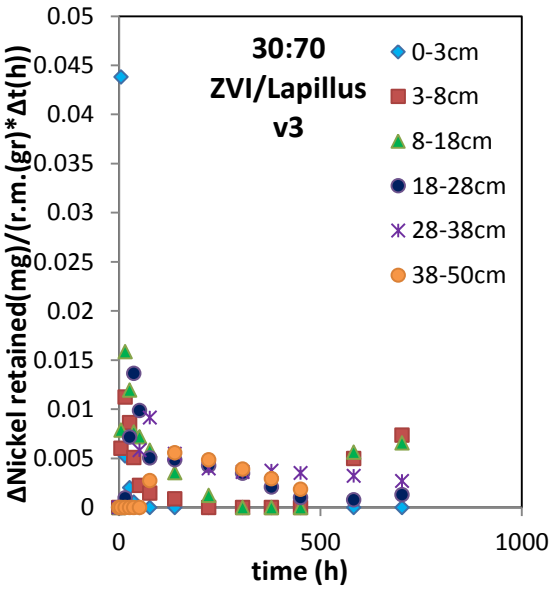

Figure 5-47 specific removal rate evolution with time for each filter sector for v3 test.

5.6.4 Initial concentration influence

Three column tests were performed to study the influence of the initial contaminant concentration on long-term Nickel removal efficiency and hydraulic behaviour. 30:70 ZVI:Lapillus mixtures filters have been used with solutions contaminated by Nickel at 10, 50 and 100 mg/L of initial concentration. The characteristics of column tests and their benchmarks (pure ZVI and pure Lapillus) are reported in Table 5-9.

React. Mat.	Weig. ratio	Initial cont. conc. (mg/L)	React. thick. (cm)	Reactive area (cm)	React. Vol. (cm^3)	Fe^0 (gr)	Lapil (gr)	n (%)	Flow veloc. (mm/min)	PV (cm^3)	Tres (h)
Lapillus		Ni 50	50	18.09	904.3		1289	35	0.276	318.5	10.6
Fe^0/ Lap	30:70	Ni 50	50	18.09	904.3	480	1120	37	0.276	334.3	11.1
Fe^0		Ni 50	3	18.09	54.26	240		44	0.276	23.76	0.8
Fe^0/ Lap	30:70	Ni 100	50	18.09	904.3	477	1113	37	0.276	337.6	11.3
Fe^0/ Lap	30:70	Ni 10	50	18.09	904.3	480	1120	38	0.276	341.4	11.4

Table 5-9 Characteristics of column tests carried out in order to study the initial concentration influence

5.6.4.1Influence of initial concentration on removal efficiency

In Figure 5-48 a) and b) the Nickel normalized concentration evolution with filter thickness at different sampling times and with time at each sampling port for the column test performed using solution contaminated by Nickel at 10 mg/L of initial concentration is shown respectively. In table 5-10 the values of pH and Eh measured at different times at the sampling port placed at 1.5, 18 and 50 cm from the inlet of the considered column are reported. As can be observed, a 3 cm long filter is able to remove efficiently the Nickel mass input in the column until about 1000 hours of interaction, corresponding to 300 mg of Nickel input, subsequently the 8 cm thick filter needs to remediate the contaminated solution until 4656 hours at least, corresponding to 1400 mg of Nickel input mass.

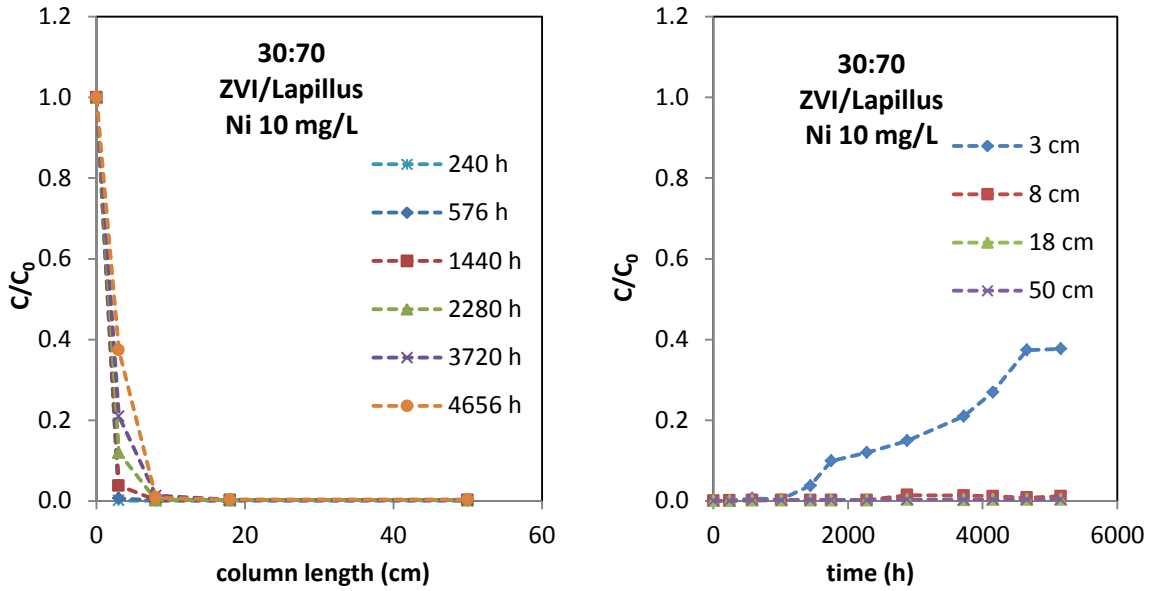

Figure 5-48 Evolution of Nickel normalized concentration a) along the column at different sampling time and b) at each sampling point with time for 30:70 ZVI/Lapillus column test carried out using a solution of Nickel at 10 mg/L initial concentration

t(h)\ dist (cm)	1.5		18		50	
	pH	Eh (mV)	pH	Eh (mV)	pH	Eh (mV)
336	6.94	-21.3	9.27	-154.2	8.6	-119.2
1344	6.7	-3.4	9.46	-152.8	8.49	-148.8
2256	6.4	30	8.2	-74	8.8	-96
3696	6.07	15.4	7.44	-54.3	8.88	-123.3
4464	6.53	47.3	9.03	-82.3	9.46	-106.9

Table 5-10 pH and Eh values at different filter length and different sampling times for 30:70 ZVI/Lapillus column test carried out using a solution of Nickel at 10 mg/L initial concentration

Looking at the pH and Eh evolution, some consideration can be made comparing them to those of column tests carried out using solution contaminated by Nickel at 50 mg/L of initial concentration. The pH is about 6 at the sampling port placed at 1.5 cm from the inlet, when the corresponding filter thickness is still highly efficient. Moreover, while for the previously analysed column tests, negative Eh values were measured when pH was more than 8, using Nickel concentration equal to 10 mg/L, chemical conditions are reducing for pH equal to 6.7. Another difference is related to the reducing chemical condition developed during the first interaction time (until

1330 hours) in the entire filter length, also in the first centimetres where this has not been observed for the previous tests.

Furthermore, more reducing conditions and higher pH value were developed at half of the total filter length than at the end of the filter during the first interaction time. The same phenomenon was observed for the test carried out at v_1 only. Usually the observed chemical conditions and measured pH values were more reducing and higher respectively as filter length increases.

In Figures 5-49 a) and b) the Nickel normalized concentration evolution with filter thickness at different sampling times and with time at each sampling port is shown respectively, for the column test carried out using solution contaminated by Nickel at 100 mg/L of initial concentration. In table 5-11, the value of pH and Eh measured at different times at the sampling port placed at 1.5, 18 and 50 cm from the column inlet are reported.

The 50 cm long filter of 30:70 ZVI/Lapillus mixture is able efficiently to remediate the contaminated solution until about 100 hours after the test beginning, corresponding to 320 mg of Nickel input mass.

Looking at the measured pH and Eh values, the first one was about 6 for all the filter length and the test duration while the latter ranged from 30 to 60 mV.

The removal efficiency of the tests performed varying the Nickel initial concentration is shown in Figure 5-50 a) as Nickel cumulative mass retained as function of Nickel mass input. It can be observed that all the three filters are able to retain 2000 mg of Nickel in input.

As the contaminant mass in input increases, the removal efficiency of the test performed with solution containing Nickel at 100 mg/L initial concentration decreases up to 50% after 8000 mg of Nickel have been flowed through it.

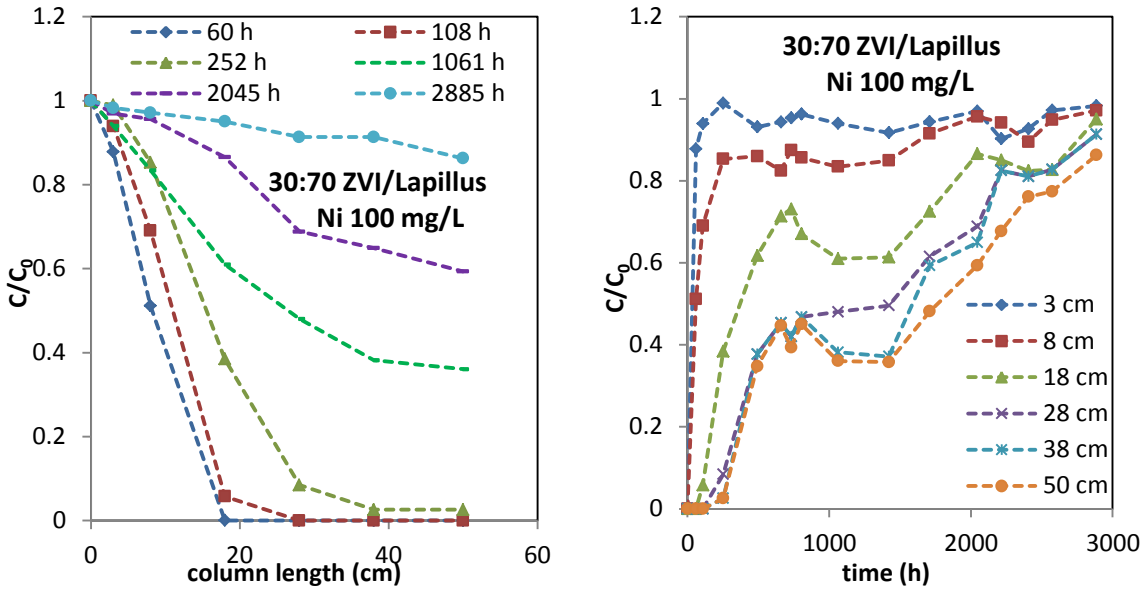

Figure 5-49 Evolution of Nickel normalized concentration a) along the column at different sampling time and b) at each sampling port with time for 30:70 ZVI:Lapillus column test carried out using a solution of Nickel at 100 mg/L initial concentration

t(h)\ dist (cm)	1.5		18		50	
	pH	Eh (mV)	pH	Eh (mV)	pH	Eh (mV)
168	6.63	35.7	6.83	37.7	6.58	26.8
672	6.13	51.7	6.01	61.7	6.22	43.3
1109	6.15	47.5	6.05	53.6	5.93	61.4
1445	6.22	42.7	6.06	53.3	5.91	63.3
2237	6.34	34.2	6.3	40.9	6.21	46.4

Table 5-11 pH and Eh values at different filter length and different sampling times for 30:70 ZVI:Lapillus column test carried out using a solution of Nickel at 100 mg/L initial concentration

The test carried out using a solution of Nickel at 50 mg/L of initial concentration keeps a high performance (99%) until 4000 mg of Nickel input mass. Afterwards, the removal efficiency of the filter decreases up to 88% after 9000 mg of Nickel input mass. The data related to the test performed with 10 mg/L Nickel initial concentration of Nickel show an efficiency equal to 99.9% for the whole duration of the test, corresponding to 2000 mg of Nickel.

In Figure 5-50 b) and 5-51 a) and b), the distribution of Nickel mass retained by different sectors is shown for the tests performed using solutions of Nickel at 10, 50 and 100 mg/L initial concentration respectively, for a preset Nickel input mass. As

can be observed, in the first considered test, the Nickel retained mass is concentrated in the first 3 cm of the filter, in the second one it is distributed in the first 18 cm of the filter, in the last in the first 28 cm.

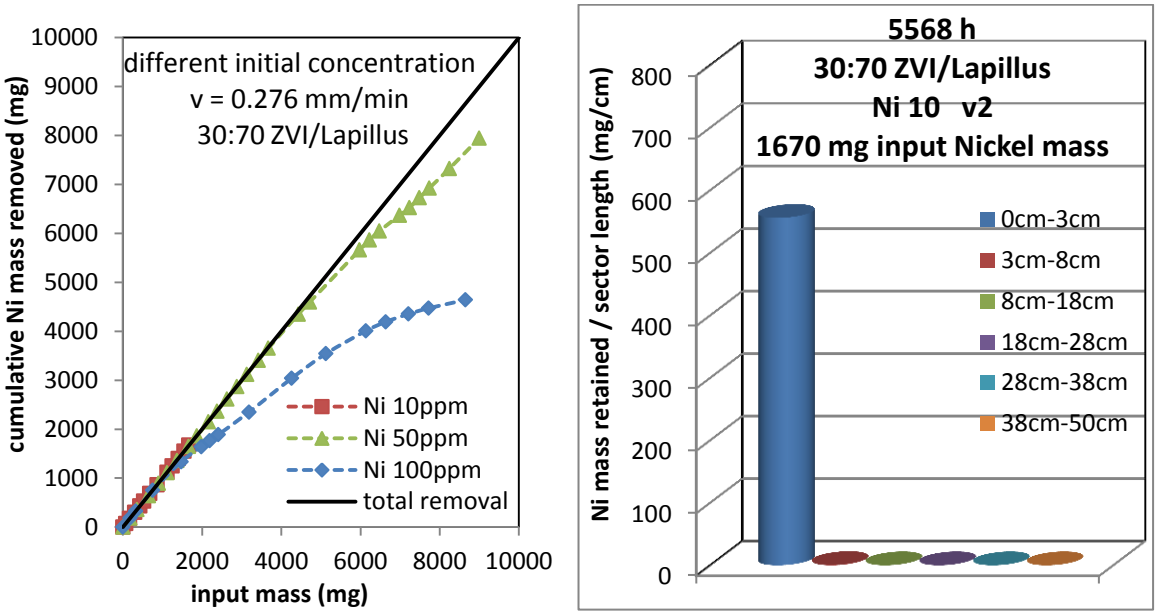

Figure 5-50 a) cumulative Nickel mass retained as function of Nickel mass input for column tests performed using solution of Nickel at 10, 50 and 100 mg/L initial concentration; b) retained Nickel mass per unit of sector length for each filter sector for test with Ni at 10 mg/L initial concentration at 5568 hours.

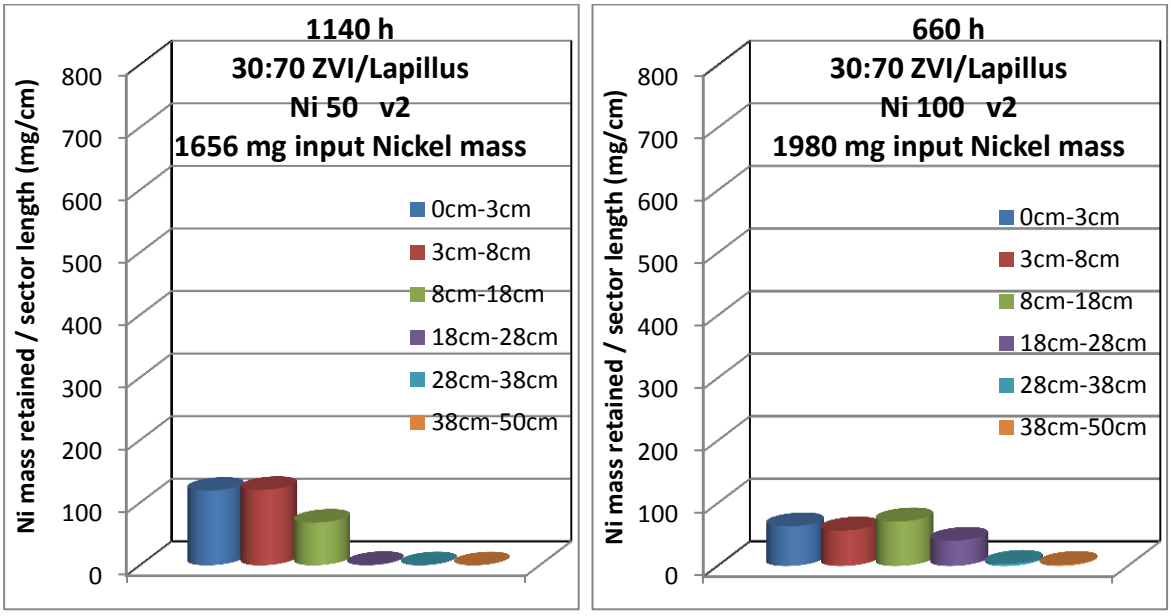

Figure 5-51 Nickel mass retained per unit of sector length for each filter sector a) for test with Ni at 50 mg/L initial concentration at 1140 hours and b) for test with Ni at 100 mg/L initial concentration at 660 hours

5.6.4.2 Influence of initial concentration on hydraulic behavior

In Figures 5-52 and 5-53, the hydraulic conductivity evolution is shown as function of time, of Nickel mass input, of water input, of cumulative Nickel retained mass for the tests performed using solutions at different Nickel initial concentrations.

The filter that has better performed under the hydraulic point of view was that with the highest Nickel initial concentration, that subject to the highest hydraulic conductivity loss was the one carried out with the lowest Nickel initial concentration.

Looking at the evolution of hydraulic conductivity as function of the above-mentioned parameters, it can be gathered that the Nickel mass input as the Nickel retained mass does not play an important role in this study. On the other hand, time and input water seem to be the parameters that mostly can influence hydraulic performance.

Comparing them to the most affecting parameters (among those considered) of hydraulic behaviour in flow velocity influence study, it seems that the water input into the column could be the parameter that can better explain the hydraulic behaviour of the column tests carried out, among the considered parameters.

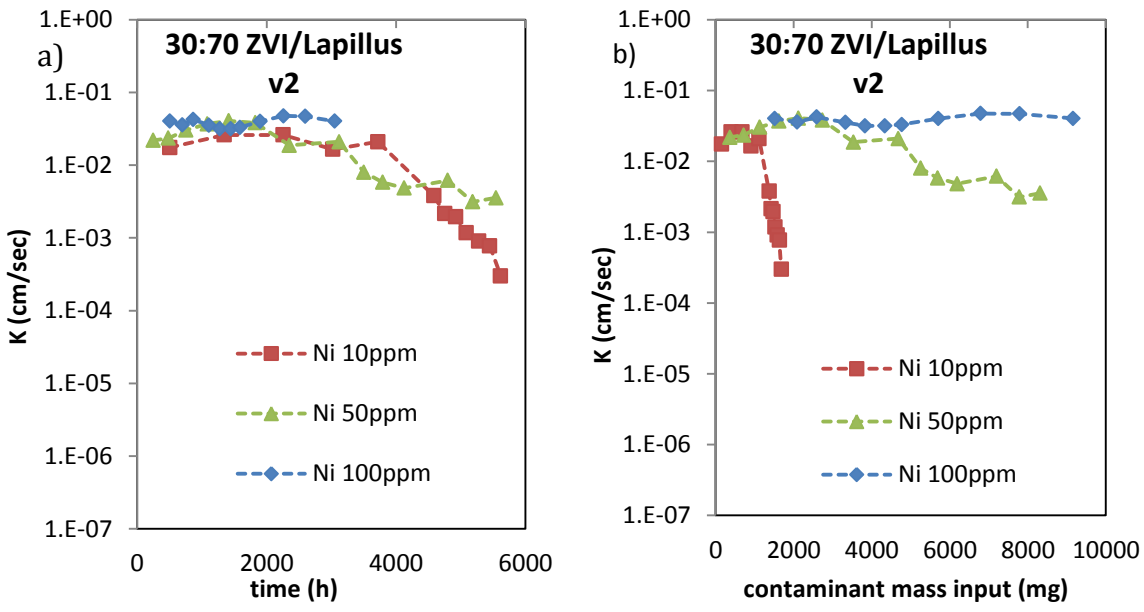

Figure 5-52 Hydraulic conductivity evolution a) as function of time and b) as function of input contaminant mass

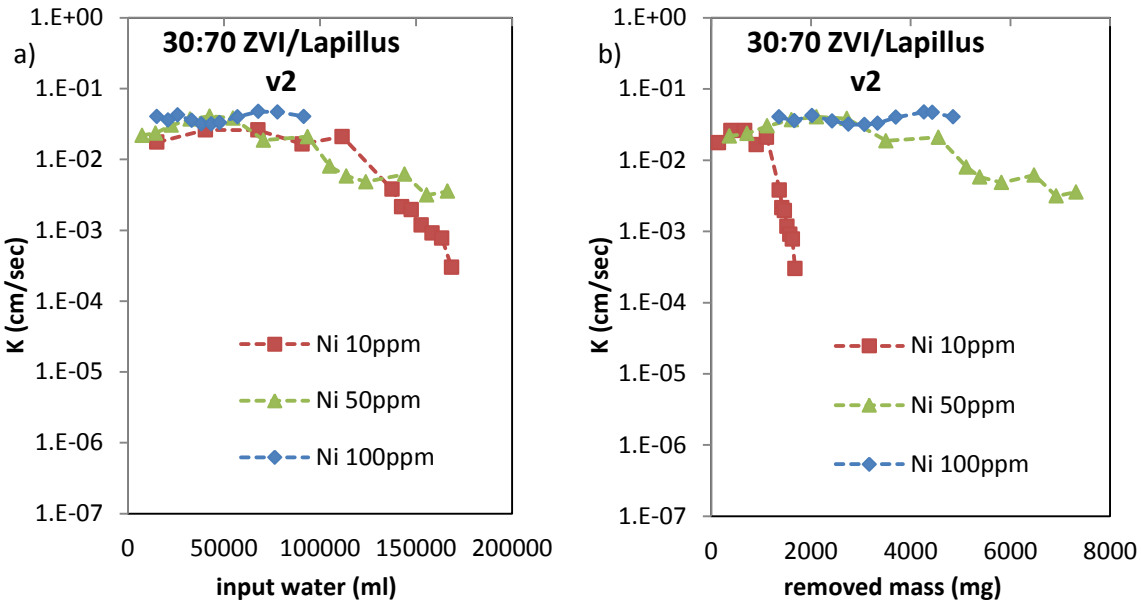

Figure 5-53 Hydraulic conductivity evolution a) as function of input water and b) as function of contaminant removed mass

5.6.4.3 Influence of initial concentration in specific removal rate

In Figure 5-54 a) and b) and 5-55, the specific removal rate evolution is shown for each filter thickness sector as function of time for the tests performed using solutions of Nickel at 10, 50 and 100 mg/L initial concentration respectively.

The first value of specific removal rate for the first sector is higher the higher is the Nickel initial concentration, although the values calculated for different sectors of the tests carried out using solution of Nickel at 50 and 100 mg/L initial concentration for the different times are in the same range. In addition, the evolution of specific removal rates with time in the test carried out with 10 mg/L Nickel initial concentration solution is different from that observed in the other. In fact, in the first test, the value related to each sector stays constant and that of the first 3 cm long filter is about 0.003 mg/(gr*h) while that of the others sectors is very low. Looking at the graphs corresponding to the other two tests, a certain variation of specific removal rate values with time and with filter thickness is observed. In particular, a clear behaviour of specific removal rate evolution with time can be distinguished among the different filter thickness sectors for the test carried out using solution of Nickel at 50 mg/L initial concentration, whereas the specific removal rate calculated

for the first 28 cm of the filter vary around the same average value, equal about 0.002 mg/(gr*h) in the case of the test performed using solution of Nickel at 100 mg/L initial concentration.

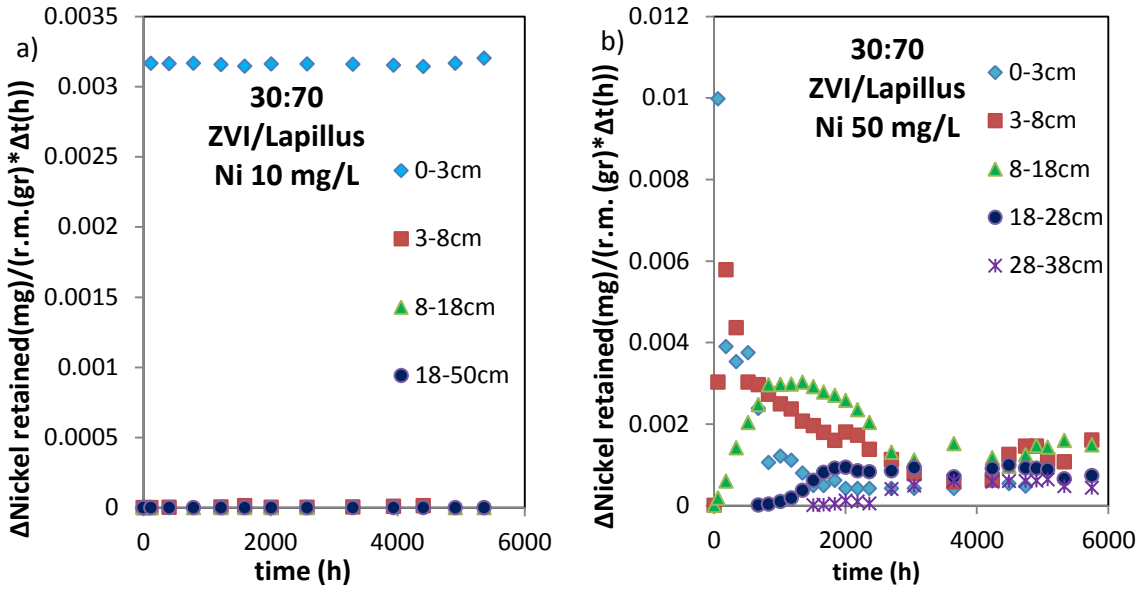

Figure 5-54 specific removal rate evolution with time for each filter sector a) for column test performed using solution of Nickel at 10 mg/L of initial concentration and b) for test performed using solution of Nickel at 50 mg/L of initial concentration

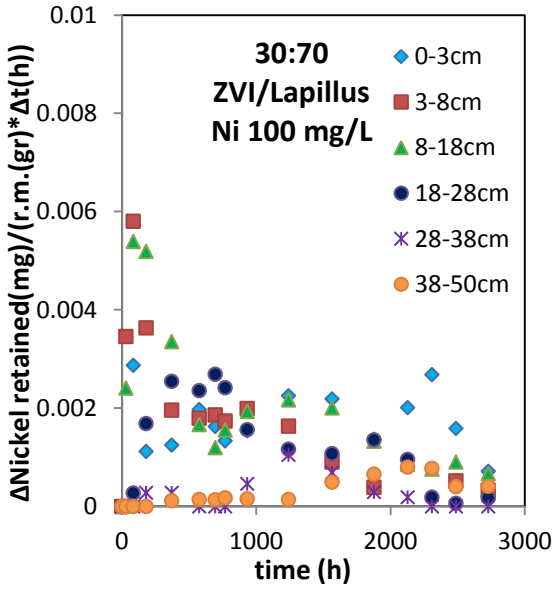

Figure 5-55 specific removal rate evolution with time for each filter sector a) for column test performed using solution of Nickel at 100 mg/L of initial concentration

5.6.5 Influence of filter thickness

In this paragraph, a study to investigate the influence of the filter thickness on long-term Nickel removal efficiency and hydraulic behaviour is proposed. Two columns were used in this study on 30:70 ZVI:Lapillus weight ratio mixture: one 50 cm and one 100 cm long. In table 5-12 the characteristics of the column tests carried out are reported. The 50 cm long filter will be called below Short Column (SC), while Long Column (LC) will refer to the 100 cm long filter.

React. mat.	Weig. ratio	Initial cont. conc. (mg /L)	React. Thick. (cm)	React. area (cm)	React. Vol. (cm^3)	Fe^0 (gr)	Lap. (gr)	n (%)	Flow veloc. (mm/ min)	PV (cm^3)	Tres (h)
Fe^0/ Lap	30:70	Ni 50	50	18.09	904.3	480	1120	37	0.276	334	11.1
Fe^0/ Lap	30:70	Ni 50	100	18.09	1808	1098	2562	34	0.276	607	20.2

Table 5-12 Characteristics of column tests carried out in order to study the configuration influence

5.6.5.1 Influence of filter thickness on removal efficiency

In Figure 5-56 a) and b) the Nickel normalized concentration evolution with the filter thickness at different sampling times and with time at each sampling port is shown respectively, for the LC test. An 80 cm long filter can reduce efficiently (with a removal efficiency of 99%) the Nickel concentration until 6500 hours of interaction test, corresponding to 9000 mg of Nickel input mass.

In Figure 5-57 the evolution of Nickel concentration with time for the same sampling ports of the LC and SC tests is reported. A similar removal efficiency can be observed. Whereas the long-term hydraulic behaviour has been not similar, as will be discussed in the next sub-paragraph.

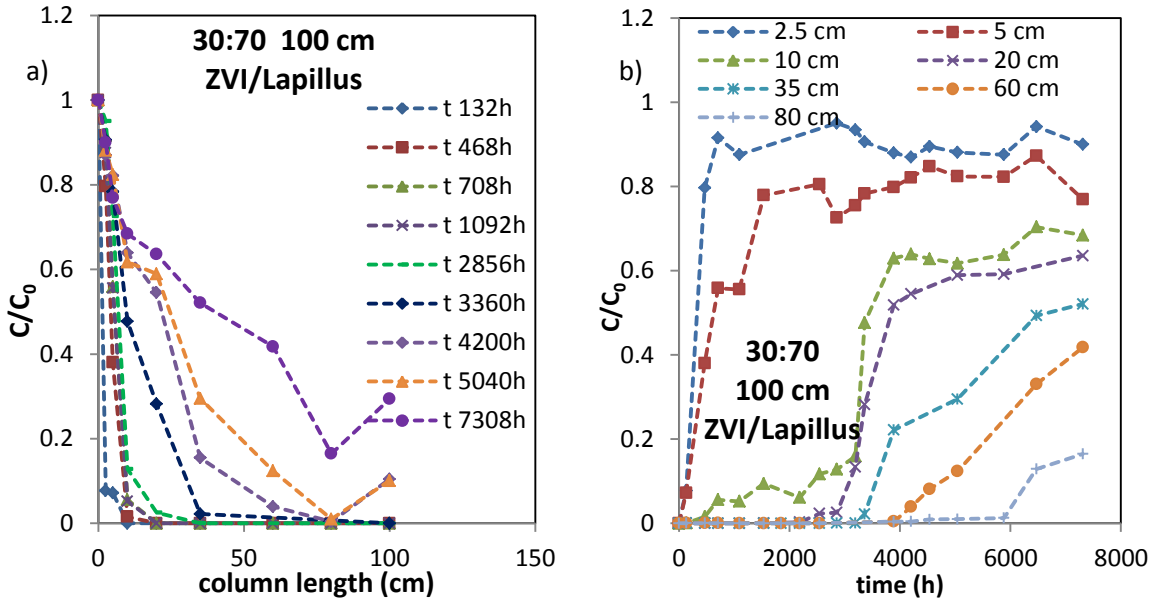

Figure 5-56Evolution of Nickel relative concentration a) along the column at different sampling time and b) at each sampling portwith time for 30:70 ZVI:Lapillus column test carried out using 100 cm long column

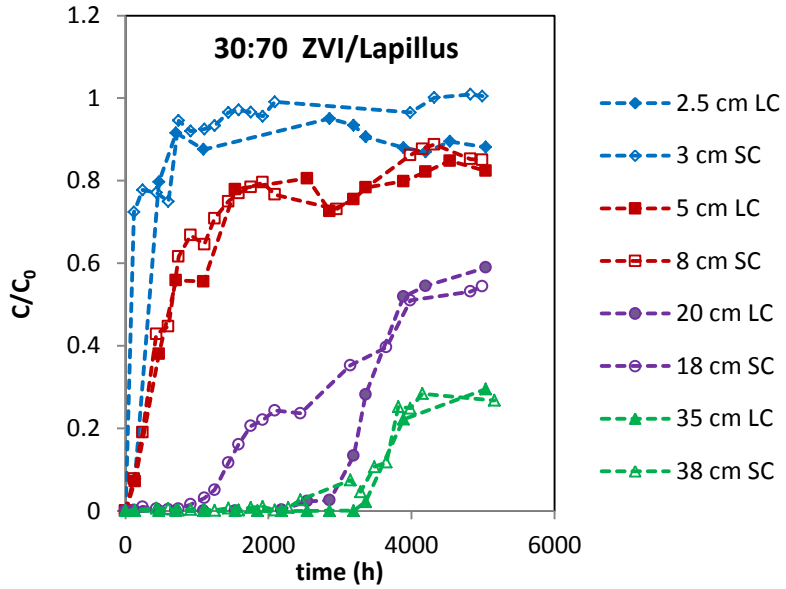

Figure 5-57 Evolution of Nickel relative concentration at each sampling point with time for 30:70 ZVI:Lapillus column test carried out using 50 cm and 100 cm long columns

5.6.5.2 Influence of filter thickness on hydraulic behavior

In Figure 5-58 and 5-59 a) and b) the hydraulic behaviour of the LC will be compared to that of the filter tested in the study on the influence of the initial Nickel concentration, while in Figure 5-60 and 5-61 a) and b) it will be compared to that of the hydraulic performance of the filter tested varying the flow velocity. In fact, the hydraulic conductivity of LC stays constant for the test duration, while that of SC decreases of one order of magnitude in a shorter time. A hydraulic behaviour similar to that performed by the LC can be observed for the filter tested at v_1 and v_3 flow velocity. The difference on the hydraulic behaviour between the two filters tested using the solution at the same contaminant initial concentration and the same flow velocity can deal with different chemical conditions development.

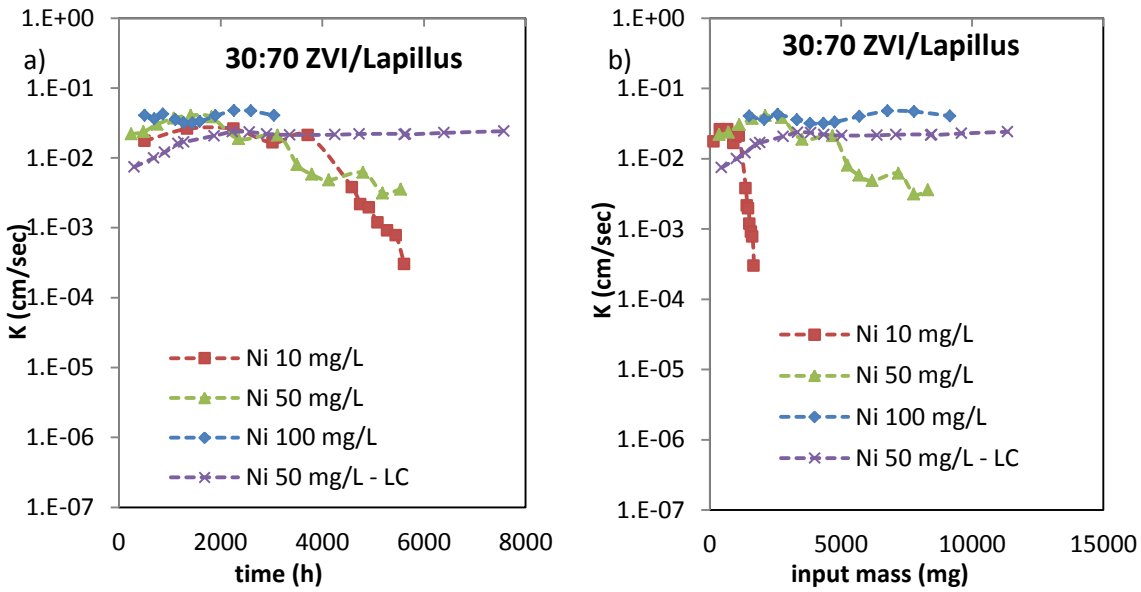

Figure 5-58 Hydraulic conductivity evolution a) as function of time and b) as function of input contaminant mass for tests at different contaminant initial concentration

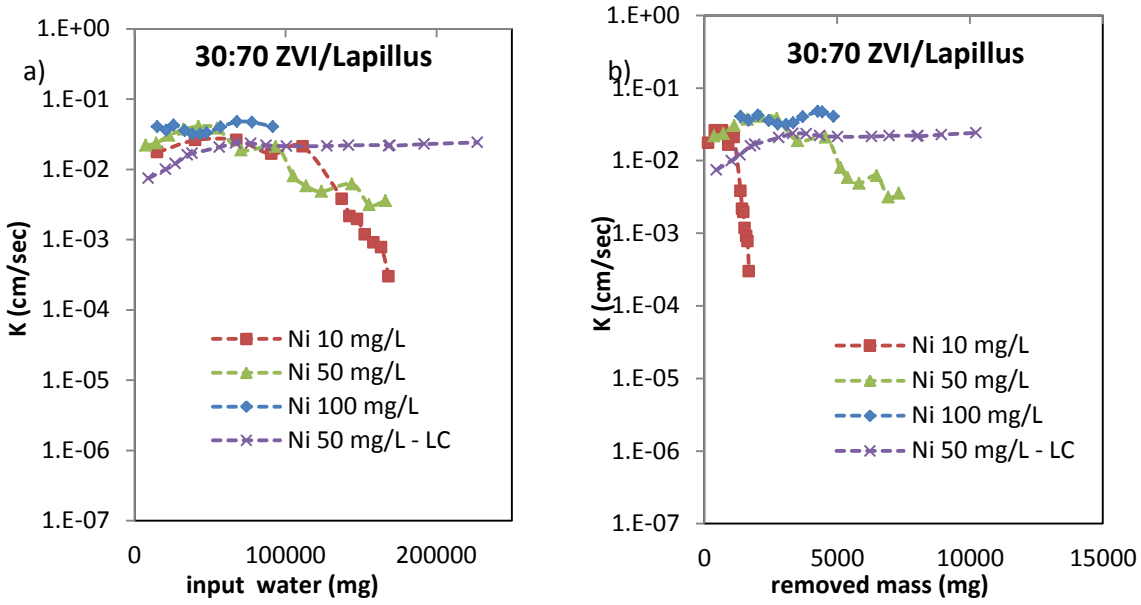

Figure 5-59 Hydraulic conductivity evolution a) as function of input water and b) as function of contaminant removed mass for tests at different contaminant initial concentration

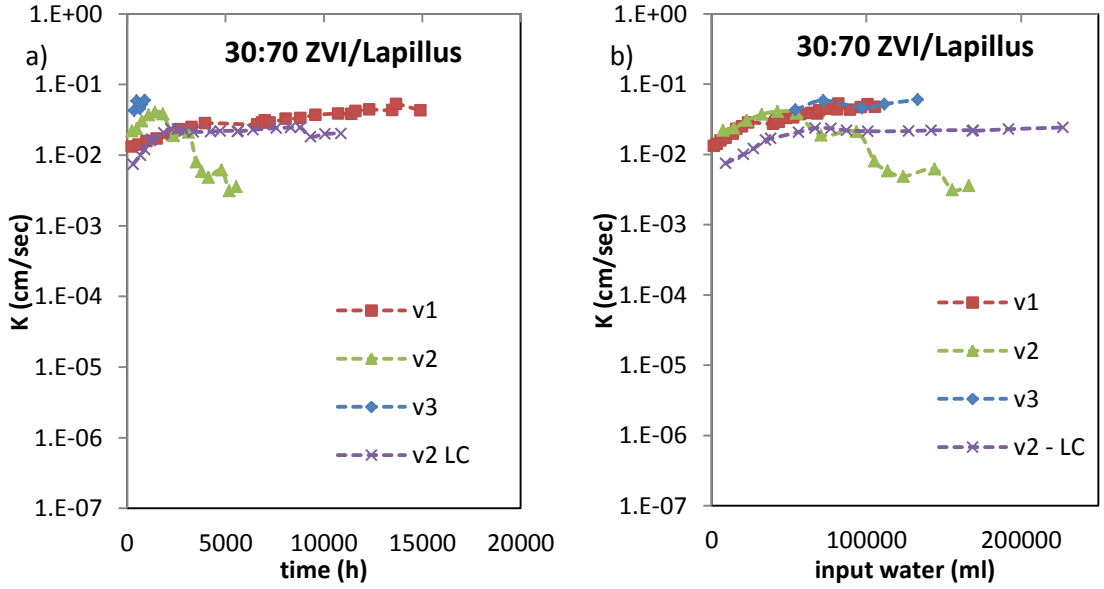

Figure 5-60 Hydraulic conductivity evolution a) as function of time and b) as function of input contaminant mass for tests at different constant flow velocity

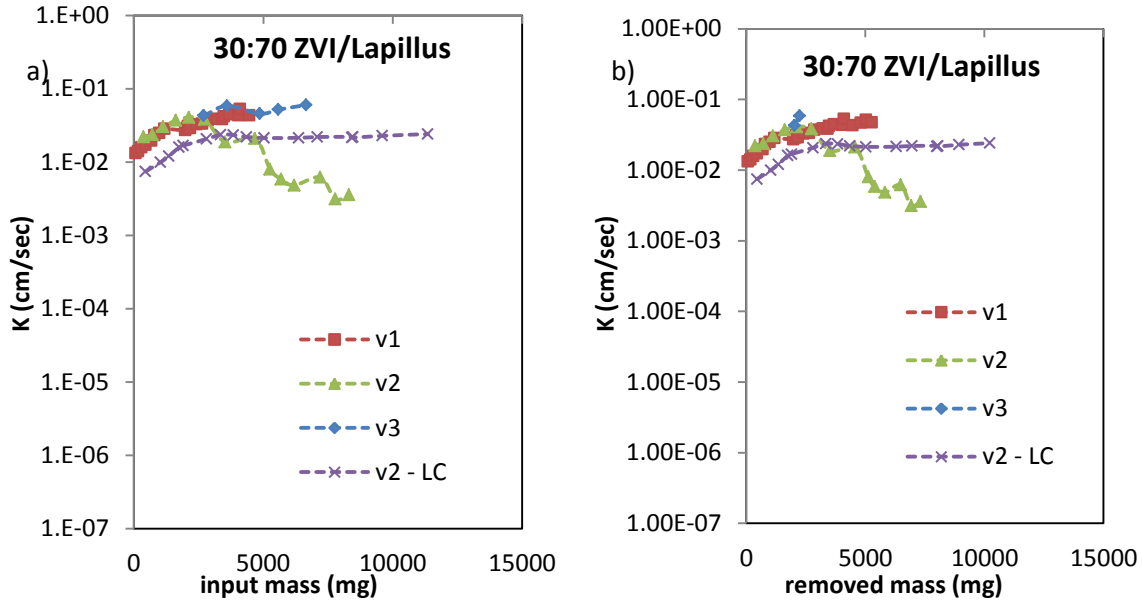

Figure 5-61 Hydraulic conductivity evolution a) as function of input water and b) as function of contaminant removed mass for tests at different constant flow velocity

5.7 Results of column tests carried out with zinc-contaminated solution

In this section the results of column tests carried out using zinc-contaminated solution are discussed. In table 5-13 the characteristics of column tests are summarized.

Firstly, results of column Fe^0/Lap 50:50 weight ratio realized using a solution of Zinc at 50 ppm of initial concentration and a constant flow velocity of input solution equal to 0.276 mm/min are analysed.

React. Mat.	Weigr atio	Initial cont. conc. (mg/ L)	React. Thick. (cm)	React. area (cm^2)	React. Vol. (cm^3)	Fe^0 (gr)	Lap. (gr)	n (%)	Flow veloc. (mm/ min)	PV (cm^3)	Tres (h)
Fe^0/ Lap	50:50	Zn 50	50	18.09	904.3	970	970	38	0.276	340.1	11.3
$Fe^{0,*}$	-	Zn 50	3	18.09	54.26	240		43	0.276	23.41	0.8

Table 5-13 Characteristics of carried out column tests to study the zinc removal
(*) (Bilardi, 2012)

5.7.1 Removal efficiency

In Figure 5-62 a) and b) the Zinc normalized concentration is shown as function of time at each sampling port and as function of filter thickness for each sampling time. The 8 cm thick filter is able to efficiently remediate until 400 hours from the test beginning. Afterwards, the 18 cm thick filters are enough to remediate until 1600 hours. Moreover, at sampling port placed at 28 cm from the inlet, highly reduced Zinc concentration was revealed.

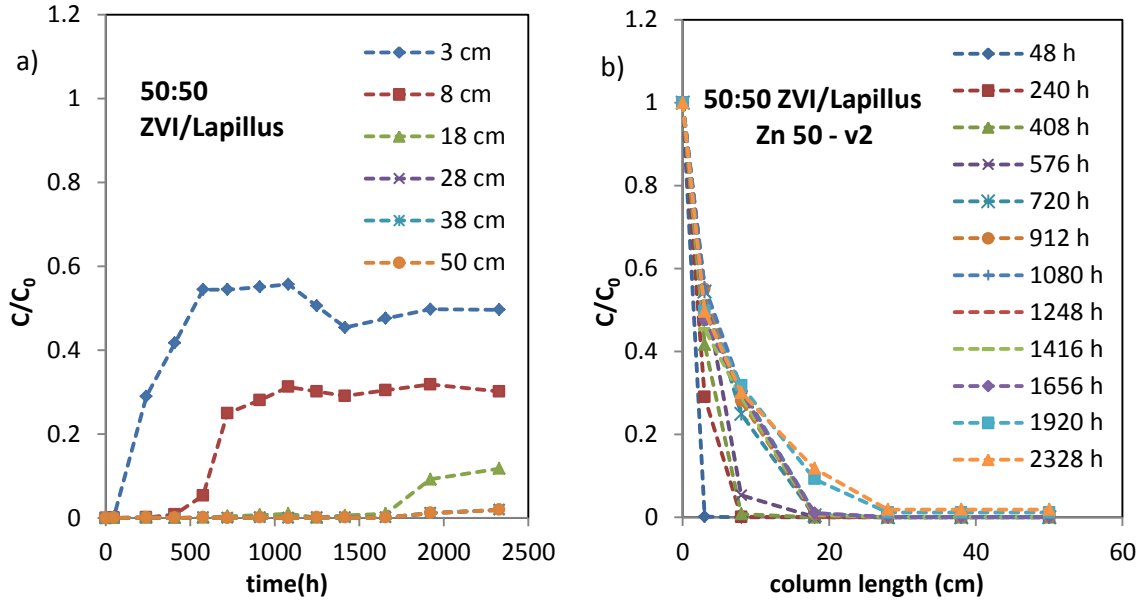

Figure 5-62 Zinc normalized concentration a) as function of time at each sampling port and b) as function of filter thickness for each sampling time.

In Figure 5-63 a) the Zinc mass retained is shown as function of Zinc mass input for the tests performed respectively with pure ZVI and with 50:50 ZVI/Lapillus w.r. mixture at different filter thickness, corresponding to ZVI content. The removal efficiency seems not be dependent on the residence time as well as the Nickel removal is, while it is rather influenced by the ZVI content. In fact, a higher removal efficiency can be observed for the pure ZVI test, that is 3 cm long and contains 240 g of reactive medium, than a 8 cm long filter of 50:50 ZVI/Lapillus w.r. mixture, containing 152 g. The results obtained performing the pure ZVI test can be comparable with that of the 18 cm long mixture filter.

In Figure 5-63 b) the Zinc mass retained mass per unit of sector length for different filter sectors at 2328 hours is shown. It can confirm the high Zinc removal of the first centimetres, also after a long time of interaction.

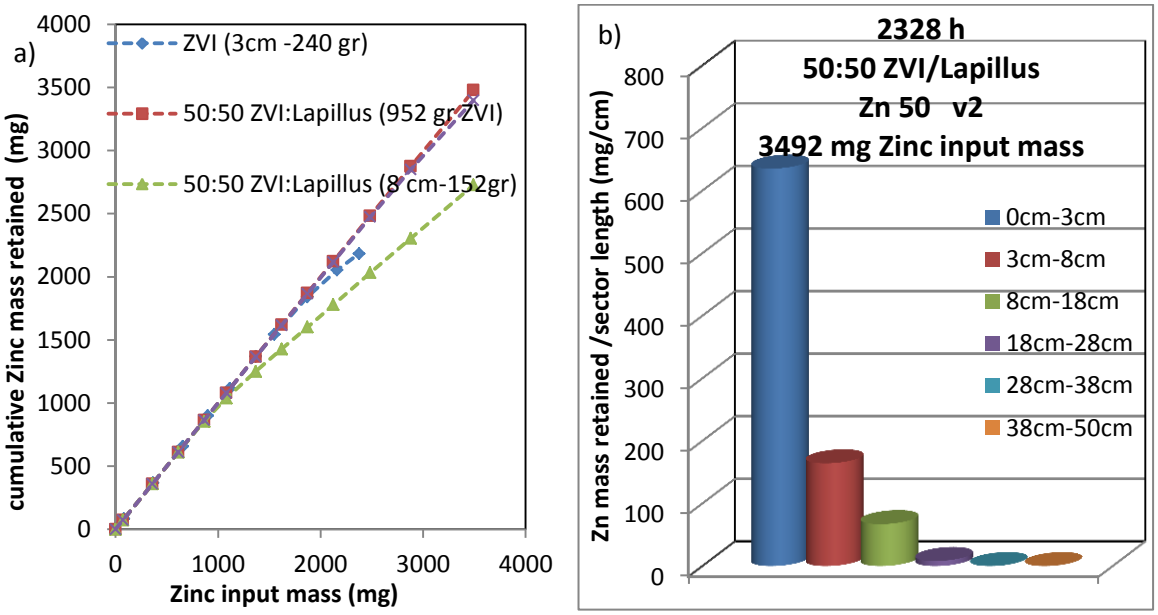

Figure 5-63 a) cumulative zinc mass retained mass as function of zinc mass input b) Zinc mass retained per unit of sector length for different filter sectors.

5.7.2 Hydraulic behaviour and specific removal rate coefficients

In Figure 5-64 a), the evolution of hydraulic conductivity as function of Zinc retained mass is shown. The pure ZVI test is subject to a high hydraulic conductivity loss corresponding to about four orders of magnitude, while no important hydraulic changes were observed for the 50:50 ZVI:Lapillus w.r. mixture.

In Figure 5-63 b), the evolution of specific removal rate for each filter sector as function of time is shown. For the entire test duration, the highest values can be found for the first 3 centimetres, while the second highest values can be observed for the 3-8 cm filter sector.

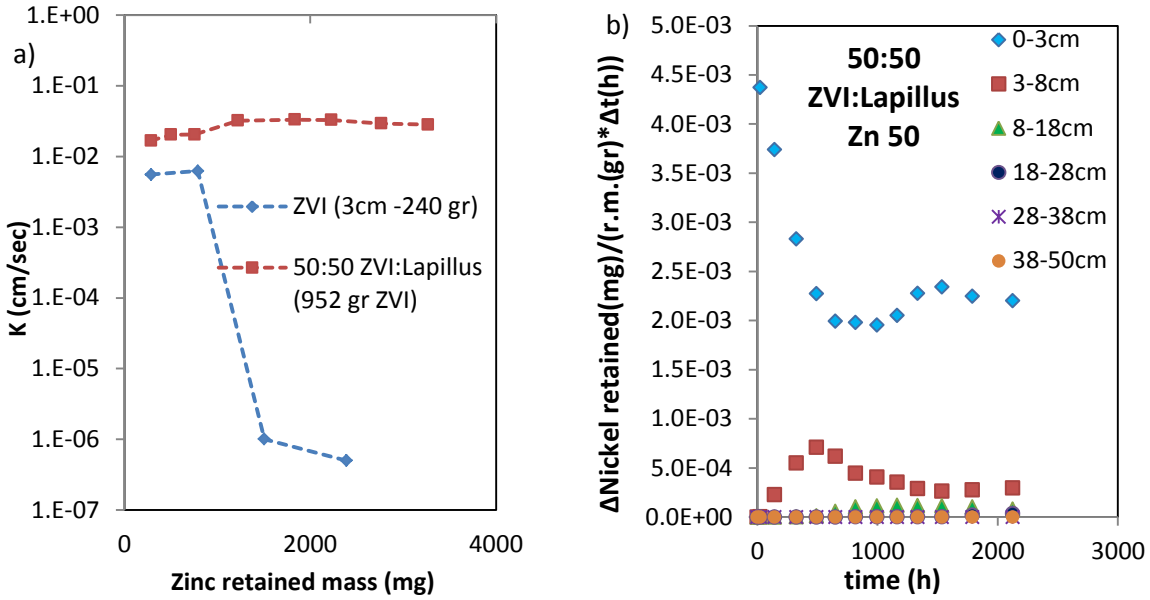

Figure 5-64 a) Hydraulic conductivity evolution as function of Zinc retained mass; b) removal specific rate evolution with time for each filter sector for column test performed using solution of Zinc at 50 mg/L of initial concentration

5.8 Results of column tests carried out with pluri-contaminated solution

The study proposed in this section is focused on the investigation of long-term removal efficiency performance and hydraulic behaviour of 50:50 ZVI:Lapillus weight ratio mixture to be used in pluri-contaminated solution remediation. A solution containing Nickel, Copper and Zinc at 50, 500 and 50 mg/L initial concentration respectively was used in the test. The obtained results and their comparison with that of column tests performed with the same weight ratio mixture and mono-contaminant solutions are introduced. The benchmarks of (pure ZVI filter) tested with the same mono-contaminant and three-contaminant solutions in the same experimental conditions (Suraci, 2011; Bilardi, 2012) were taken into account in the analysis. The characteristics of the considered column tests are reported in Table 5-14.

React. mat.	Weig. ratio	Initial cont. conc. (mg/ L)	React. Thick. (cm)	React. area (cm)	React. Vol (cm^3)	Fe^0 (gr)	Lapil. or Pum. (gr)	n (%)	Flow veloc. (mm/ min)	PV (cm^3)	Tres (h)
Fe^0/ Lap	50:50	Ni 50	50	18.09	904.3	970	970	38	0.276	340.1	11.3
Fe^0/ Lap	50:50	Zn 50	50	18.09	904.3	970	970	38	0.276	340.1	11.3
Fe^0/ Lap	50:50	Ni 50, Cu 500, Zn 50	50	18.09	904.3	963	963	38	0.276	344.5	11.5
Fe^0/ Lap	30:70	Ni 50, Cu 500, Zn 50	50	18.09	904.3	904	480	37	0.276	334.3	11.1
$Fe^{0,*}$	-	Ni 50	3	18.09	54.26	240	-	44	0.276	23.76	0.8
$Fe^{0,**}$	-	Zn 50	3	18.09	54.26	240	-	43	0.276	23.41	0.8
$Fe^{0,*}$	-	Cu 500	3	18.09	54.26	240	-	44	0.276	23,76	0.8
$Fe^{0,**}$	-	Ni 50, Cu 500, Zn 50	3	18.09	54.26	240	-	48	0.276	26.15	0.9

Table 5-14 Characteristics of carried out column tests to study the tri-contaminant removal
*(Suraci, 2011);**(Bilardi 2012)

5.8.1 Removal efficiency

The investigation about removal efficiency is developed in three steps. The first consists of comparing the contaminant concentration evolution in mono-contaminant and three-contaminant tests. The second is focused on studying whether a priority in removal exists and whether a difference between mono-contaminant and three-contaminant cases can be observable, as well as in the similar study performed using ZVI/Pumice mixtures. (Bilardi et al., 2014). Finally, the results obtained using 50:50 ZVI:Lapillus weight ratio will be compared with those of pure

ZVI filters tested under the same experimental conditions with mono and three-contaminant solutions.

In Figure 5-65 a) and b) the results concerning the 50:50 weight ratio ZVI:Lapillus mixture and the pure ZVI filters tested using mono-contaminant and three-contaminant solutions for Nickel and Zinc contaminants respectively are shown. The 18 cm thick filter of 50:50 ZVI:Lapillus mixture corresponds to about 340 gr of ZVI, while in the 3 cm of pure ZVI filter the mass of reactive material is 240 gr. Concerning Nickel removal, the 3 cm thick pure ZVI filter is not able to reduce efficiently the contaminant concentration in any case, neither in mono-contaminant nor in three-contaminant tests. On the other hand, when Zinc contaminant is used, the 3 cm of pure ZVI filter are able to remove efficiently the contaminant in mono-contaminant solution, while it does not have the same efficiency when three-contaminant solution is used. Probably, this difference is due to the presence in three-contaminant solution of Copper, that can be rapidly removed by redox processes (Bilardi et al., 2014).

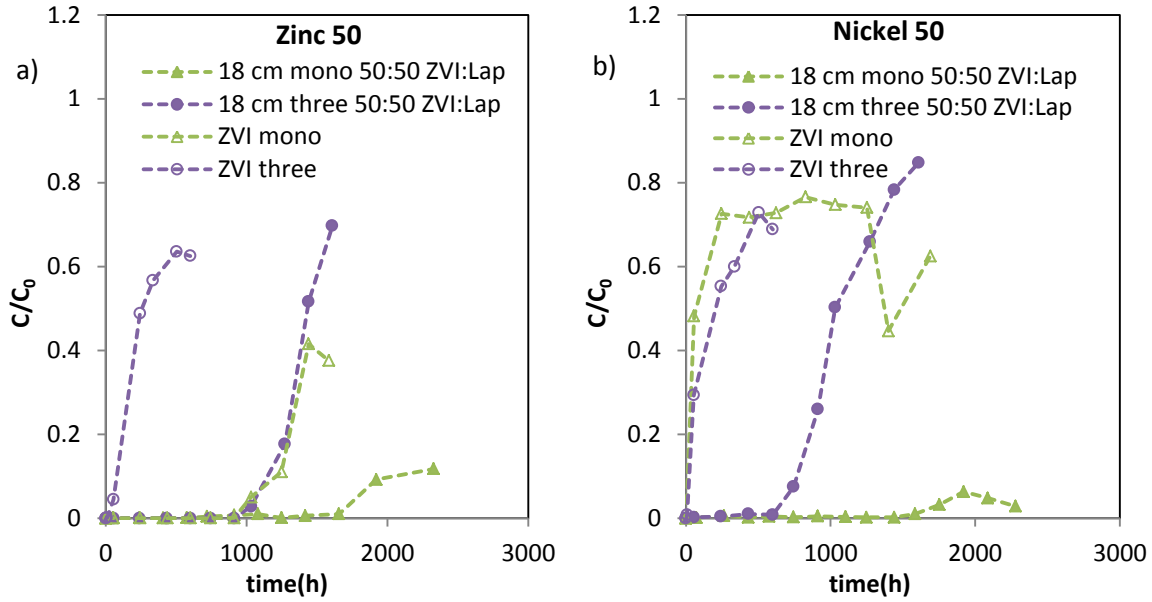

Figure 5-65 a) Zinc and b) Nickel normalized concentration evolution at 18 cm long 50:50 ZVI:Lapillus w.r. mixtures and at outlet of pure ZVI filters carried out using mono and three-contaminant solutions

In Figure 5-66 a) and b) the cumulative contaminant mass as function of input contaminant mass is shown for the 18 cm long 50:50 ZVI:Lapillus w.r. mixture (340 gr of ZVI) and for the pure ZVI (240 gr of XVI) filters of mono and three- contaminant tests, for Zinc and Nickel respectively. This comparison based on similar ZVI content shows the different influence of ZVI content on the removal of the two contaminants.

It mostly influences Zinc removal, while it is not the most affecting parameter of Nickel removal.

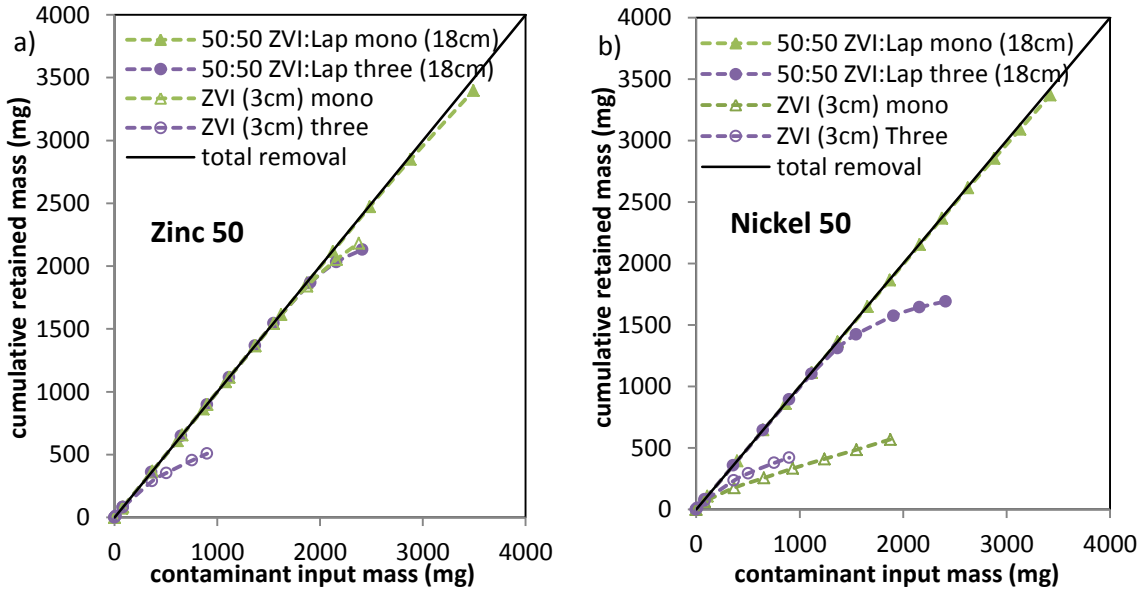

Figure 5-66 a) Zinc and b) Nickel cumulative retained mass as function of contaminant input mass for 18 cm long 50:50 ZVI:Lapillus w.r. mixtures and pure ZVI filters carried out using mono and three-contaminant solutions

5.8.2 Hydraulic behaviour

The investigation of the long-term hydraulic behaviour will be focused on comparing the calculated hydraulic conductivity evolution for the column tests carried out using mono-contaminant solutions of Nickel and Zinc and the value obtained for the three-contaminant solution tests.

In Figure 5-69 a) the evolution of hydraulic conductivity with time for column testes performed using 50:50 weight ratio ZVI:Lapillus and solutions contaminated respectively by Nickel (50 mg/L), Zinc (50 mg/L) and Nickel, Copper and Zinc (50, 500 and 50 mg/L respectively).

The three filters have not developed the same long-term hydraulic behaviour. Considering that the composition of the used mixtures, the used ZVI mass and the experimental conditions (e.g. water flowed and residence time) were the same, the observed difference in hydraulic performance probably deals with the mass of retained contaminants or their compounds and reactions involving Iron, contaminants.

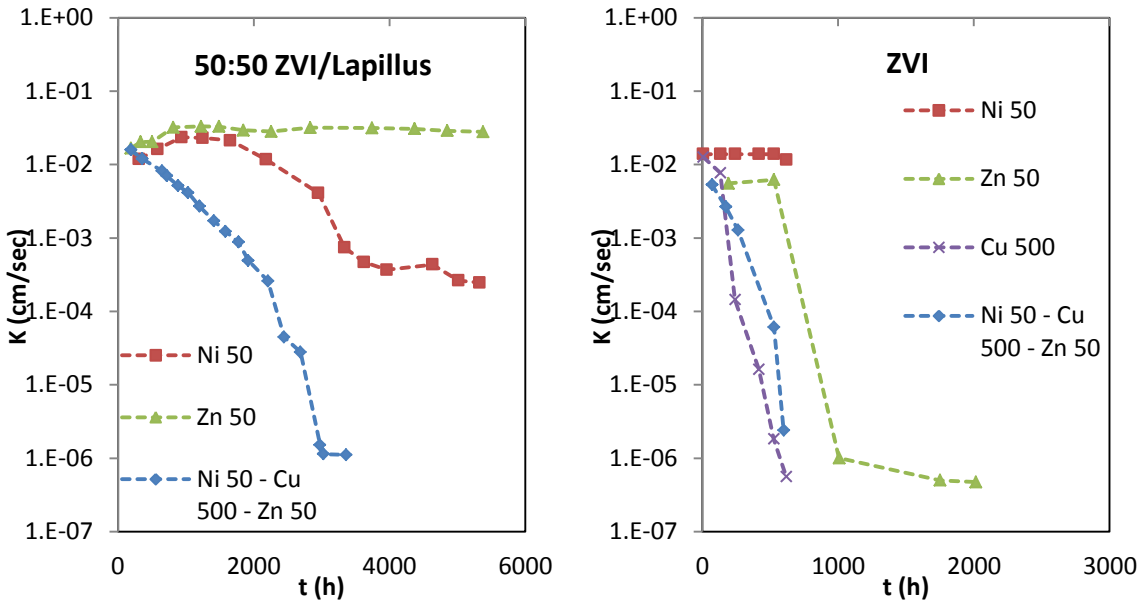

Figure 5-67 Hydraulic evolution with time a) for 50:50 ZVI/Lapillus w.r. mixtures and b) for pure ZVI tests.

To investigate whether the same order in hydraulic conductivity loss is observed using pure ZVI, the values measured in the 3 cm long pure ZVI filters performed with Nickel-contaminated (C_0=50 mg/L), Zinc-contaminated (C_0=50 mg/L), Copper-contaminated (C_0=500 mg/L) and three-contaminated (C_0=50 mg/L for Nickel and Zinc, C_0=500 mg/L for Copper) solutions are reported in Figure 5-69 b). As can be expected, the ZVI filters rapidly lost their initial hydraulic conductivity and its final value was about 5E-07 cm/sec for all the tests, except for that performed using Nickel-contaminated solution. This difference can be sought in chemical conditions development or in the filter length being not high enough to develop hydraulic issue, taking into account the importance of residence time to remove Nickel.

The hydraulic conductivity loss in pure ZVI filters takes more time to develop in experiments using Zinc-contaminated than those with Copper-contaminated and three-contaminated solutions. Moreover, the loss of hydraulic conductivity has the same rate for all the tests. Also for the tested 50:50 ZVI:Lapillus weight ratio mixtures, that with the three-contaminant solution is subject to the earliest and fastest loss in hydraulic conductivity. That performed using Zinc-contaminated solution is not subject to hydraulic issue in the experimental test time.

5.9 Conclusion

In this chapter it is proposed the use of natural volcanic lapillus as new admixing agent for ZVI. The granular mixture composed by ZVI and lapillus was tested toward nickel removal through column tests and the effect of the mixture weight ratio, flow velocity and contaminant initial concentration on the long-term removal efficiency and hydraulic behavior was investigated.

It was observed as pure Lapillus tested in column with a solution of nickel at 50 mg/L of initial concentration and a 0.276 mm/min constant flow velocity performs a not negligible nickel removal efficiency. Considering the same ZVI content (240 g), the removal efficiency after the input of 2.5 g of nickel mass was 99.3%, 98.9%, 95.1% and 34% for the granular mixtures at weight ratios of 10:90 (for which the maximum ZVI content available was 138g), 30:70 and 50:50 and pure ZVI filter respectively.

Hydraulic conductivity determinations have shown the highest permeability reduction for the granular mixture at weight ratio equal to 50:50. For the 10:90 and 30:70 w.r. mixtures, the nickel mass retained was almost homogenously distributed along the first 18 cm from the column inlet, while for 50:50 w.r. mixture the nickel mass is retained mainly in the first 8 cm leading to a higher reduction of the hydraulic conductivity. The flow velocity plays an important role in nickel removal, in fact the higher the flow velocity and the lower the contact time and the removal efficiency. Furthermore, the removed nickel mass was retained in the first 8 cm of the filter in the test carried out at 0.079 m/d, it is equally distributed in the first 18 cm of the filter for the test carried out at 0.4 m/d, whereas the entire filter is involved in nickel removal processes in the test carried out at 1.9 m/d. The removal efficiency of the reactive medium decreases as contaminant concentration in input increases. In particular, the test performed with 10 mg/L of initial nickel concentration shows an efficiency equal to 99.9%. and the nickel retained mass was concentrated in the first 3 cm of the filter, whereas it was distributed in the first 28 cm of the filter in the test carried out with the higher value of initial nickel concentration (i.e. 100 mg/L).

Repeatability of tests should be studied to understand more precisely the influence of ZVI and lapillus in long-term removal efficiency and hydraulic behaviour.

In Chapter 6, a model to simulate the experimental results observed in column tests performed with mixtures is developed.

6 Column test modelling Mono-dimensional Model Development

6.1 Introduction

As observed in Chapter 5, the removal efficiency and hydraulic behavior of mixtures based on ZVI and internally porous materials can be influenced significantly by different factors.

In this section, the development of a model to be used to simulate the long-term removal efficiency and the hydraulic behavior is outlined. Moreover, the model is useful to understand the mechanisms that occur during pollutants removal.

Firstly, the methodology used to develop the model will be described as well as the approach adopted and the fundamentals of equations that constitute the basis of the model.

A brief discussion on the mechanisms of heavy metal removal using ZVI, Pumice and Lapillus will be proposed to be able to choose the more appropriate model concerning the removal term. Once the most adequate has been hypothesized, the methodology followed to choose the values of coefficients and simulate the experimental results will be described. Finally the simulations and sensitivity analysis results will be shown.

6.2 Methodology

The model of column, considered as filter of doubly porous material, has been conceived in order to develop a tool to simulate the long-term removal efficiency and hydraulic behavior, as coupled, and to understand the removal processes and the mechanisms leading to hydraulic conductivity loss as well as how they evolve with time and along the filter thickness into the reactive packed bed.

The general steps for model development are described in Figure 6-1. The mass balance represents the first step and it has been based on mechanisms of diffusion, advection and reaction. Afterwards, the observation of microstructure evolution represents the basis of interpretation and understanding of permeability evolution. Both removal efficiency and hydraulic behavior can be influenced by microstructure evolution and this should be introduced through a coupled model. Furthermore, this

path has been constantly based on observation of experimental data, geometrical hypothesis and back-analysis.

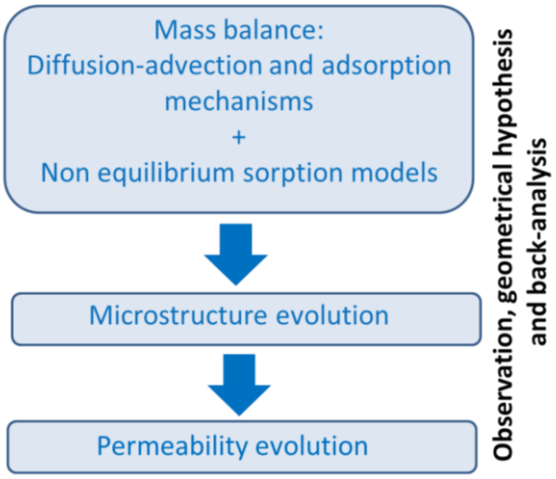

Figure 6-1 Scheme of methodology

6.3 Continuum approach

To simulate the column tests, the models of flow and solute transport through the subsurface porous media have been considered. They consist of partial differential equations and are based on considering the porous medium as a continuum domain that is occupied by different phases, solid matrix and void space and for which a representative elementary volume (REV) can be found. (Bear, 2010). The void space can be occupied by liquid and gaseous phases in different proportions, as function of saturation. A phase can be defined as a portion of space that is separated from others by an interface or that is occupied by a material characterized by a single set of constitutive relations describing its behavior. The gaseous phase can be only one, gas being miscible, while the liquid phases can be more than one. A domain occupied by a phase can be considered a continuum if state variables and properties can be assigned to every point within it.

Considering a porous medium domain made of solid matrix and at least one fluid phase, subdomains occupied by the first and the latter can be identified. The subdomain occupied by a solid is characterized by a behavior as a continuum with respect to a solid, it is so for that occupied by water. The continuum approach applied to one phase is based on averaging its behavior at molecular level, in order to obtain a microscopic level description. To overcome the difficulties concerning the solving of

problems at this level, a macroscopic level can be introduced, in which properties can be assigned for every point in the porous macroscopic level domain.

Thus, the real porous medium domain, made of at least two phases, each one considered as a continuum at microscopic level and together completely occupying the porous medium domain, is modeled as a continuum in which each phase behaves as a continuum filling up the porous medium domain as a whole (overlapping continua).

Average values of variables describing the behavior of a phase can be assigned at each point of porous medium domain taking them over an elementary volume centered into the point. Moving it into the porous medium domain, a field of macroscopic variables, as differentiable functions of spatial coordinates can be obtained. Coefficients result from the averaging process, e.g. porosity, permeability and dispersivity. In fact, the REV should be sufficiently large that, taken at different locations of the entire domain, it will contain a solid phase and a void space. (Bear, 2010).

6.4 Fundamentals of equations

The development and use of a model allows us to predict the behavior of an aquifer in response to excitations due to the implementation of management decisions, to better understand a system from different points of view, to provide information for field experiments design, for monitoring networks and for complying with regulations. (Bear, 2010). The aim of this work is to develop a numerical model to simulate dynamic laboratory tests carried out to study the long-term heavy metal removal efficiency and hydraulic behavior of zero valent iron and pumice or lapillus mixtures to be used in Permeable Reactive Barrier application.

Because of the complexity of different practical problems it is often not possible to solve the mathematical models analytically. Thanks to the ability to model more complex conditions than analytical solutions, numerical models are used to solve the mathematical ones using computer programs. Estabragh et al.(2013) describe the differences in terms of results between the two kinds of solution approaches.

The model used to search the best fitting of carried out column tests results is based on the one-dimensional advection-dispersion-sorption equation derived by the

equation for three dimensional solute transport in saturated media under uniform steady flow presented by Bear (1979).

The hypothesis of the well-known above-mentioned equation consists of homogeneous, isotropic and saturated porous media with flow conditions valid for Darcy's law. The model is based on the conservation of a mass of solute in a small representative elementary volume. (Fetter, 1992).

The results that will be shown at a later stage are obtained from some simulations of a numerical model based on a system of five or six equations with five or six unknowns respectively.

Comparing the batch tests and column tests results, it was possible to deduce and hypothesize non-equilibrium sorption conditions.

$$\varphi_e \frac{\partial C}{\partial t} - \varphi_e D_L \frac{\partial^2 C}{\partial x^2} + \varphi_e v_x \frac{\partial C}{\partial x} + \sum_i R_i = 0 \qquad (6-1)$$

$$\frac{\partial \varphi_{macro}}{\partial t} = -\alpha(\eta - 1)\theta_z \qquad (6-2)$$

$$\frac{\partial \varphi_{micro}}{\partial t} = 0 \qquad (6-3)$$

$$\varphi_{macro} + \varphi_{micro} = \varphi \qquad (6-4)$$

$$D_L = \alpha_L v_x + D^* \qquad (6-5)$$

$$\varphi_{macro} = \frac{V_v}{Vol} \qquad (6-6)$$

In equation (6-1) the terms of variation of solute concentration C with time, the diffusion-dispersion D_L term expressed by Fick's law, the advection term depending on the v_x flow rate and the reaction terms Ri. The D coefficient is expressed by the equation (6-5) and this includes the D* diffusion coefficient and the hydrodynamic dispersion coefficient parallel to the principal direction of flow, defined as α_L longitudinal dynamic dispersion times the seepage velocity v_x. Each term of equation

(6-1) is multiplied by the φ_e effective porosity value to refer all the numerical models and then the results to a unit volume. The equations (6-2) and (6-3) express the total porosity variation with time. θ_z represents the volumetric fraction occupied by ZVI, α a is the depletation rate, η represents the coefficient of volumetric expansion (Caré et al, 2013, Bilardi et al., 2013a). The φ_{macro} macro-porosity term used in equation (6-2) is defined by equation (6-6) and it is equal to the ratio between the void volume V_v and the total volume Vol of the column physical model. Where φ_{micro} is the pumice intra-particles porosity equal to the ratio between the pumice particles internal void volume V_{vp} and total volume Vol. Before discussing and defining the reaction terms, a review of available models will be introduced to explain the choice of the model used .

6.5 General review of available models

A number of numerical models are available to represent the transport through unsaturated and saturated soil. Vleach, CHEMFLO 2000, Sesoil, Sutra, Mofat, VS2DTI, Pestan, Bioplume III, HELP are used for unsaturated conditions, while Bioscreen, Modflow, Phast, WhAEM2000, AT123D and FEFLOW 5.4 are useful for saturated conditions.

In Figure 6-2 a scheme regarding modelling approaches available for the description of transformation processes of contaminants in transport equations is shown.

Some approaches for the simulation of contaminants transport are based on multicomponent transport codes that incorporate different chemical models to describe the interaction between dissolved species and immobile solid surfaces. (Kantar, 2007). For each kind of chemical process considered, there are different developed models. One example is the MIN3P model developed by Mayer (1999) and Mayer et al. (2002) consisting of a multicomponent reactive transport model for variably saturated porous media (Bilardi et al., 2012 b).

The single component models are not chemically explicit and are not based on considering the various sorption processes separately. They are focused on the overall result of processes resulting in solute removal from solution. This kind of model has a more limited number of parameters to be defined than the multi-component ones and therefore are easier to calibrate.

To choose the more appropriate model, removal mechanisms of heavy metal (and Nickel in particular) onto Pumice (or Lapillus) and ZVI will be summarized.

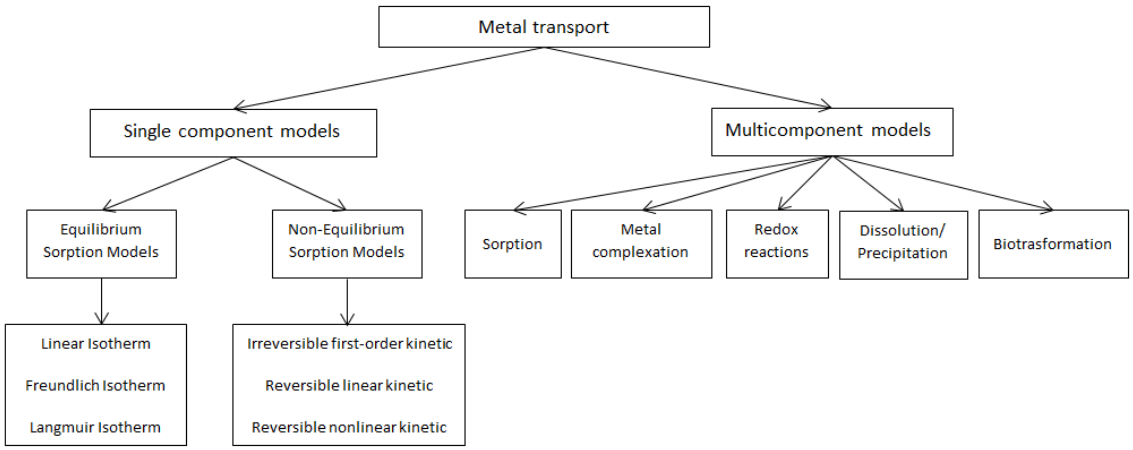

Figure 6-2 Scheme of description of transformation processes of contaminant in transport equation (adapted from Kantar, 2006)

6.6 Nickel removal on Pumice, Lapillus and ZVI

The heavy metal removal in zero valent iron can take place by means of reductive precipitation and co-precipitation, adsorption onto iron surface and onto iron corrosion products (Suponik et al., 2014). The kind of removal mechanism depends on the characteristics of the metal to remove, on the presence of other substances and physicochemical conditions of the ZVI and surrounding zones. On the other hand, in groundwater the corrosion of zero valent iron, oxidized to ferrous and ferric iron, causes an increase in pH, an decrease in ORP, the consumption of dissolved oxygen and the generation of hydrogen (Puls et al., 1999). The reactions involved during the oxidation of iron in the water are described by equations 6-7 to 6-11.

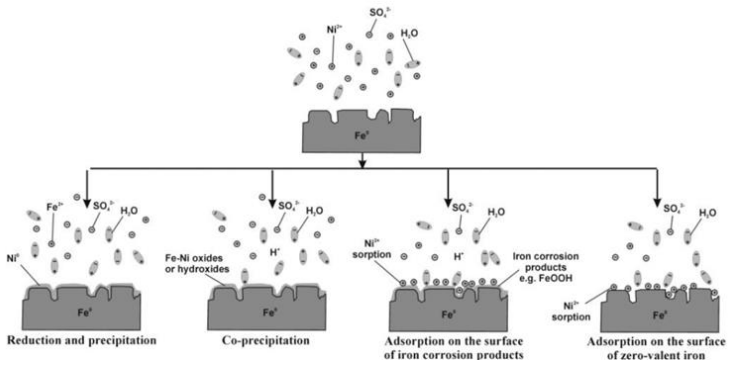

Figure 6-3 Nickel removal using ZVI (Suponik et al., 2014)

$$2Fe^{0}_{(s)} + O_2 + 2H_2O \rightarrow 2Fe^{2+} + 4OH^- \quad (6\text{-}7)$$

$$Fe^{0}_{(s)} + 2H_2O \rightarrow Fe^{2+} + H_2 + 2OH^- \quad (6\text{-}8)$$

$$2Fe^{2+} + 2H_2O \rightarrow 2Fe^{3+} + H_2 + 2OH^- \quad (6\text{-}9)$$

$$2Fe^{2+} + \tfrac{1}{2}\, H_2O + 2H^+ \rightarrow 2Fe^{3+} + H_2O \quad (6\text{-}10)$$

$$2Fe^{3+} + 6\, H_2O \rightarrow 2Fe(OH)_{3(s)} + 6H^+ \quad (6\text{-}11)$$

As described in the paper written by Li and Zhang (2007), the removal mechanism of metal ions with a standard potential very close to that of iron are sorption/surface complex formation and/or reductive precipitation (Figure 6-3). The small difference of standard electrode potential of Fe^0 and Ni^0 reduces at minimum the possibility of reductive precipitation process in metallic form. It is possible to say that the main processes for Nickel (II) removal are adsorption on the iron corrosion products surface and less likely directly onto zero valent iron surface. There is the possibility that the co-precipitation with iron, forming oxides and hydroxides, takes place, too.

As has been described in Chapter 3, heavy metals removal by pumice as well as lapillus can depend on the high internal porosity and the content of iron and aluminium oxides that are very effective in removing heavy metal contaminants due to their high specific surface areas and reactive surface functional groups.

The adsorption proceeds through the diffusion consisting of transfer of adsorbate from solution to adsorbent surface, the migration of adsorbate into pores and interaction with available sites on the interior surface of pores (Figure 6-4).

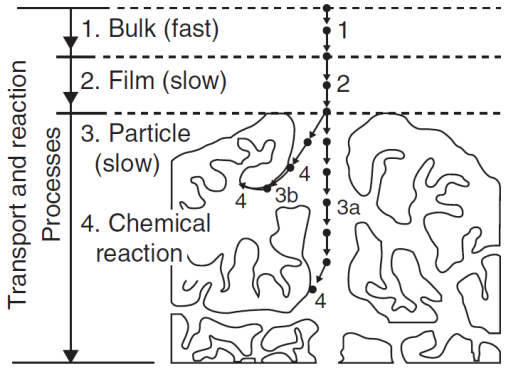

Figure 6-4 reaction processes in a porous medium (Weber and Smith, 1987, Appelo, 2005).

The factors influencing the adsorption are surface area of adsorbent, contact time or residence time, particle size of adsorbent, solubility of substances, affinity of the solute for the adsorbent, size of the molecule with respect to size of the pores, degree of ionization of the adsorbate molecule, pH and initial concentration.

6.7 Sorption models

The sorption processes are adsorption, by which a solute clings to a solid-surface, ion exchange, during which a charged ion is exchanged with another of the same sign present on the solid surface, chemisorption, when the solute is incorporated in solid phase by chemical reactions and absorption, that occurs when the solute can diffuse into the internal pores of a porous particle and be sorbed onto interior surfaces. (Fetter, 1992).

The aim of this kind of model is focused on the practical interest of considering the removal of the solute from solution and its partitioning between solution and solid phase.

Considering the sets of chemical reactions and the ground-water flow rates, Rubin (1983) classified all reactions into two kinds consisting in equilibrium and non-equilibrium or kinetic reactions. The first are sufficiently fast reactions related to the groundwater flow rate so that it is possible to assume a local equilibrium between solute and surrounding. The non-equilibrium reactions are slow sorption processes compared to the rate of fluid flow in the porous media, so that it is not possible to hypothesize the development of equilibrium conditions between solute and sorbed phase.

The resulting model for linear equilibrium adsorption is easy but has shown some inadequacies comparing with experimental data. For this reason, more complex models were introduced taking into account the different rates of sorption processes in different parts of soil medium. (Van Genuchten, 1981).

Considering the experimental data of the reactive materials tested in this research activity, the reaction time, is considered as the time that the reactive material needs to remediate efficiently contaminated water in batch tests, and the residence time, that the column test can ensure. In table 6-1 the reaction times observed for the batch tests performed using different weight ratios of ZVI:Pumice mixtures and solution of

Nickel at 5 and 50 mg/L initial concentrations are reported. In table 6-2 the characteristics of column tests performed using different weight ratios of ZVI:Pumice mixtures and solution of Nickel at 50 mg/L initial concentrations are reported. It can be observed that the residence time is always lower than the time necessary for the total development of removal reaction, as observed in batch tests. Of course, this should be considered as a preliminary comparison, taking into account the different experimental conditions. Moreover, this observation can justify the choice of the tipe of sorption model (i.e. non-equilibrium (kinetic) sorption model). Different simulations and the results of batch tests modelling (Chapter 3) can validate this choice.

Reaction time (h)					
Ni Co (mg/l)	0:100 w.r.	10:90 w.r.	30:70 w.r.	50:50 w.r.	100:0 w.r.
5	>48	24	24	8	8
50	>120	120	48	48	24

Table 6-1 reaction time as observed by batch tests results

w.r	M_{tot}(g)	V_c(cm^3)	n(%)	PV(cm^3)	T_R(h)
0:100	560	902	45	411	13.7
10:90	650	981	46	459	15.3
30:70	800	981	46	459	15.3
50:50	1060	981	46	448	15
100:0	1680	435	51	222	7.4

Table 6-2 column tests characteristics

6.8 Column model

A mono-dimensional advection-dispersion-diffusion equation is applied to the representative elemental volume (REV) of the column and the equation (6-1) can be rewritten as :

$$\varphi_e \frac{\partial C}{\partial t} = \varphi_e D_L \frac{\partial^2 C}{\partial x^2} - \varphi_e v_x \frac{\partial C}{\partial x} - \varphi_e \sum_i \frac{\partial C_i^*}{\partial t} \qquad (6-12)$$

where the φ_e is the effective porosity, smaller than the total porosity φ (equal to voids volume to total volume ratio), is the porosity through which flow can occur, considering that sometimes, part of void space is unavailable for fluid flow or contains immobile fluid. C is the solute concentration, D_L is the hydrodynamic dispersion coefficient parallel to the principal direction of flow that can be written also as:

$$D_L = \alpha_L v_x + D^* \qquad (6-13)$$

where α_L represents the longitudinal dynamic dispersivity, v_x is the average linear velocity in the longitudinal direction and D^* is the effective diffusion coefficient that is equal to:

$$D^* = \omega D_d \qquad (6-14)$$

where ω is a coefficient that is related to the tortuosity (Bear 1972) and D_d is the diffusion coefficient in water. Tortuosity can be defined in different ways. It consists of an index of the shape of the flow path followed by water molecules flowing through a porous medium (Fetter, 1999). v_x represents the average velocity of the fluid flowing through a porous medium, referred to seepage velocity too. It is given by the Darcy velocity v divided by the effective porosity φ_e:

$$v_x = \frac{Ki}{\varphi_e} \qquad (6-15)$$

where K is the hydraulic conductivity and i represents the hydraulic gradient.
The term C_i^* represents the removed solute mass by i-th reactive material divided by the solution volume. This term is replaced by the model hypothesized as to be able to represent the experimental results and the remediation mechanisms developed by the used reactive materials as described in the literature.

6.9 Choice of model parameters coefficients

The hydrodynamic dispersion is given by the sum of diffusion and dispersion. This means that it can be divided into the two components. Practically, the diffusion is often neglected in groundwater flow conditions. To evaluate the relative contribution of mechanical dispersion and diffusion to solute transport in column tests, the number of Peclet, described by equation 6-16 for column studies, can be calculated.

$$Pe = \frac{v_x d}{D_d} \qquad (6-16)$$

where v_x is the advection velocity, d is the average grain diameter and D_d the molecular diffusion coefficient. The Peclet number, as applied to the column studied, represents the ratio of mass transport by advection to mass transport by molecular diffusion (Fetter, 1999). Considering an average diameter (d_{50}) varying among 0.3, 0.4 and 0.5 mm, the D_d coefficient varying between the maximum (1.5×10^{-9} m^2sec^{-1}) and minimum (0.7×10^{-9} m^2sec^{-1}) values (Gui *et al.*, 2009; Jeen *et al.*, 2007; Mayer *et al.*, 2002; O *et al.*, 2009, Moraci et al., 2014) and the seepage velocity used to perform column tests, Peclet number was calculated for the column tests carried out (table 6-3).

Dd_{min}				Dd_{max}			
d_{50} (mm)	0.3	0.4	0.5	d_{50} (mm)	0.3	0.4	0.5
v1	2.5	3.3	4.1	v1	1.2	1.5	1.9
v2	12.3	16.5	20.6	v2	5.8	7.7	9.6
v3	61.7	82.3	102.8	v3	28.8	38.4	48

Table 6-3 Peclet number for carried out column tests varying d_{50}, Dd and v

Figure 6-5 shows the results of experimental measurements using uniform sand columns and tracers (Perkins and Johnson, 1963). Although only pure ZVI can be classified as uniform sand, while Pumice and Lapillus are sand with a low percentage classified as silt, the observation of the graph considering the number of Peclet calculated for performed column tests, can provide important information.

Looking at the graph, for very low velocities, the D_L to D_d ratio is constant and about 0.7. For the Peclet number lower than 0.4, diffusion is the key-phenomenon for solute transport and dispersion can be neglected, for its values higher than 6 dispersion is the most effective mechanism of mass transport, while for value between 0.4 and 6 there is a transition zone, where the effectiveness of dispersion and diffusion is the same.

Considering the Peclet number as calculated for performed column tests, for all the tests performed using v_2 and v_3 hypothesizing both values of D_d the advective dispersion is the main mass transport phenomenon. The experiments performed using v_1 correspond to the transition zone, where an influence of both dispersion and diffusion is valid.

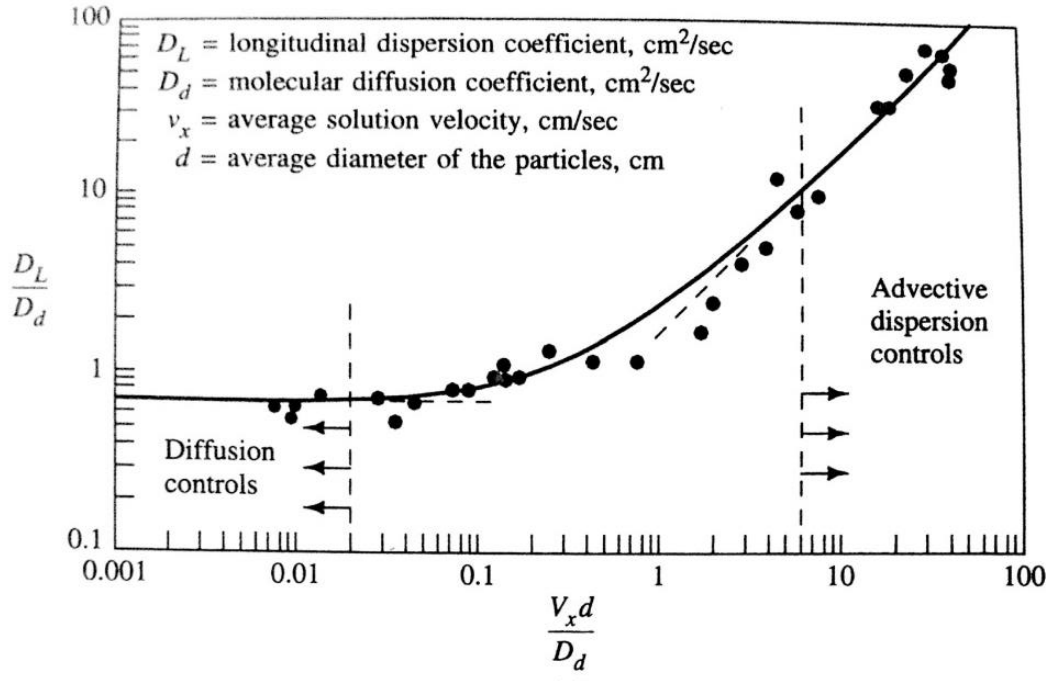

Figure 6-5 Graph of dimensionless dispersion coefficient versus Peclet number (Perkins and Johnson, 1963).

A study of the ratio of dispersion coefficient D_L over the diffusion coefficient D_d in pure water as function of Peclet number Pe was proposed by Bear (1972) for a column study for given packed columns, using tracers. Two main domains have been discerned: one corresponding to Pe < 0.5 where diffusion is the dominant mechanism and the other characterized by Pe > 0.5 where dispersion is the main process (Bear,1972; Plumb and Whitaker, 1988; Appelo, 2005).

The dispersivity coefficient α_L in column tests is equal to the representative grain diameter used in packing the column (Appelo, 2005). The dispersivity coefficient α_L has been used equal to d_{50} .

6.9.1 Methodology for model development

6.9.2 Batch tests and column tests

In this paragraph simulations using removal coefficients obtained by analysis of batch tests introduced in Chapter 3 will be described, showing the results.

In the following application, the effective porosity φ_e will be considered equal to the total inter-particles porosity φ_{macro} and referred to n.

$$\frac{\partial C_i^*}{\partial t} = \frac{\rho_b}{n} \frac{\partial S_i^*}{\partial t} \qquad (6-17)$$

where ρ_b is the bulk density, defined by solid mass to total volume ratio, S_i^* is the solute mass retained by unit mass of i-th reactive material.

In equation 6-18 a non-equilibrium sorption model is described as more general than possible, considering a reactive media made of more than one material. Different reactive materials can be characterized by their solute removal efficiency, if taken as pure material but their efficiency can be affected by the presence of other reactive material, when they are used as mixed. The equation 6-18 represents the used model to simulate experimental column tests results using coefficients obtained by batch tests. It assumes that the first-order rate coefficient evolution as function of solid to liquid ratio can be described by a linear relation.

$$\frac{\rho_b}{n}\frac{\partial S_i^*}{\partial t} = \frac{\partial C_i^*}{\partial t} = P_i \frac{M_i}{Vol \cdot n} C - k_{3i} C_i^* - \sum_j f_{ij} \qquad (6-18)$$

where P_i (m^3/(kg*s)) is a first-order rate coefficient divided by the reactive mass and multiplied by the solution volume. P_i value is derived by the batch tests and takes into account the solid to liquid ratio, in batch tests performed using the i-th reactive material. M_i represents the reactive mass of the i-th reactive material contained in the column. Vol is the total internal volume of the column. k_{3i} is the backward rate coefficient meaning that the rate of solute sorption depends on the amount that has already been sorbed. The terms f_{ij} represent the influence on solute removal efficiency of the i-th reactive material due to the presence of the j-th reactive material.

Considering that by observing and analyzing batch test results, P_i and k_{3i} coefficients can be obtained easily, one step of simulation development has been focused on use of the two parameters (P_i and k_{3i}) as found for reactive materials used as pure. The term of mutual influence has been neglected. With this assumption the equations used in the simulation to describe sorption term are represented by (6-19) and (6-20).

$$\frac{\partial C_p^*}{\partial t} = P_p \frac{M_p}{Vol \cdot n} C - k_{3p} C_p^* \qquad (6-19)$$

$$\frac{\partial C_z^*}{\partial t} = P_z \frac{M_z}{Vol \cdot n} C - k_{3z} C_z^* \qquad (6-20)$$

where C_p^* and C_z^* represent the solute mass removed to solution volume ratio. P_p and P_z (m^3/(kg*s)) are the first-order rate coefficients divided by the reactive mass and multiplied by the solution volume obtained by analysis of the batch tests carried out using pure pumice and pure ZVI respectively. M_p and M_z represent the reactive mass of pumice and ZVI contained in the column performed using mixture at different weight ratios. k_{3p} and k_{3z} are the backward rate coefficients obtained by analyzing batch tests results performed using pure pumice and pure ZVI.

In the Figures 6-6 and 6-7 the batch tests results used to calculate the first-order rate coefficient (k_{2p} and k_{2p}) for the firsts two hours of interaction are shown. They

concern the batch tests performed using solution of Nickel at 50 mg/L initial concentration, LM and HM solid to liquid ratios, pure ZVI (Figures 5.6 a) and b), pure Pumice (Figure 6-7 a) and 30:70 w.r. mixture (Figure 5.7 b). The sorption model equations applied to batch tests with pure pumice and pure ZVI to calculate the necessary coefficients are:

$$\frac{\partial C_p^*}{\partial t} = k_{2p}C - k_{3p}C_p^* \qquad (6-21)$$

$$\frac{\partial C_z^*}{\partial t} = k_{2z}C - k_{3z}C_z^* \qquad (6-22)$$

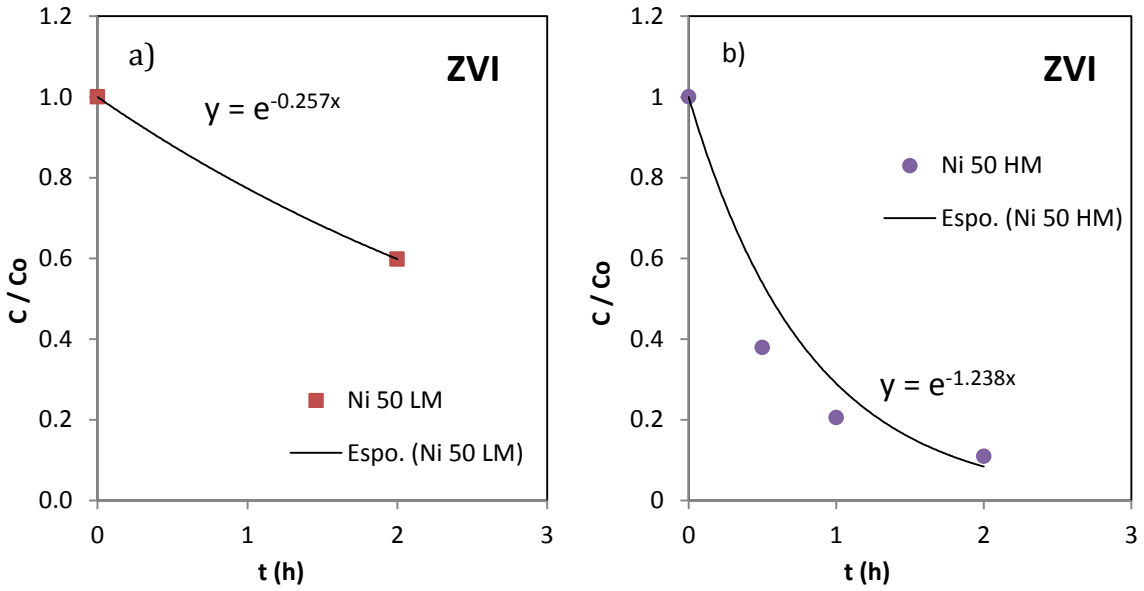

Figure 6-6 first-order rate coefficients for batch tests performed using solution of Nickel at 50 mg/L initial concentration and pure ZVI at a) LM and b) HM solid to liquid ratios

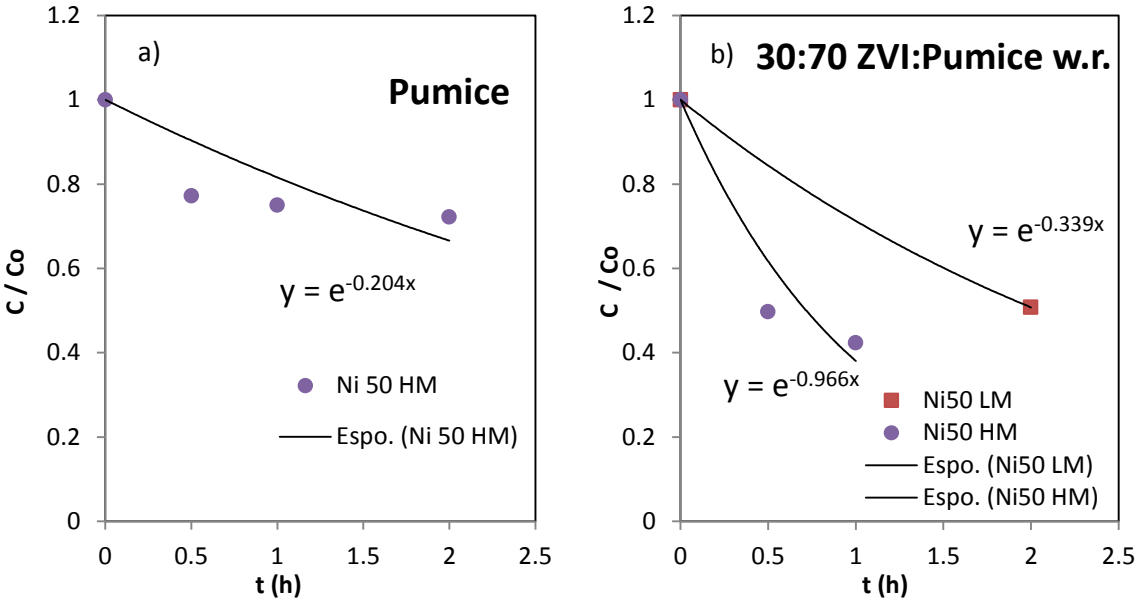

Figure 6-7 first-order rate coefficients for batch tests performed using solution of Nickel at 50 mg/L initial concentration and a) pure Pumice at HM solid to liquid ratio and b) 30:70 w.r. mixture at LM and HM solid to liquid ratios

The k_{3z} and k_{3p} coefficients have been calculated for the condition expressed by equations:

$$k_{2p}C - k_{3p}C_p^* = 0 \qquad (6-23)$$

$$k_{2z}C - k_{3z}C_z^* = 0 \qquad (6-24)$$

Coefficients for batch test performed using 30:70 ZVI:Pumice w.r. mixture were calculated using the same procedure. In Table 6-4 the k_2 and k_3 values as calculated for each reactive material are reported. In Table 6-5 the P_i coefficients equal to k_2 obtained by a done batch tests, divided by the reactive mass and multiplied by the solution volume used in the same batch test are shown.

reactive material	k2 (1/h)		k3 (1/h)	
	LM	HM	LM	HM
ZVI	2.57E-01	1.24E+00	3.83E-01	7.56E-01
Pumice	3.00E-03	2.04E-01	9.67E-05	6.91E-01
30:70	3.39E-01	9.66E-01	3.49E-01	9.56E-01

Table 6-4 k2 (1/h) and k3 (1/h) coefficients as found analyzing batch tests

reactive material	P_i [ml/(h*g)]		
	LM	HM	average
ZVI	2.57E+00	4.95E+00	3.76E+00
Pumice	3.00E-02	8.16E-01	4.23E-01
30:70	3.39E+00	3.86E+00	3.63E+00

Table 6-5 Pi coefficients evaluated considering k2 coefficient and the solid to liquid ratio in batch test

In Figures 6-8 and 6-9, the results of simulations of 30:70 ZVI:Pumice w.r. mixture column test using a solution of Nickel at 50 mg/L initial concentration and a constant flow velocity equal to v_2 (0.276 mm/min) and coefficients obtained by batch tests analysis are shown. In Figure 6-8 the results of simulation based on the two equations (6-19) and (6-20) concerning one the efficiency of Pumice and one that of ZVI are shown. In Figure 6-9 the results of simulation were obtained using one equation to describe the sorption onto mixtures particles:

$$\frac{\partial C^*_{mix}}{\partial t} = P_{mix}\frac{M_{mix}}{Vol \cdot n}C - k_{3mix}C^*_{mix} \qquad (6-25)$$

where the P_{mix} has been calculated by the k_{2mix} coefficient reported in table 6-4 and k_{3mix} were obtained using the following equation:

$$k_{2mix}C - k_{3mix}C^*_p = 0 \qquad (6-26)$$

k_{2mix} and k_{3mix} coefficients were obtained by batch tests performed using 30:70 ZVI:Pumice w.r. mixtures.

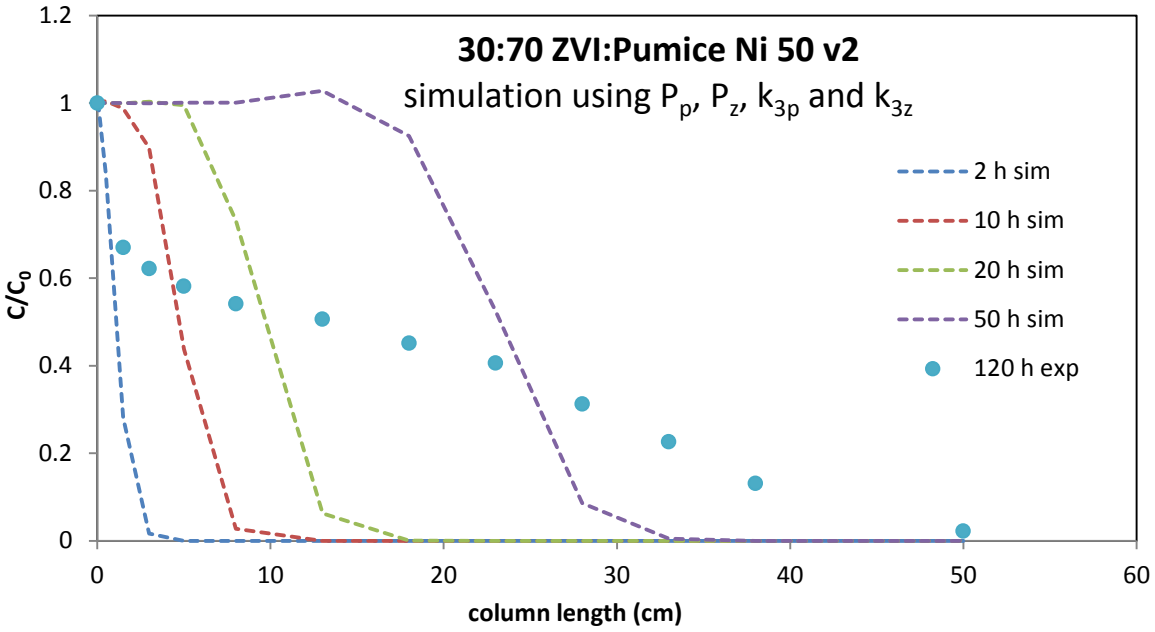

Figure 6-8 simulation results based on the use of coefficients related to batch tests performed using pure reactive materials

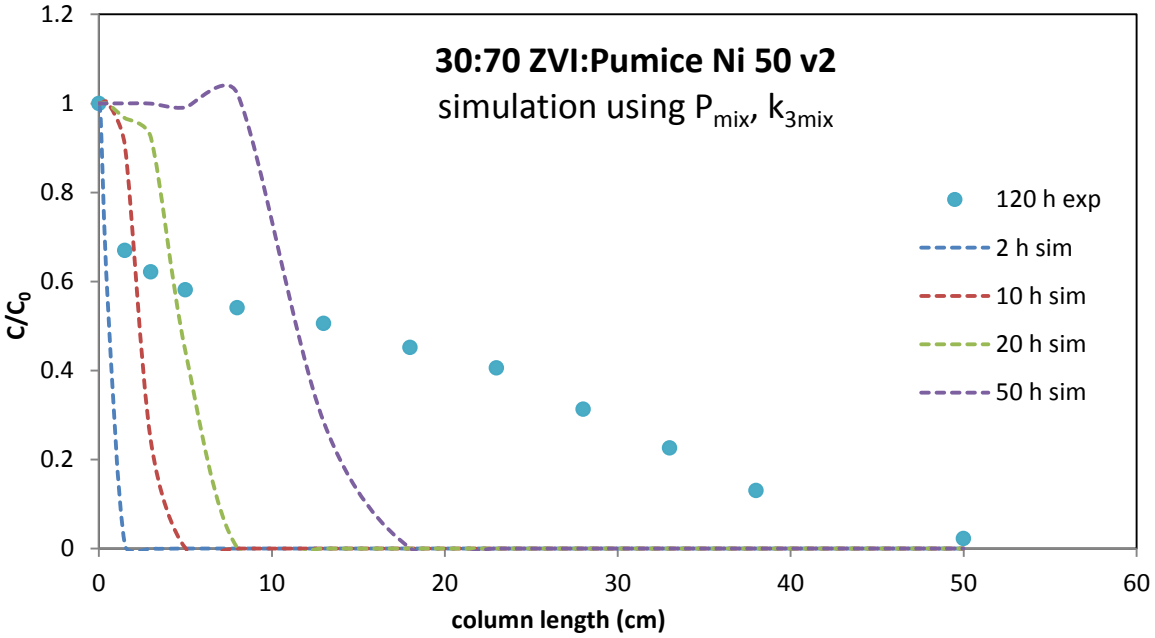

Figure 6-9 simulation results based on the use of coefficients related to batch tests performed using 30:70 ZVI:Pumice w.r. mixture

Two main considerations can be made observing Figures 6-8 and 6-9. Firstly, the coefficients obtained by batch tests seem not to be able to represent the sorption effects in column tests. This can deal with a number of different experimental conditions, e.g. solid to liquid ratio and the contaminant mass to reactive mass ratio reported in Table 6-6. The observation of this latter and of simulation results can

suggest a non-linear relation between first-order rate coefficient and solid to liquid ratio. The initial solid to liquid ratio of a column test performed using a 30:70 ZVI:Pumice mixture is about 2, while it is 0.1 and 0.25 for LM and HM batch tests. Considering that this column test was performed using a flow velocity equal to 0.276 mm/min and all the considered tests (batch and column) were carried out using a solution of Nickel at 50 mg/L, the reactive mass to contaminant mass ratio is about 2, 5 and 40 for LM and HM batch tests and column tests respectively. In particular the data related to the batch test is related to 1 PV (the first one) flowed and the entire reactive mass. The same reactive mass to contaminant mass of LM and HM batch tests can be reached in the first 3 cm of the column after 16 and 6 hours from the test beginning.

Secondly, a certain difference in simulation results can be observed between the test simulated using equation and coefficients related to each pure reactive material and that performed using one equation and coefficient related to test carried out with the mixture. This can be an evidence of not superposing effects, probably due to each influencing the other in removal efficiency.

Batch or column tests	reactive mass (gr)	cont. mass (mg)	solid/liquid	reactive mass/ cont. mass
LM	5.4	2.7	0.10	2
HM	8	1.6	0.25	5
column test 30:70 ZVI:Pum.	800	19.90	2.01	40.21 (1PV)

Table 6-6 solid to liquid ratio and reactive mass to contaminant mass ratio for LM and HM batch test and for 30:70 ZVI:Pumice w.r. mixture performed with 0.276 mm/min constant flow velocity (and solution of Nickel at 50 mg/L initial concentration)

6.9.3 Model application to mixture filters

Considering what has been observed through the previous simulation results the sorption onto the mixtures has been modeled as developed by only one material that has the characteristics of the mixture.

This means that one term of sorption has been used in the dispersion-advection equation. Considering the values of P_{mix} and k_{3mix} obtained from batch tests, they

have been changed in order to search the best values for this parameters, referred to $P_{mix,o}$ and $k_{3mix,o}$, where the subscripted o means optimization.

$$\frac{\partial C^*_{mix}}{\partial t} = P_{mix,o}\frac{M_{mix}}{Vol \cdot n}C - k_{3mix,o}C^*_{mix} \qquad (6-27)$$

In Figures 6-10 – 6-17, the simulation results and experimental data are reported for some ZVI:Pumice and ZVI:Lapillus mixtures. Varying the mixtures all the values referred to the material were changed, e.g. apparent and real density for porous materials, initial porosity. Varying the flow velocity and the contaminant initial concentration the related parameter values and boundary conditions were changed to be equal to experimental conditions.

The values of $P_{mix,o}$ and $k_{3mix,o}$ found for the different column tests simulated are reported in table 6-7.

As can be observed, the values of both coefficients are lower than the correspondent found by batch tests analysis. In particular P_{mix} values, related to batch tests, seem to be 5, 15 or 50 times higher than the corresponding $P_{mix,o}$. This can give some indications to performed batch tests with conditions more similar to those of column test. The k_{3mix} values as found for batch tests are two or three orders of magnitude higher than the corresponding $k_{3mix,o}$. Further investigations can be effected to understand what are the main factors affecting the term k_3 representing the reversibility of sorption or the influence of already sorbed mass on sorption rate.

Furthermore, it can be observed that the column tests with 30:70 ZVI:Pumice mixture using a solution of Nickel at 40 and v1 and v3 flow velocity can be simulated using the same values of $P_{mix,o}$ and $k_{3mix,o}$ parameters. These values can be used to simulate the tests with 30:70 ZVI:Lapillus w.r. mixture performed using a solution of Nickel at 50 mg/L and v2 flow velocity (but not for v1 and v3 flow velocities). Concerning the column tests performed using 30:70 ZVI:Pumice mixture and solution of Nickel at 8 mg/L initial, the values of $P_{mix,o}$ parameter vary in a large range.

This can suggest that the sorption in packed column is mainly dependent on the contaminant concentration. For low values of the latter, the sorption is highly affected by flow velocity.

mixtures	Ni i.c. (mg/L)	velocity (mm/min)	$P_{mix,o}$ [ml/(h*g)]	$k_{3mix,o}$ (1/h)
30:70 Fe:Pum	Ni 40	0.06	7.25E-02	6.53E-04
30:70 Fe:Pum	Ni 40	1.38	7.25E-02	6.53E-04
30:70 Fe:Pum	Ni 8	0.06	1.81E-03	3.26E-04
30:70 Fe:Pum	Ni 8	0.28	2.42E-01	3.26E-04
30:70 Fe:Pum	Ni 8	1.38	1.13E+00	9.60E-04
30:70 Fe:Pum	Ni 95	1.38	2.42E-01	3.26E-03
30:70 Fe:Lap	Ni 50	0.28	7.25E-02	6.53E-04

Table 6-7 coefficients of non-equilibrium sorption model as found by optimization

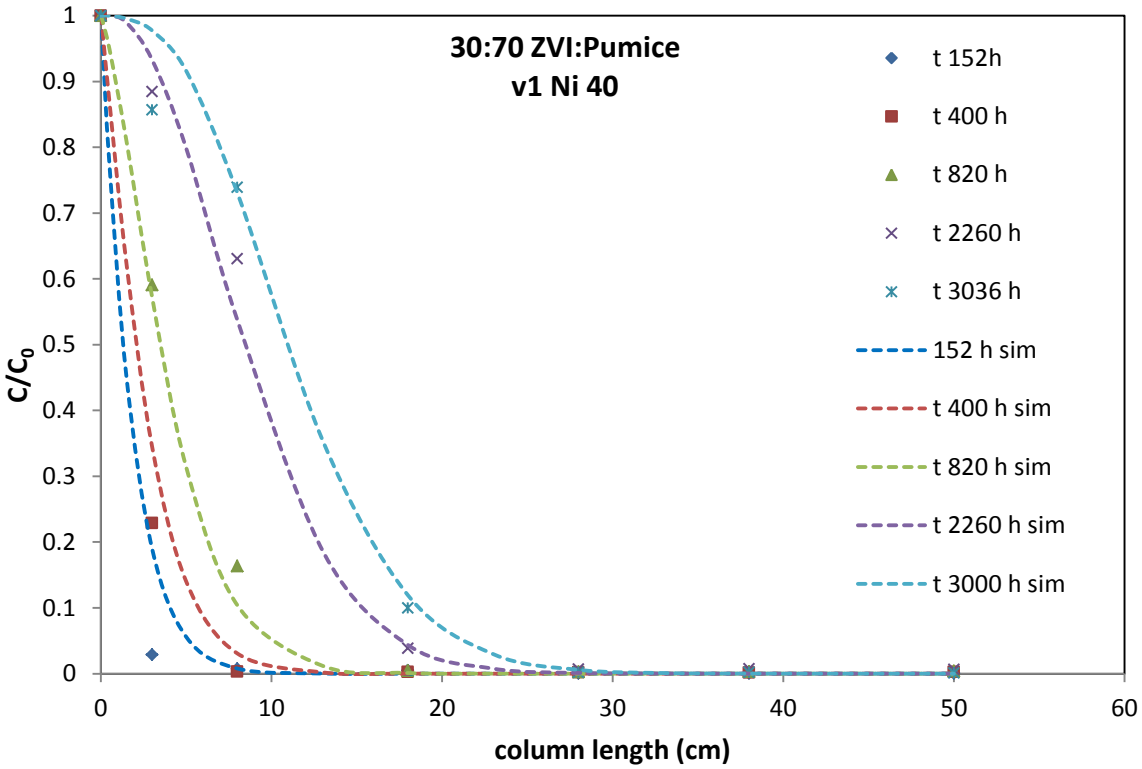

Figure 6-10 simulation and experimental results of column test performed with 30:70 ZVI:Pumice w.r. mixture, solution of Nickel at 50 mg/L initial concentration and v1 flow velocity.

It is possible to observe that the first-order rate coefficient $P_{mix,o}$ depends on the initial concentration value. In fact, for values of 40-50 mg/L, it does not vary with the flow velocity, while this happens for lower initial concentration values (8 mg/L) and $P_{mix,o}$ value increases as the flow velocity increases. The $k_{3mix,o}$ backward rate, that takes into account the mass already absorbed onto the reactive material, is of the same order of magnitude for all the tests, unless for that performed at the highest initial concentration value (95 mg/L). This makes sense because in this latter case the

mass retained after a certain time is higher than in tests performed using lower initial concentration under the same conditions.

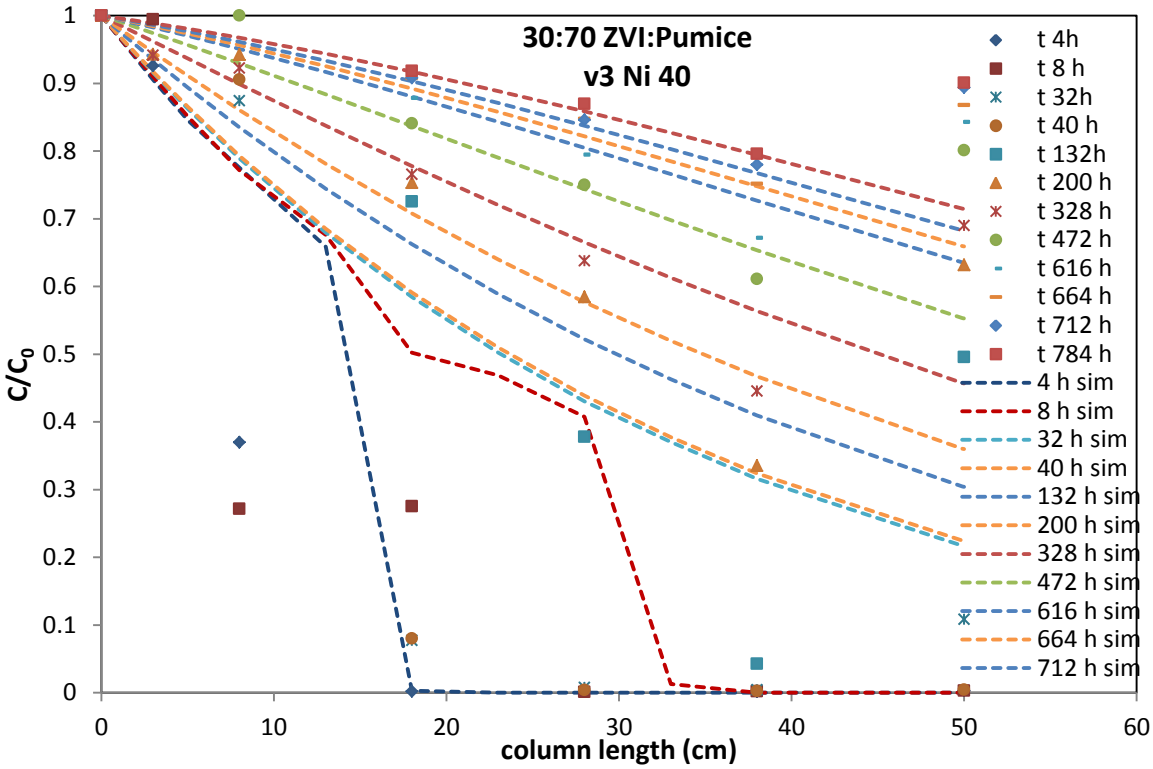

Figure 6-11 simulation and experimental results of column test performed with 30:70 ZVI:Pumice w.r. mixture, solution of Nickel at 50 mg/L initial concentration and v3 flow velocity.

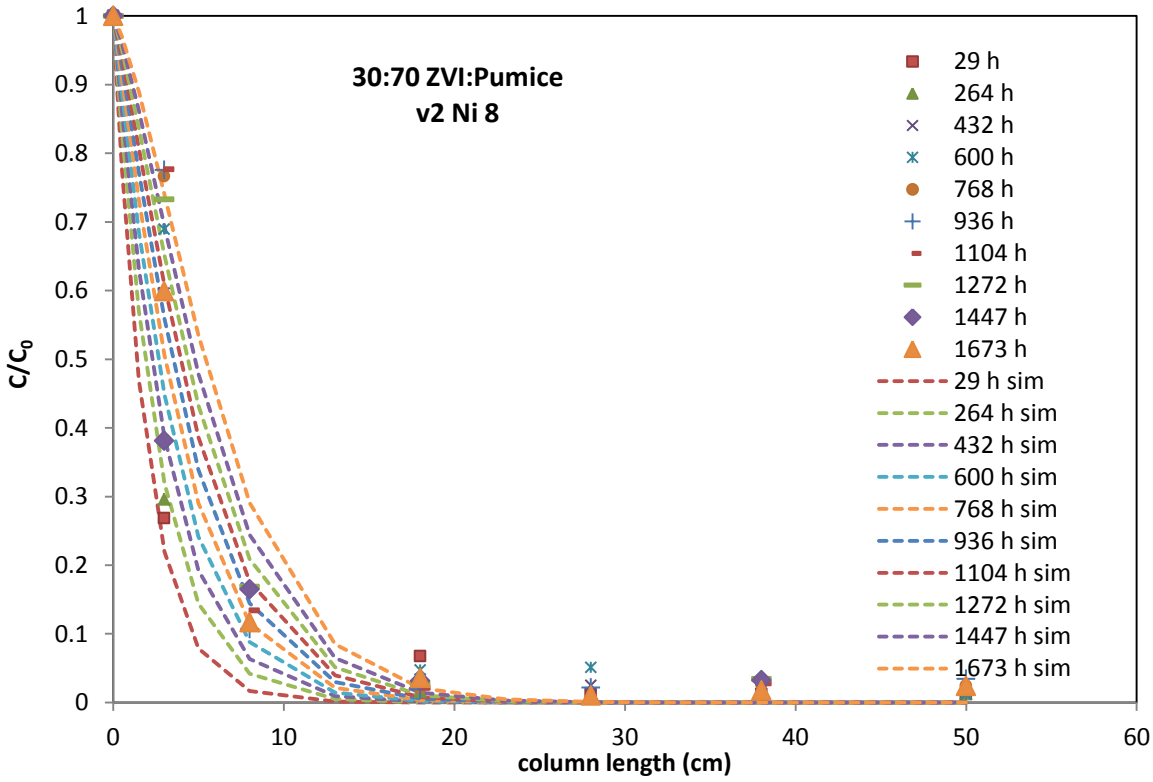

Figure 6-12 simulation and experimental results of column test performed with 30:70 ZVI:Pumice w.r. mixture, solution of Nickel at 8 mg/L initial concentration and v2 flow velocity.

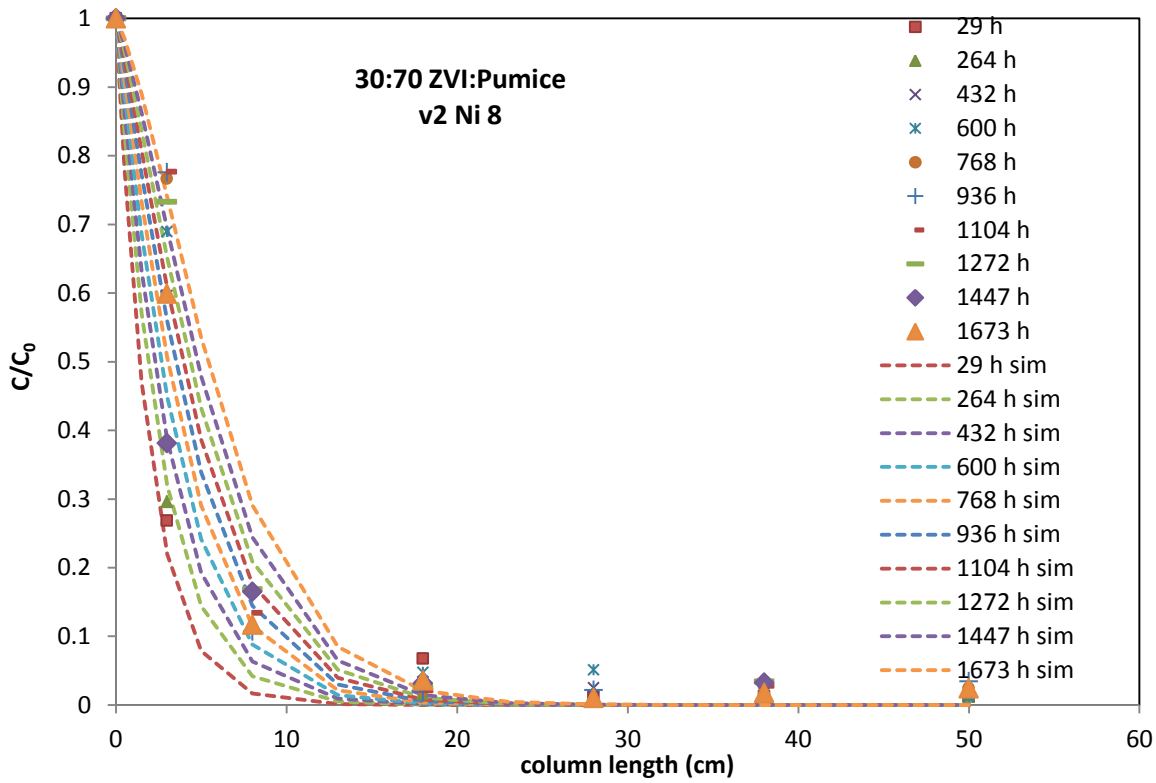

Figure 6-13 simulation and experimental results of column test performed with 30:70 ZVI:Pumice w.r. mixture, solution of Nickel at 8 mg/L initial concentration and v3 flow velocity.

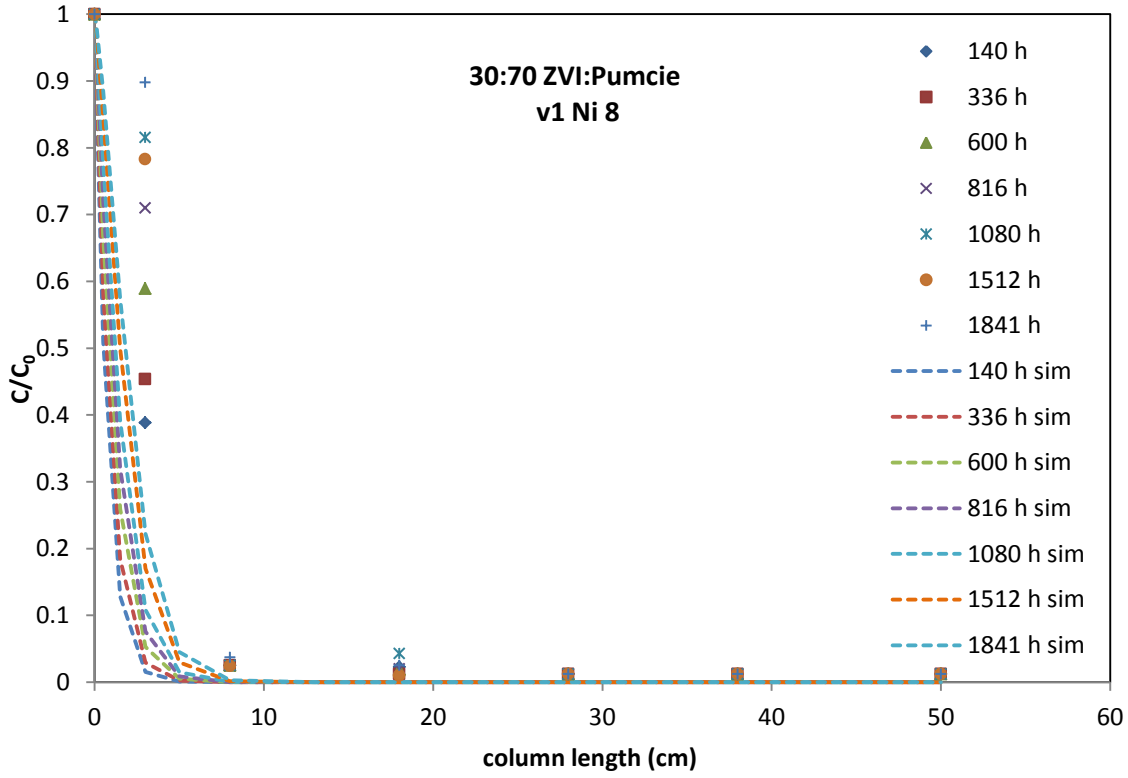

Figure 6-14 simulation and experimental results of column test performed with 30:70 ZVI:Pumice w.r. mixture, solution of Nickel at 8 mg/L initial concentration and v1 flow velocity.

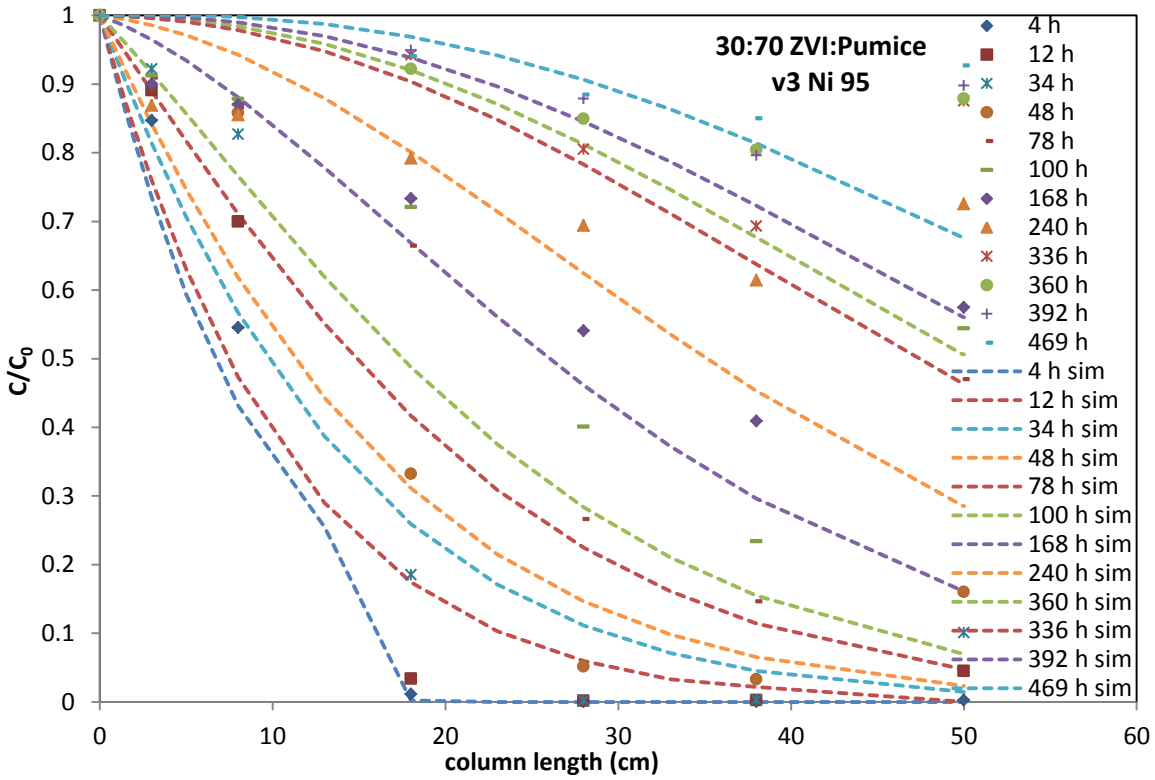

Figure 6-15 simulation and experimental results of column test performed with 30:70 ZVI:Pumice w.r. mixture, solution of Nickel at 95 mg/L initial concentration and v3 flow velocity.

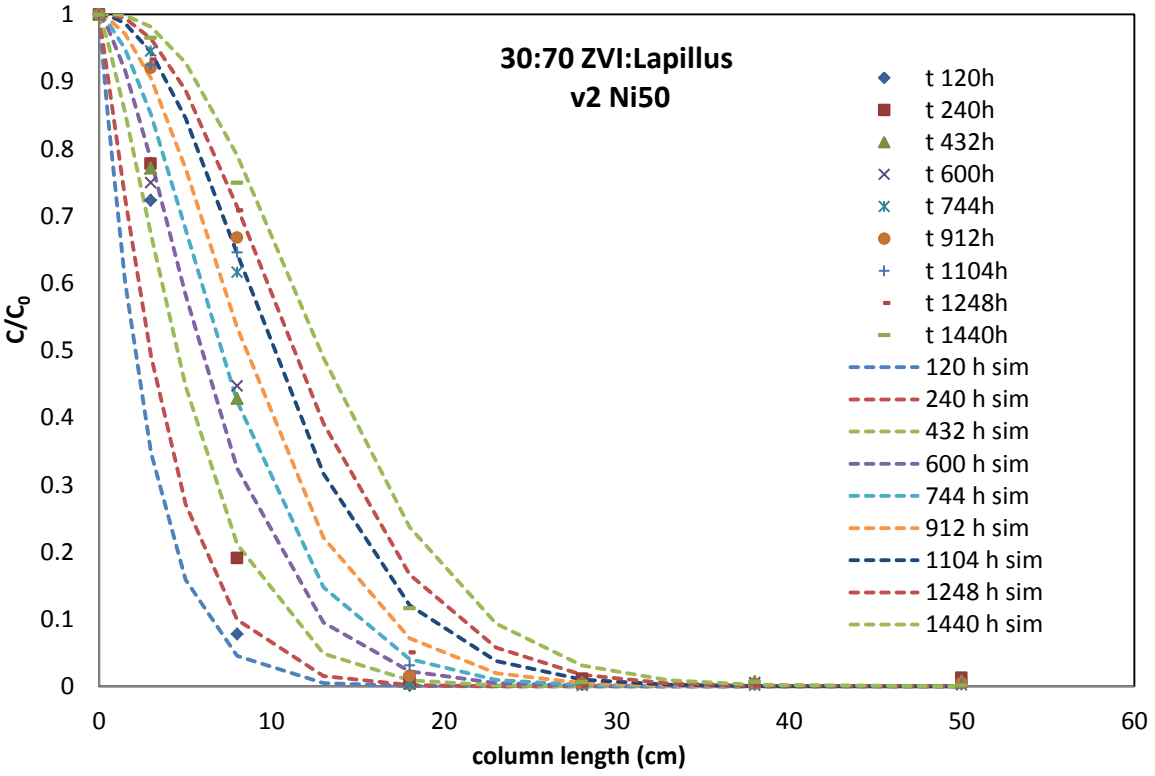

Figure 6-16 simulation and experimental results of column test performed with 30:70 ZVI:Lapillus w.r. mixture, solution of Nickel at 50 mg/L initial concentration and v2 flow velocity.

6.10 Conclusions

A mono-dimensional advection-dispersion-diffusion equation was applied to the representative elemental volume (REV) of the column. To evaluate the influence of dispersion and diffusion term on the contaminant mass transport through the porous media, the Peclet number was calculated for all the column tests to be simulated. This parameter, as applied to the column studied, represents the ratio of mass transport by advection to mass transport by molecular diffusion. Considering the evaluation of Peclet number, advection-dispersion term seems to be more influent for the performed column tests and v3 (1.382 mm/min), while for the other tests the terms of diffusion and the advection-dispersion can have equal influence on contaminant transport.

Concerning the reaction term, a non-equilibrium sorption model was used.

The sorption onto the mixtures was modeled considering the mixture as one material. This means that one term of sorption was used in the dispersion-advection equation. To simulate the results and experimental data of some ZVI:Pumice and ZVI:Lapillus mixtures tested, the values of different parameters as well as the initial and boundary conditions were changed to be equal to experimental conditions.

The values found for sorption term are lower than the correspondent found by batch tests analysis. In particular the values used for column simulation related to the ZVI:Pumice mixture are 5, 15 or 50 times higher than the corresponding value found experimentally from batch tests. Furthermore, it can be observed that the column tests with 30:70 ZVI:Pumice mixture using a solution of Nickel at 40 and v1 and v3 flow velocity can be simulated using the same values of sorption term parameters.

In Chapter 7, a comparison of experimental results of ZVI:Pumice and ZVI:Lapillus mixtures tested in column is performed to understand the factors that influence their long-term removal efficiency and hydraulic behavior and what is their different influence on the performance of the two mixtures.

7 Pumice-lapillus comparison study

7.1 Introduction

As observed in Chapter 6, a deeper interpretation of column tests results obtained using ZVI:Pumice and ZVI:Lapillus mixtures needs, to understand the factors of their long-term removal efficiency and hydraulic behavior and how they influence the sorption processes. In fact, a non-equilibrium sorption model seems to be able to simulate the column tests results.

In this chapter, a comparative analysis of column tests results obtained testing ZVI:Pumice and ZVI:Lapillus mixtures is carried out. Firstly, results concerning the remediation of Nickel-contaminated solutions will be considered. The comparison regarding long-term removal efficiency and hydraulic behavior will concern the benchmark tests, the column tests carried out using mixtures at different weight ratio, those performed using Nickel-solution at different initial concentrations and those carried out varying the flow velocity.

Afterwards, the results concerning the tested ZVI:Pumice and ZVI:Lapillus mixtures using Zinc-contaminated solutions and three-contaminated solutions will be compared.

7.2 Comparison about Nickel-contaminated tests

The column tests performed using ZVI:Pumice and ZVI:Lapillus mixtures placed in contact with Nickel-contaminated solutions will be analyzed by comparing them. Firstly, pure Pumice and pure Lapillus column tests results will be considered. The comparison regarding performance of mixtures at the same weight ratio will be based on equal ZVI content, equal residence time and equal removal efficiency. Results obtained by ZVI:Pumice and ZVI:Lapillus mixtures column tests performed with solutions at the same Nickel initial concentration will be compared, as well as those get from testes performed at the same flow velocity.

7.2.1 Benchmark columns

An analysis of long-term Nickel removal efficiency using pure volcanic materials is possible basing it on the experimental results of pure Pumice and pure Lapillus column tests carried out with Nickel-contaminated solution at an initial concentration equal to 50 mg/L flowing into the column at 0.276 mm/min constant flow velocity. Porosity, Pore Volume and residence time have been calculated as described in equations (4-9), (4-7) and (4-8) respectively.

In Table 7-1 the characteristics of the two benchmark column tests are reported. The experimental data and characteristics of pure Pumice column test concern the 30:70 weight ratio ZVI:Pumice column test, where the two reactive materials are placed in two layers in serie, not mixed (Moraci and Calabrò, 2010). Pumice was placed as first layer at the bottom of the column, while ZVI occupied 3 cm as upper layer (Moraci and Calabrò, 2010). The characteristics and the experimental data which will be reported are relative only to the Pumice layer.

React. mat.	Initial cont. conc. (mg/L)	React. Thick. (cm)	React. area (cm^2)	React. Vol. (cm^3)	Lapill. or Pum. (gr)	n (%)	Flow veloc. (mm/ min)	PV (cm^3)	Tres (h)
Lapill.	Ni 50	50	18.09	904.3	1289	35	0.276	318.5	10.6
Pum.	Ni 50	47	18.09	850	560	45	0.276	383.4	12.8

Table 7-1 Characteristics of pure Pumice and pure Lapillus carried out column tests

The evolution of Nickel normalized concentration with time is shown in Figure 7-1 a) and b) comparing the experimental data obtained at two different lengths of pure Pumice and pure Lapillus filters, specifically at 3 cm and 38 cm respectively. 3 cm is the filter length corresponding to the first sampling port, 38 cm is the highest length for which experimental data of pure Pumice filter are available.

A certain Nickel removal efficiency is already performed in 3 cm reactive granular filter length, although it is limited, for both tests. Looking at the data concerning this length, a light Nickel retention capacity is observable for tested Pumice; in fact after 120 hours from the beginning of the test , the relative Nickel concentration is about half of the initial value. After 245 hours, a constant value of residual concentration is

reached and it is constantly equal about 0.9 until 1500 hours. In the case of the pure Lapillus test, 3 cm filter thickness can be passed through in a lower residence time than the same length Pumice filter, performing a Nickel removal efficiency higher than Pumice. In fact, the contaminant normalized concentration is about 0.6 after 600 hours of test duration. This value of relative concentration increases with time to about 0.8 after 2300 hours.

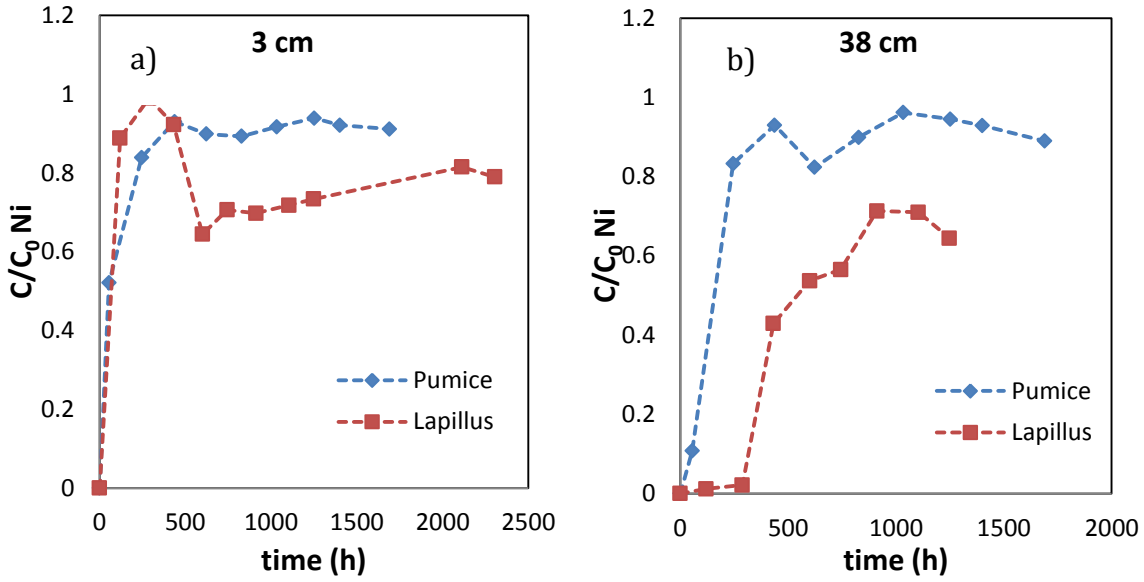

Figure 7-1 Nickel normalized concentration evolution with time using a) 3 cm filter length and b) 38 cm filter length of pure Pumice and pure Lapillus reactive materials

The difference regarding Nickel removal efficiency between the two tested volcanic porous materials is more evident considering the experimental data at 38 cm filter length (Figure 7-1 b). In fact, a faster reduction of Nickel removal efficiency for pure Pumice filter than for pure Lapillus can be observed. After about 245 hours, the Nickel normalized concentration reached values about 0.8 (demonstrating the low influence of diffusion and dispersion in contaminant transport). 38 cm long Lapillus filter has a high Nickel removal efficiency. It is able, in effect, to reduce initial concentration to values lower than 0.02 until about 300 hours from the test beginning.

However, after this time the Nickel removal efficiency of 38 cm pure Lapillus filter length decreases more slowly than that of pure Pumice filter and at about 1200 hours the Nickel relative concentration is about 0.6.

7.2.2 Comparison of weight ratio influence

Let us analyze and compare the weight ratio influence on Nickel removal efficiency of ZVI:Pumice and ZVI:Lapillus mixtures. The three tested weight ratios of ZVI:Pumice and ZVI:Lapillus and the benchmark tests will be considered. They consist of 10:90, 30:70 and 50:50 for both ZVI:Pumice w.r. and ZVI:Lapillus w.r., pure Pumice, pure Lapillus and pure ZVI column tests carried out under the same experimental boundary conditions.

Table 7-2 summarizes the characteristics of the considered column tests.

The comparative analysis among these tests to study the weight ratio influence of the two different mixtures on Nickel removal can be based mainly on two parameters: ZVI content and removal efficiency.

7.2.2.1 Equal ZVI content

The first analysis proposed is about experimental data interpretation obtained considering couples of filter lengths corresponding to equal ZVI content between ZVI:Lapillus and ZVI:Pumice columns at the same weight ratio. Under the hypothesis of complete homogenous mixing of the two reactive materials constituting each mixture filling the column, filter lengths containing the same ZVI quantity in both kinds of mixtures were identified in order to compare their performance, at fixed weight ratio. In the following Table 7-3, filter lengths and correspondent ZVI contents are reported for each weight ratio and each kind of mixture. They were chosen in order to individuate the lowest and the highest possible ZVI contents in common for the two kinds of mixture at a fixed weight ratio for which experimental data are available. Intermediate conditions of ZVI content are also investigated.

React. mat.	Weig. ratio	Init. cont. conc. (mg/ L)	React. Thick. (cm)	React. area (cm^2)	Reac. vol. (cm^3)	Fe^0 (gr)	Lapill or Pum. (gr)	n (%)	Flow veloc. (mm/ min)	PV (cm^3)	Tres (h)
Lapil.		Ni 50	50	18.09	904.3		1289	35	0.276	318.5	10.6
Fe^0/ Lap	10:90	Ni 50	50	18.09	904.3	138	1242	36	0.276	322.2	10.7
Fe^0/ Lap	30:70	Ni 50	50	18.09	904.3	480	1120	37	0.276	334.3	11.1
Fe^0/ Lap	50:50	Ni 50	50	18.09	904.3	970	970	38	0.276	340.1	11.3
Fe^{0*}		Ni 50	3	18.09	54.26	240		44	0.276	23.76	0.8
Pum.*		Ni 50	47	18.09	850		560	45	0.276	383.4	12.8
Fe^0/ Pum*	10:90	Ni 50	100	18.09	1809	153	1374	36	0.276	644.6	21.5
Fe^0/ Pum*	30:70	Ni 50	50	18.09	904.3	244	570	44	0.276	398.5	13.3
Fe^0/ Pum*	50:50	Ni 50	50	18.09	904.3	531	531.2	44	0.276	394.2	13.1

Table 7-2 Characteristics of column tests considered in comparison of weight ratio influence between ZVI:Pumice and ZVI:Lapillus mixtures

(* Suraci P., 2010)

In Figures 7-2 and 7-3, comparisons between column tests results of ZVI:Pumice and ZVI:Lapillus mixtures at 10:90 w.r. are shown, for the same ZVI mass used.

In Figure 7-2 a) Nickel normalized concentration evolution is reported for 3 cm of ZVI:Lapillus and 8 cm of ZVI:Pumice mixtures filters. Both filter lengths contain about 10 gr of ZVI (Table 7-3). Although Nickel initial concentration is reduced by 30% at 120 hours, the 8 cm of ZVI:Pumice filter seems to be more efficient than the 3 cm of ZVI:Lapillus, which can be due to the higher residence and contact time or to the higher dispersion effect of the longer ZVI:Pumice filter than that of the ZVI:Lapillus. However, removal efficiency decreases for both considered filters.

Weight ratio	10:90		30:70		50:50	
Mixtures	Fe^0/Pum	Fe^0/Lap	Fe^0/Pum	Fe^0/Lap	Fe^0/Pum	Fe^0/Lap
Thickness (cm)	8	3	5	3	5	3
ZVI (gr)	12.24	8.2	24.4	28.8	53.1	58.2
Thickness (cm)	18	8	13	8	13	8
ZVI (gr)	27.54	22.1	63.5	76.8	138.1	155.2
Thickness (cm)	28	18	38	18	33	18
ZVI (gr)	42.8	49.6	185.7	172.8	350.6	349.2
Thickness (cm)	58	28	50	28	50	28
ZVI (gr)	88.7	77.3	244.4	268.8	531.15	543.2

Table 7-3 Filter lengths and correspondent ZVI mass for mixtures of ZVI:Pumice and ZVI:Lapillus at different weight ratios.

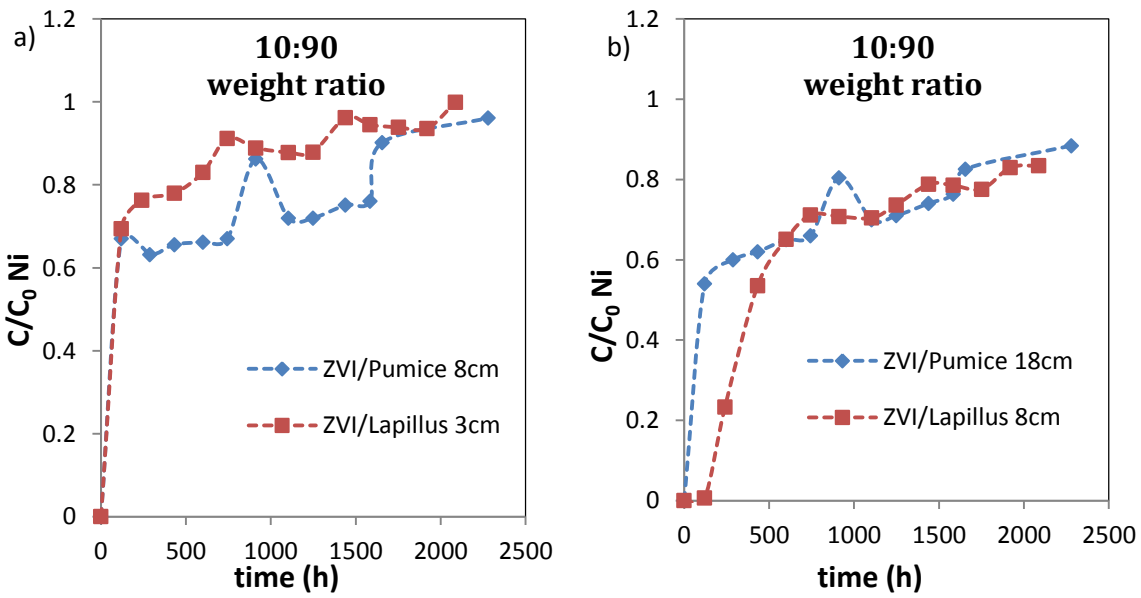

Figure 7-2 Nickel normalized concentration evolution in 10:90 w.r. column tests at a) 8 cm long ZVI:Pumice and 3 cm long ZVI:Lapillus filters and at b) 18 cm long ZVI:Pumice and 8 cm long ZVI:Lapillus filters.

In Figure 7-2 b) data related to the 18 cm long ZVI:Pumice filter are compared to that of the 8 cm long ZVI:Lapillus filter. At 120 hours after the beginning of the test, in the ZVI:Pumice filter the Nickel initial concentration value is reduced by half, while the 8 cm of ZVI:Lapillus filter are enough to reduce it to a 0.006 value. Afterwards, the removal efficiency decreases up to 50% at 432 hours. From this time, the evolution of Nickel relative concentration is the same for both mixtures.

In Figures 7-3 a) and b) data concerning 45 and 85 gr of ZVI are shown respectively. It can be observed that the ZVI:Lapillus filter is always more efficient than the ZVI:Pumice filter length containing approximately the same ZVI quantity. Even though the 18 cm and 28 cm long ZVI:Lapillus filters are compared to the 28 cm and 58 cm long ZVI:Pumice filters respectively, the first can reduce Nickel initial concentration to 0.004 value until 432 hours and 900 hours, while the second can reduce it by 50-60% at maximum already at the first sampling time. This can demonstrate the higher Nickel removal efficiency of Lapillus compared to Pumice. Furthermore, it should be considered that the residence time in the ZVI:Lapillus filters is lower than the ZVI:Pumice filters in the above comparisons and especially for 10:90 mixtures.

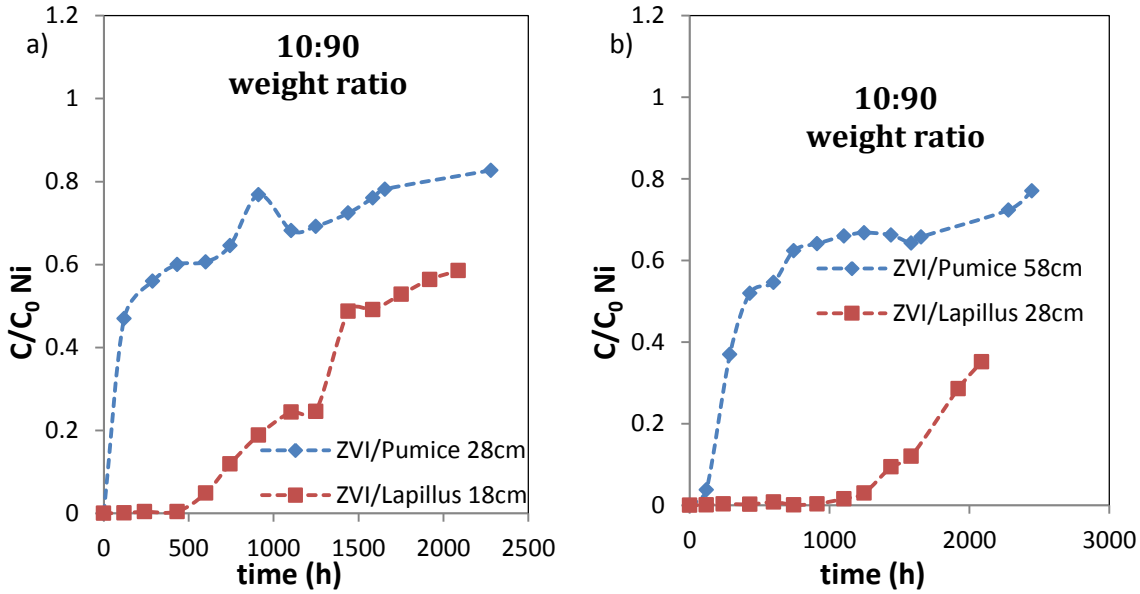

Figure 7-3 Nickel normalized concentration evolution in 10:90 w.r. column tests at a) 28 cm long ZVI:Pumice and 18 cm long ZVI:Lapillus filters and at b) 58 cm long ZVI:Pumice and 28 cm long ZVI:Lapillus filters.

In Figures 7-4 and 7-5, data related to 30:70 weight ratio column tests are shown.

Analyzing the results related to the 30:70 w.r. column tests, the behavior previously observed can be confirmed. In fact, also using 25 gr of ZVI distributed in the 3 cm of ZVI:Lapillus mixture filter and in the 5 cm of ZVI:Pumice mixture filter, the considered filter length and ZVI content seem not to be enough to reduce the Nickel initial concentration significantly (Figure 7-4 a).

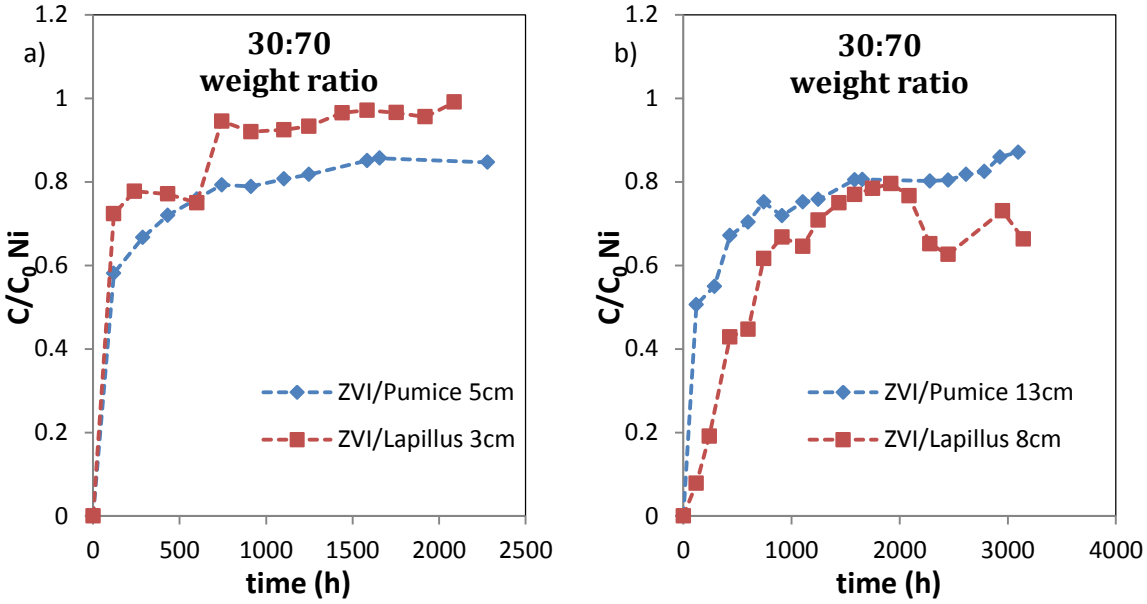

Figure 7-4 Nickel normalized concentration evolution in 30:70 w.r. column tests at a) 5 cm long ZVI:Pumice and 3 cm long ZVI:Lapillus filters and at b) 13 cm long ZVI:Pumice and 8 cm long ZVI:Lapillus filters.

Using about 70 gr of ZVI in the 30:70 w.r. filters, the ZVI/Pumice mixtures tested in the column has a length of 13 cm, while the ZVI/Lapillus mixture is 8 cm long. As represented in Figure7-4 b, the Nickel removal efficiency is higher in the ZVI:Lapillus filter, even if the behavior of the two mixtures using the considered lengths is almost the same.

Using 180 gr and 250 gr of ZVI mixed with Pumice or Lapillus to obtain 30:70 w.r. mixtures, data related to the 38 cm of ZVI/Pumice mixture and the 18 cm of ZVI/Lapillus mixture filter lengths should be considered for the first ZVI content, while that concerning the 50 cm long ZVI/Pumice mixture filter and the 28 cm long ZVI/Lapillus mixture filter can be compared on the basis of the latter's ZVI content (Table 7-3). In these two cases, as reported in Figure 7-5 a) and b) the considered filter of ZVI/Lapillus is highly more efficient than that of ZVI/Pumice containing the same ZVI quantity. Furthermore, the ZVI/Lapillus mixture filters can reduce to 0.005 value the Nickel normalized concentration until 1000 and 2000 hours, if 180 gr and 250 gr of ZVI are respectively used. The ZVI/Pumice mixture lengths containing the same ZVI quantity have a limited Nickel removal capacity.

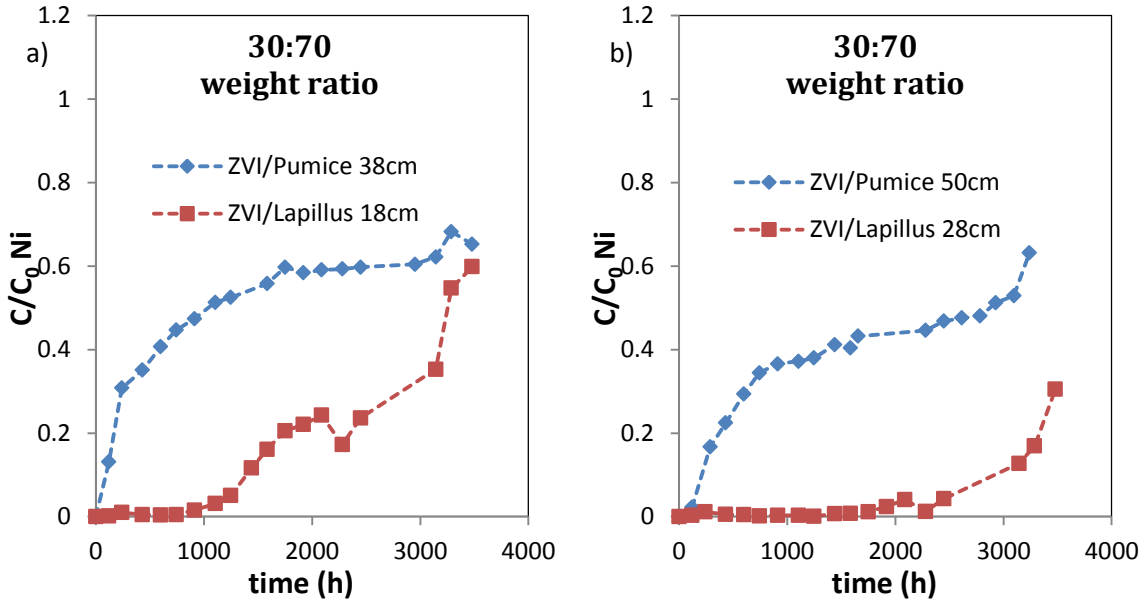

Figure 7-5 Nickel normalized concentration evolution in 30:70 w.r. column tests at a) 38 cm long ZVI:Pumice and 18 cm long ZVI:Lapillus filters and at b) 50 cm long ZVI:Pumice and 28 cm long ZVI:Lapillus filters.

In Figures 7-6 and 7-7, the experimental data for Nickel concentration evolution with time concerning 50:50 weight ratio column tests are shown.

Considering the data as reported in Figure 7-6 and 7-7 a) and b), it is possible to observe the influence of the residence time of the contaminant solution during its passage through the porous reactive media on removal efficiency, as well as for the previously analyzed weight ratio filters. In fact, using about 55 gr of ZVI filling the column mixed with the same quantity of Lapillus or Pumice, the 3 cm of ZVI/Lapillus mixture filter and the 5 cm of ZVI/Pumice mixture filter do not assure the necessary residence time in order to reduce the initial Nickel concentration significantly.

However, the same ZVI quantity used in a 10:90 ZVI/Lapillus w.r. column test corresponds to 18 cm filter length, that can reduce to 0.004 the Nickel normalized concentration until 400 hours.

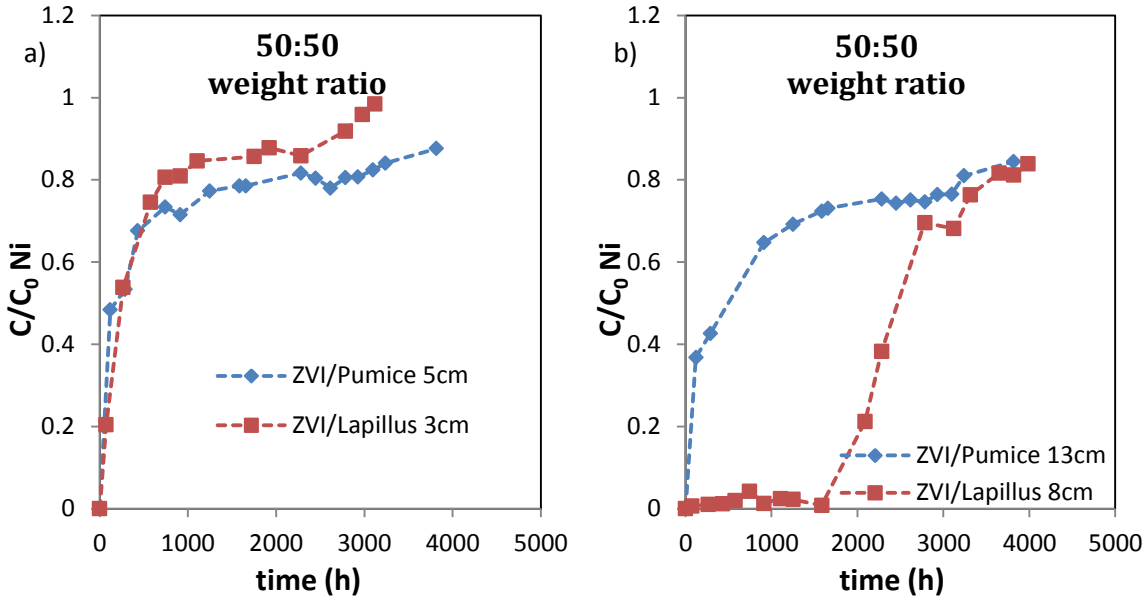

Figure 7-6 Nickel normalized concentration evolution in 50:50 w.r. column tests at a) 5 cm long ZVI:Pumice and 3 cm long ZVI:Lapillus filters and at b) 13 cm long ZVI:Pumice and 8 cm long ZVI:Lapillus filters.

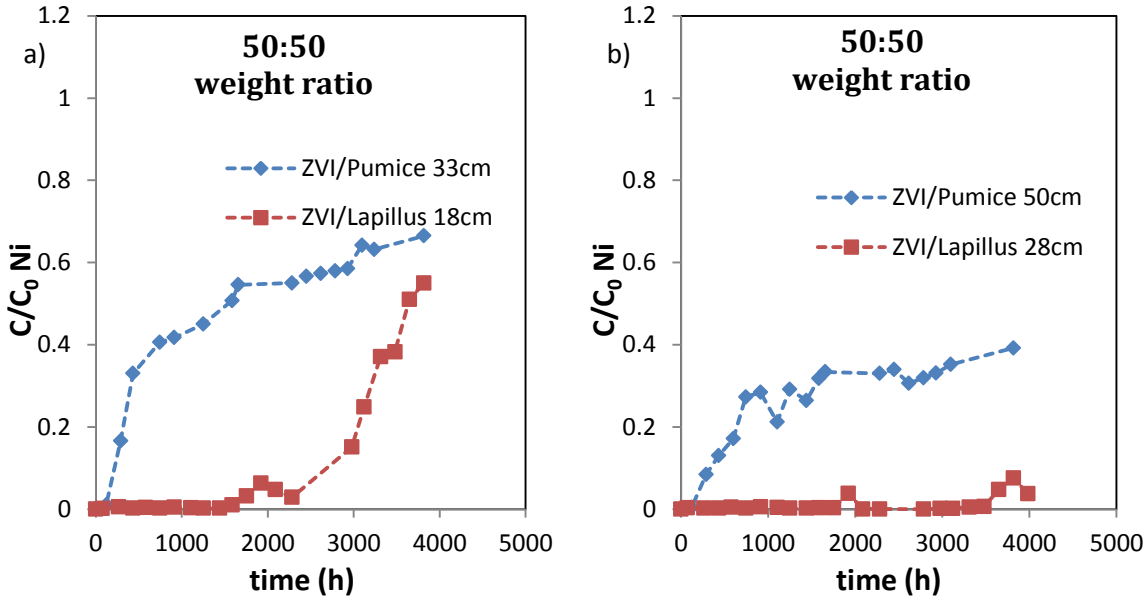

Figure 7-7 Nickel normalized concentration evolution in 50:50 w.r. column tests at a) 33 cm long ZVI:Pumice and 18 cm long ZVI:Lapillus filters and at b) 50 cm long ZVI:Pumice and 28 cm long ZVI:Lapillus filters.

In Figure 7-6 b), the Nickel normalized concentration evolution with time refers to 145 gr of ZVI. The ZVI/Pumice mixture filter, 13 cm long, manifests a residual Nickel removal capacity, while the 8 cm ZVI/Lapillus mixture filter length is enough to reduce to 0.008 value the normalized Nickel concentration until 1600 hours. After this time, reactive media exhaustion is rapid. On the other hand, it is possible to observe that using the same ZVI quantity mixed with Lapillus in order to obtain a

30:70 w.r. mixture, having a 18 cm long filter, the high Nickel removal efficiency, reducing the contaminant normalized concentration to 0.005, lasts until 800 hours.
The comparisons between the 50:50 ZVI/Pumice and the ZVI/Lapillus weight ratio proposed in Figure 7-7 a) and b) are based on 350 gr and 535 gr of ZVI quantity respectively. In both cases, the ZVI/Pumice mixture filter lengths significantly reduce the normalized Nickel concentration until 80 hours, while after this time the residual Nickel removal efficiency tends to increase resulting in 0.6 and 0.4 value of normalized Nickel concentration at 4000 hours using 350 and 535 gr of ZVI respectively (Figure 7-7 a and b). The ZVI/Lapillus filter manifests high efficiency, reducing the normalized Nickel concentration to 0.009 value until 1600 hours if mixed with 350 gr of Lapillus in 18 cm long filter (Figure 7-7 a) and to 0.006 until 3400 hours if mixed with 535 gr of Lapillus occupying 28 cm of the column (Figure 7-7 b).

7.2.2.2 Equal efficiency

The third analysis to study the difference of weight ratio influence on Nickel removal efficiency between ZVI/Pumice and ZVI/Lapillus mixtures can be conducted searching the filter lengths that can have the same Nickel removal efficiency evolution, preset the weight ratio.
After having compared the different evolution of normalized Nickel concentration with time at different sampling ports of each column test carried out at a certain weight ratio, regarding those that demonstrate greater similarity, the corresponding ZVI content and the residence time have been calculated.

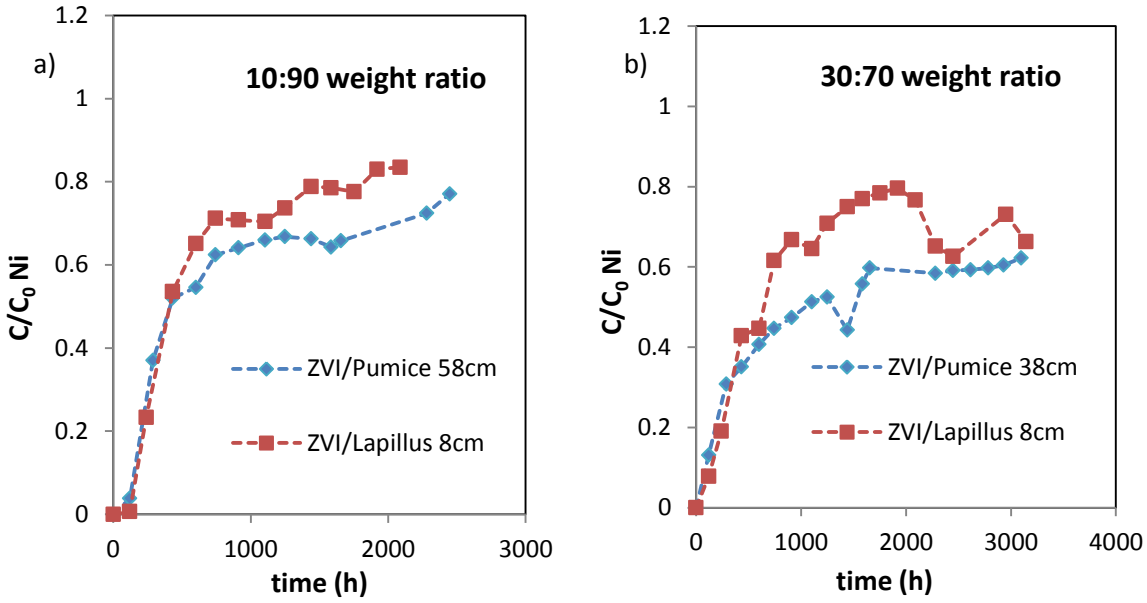

Figure 7-8 Nickel normalized concentration evolution a) in 10:90 w.r. column tests at 58 cm long ZVI:Pumice and 8 cm long ZVI:Lapillus filters and b) in 30:70 w.r. column tests at 38 cm long ZVI:Pumice and 8 cm long ZVI:Lapillus filters.

In Figures 7-8 and 7-9 comparison referring to 10:90, 30:70 and 50:50 weight ratio are shown respectively. Regarding the 10:90 weight ratio, the lower difference between evolution of Nickel removal efficiency in the ZVI:Pumice and ZVI:Lapillus mixtures column tests was found for the 58 cm long ZVI:Pumice mixture filter and for the 8 cm long ZVI:Lapillus mixture filter. The corresponding ZVI content is about 88.74 gr and 11 gr respectively. While the residence time is about 12.5 and 1.7 hours so that the 58 cm of ZVI:Pumice mixture filter and for the 8 cm of ZVI:Lapillus mixture filter are passed through by the contaminant solution respectively.

Concerning the 30:70 weight ratio column tests, the more similar behavior in Nickel removal efficiency between the ZVI:Pumice and ZVI:Lapillus mixtures filters was found for the 38 cm long ZVI:Pumice mixture filter and for the 8 cm long ZVI:Lapillus mixture filter. The corresponding ZVI content is about 185 gr and 76 gr for the ZVI:Pumice and ZVI:Lapillus mixtures respectively, while the residence time is about 10 and 1.8 hours respectively.

Regarding the 50:50 weight ratio column tests, the more similar behavior of long-term Nickel removal efficiency can be found for the 33 long ZVI:Pumice mixture filter and the 8 cm long ZVI:Lapillus mixture filter. The corresponding ZVI content is about 350 gr and 155 gr for the considered filter lengths respectively, while the residence times are 8.6 and 1.8 hours respectively.

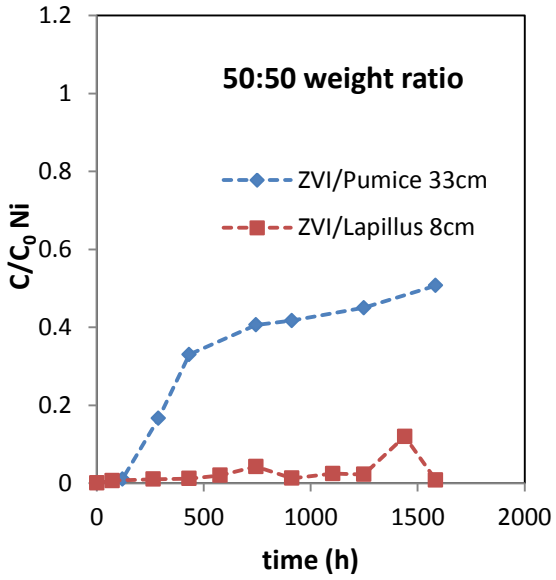

Figure 7-9 Nickel normalized concentration evolution in 50:50 w.r. column tests at 33 cm long ZVI:Pumice and 8 cm long ZVI:Lapillus filters

7.2.2.3 Contaminant mass balance and specific removal rate evolution

A mass balance for contaminant mass was carried out for each column test performed with the ZVI:Pumice and ZVI:Lapillus mixtures at different weight ratios. In Figures 7-10, 7-11 and 7-12 the Nickel mass retained in each filter sector divided by the sector length is shown for the same time (2448 h) after test beginning for 10:90, 30:70 and 50:50 w.r. mixtures. Data referred to the ZVI:Pumice and ZVI:Lapillus are shown in a) and b) Figures respectively. In this way, it is possible to observe the distribution of the Nickel retained along the filter and to find the difference among the ZVI:Pumice and ZVI:Lapillus. Looking at the figures concerning the ZVI:Pumice mixtures (Figure 7-10 a, 7-11 a and 7-12 a), it seems that the highest quantity of Nickel retained by unit of filter length is found in the first 3 cm for all three w.r. ZVI:Pumice mixtures. Furthermore, comparing them to the respective ZVI:Lapillus mixtures filter (Figure 7-10 b, 7-11 b and 7-12 b), a significant difference in the distribution of Nickel retained per unit of filter length along the column can be observed for each weight ratio. In fact, while in the ZVI:Lapillus mixtures, the Nickel retention involves higher filter length the lower the ZVI content in the mixture, in the ZVI:Pumice mixture the Nickel is mainly retained by the first centimeters. In the

ZVI:Lapillus tests, the distribution is more homogeneous along the column as the ZVI content decreases.

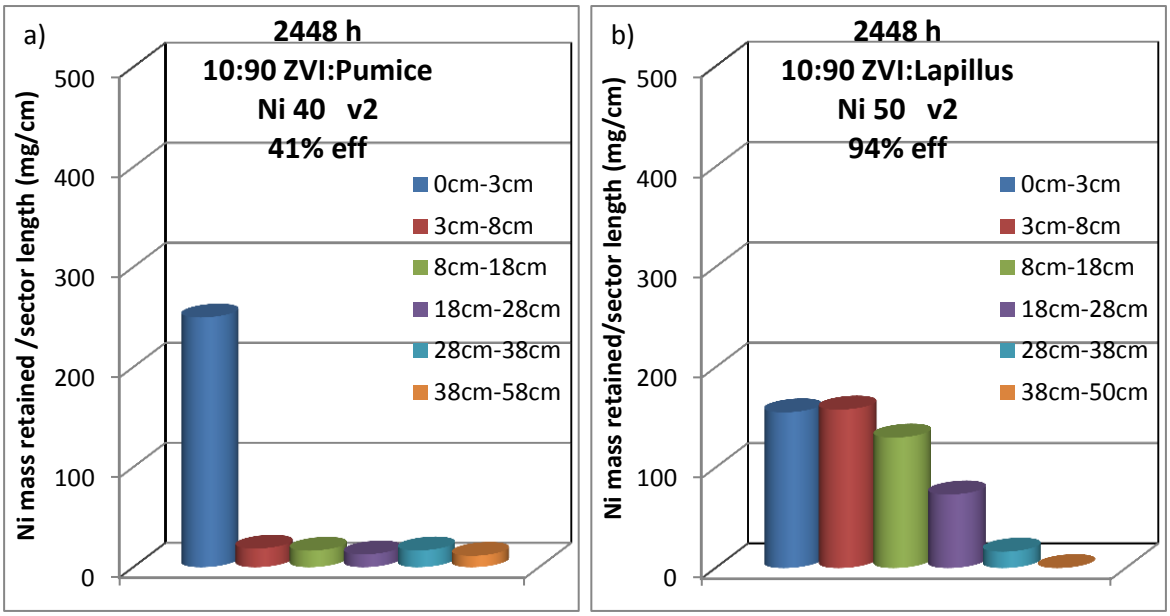

Figure 7-10 Nickel mass retained in each sectors divided by the length of the sector in 10:90 w.r. of a) ZVI:Pumice and b) ZVI:Lapillus mixtures column tests at 2448 hours from the test beginning

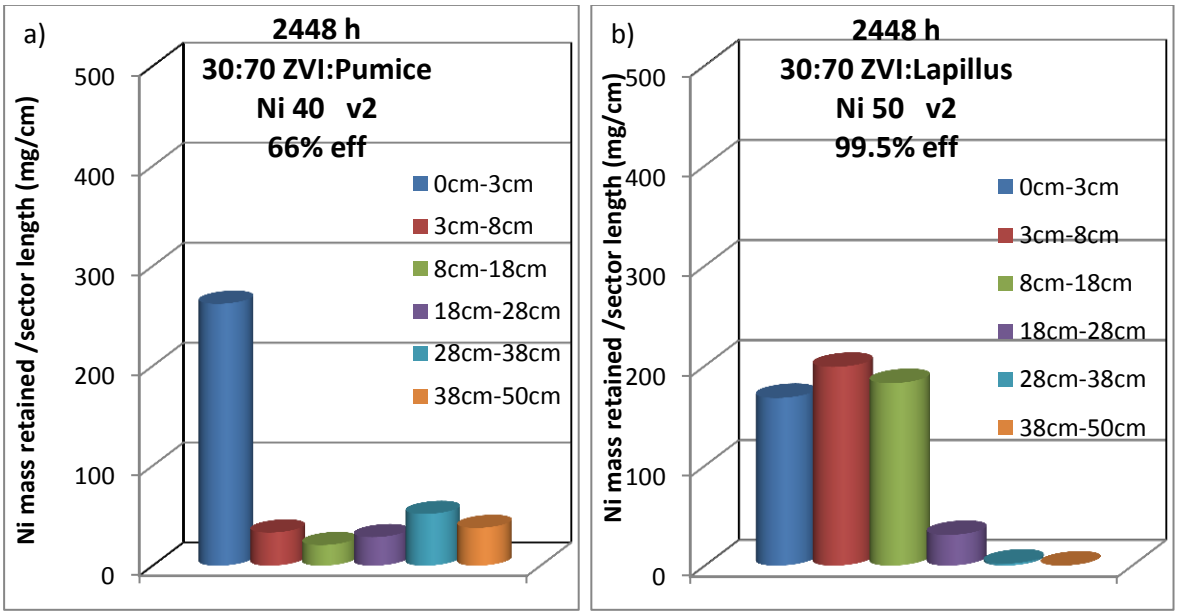

Figure 7-11 Nickel mass retained in each sectors divided by the length of the sector in 30:70 w.r. of a) ZVI:Pumice and b) ZVI:Lapillus mixtures column tests at 2448 hours from the test beginning

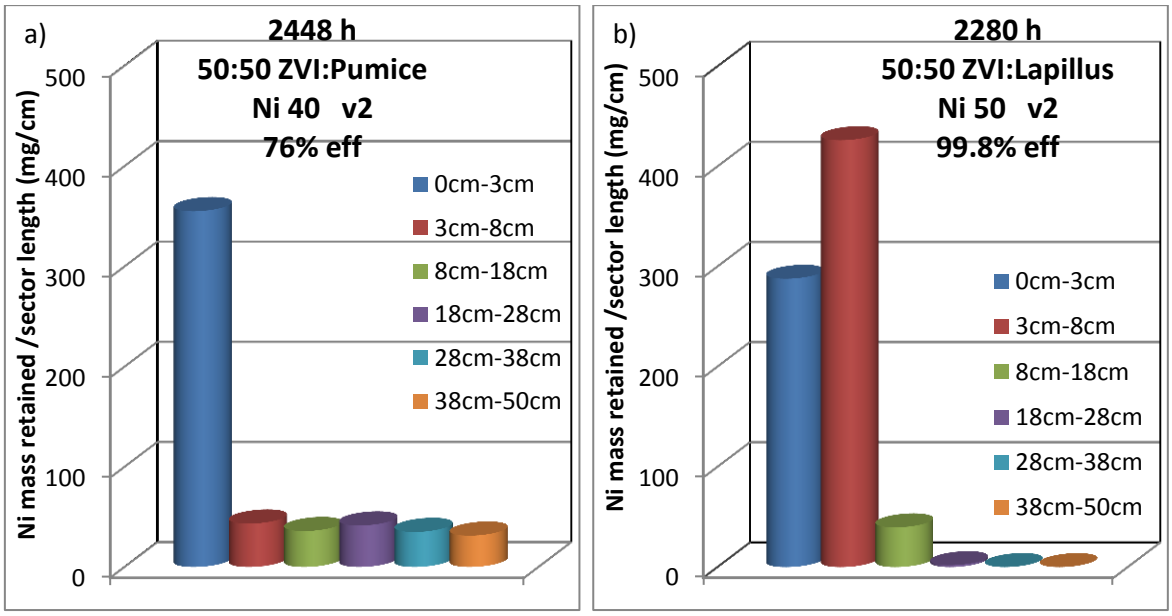

Figure 7-12 Nickel mass retained in each sectors divided by the length of the sector in 50:50 w.r. of a) ZVI:Pumice and b) ZVI:Lapillus mixtures column tests at 2448 hours from the test beginning

In Figures 7-13, 7-14 and 7-15, the evolution of specific removal rate for 10:90 , 30:70 and 50:50 w.r. tested for ZVI:Pumice and ZVI:Lapillus mixtures are respectively shown.

Their evolution confirms the highest quantity of Nickel retained by unit of reactive media in the unit of time as calculated for the first 3 cm of the ZVI:Pumice w.r. tests.

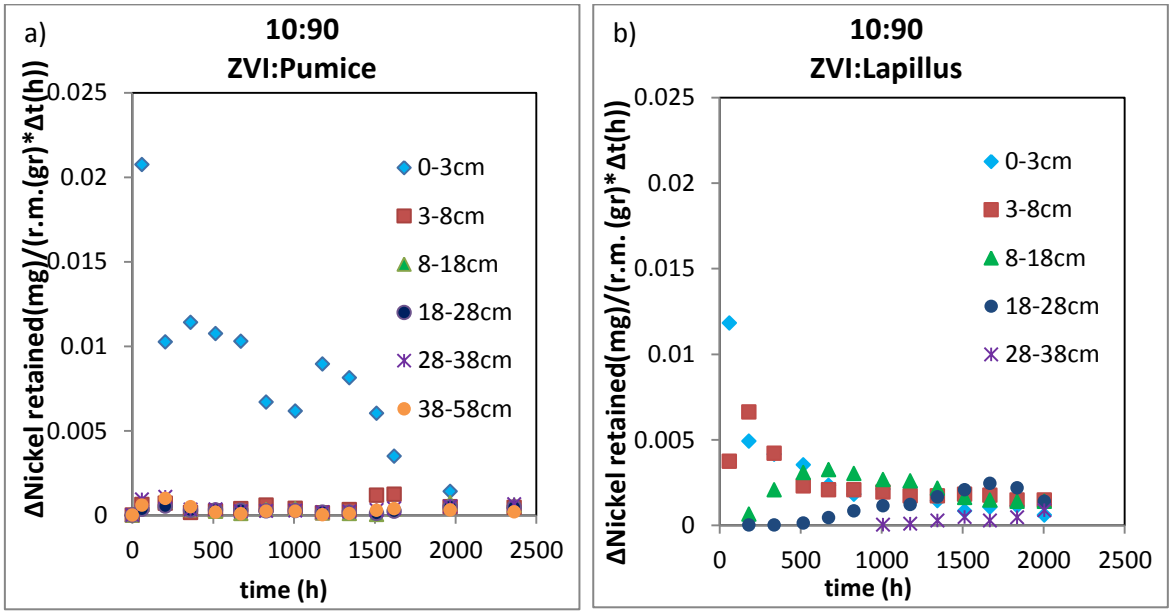

Figure 7-13 Partial Nickel mass retained in each filter sectors during each time interval divided by the reactive media mass contained in the sector per unit time for 10:90 a) ZVI:Pumice w.r. and b) ZVI:Lapillus w.r.

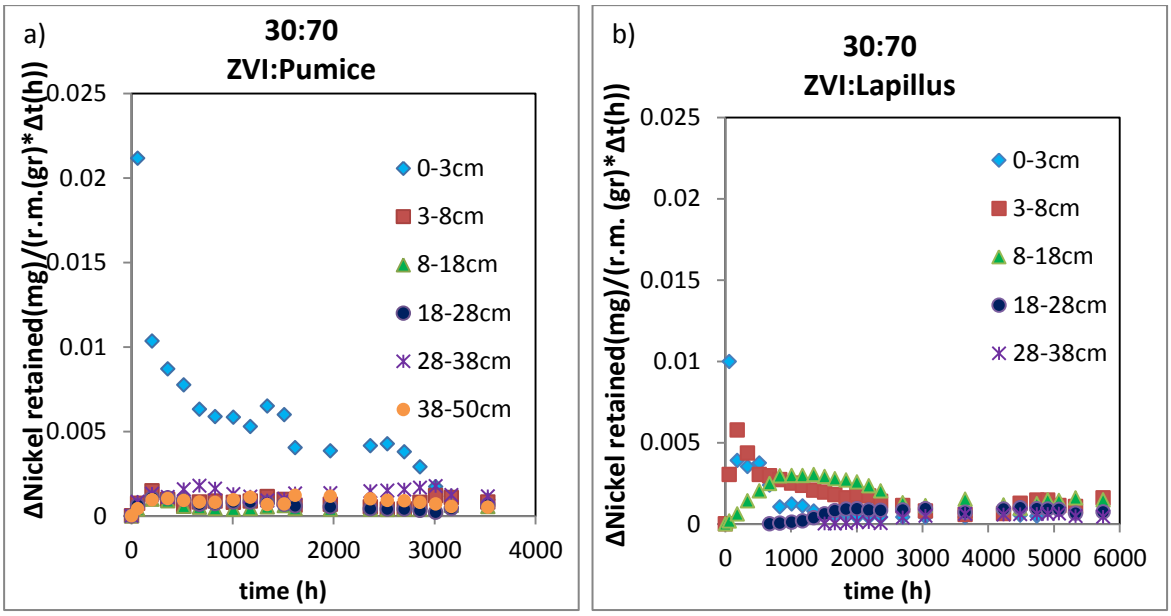

Figure 7-14 Partial Nickel mass retained in each filter sectors during each time interval divided by the reactive media mass contained in the sector per unit time for 30:70 a) ZVI:Pumice w.r. and b) ZVI:Lapillus w.r.

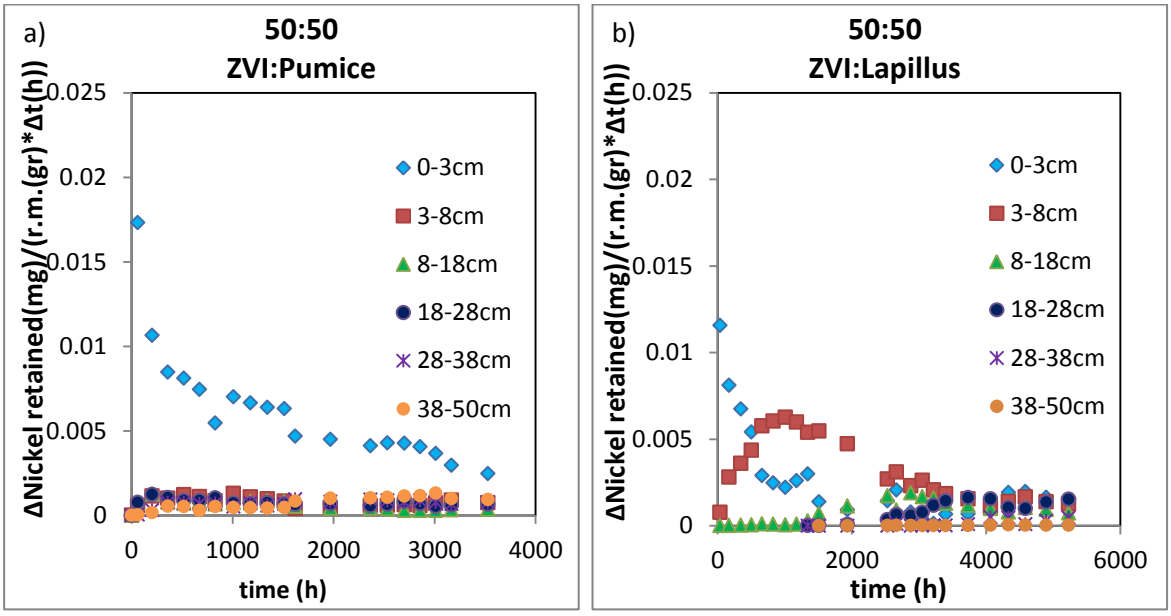

Figure 7-15 Partial Nickel mass retained in each filter sectors during each time interval divided by the reactive media mass contained in the sector per unit time for 50:50 a) ZVI:Pumice w.r. and b) ZVI:Lapillus w.r.

These values are the highest that can be observed among the specific removal rate values of tests performed at the same w.r. While the specific removal rate values calculated for the ZVI:Pumice filter length higher than 3 cm are really slower than the correspondent of the ZVI:Lapillus mixtures tests. Furthermore, a certain evolution of specific removal rate coefficient with time and with filter thickness can be observed

for the ZVI:Lapillus tests, while the specific removal rate concerning the filter thickness of the ZVI:Pumice mixtures higher than 3 cm seem to remain constant.

7.2.3 Comparison of flow velocity influence

The third step in the study concerning the difference on Nickel removal efficiency between the ZVI:Pumice and the ZVI:Lapillus mixtures regards the influence of flow velocity on long-term Nickel removal efficiency and hydraulic behavior. In Table 7-6, the characteristics of the considered column tests are reported.

The fixed weight ratio is 30:70 for both the ZVI:Pumice and ZVI:Lapillus mixtures tests. The initial Nickel concentration is about 50 mg/L for the ZVI:Lapillus tests and 40 mg/L for the ZVI:Pumice tests. The constant flow velocities used were 0.055 mm/min (v_1), 0.276 mm/min (v_2) and 1.382 mm/min (v_3).

React. mat.	Initial cont. conc. (mg/L)	React. thick. (cm)	React. area (cm^2)	React. Vol. (cm^3)	Fe^0 (gr)	Lapill. or Pum. (gr)	n (%)	Flow veloc. (mm/min)	PV (cm^3)	Tres (h)
Fe^0/ Lap	Ni 50	50	18.09	904.3	473	1104	37	0.055	336.7	56.1
Fe^0/ Lap	Ni 50	50	18.09	904.3	480	1120	37	0.276	334.3	11.1
Fe^0/ Lap	Ni 50	50	18.09	904.3	468	1093	38	1.382	348.1	2.3
Fe^0/ Pum	Ni 50	50	18.09	904.3	244	570	47	0.055	428.6	71.4
Fe^0/ Pum	Ni 50	40	18.09	904.3	240	560	44	0.276	398.5	13.3
Fe^0/ Pum	Ni 50	40	18.09	904.3	240	560	48	1.382	432.6	2.9

Table 7-4 Characteristics of column tests considered in comparison of flow velocity influence between ZVI:Pumice and ZVI:Lapillus mixtures

7.2.3.1Long-term removal efficiency

In Figures 7-16 and 7-17, the Nickel retained per unit reactive mass in each filter sector is shown for the ZVI:Pumice (Figures a) and ZVI:Lapillus (Figures b) mixtures tested with a v1 flow velocity, after about 2200 and 10000 hours after test beginning respectively. For the first considered time, around 2200 hours, it can be observed that both mixtures are highly efficient and that the Nickel retention is mostly concentrated in the first 3 cm of the ZVI:Lapillus filter (Figures 7-16 a), while it is better distributed along the filter in the ZVI:Pumice column test (Figures 7-16 b). This difference in Nickel retention distribution along the column is highlighted as time increases. In fact, at about 10000 hours after the test beginning, the input Nickel mass is almost totally removed by the first 8 cm of the ZVI:Lapillus filter length, mainly by the first 3 cm, while the input Nickel mass in the ZVI:Pumice is removed in a more homogeneous way by the filter and with a lower efficiency than the ZVI:Lapillus filter does.

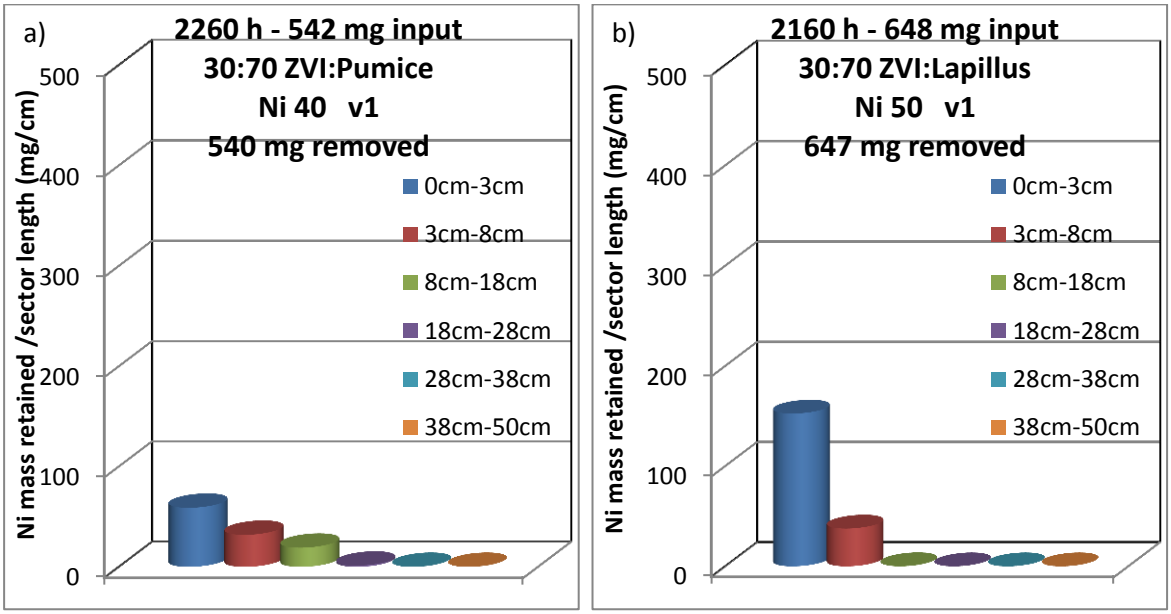

Figure 7-16 Nickel retained mass in each sector divided by the length of the sector in v1 tests with a) ZVI:Pumice and b) ZVI:Lapillus mixtures column tests at about 2200 hours from the test beginning

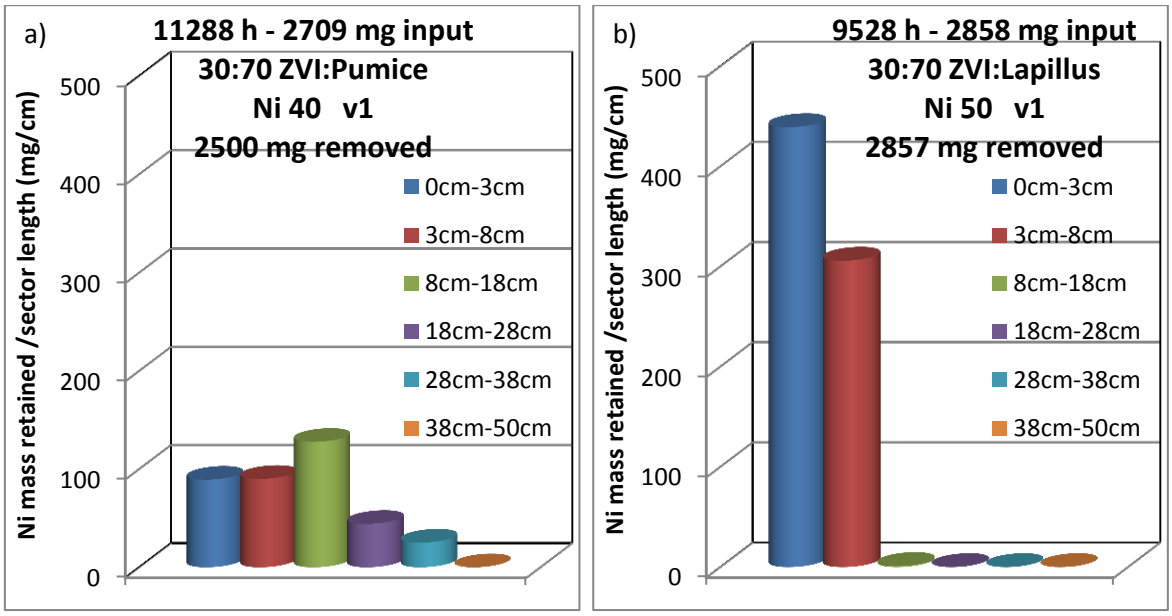

Figure 7-17 Nickel retained mass in each sector divided by the length of the sector in v1 tests with a) ZVI:Pumice and b) ZVI:Lapillus mixtures column tests at about 10000 hours from the test beginning

In Figures 7-18 and 7-19, the Nickel retained per unit reactive mass in each filter sector is shown for the ZVI:Pumice (Figures a) and the ZVI:Lapillus (Figures b) mixtures tested with a v3 flow velocity, after about 60 and 400 hours after test beginning respectively.

At about 60 hours, the Nickel input mass has been retained with high efficiency by both filters. Concerning the Nickel retention distribution along the filter, it seems to be more homogeneous in the ZVI:Lapillus filter than in the ZVI:Pumice one. This is more evident if a higher interaction time is considered, as shown in Figures 7.19. However, the Nickel removal efficiency seems not to vary much between the two mixtures when v3 flow velocity tests are considered.

The Nickel retained mass as function of Nickel input mass is shown for the three tested flow velocities in Figures 7-20 a) and b) for the ZVI:Pumice and the ZVI:Lapillus mixtures respectively. Comparing them, the higher removal efficiency of the ZVI:Lapillus than ZVI:Pumice mixtures is confirmed for each flow velocity used. The v1 test seems to be highly efficient for all the tests' duration in both filters. Concerning the v2 tests, the ZVI:Lapillus filter maintains a high removal efficiency for all of the test duration. In fact, its Nickel removal efficiency is about 88% after 9000 mg of Nickel input , while using the ZVI:Pumice mixture, it is about 58%, corresponding to 6000 mg.

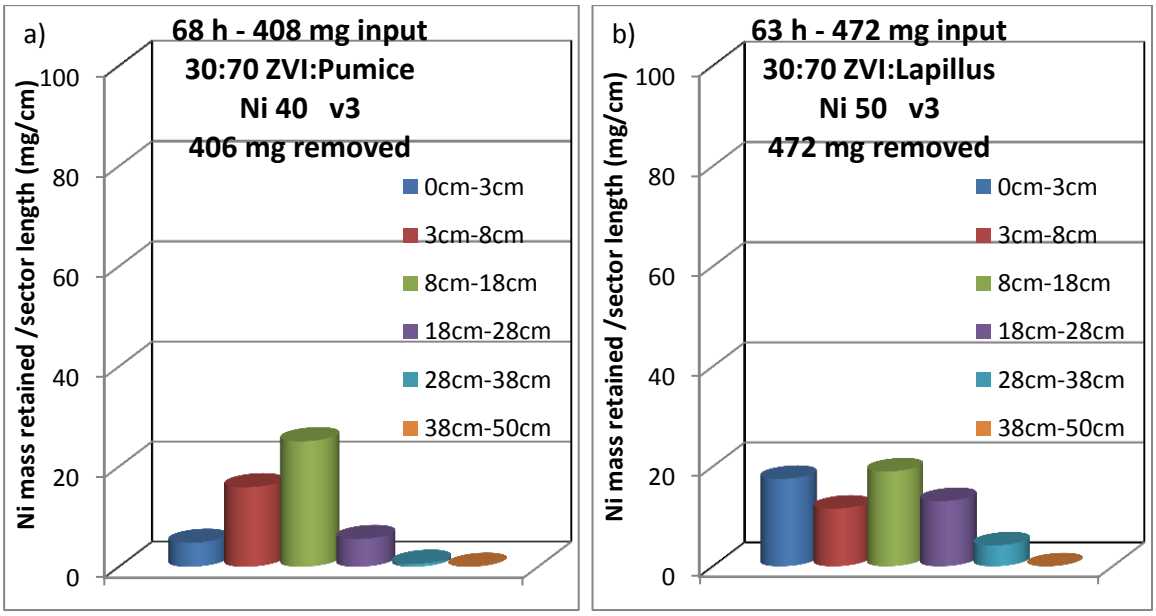

Figure 7-18 Nickel mass retained in each sector divided by the length of the sector in v3 tests with a) ZVI:Pumice and b) ZVI:Lapillus mixtures column tests at about 63 hours from the test beginning

Regarding the mixtures tested using v3 flow velocity, it can be observed that the Nickel removal efficiency evolution as function of Nickel input mass is almost the same and it is about 60% after 400 mg of Nickel input.

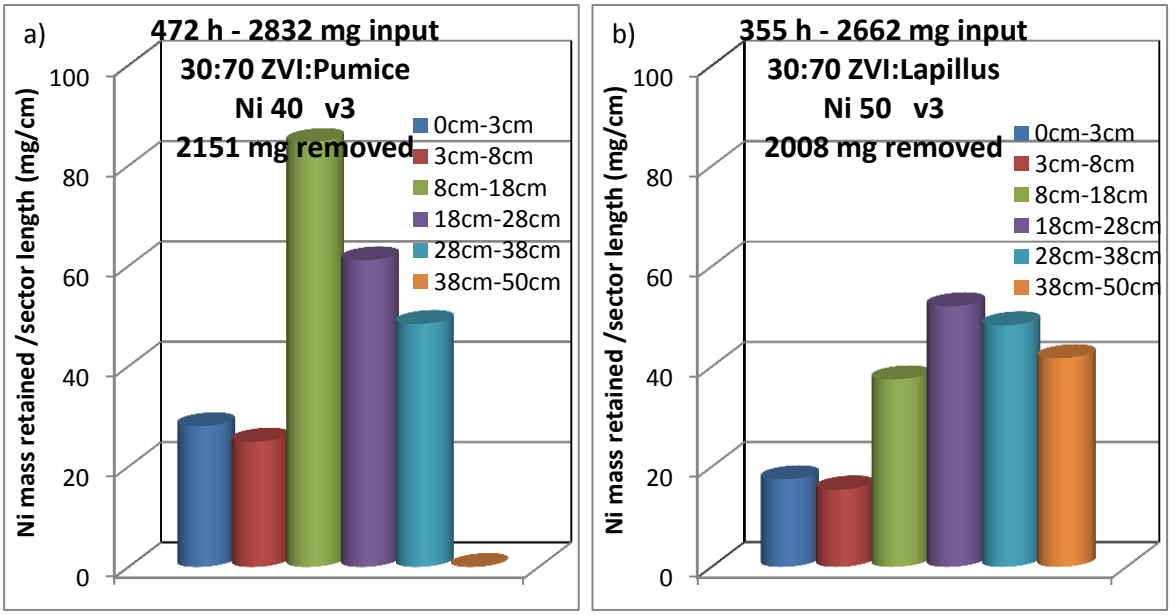

Figure 7-19 Nickel retained mass in each sector divided by the length of the sector in v3 tests with a) ZVI:Pumice and b) ZVI:Lapillus mixtures column tests at about 400 hours from the test beginning

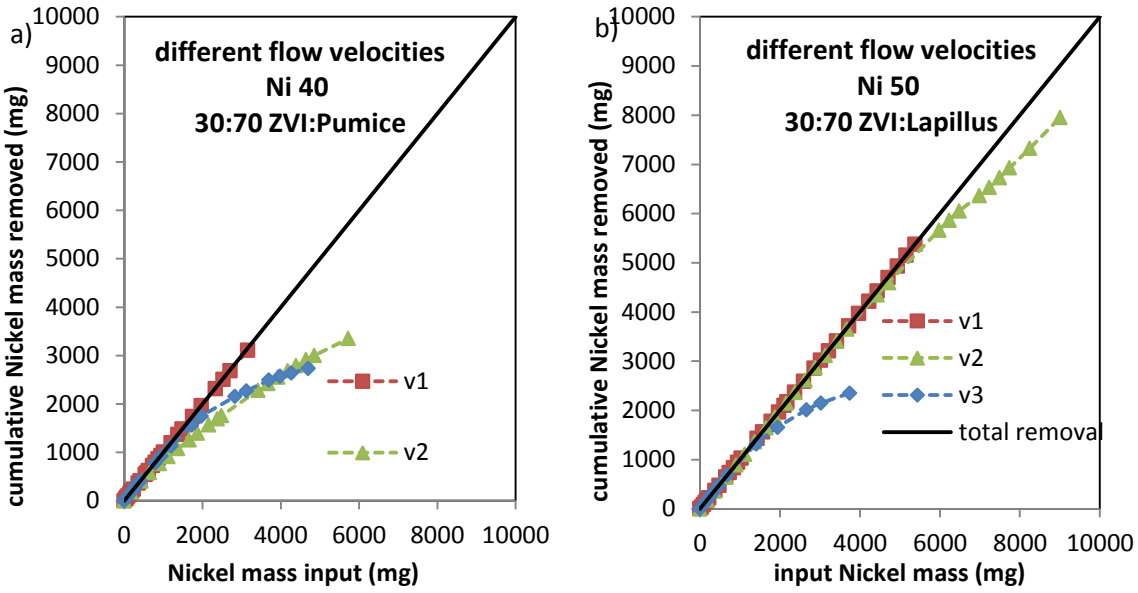

Figure 7-20 Nickel mass removed as function of Nickel mass input for v1, v2 and v3 tests performed with 30:70 w.r. a) ZVI:Pumice and b) ZVI:Lapillus mixtures.

7.2.3.2 Long-term hydraulic behavior

Concerning long-term hydraulic behavior, the evolution of hydraulic conductivity will be proposed for the column tests performed at different flow velocity, comparing what has been observed in ZVI:the mixtures and the ZVI:Lapillus mixtures column tests.

In Figures 7-21, 7-22 and 7-22, the evolution of hydraulic conductivity will be shown as function of input mass, water input and time. The a figures concern the ZVI:Pumice mixture, while the b ones refer to the ZVI:Lapillus mixtures.

As can be observed, the hydraulic conductivity changes into almost the same range for all the considered tests, except for the v1 test of the ZVI:Pumice mixture.

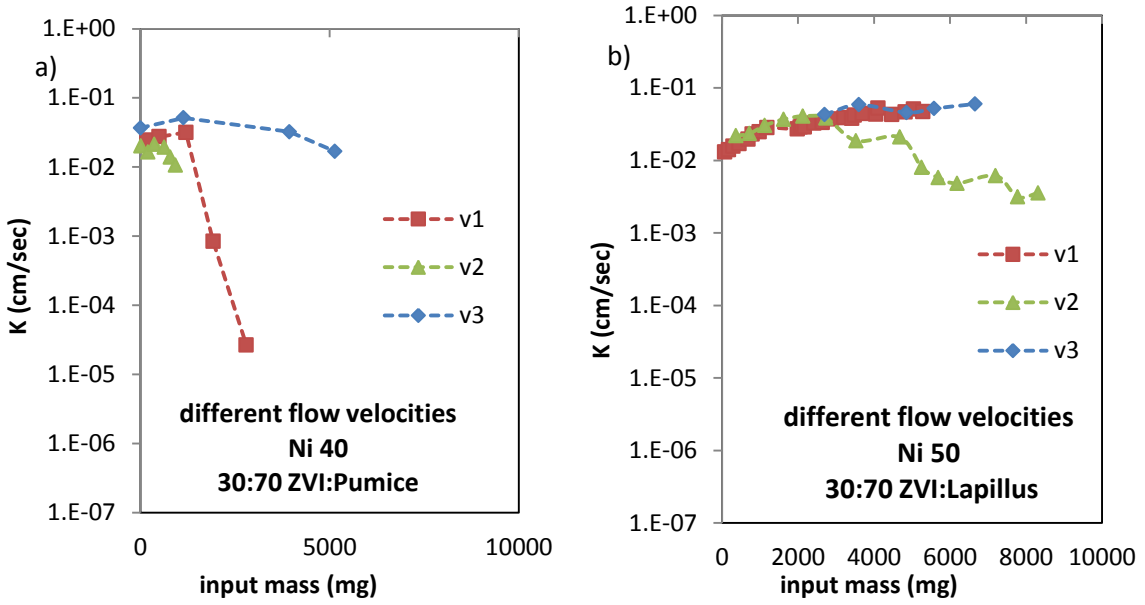

Figure 7-21 permeability evolution as function of the Nickel mass input for v1,v2 and v3 tests performed with 30:70 w.r. a) ZVI:Pumice and b) ZVI:Lapillus mixtures.

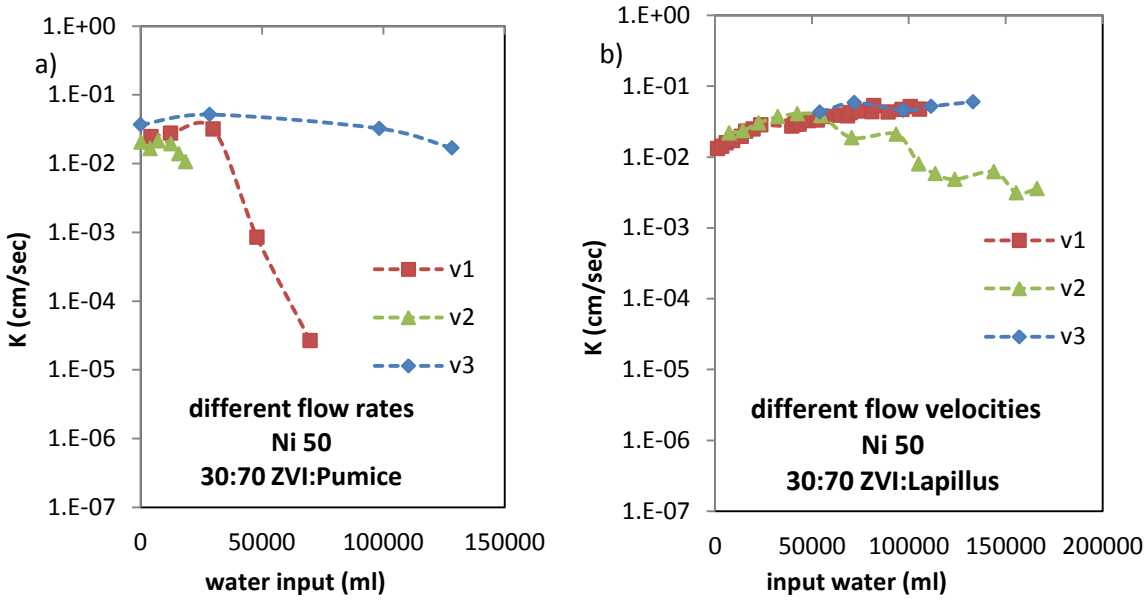

Figure 7-22 permeability evolution as function of the input water for v1,v2 and v3 tests performed with 30:70 w.r. a) ZVI:Pumice and b) ZVI:Lapillus mixtures.

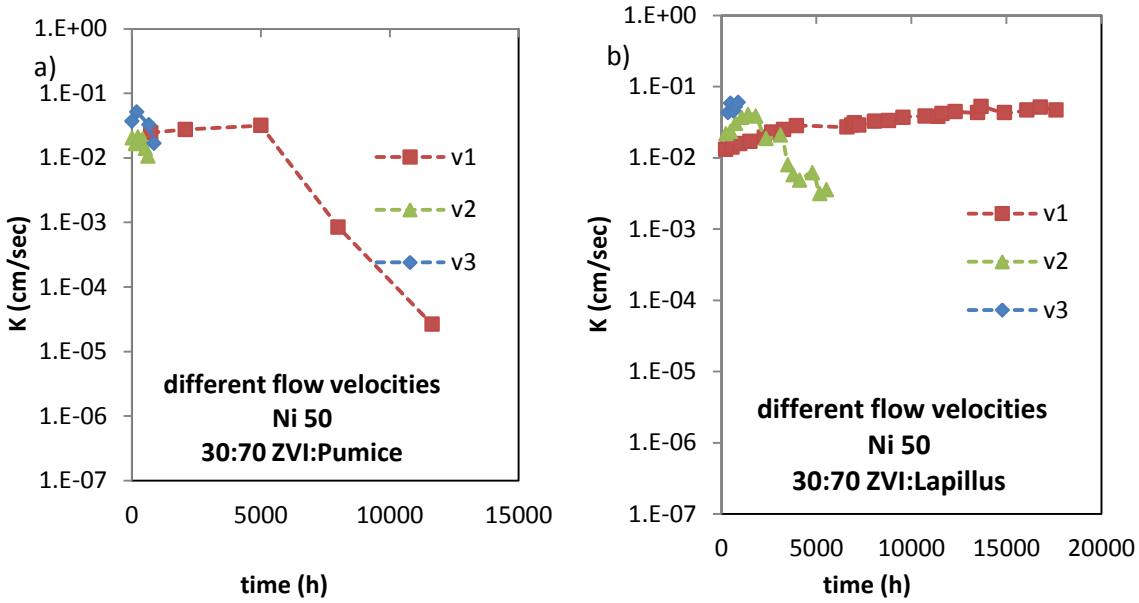

Figure 7-23 permeability evolution as function of time for v1,v2 and v3 tests performed with 30:70 w.r. a) ZVI:Pumice and b) ZVI:Lapillus mixtures.

7.2.4 Comparison of initial contaminant concentration

In this section, a comparison based on the influence of contaminant initial concentration between the long-term Nickel removal efficiency and hydraulic behavior of the ZVI:Pumice mixtures and that of the ZVI:Lapillus will be proposed. The weight ratio used was 30:70 for both mixtures and the constant flow velocity was 0.276 mm/min. In Table 7-9, the characteristics of the column tests carried out and useful for this study are reported.

React. mat.	Initial cont. conc. (mg/L)	React. Thick. (cm)	React. area (cm^2)	React. Vol. (cm^3)	Fe^0 (gr)	Lapill. or Pum. (gr)	n (%)	Flow veloc. (mm/ min)	PV (cm^3)	Tres (h)
Fe^0/ Lap	Ni 50	50	18.09	904.32	480	1120	37	0.276	334.34	11.1
Fe^0/ Lap	Ni 100	50	18.09	904.32	477	1113	37	0.276	337.58	11.3
Fe^0/ Lap	Ni 10	50	18.09	904.32	480	1120	38	0.276	341.36	11.4
Fe^0/ Pum	Ni 8	50	18.09	904.32	240	560	46	0.276	444	14.8
Fe^0/ Pum	Ni 50	50	18.09	904.32	244	570	44	0.276	644.6	21.5

Table 7-5 Characteristics of column tests considered in comparison of contaminant initial concentration influence between ZVI:Pumice and ZVI:Lapillus mixtures

7.2.4.1Long-term Nickel removal efficiency

In Figures 7-24 a) and b), the Nickel retained mass is shown as function of the Nickel input mass for the 30:70 ZVI:Pumice w.r. mixture and for the 30:70 ZVI:Lapillus w.r mixture respectively.

Regarding the Nickel mass input in column tests performed with the lowest Nickel initial concentration, the removal efficiency is high for both filters. Looking at the tests carried out with the intermediate Nickel initial concentration the removal efficiency rapidly decreased in the ZVI:Pumice mixture filter, while it remained high for the ZVI:Lapillus mixture, as previously observed.

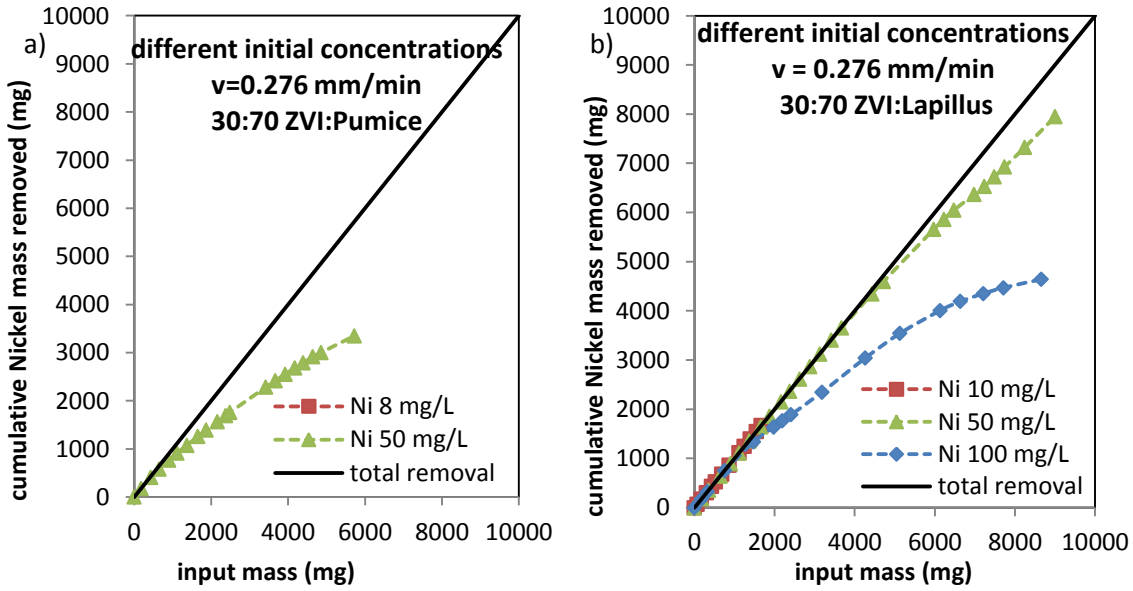

Figure 7-24 Nickel mass removed as function of Nickel mass input for tests performed with 30:70 w.r. a) ZVI:Pumice using solutions of Nickel at 10, 50 and 100 mg/L initial concentrations and b) ZVI:Lapillus mixtures using Nickel solution at 8 and 50 mg/L initial concentrations

7.2.4.2Long-term hydraulic behavior

In Figure 7-25 a) and b), the evolution of hydraulic conductivity is shown as function of time for the ZVI:Pumice and ZVI:Lapillus mixture column tests respectively.

Concerning the first 2000 hours of interaction, no important hydraulic conductivity changes are observed. After this time, that is, the duration of the ZVI:Pumice mixture column tests, the ZVI:Lapillus filters tested using solutions of Nickel at 10 and 50

mg/L are subject to hydraulic conductivity decrease of two and one order of magnitude respectively.

Regarding the pH and Eh evolutions, a difference can be observed comparing the data related to the ZVI:Pumice and ZVI:Lapillus mixtures. In fact, considering the tests where pH and Eh do not stay constant (those carried out at v_3 and Nickel solution at 100 mg/L initial concentration), in the ZVI:Pumice mixture filters the pH increases with the filter thickness, while the Eh decreases with it. Furthermore, they tend to reach the same value along the column with time. In ZVI:Lapillus, this general behaviour is not followed during the first interaction time, during which the pH at half filter length is higher and Eh is lower than at outlet (for 170 hours for tests carried out with v_1 and 1400 hours for tests carried out using solution with initial Nickel concentration equal to 10 mg/L, at least).

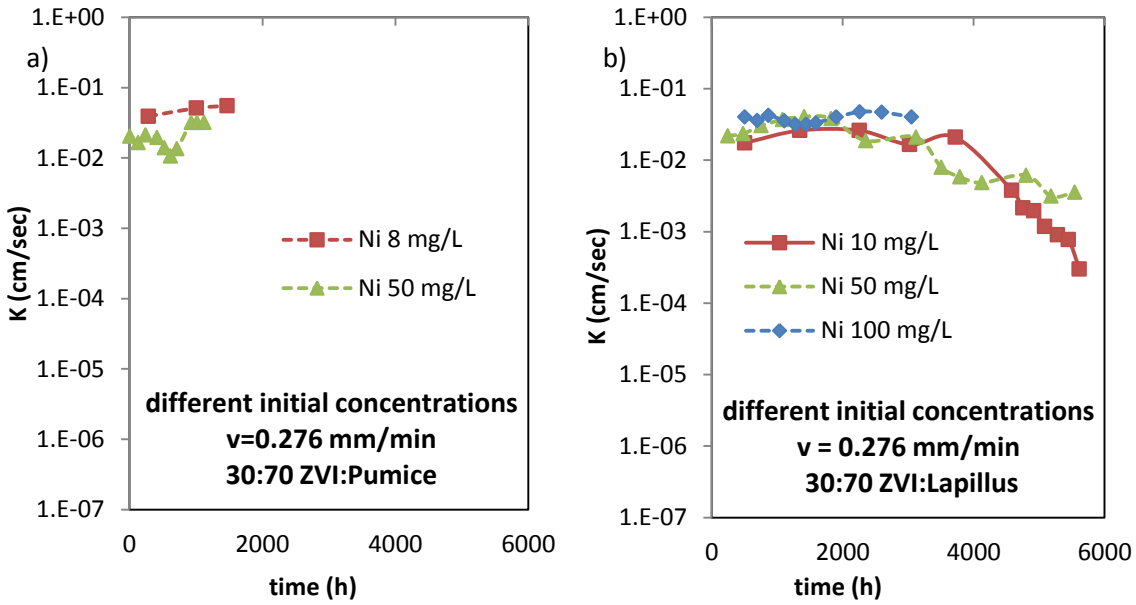

Figure 7-25 hydraulic conductivity evolution with time for tests performed with 30:70 w.r. a) ZVI:Pumice using solutions of Nickel at 10, 50 and 100 mg/L initial concentrations and b) ZVI:Lapillus mixtures using Nickel solution at 8 and 50 mg/L initial concentrations

7.3 Comparison about Zinc-contaminated tests

In this paragraph, a study of the long-term Zinc removal efficiency and hydraulic behaviour of the 50:50 ZVI:Pumice and ZVI:Lapillus w.r. mixtures is proposed. In Table 7-10, the characteristics of considered column tests are reported. Solution of Zinc at 50 mg/L was flowed in the column at 0.276 mm/minconstant flow velocity in both tests.

React. mat.	Weig. ratio	Initial cont. conc. (mg/L)	React. Thick. (cm)	React. area (cm^2)	Reac. Vol. (cm^3)	Fe^0 (gr)	Lapil. or Pum. (gr)	n (%)	Flow veloc. (mm/min)	PV (cm^3)	Tres (h)
Fe^0/ Pum	50:50	Zn 50	50	18.09	904.32	481	481	49	0.276	442.29	14.7
Fe^0/ Lap	50:50	Zn 50	50	18.09	904.32	970	970	38	0.276	340.16	11.3
$Fe^{0,*}$	-	Zn 50	3	18.09	58.9	240	-	50	0.276	28	0.9

Table 7-6 Characteristics of column tests considered in comparison of long-term Zinc removal efficiency between ZVI:Pumice and ZVI:Lapillus mixtures
(* Bilardi, 2012)

7.3.1 Long-term Nickel removal efficiency

In Figures 7-26 a) and b) the evolution of Zinc normalized concentration as function of filter thickness for different sampling times is shown for the ZVI:Pumice and ZVI:Lapillus mixtures respectively. As can be observed, both filters are able initially to reduce Zinc concentration efficiently in the available filter thickness (50 cm). This is true for the ZVI:Pumice mixture filter until about 500 hours of interaction, while the ZVI:Lapillus mixture filter is highly efficient after 2328 hours also. Furthermore, the latter maintains a constant high removal efficiency until about 500 hours using a 8 cm long filter.

In this comparison, the different ZVI content between the two filters should be considered. In fact, the ZVI:Pumice and ZVI:Lapillus mixtures contain 481 gr and 970 gr of ZVI respectively, one almost the double of the other (Table 7-10). Taking into account this aspect, a comparison between the available data at the sampling ports placed at 28 cm from the inlet and at the outlet of the ZVI:Lapillus and ZVI:Pumice mixtures filters will be proposed. In Figure 7-27 a) the Zinc normalized concentration evolution at sampling ports placed at 28 cm from inlet and at outlet of the ZVI:Lapillus and ZVI:Pumice mixtures filters respectively is shown as function of time. As can be observed, the ZVI:Pumice mixture filter is able to reduce the Zinc

concentration efficiently until the first 255 hours of interaction, after which the Zinc normalized concentration increases rapidly. When the 28 cm long ZVI:Lapillus filter is used, the removal efficiency remains constant at high values for all of the test duration (more than 2000 hours).

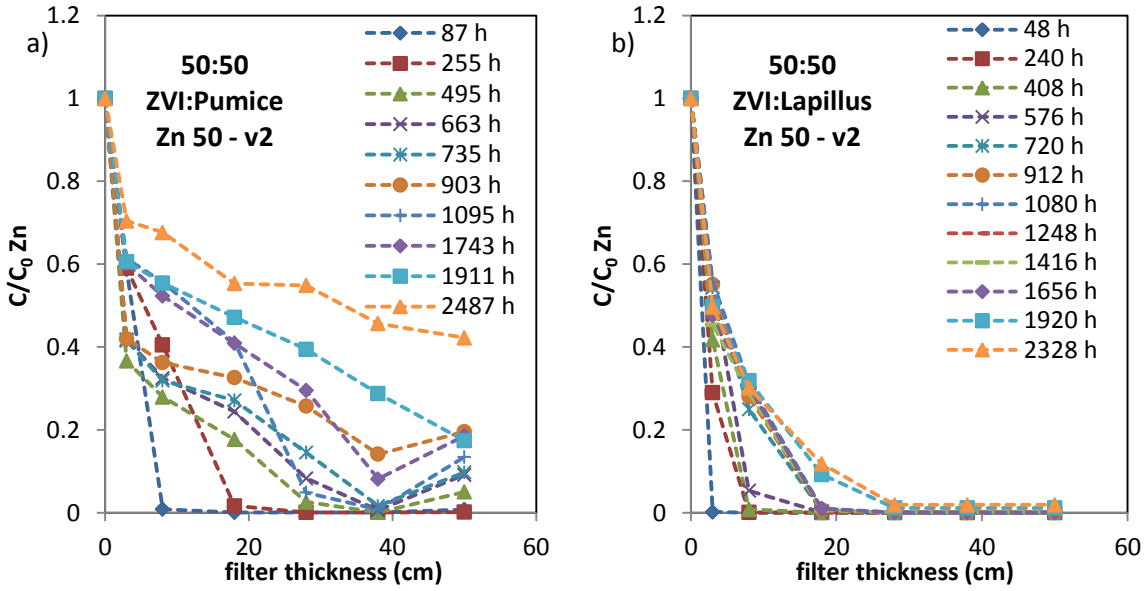

Figure 7-26 Evolution of Zinc normalized concentration with filter thickness at different sampling times for a) 50:50 ZVI:Pumice w.r. mixture test and b) 50:50 ZVI:Lapillus w.r. mixture test

Furthermore, a contaminant mass balance was carried out for the two filters lengths containing equal ZVI mass. In Figure 7-27 b), the Zinc retained mass is shown as a function of Zinc input mass for the 28 cm long ZVI:Lapillus mixture filter and for the 50 cm long ZVI:Pumice mixture filter. Both filters seem to have a high Zinc removal efficiency, that is, about 86% and 99% for the ZVI:Pumice and ZVI:Lapillus mixtures filters respectively, corresponding to 3000 mg of Nickel input mass.

7.3.2 Long-term hydraulic behavior

Concerning the long-term hydraulic behaviour, a comparison of hydraulic conductivity evolution with time for the ZVI:Pumice mixture, ZVI: the Lapillus mixture and the pure ZVI filters tested under the same experimental conditions is proposed in Figure 7-28 a). The two mixtures were not subject to hydraulic

conductivity reduction during the time, while a reduction of four orders of magnitude was observed for the pure ZVI test.

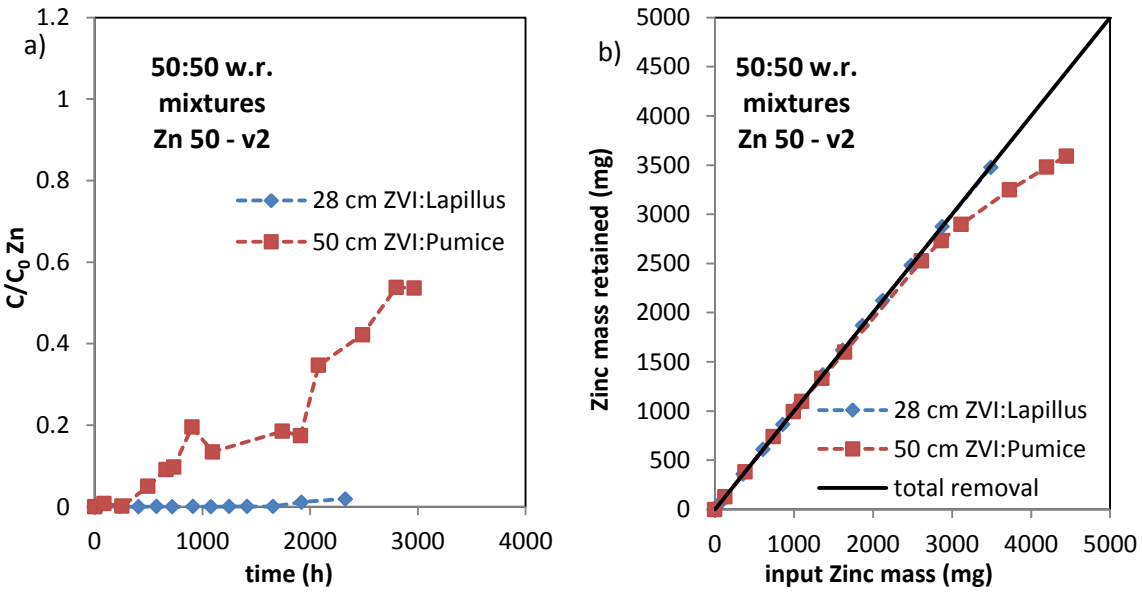

Figure 7-27 a) Zinc normalized concentration evolution as function of time and b) Zinc retained mass as function of input Zinc mass for 28 cm long ZVI:Lapillus mixture filter and 50 cm long ZVI:Pumice mixture filter.

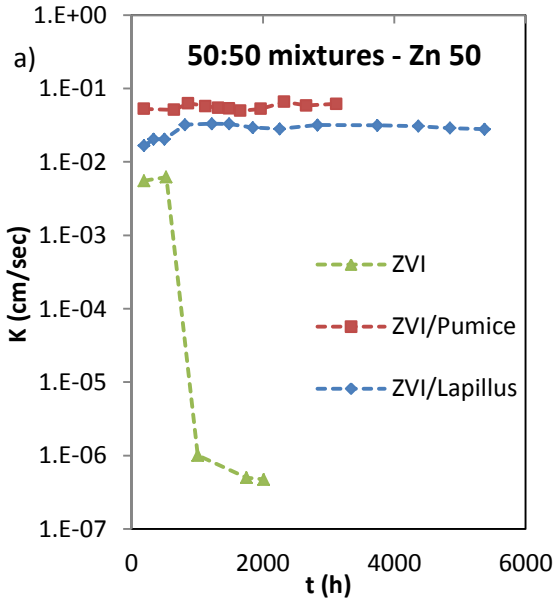

Figure 7-28 hydraulic conductivity evolution with time for 50:50 ZVI:Pumice and ZVI:Lapillus w.r. mixtures and pure ZVI filters performed using solution of Zinc at 50 mg/L initial concentration and v2 constant flow velocity.

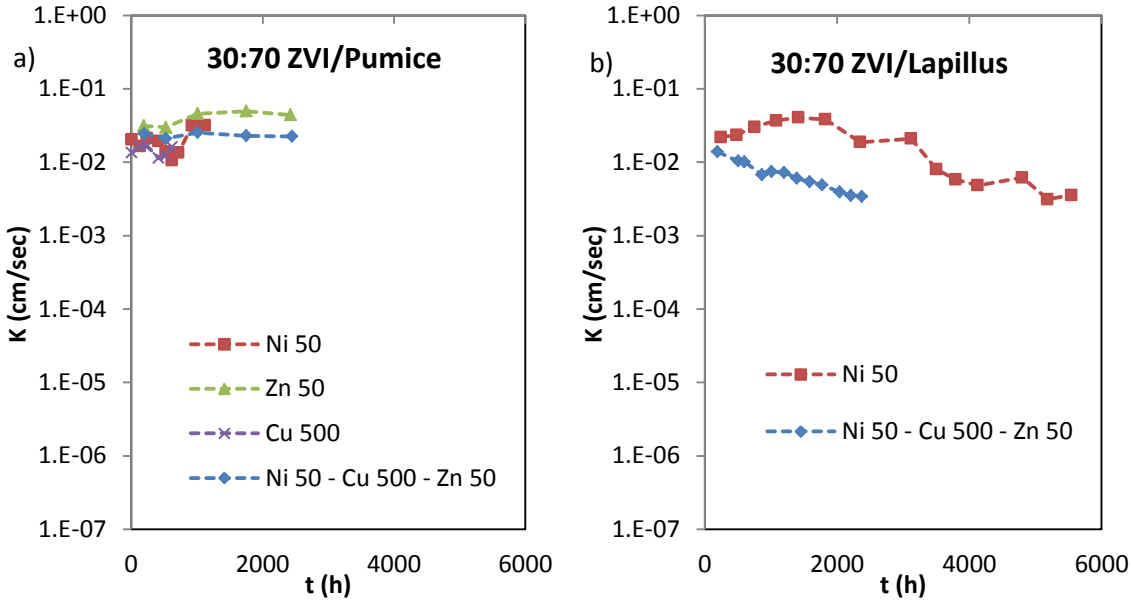

Figure 7-29 Hydraulic conductivity evolution with time for a) 30:70 ZVI:Pumice w.r. mixture and b) 30:70 ZVI:Lapillus w.r. mixture filters tested with mono-contaminant and three-contaminant solutions.

7.4 Conclusions

The comparative analysis between results of column tests performed using ZVI:Pumice mixture and those obtained using ZVI:Lapillus mixtures was based on Nickel and Zinc removal. The first step of analysis of column tests based on the Nickel-contaminated groundwater remediation regarded the comparison of long-term removal efficiency of tested pure volcanic materials, pure Pumice or pure Lapillus, carried out with Nickel-contaminated solution at an initial contaminant concentration equal to 50 mg/L put into the column at 0.276 mm/min constant flow velocity. A certain Nickel removal efficiency is already performed in 3 cm reactive granular filter length, although it is limited, for both tests and higher in pure Lapillus test. This difference is more evident considering the experimental data at 38 cm.

Therefore, a comparison among the different weight ratio mixtures tested was made. It was based on analysis of results of column tests performed using 10:90, 30:70 and 50:50 ZVI:Pumice w.r. and ZVI:Lapillus w.r mixtures under the same experimental conditions, considering the same ZVI content, same residence time and same removal efficiency. According to the first two criteria, the ZVI:Lapillus w.r mixtures are always more efficient. In fact, considering the third one for 10:90 w.r. mixtures, 8 cm of ZVI:Lapillus mixture have the same efficiency of 58 cm of ZVI:Pumice filter, for 30:70

w.r. mixtures, 8 cm of ZVI:Lapillus mixture have the same efficiency of 38 cm of ZVI:Pumice filter and for 50:50 w.r. mixtures, 8 cm of ZVI:Lapillus mixture have the same efficiency of 33 cm of ZVI:Pumice filter.

Regarding the comparison among column tests with 30:70 ZVI:Pumice w.r. and ZVI:Lapillus w.r. mixtures performed using different flow velocities (0.055, 0.276 and 1.382 mm/min), the higher removal efficiency of the ZVI:Lapillus than ZVI:Pumice mixtures is confirmed for each flow velocity used. The v1 test seems to be highly efficient for all the tests duration (14000 h for ZVI:Pumice and 19000 for ZVI:Lapillus) in both filters. Concerning the v2 tests, the ZVI:Lapillus filter maintains a high removal efficiency for all the test duration. In fact its Nickel removal efficiency is about 88% after 9000 mg of Nickel input , while using ZVI:Pumice mixture it is about 58% corresponding to 6000 mg. Regarding the mixtures tested using v3 flow velocity, it can be observed that the Nickel removal efficiency evolution as function of Nickel input mass is almost the same and it is about 60% after 400 mg of Nickel input. The hydraulic conductivity changes into almost the same range for all the considered tests, excep for the v1 test of ZVI:Pumice mixture for which it decreases of 3 orders of magnitude.

Concerning the comparison among column tests with 30:70 ZVI:Pumice w.r. and ZVI:Lapillus w.r. mixtures performed using different Nickel initial concentrations (10, 50 mg/L), the removal efficiency is high for both filters performed in column tests with the lowest Nickel initial concentration. Regarding the tests carried out with the intermediate Nickel initial concentration the removal efficiency rapidly decreases in the ZVI:Pumice mixture filter, while it remains high for ZVI:Lapillus mixture. Until the duration of ZVI:Pumice mixtures column test no important hydraulic conductivity changes are observed. After this time, the ZVI:Lapillus filters tested using solutions of Nickel at 10 and 50 mg/L are subject to hydraulic conductivity decrease of two and one order of magnitude respectively.

Concerning tests performed to remediate Zinc contaminated water (at 50 mg/L initial concentration) using 50:50 ZVI:Pumice w.r and ZVI:Lapillus w.r. mixtures a comparison can be made based on the same ZVI content. Thus, 28 cm long ZVI:Lapillus mixture filter was compared to 50 cm long ZVI:Pumice mixture filter. Both filters seem to have a high Zinc removal efficiency, that is, about 86% and 99% for ZVI:Pumice and ZVI:Lapillus mixtures filters respectively, corresponding to 3000

mg of Nickel input mass. The two mixtures have not been subject to hydraulic conductivity reduction during the time, while a reduction of four orders of magnitude has been observed for the pure ZVI test.

The comparison among tests performed using three-contaminated solutions and mono-contaminant solutions and 30:70 ZVI:Pumice and ZVI:Lapillus w.r. mixtures was made regarding only the hydraulic conductivity evolution. The ZVI:Pumice mixture filters did not develop phenomena leading to hydraulic conductivity reduction during the time of test duration, while, for ZVI:Lapillus tests, a certain reduction about one order of magnitude, developed in 2000 hours in three-contaminant and in 6000 hours in test with Nickel-contaminant solution, was observed.

In Chapter 8 the results of release tests performed for some column tests and the iron and nickel concentration evolution is shown and discussed.

8 Further information about removal efficiency

8.1 Introduction

As observed in Chapter 7, some differences in long-term removal efficiency and hydraulic behavior were found between ZVI:Pumice and ZVI:Lapillus mixtures.
In this chapter, some further analysis is performed to evaluate whether ZVI:Lapillus mixtures release nickel after the test end and how the iron concentration varies as function of time and filter thickness. The evolution of iron concentration along the column and with time is shown and discussed, comparing it with the evolution of Nickel for the same considered column tests.
Furthermore, results of release tests, performed to evaluate the possibility of release of contaminant by exhausted reactive materials when fresh water flows through it, are shown and described for two column tests.

8.2 Iron and Nickel concentration evolution

The Iron concentration was measured in samples withdrawn from the solution flowing into the column at different sampling times and ports for some column tests. Knowing the evolution of Iron along the column with time can be an important information to understand whether Iron is released in the water during the removal processes and to hypothesize what processes lead to its release.
In this paragraph, two column tests are considered through which the mixture 30:70 ZVI:Lapillus w.r. was tested using a solution of Nickel at 50 mg/L initial concentration: one was performed using a 50 cm long filter under a 1.382 mm/min constant flow velocity (v_3), the second using a 100 cm long filter under a 0.276 mm/min constant flow velocity (v_2). In Figures 8-1 and 8-3, the Nickel concentration evolution along the column length from the beginning of the test until about 60 h and from 90 to 500 h are shown respectively, for the test performed using v_3. In Figures 8-2 and 8-4, the Iron concentration evolution along the column length from the beginning of the test until about 60 h and from 90 to 500 h are shown respectively for the same test.

In Figures 8-5 and 8-7, the Nickel concentration evolution along the column length from the beginning of the test until about 2500 h and from 4200 to 7300 h is shown respectively, for the test performed using v2. In Figures 8-6 and 8-8, the Iron concentration evolution is shown for the same test and sampling times.

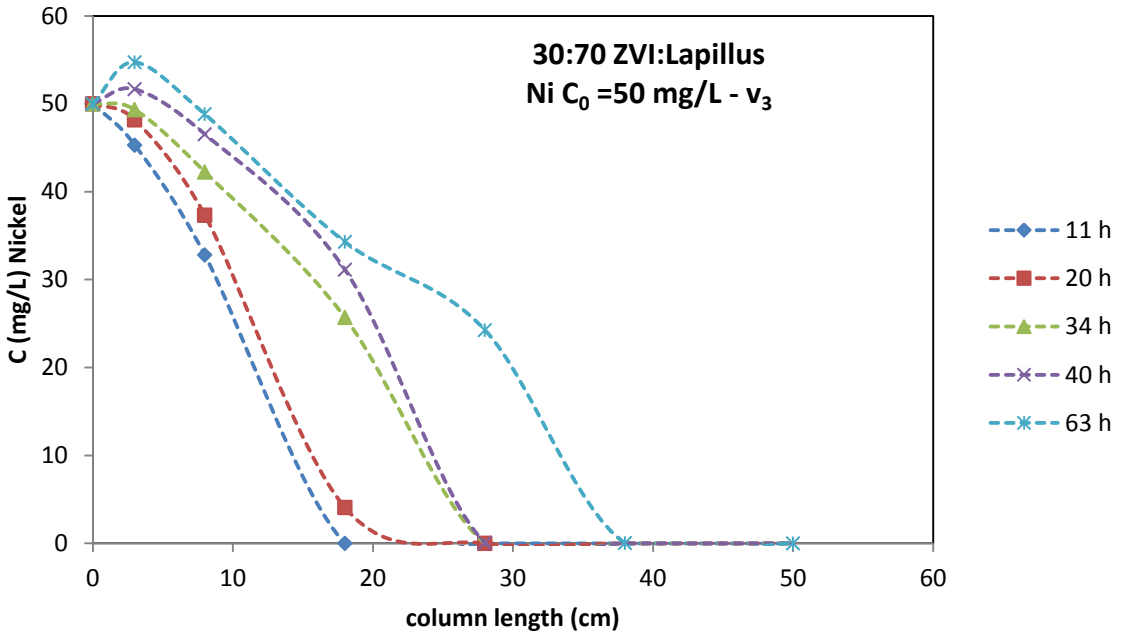

Figure 8-1 Nickel concentration evolution as function of filter thickness for different sampling times for test with 30:70 ZVI:Lapillus w.r. mixture, Ni solution at 50 mg/L initial concentration and v3 flow velocity (until 63 h)

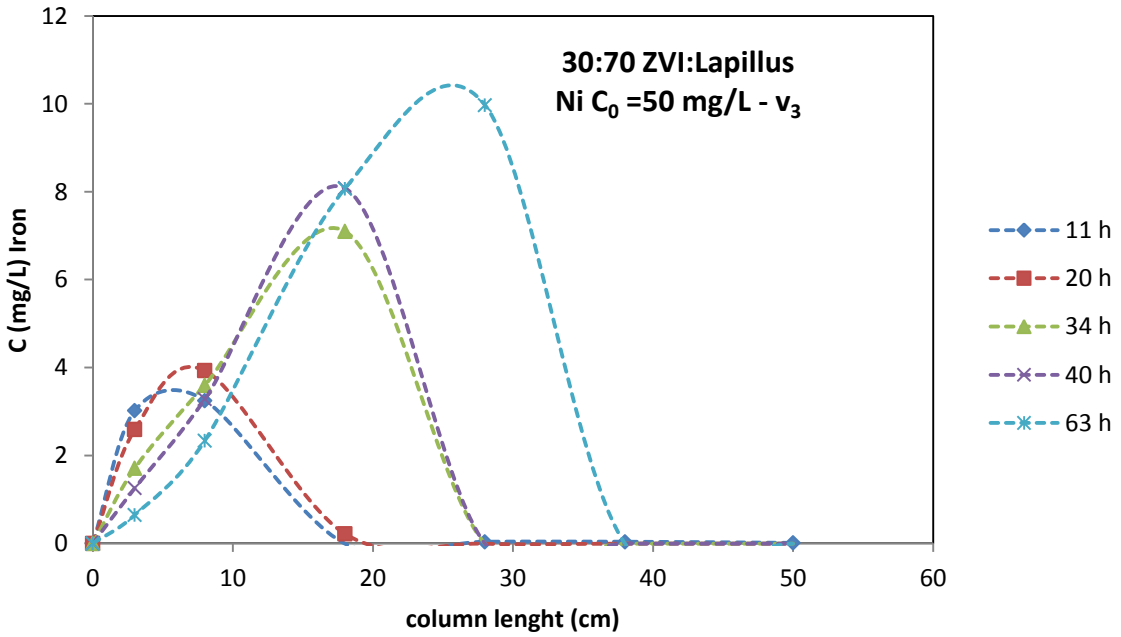

Figure 8-2 Iron concentration evolution as function of filter thickness for different sampling times for test with 30:70 ZVI:Lapillus w.r. mixture, Ni solution at 50 mg/L initial concentration and v3 flow velocity (until 63 h)

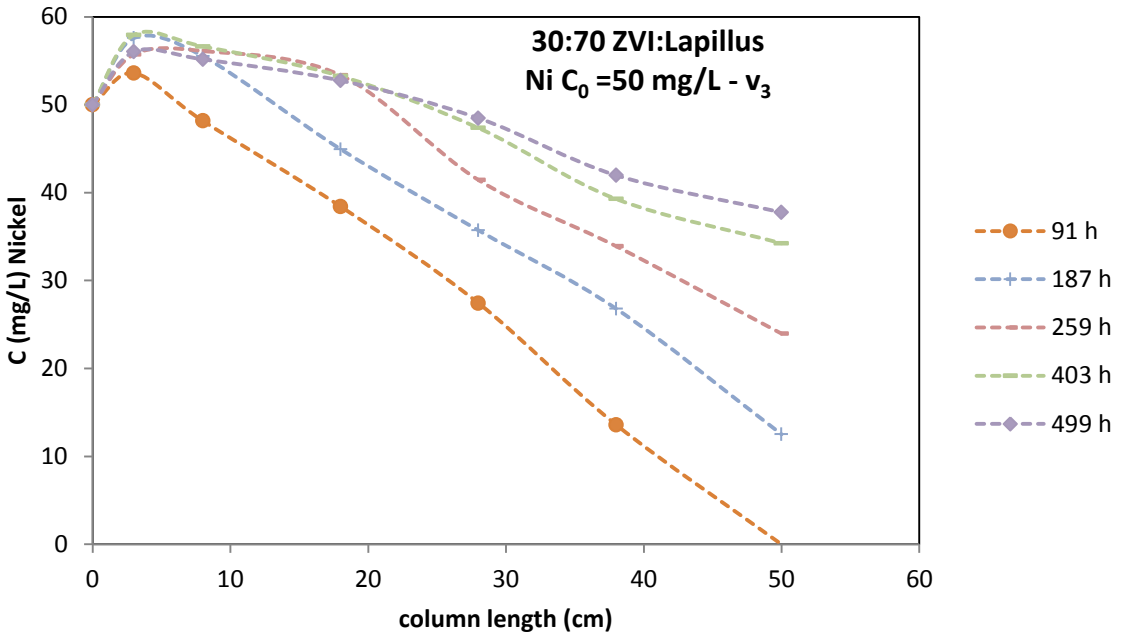

Figure 8-3 Nickel concentration evolution as function of filter thickness for different sampling times for test with 30:70 ZVI:Lapillus w.r. mixture, Ni solution at 50 mg/L initial concentration and v3 flow velocity (since 90 h)

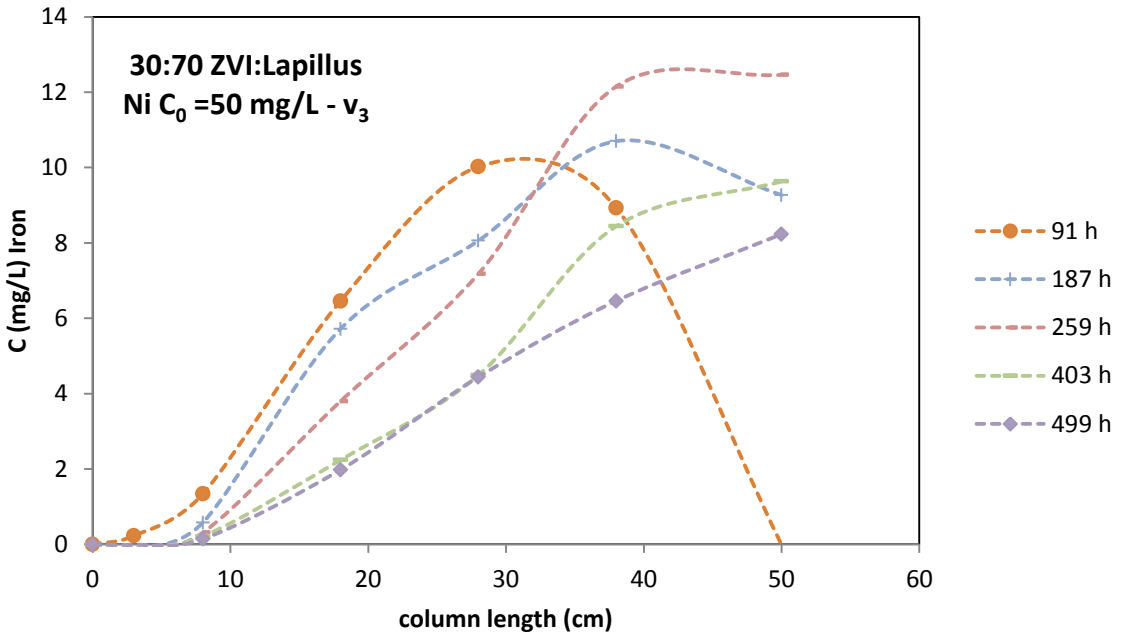

Figure 8-4 Iron concentration evolution as function of filter thickness for different sampling times for test with 30:70 ZVI:Lapillus w.r. mixture, Ni solution at 50 mg/L initial concentration and v3 flow velocity (since 90 h)

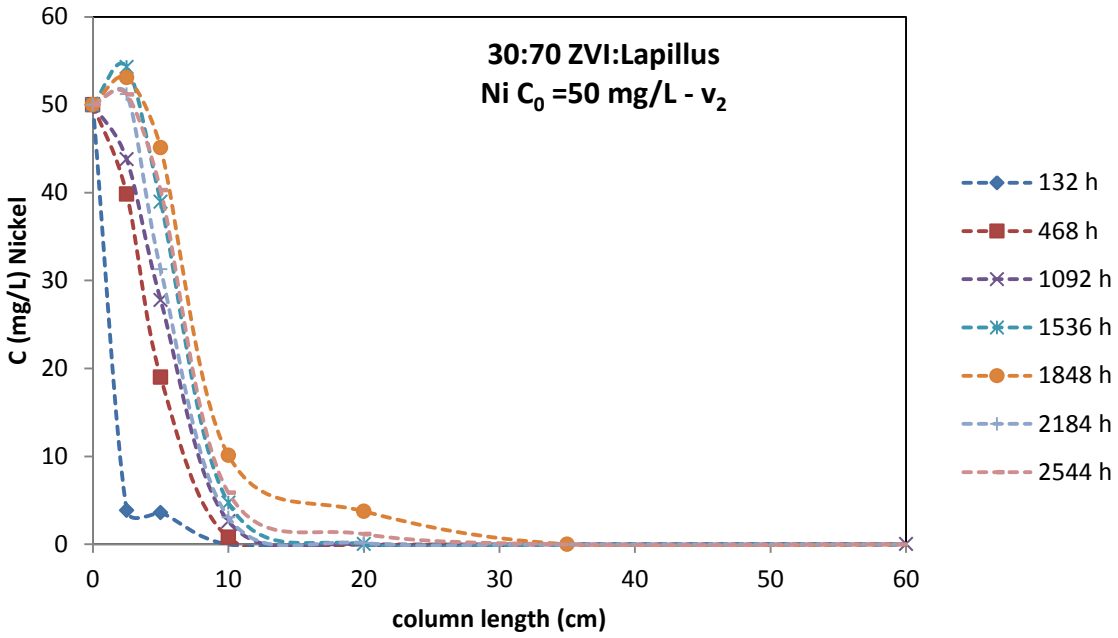

Figure 8-5 Nickel concentration evolution as function of filter thickness for different sampling times for test with 30:70 ZVI:Lapillus w.r. mixture, Ni solution at 50 mg/L initial concentration and v2 flow velocity (until 2500 h)

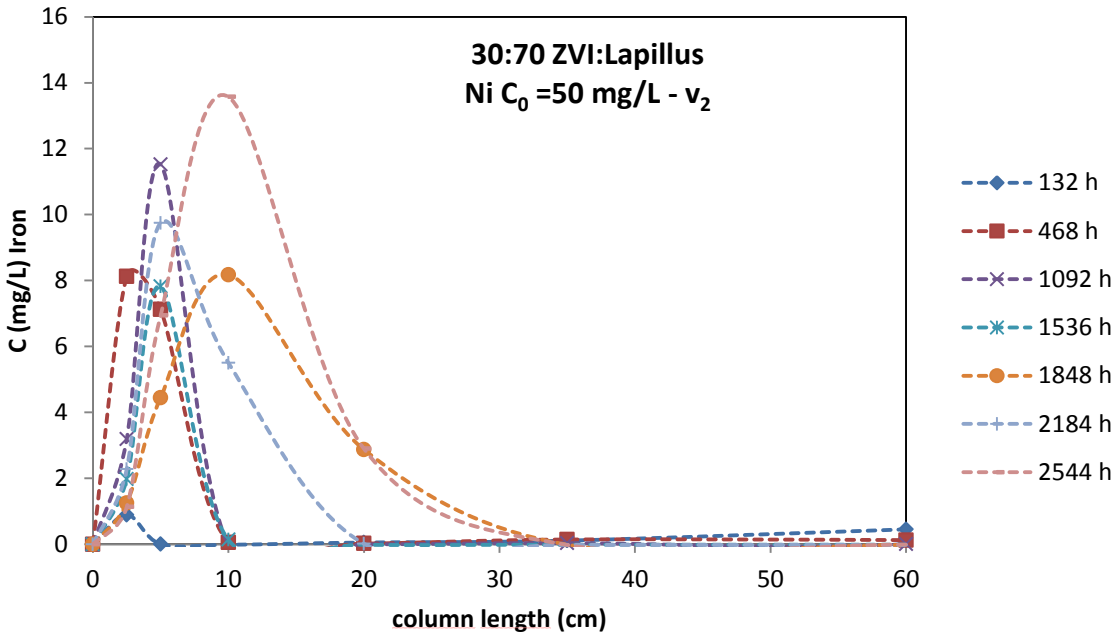

Figure 8-6 Iron concentration evolution as function of filter thickness for different sampling times for test with 30:70 ZVI:Lapillus w.r. mixture, Ni solution at 50 mg/L initial concentration and v2 flow velocity (until 2500 h)

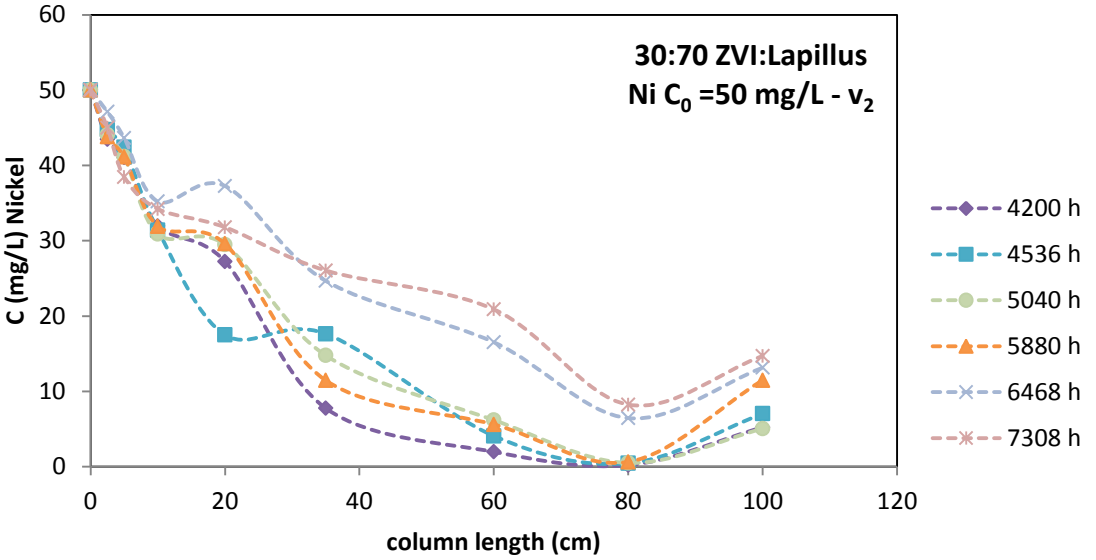

Figure 8-7 Nickel concentration evolution as function of filter thickness for different sampling times for test with 30:70 ZVI:Lapillus w.r. mixture, Ni solution at 50 mg/L initial concentration and v2 flow velocity (since 4200 h)

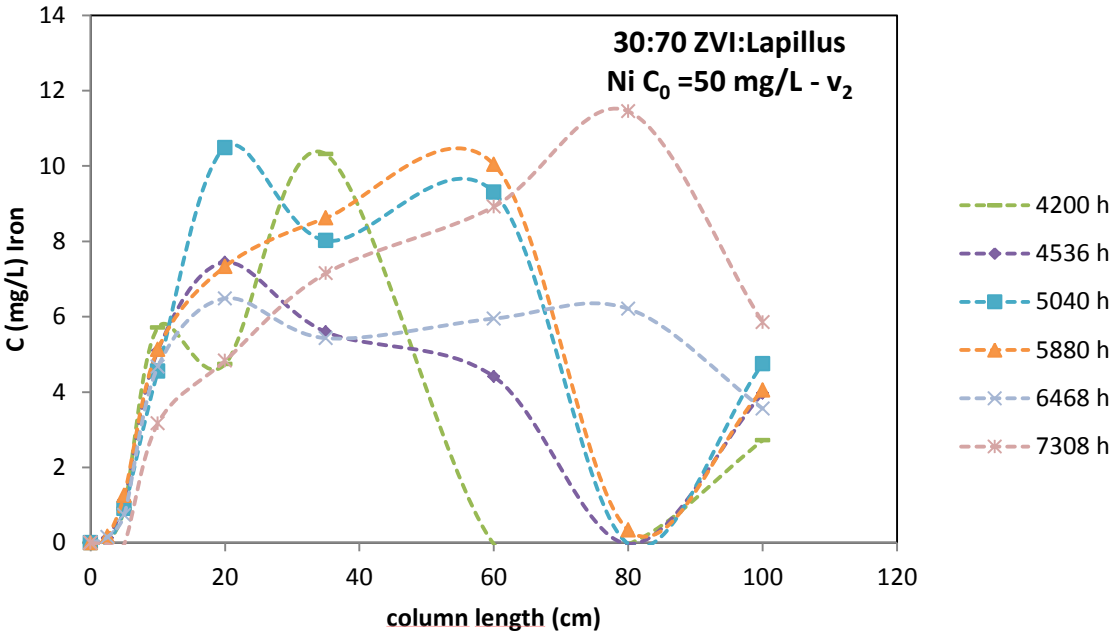

Figure 8-8 Iron concentration evolution as function of filter thickness for different sampling times for test with 30:70 ZVI:Lapillus w.r. mixture, Ni solution at 50 mg/L initial concentration and v2 flow velocity (since 4200 h)

Observing these graphs, two main considerations can be made. The first is related to the column length that is involved in Iron concentration evolution. In fact, it can be observed that the evolution of Iron is strictly related to that of Nickel. The not negligible Iron concentration is measured where and when not negligible Nickel

concentrations are measured. Considering the filter length, its evolution starts and ends where the same is observed for the evolution of concentrations of Nickel, for each sampling time. In fact, as observed in column tests performed using ZVI:Pumice mixtures (Bilardi et al. 2013a and 2013b), as the nickel breakthrough is reached, iron is released.

The second consideration is related to the peaks observed for Iron and Nickel evolution concentration along the column for each sampling time. It can be observed that the picks of Nickel and Iron do not correspond, but the peaks of Iron correspond to the position along the column where Nickel concentration is mostly reduced.

8.3 Nickel release tests

The results of release tests performed in two column tests are shown in Figures 8-9 and 8-10 in terms of Nickel concentration at the outlet of the column as function of time. The experimental data are related to the column tests carried out using a 30:70 ZVI:Lapillus w.r. mixture to remediate a solution of Nickel at 100 mg/L of initial concentration input at the inlet under 0.276 mm/min constant flow velocity. The data shown in Figure 8-10 relate to the 50 cm high column test performed using a 30:70 ZVI:Lapillus w.r. mixture, a solution of Nickel at 50 mg/L of initial concentration and a constant flow velocity of 1.382 mm/min. As can be observed in both graphs, when fresh water flows through the exhausted reactive material, Nickel mass already retained by this latter is not flushed out from it and water is kept clear. Probably, the Nickel concentration observed at the beginning of the release tests is due to the expulsion of pore water present in the column at the end of the experiment with contaminated water.

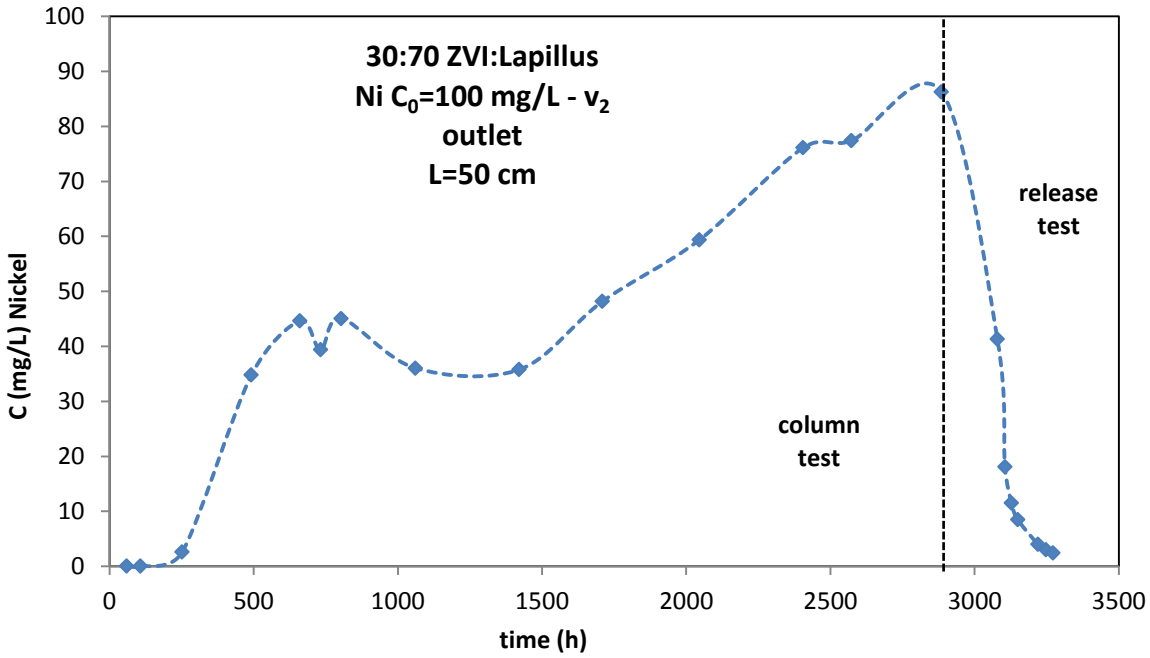

Figure 8-9 Nickel concentration evolution at outlet (50 cm) during column test and the next release test for 30:70 ZVI:Lapillus w.r. mixture tested with a solution of Nickel at 100 mg/L initial concentration and v2 flow velocity

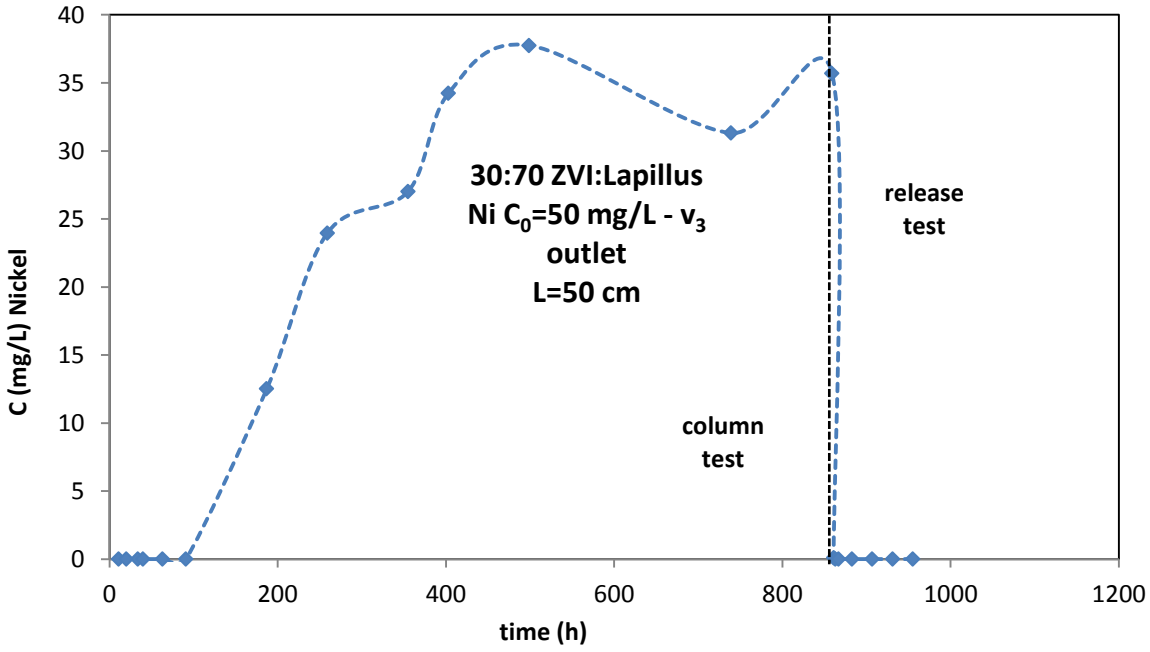

Figure 8-10 Nickel concentration evolution at outlet (100 cm) during column test and the next release test for 30:70 ZVI:Lapillus w.r. mixture tested with a solution of Nickel at 50 mg/L initial concentration and v3 flow velocity in a column test 100 cm high

8.4 Conclusions

Observing the data of nickel and iron concentration evolution along the column and during time, it can be observed that the evolution of iron is strictly related to that of nickel, because its evolution starts and ends where it is observed as the same for the evolution of concentration of Nickel and the peaks of iron concentration evolution correspond to the position along the column where nickel concentration is mostly reduced.

Concerning the results of release tests performed in two column tests using a 30:70 ZVI:Lapillus w.r. mixture to remediate a solution of Nickel at 100 mg/L of initial concentration input at the inlet under 0.276 mm/min constant flow velocity and 100 cm high column test performed using a 30:70 ZVI:Lapillus w.r. mixture, a solution of Nickel at 50 mg/L of initial concentration and a constant flow velocity of 1.382 mm/min it can be supposed that Nickel mass already retained by reactive material is not flushed out from it.

9 Final remarks and future works

The analysis of the results of experimental and modeling activities introduced in this thesis, leads to different considerations about the investigated reactive media and ideas about further work.

Firstly, the volcanic Lapillus and ZVI:Lapillus mixtures seem to be more efficient in terms of long-term heavy-metal contaminated groundwater remediation and to have a better long-term hydraulic behavior than Pumice and ZVI:Pumice mixtures.

The higher removal efficiency of Lapillus can deal with the higher content in iron oxides, the lower content in silica and the greater roughness of the surface, that increases the specific external surface, important parameter in removal processes, as well as the larger pores, that makes more easily accessible the internal surface particle by contaminated water, than Pumice.

Concerning the mixtures, the higher specific weight of Lapillus than that of Pumice allows for a higher homogeneity of the mixture composition along the column (or PRB) height depending on the filling procedure used during the installation. It allows also for a higher ZVI content per unit volume or filter unit thickness in ZVI:Lapillus than in ZVI:Pumice, which means a higher number of reactive sites, considering the ZVI as the most efficient material. Furthermore, comparing the efficiency of mixtures filters at the same weight ratio and the same ZVI content, ZVI:Lapillus mixtures allow us to obtain a higher efficiency with less thick filters. Considering the importance of residence time for some heavy metal removal (e.g. Nickel), this highlights the higher removal efficiency of Lapillus compared to Pumice.

Of course, the hypothesized causes of removal efficiency of Lapillus should be confirmed by further investigations. Physical-chemical analysis of exhausted material should be performed to understand what the main removal processes are and the most important characteristics that affect them, as well as the possible interactions between ZVI and Lapillus . Measurement of specific surface and characterization of roughness of Pumice and Lapillus using BET can be important for understanding how they influence the removal efficiency. As was observed through the SEM pictures, Pumice seems to have a high internal porosity and smooth external surface, while Lapillus seems to have a lower internal porosity with larger pores and a much rougher external surface than Pumice.

Concerning the coupled model of the column test, the sorption model seems to be good for representing long-term Nickel removal efficiency of the studied mixtures. More investigations should be carried out, to develop the removal efficiency model applied to other heavy metals removal, considering mono- and three-contaminant solutions. In effect, the introduction of other terms or equations representing other contaminant removal processes, the removal efficiency of each material constituting the mixtures as well as their influence on each other can be considered. Regarding the model of hydraulic conductivity evolution, further study and investigation is needed. Considering the different possible causes of its evolution, e.g. iron corrosion products, secondary mineral precipitates, colloids and gas formation, measurements of differential pore water pressure along the filter thickness can provide important information about the position of the layer characterized by the highest porosity reduction. A further tool to use to make a comparison study consists in the application of a chemical-hydraulic modeling to the column tests, to identity where the accumulation of the products with the most expansive nature is, and how it varies with time. Of course, this should be investigated for each contaminant and for pluri-contaminant solutions, because the evolution of removal efficiency and hydraulic behavior can vary with the considered filter thickness, the contaminant to be removed and the chemical conditions as function of time.

Since gas production can be an important phenomenon leading to hydraulic conductivity reduction, a column study performed using a gamma-densimetre, that gives information about the volumetric mass of the solid phase during time, can be carried out and their results can be compared with the other two above-mentioned investigations to identify the influence of each factor in the hydraulic performance of column tests. Thus, the hydraulic model applied for the tested mixtures can be better developed and calibrated.

A microstructural study on the exhausted reactive material will be useful to better understand the mechanisms developed during the removal processes.

Finally, tests with real contaminated groundwater should be carried out to investigate whether and how different chemical composition and condition of contaminated water affect the contaminant removal efficiency and hydraulic behavior of the used mixtures.

8 REFERENCES

Appelo C. A. J. and Postma D., 2005. Geochemistry, Groundwater And Pollution. A.A. Balkema Publishers, pp:634.

Bear, J. 1979. Hydraulics of ground water. New York City: McGraw-Hill.

Bear, J. & Cheng, A. H.-D. 2010. Theory and applications of transport in porous media. Modeling Groundwater Flow and Contaminant Transport. Springer.

Benner, S. G., D. W. Blowes, W. D. Gould, R. B. Herbert Jr., and C. J. Ptacek. 1999. "Geochemistry of a Reactive Barrier for Metals and Acid Mine Drainage," Environmental Science and Technology 33: 2793–99.

Bi, E., Devlin, J. and Huang, B., 2009. Effects of Mixing Granular Iron with Sand on the Kinetics of Trichloroethylene Reduction. Ground Water Monit. Remed, Volume 29, p. 56–62.

Bilardi S., 2012a. Short and long term behaviour of Fe0 and Fe0/Pumice granular mixtures to be used in PRB for groundwater remediation. Ph. D. Thesis in Geotechnical Engineering at the Mediterranean University of Reggio Calabria.

Bilardi, S., Amos, R. T., Blowes, D. W., Calabrò P. S. and Moraci, N., 2012b, Reactive Transport Modeling of ZVI Column Experiments for Nickel Remediation. Ground Water Monitoring & Remediation. doi: 10.1111/j1745–6592.2012.01417.x

Bilardi, S., Calabrò, P.S. and Moraci, N., 2012c. Are accelerated column tests used in permeable reactive barriers design sufficiently reliable? Proceeding of the Third International Conference on Hazardous and Industrial Waste Management, Crete, Greece. Technical University of Crete, Chania, Greece.

Bilardi, S., Calabrò, P. S., Caré, S., Moraci, N. and Noubactep, C., 2013a. Effect of Pumice and Sand on the Sustainability of Granular Iron Beds for the Aqueous Removal of CuII, NiII, and ZnII. Clean – Soil, Air, Water, 41(9), p. 835–843.

Bilardi, S., Calabrò, P. S., Caré, S., Moraci, N. and Noubactep, C., 2013b. Improving the sustainability of granular iron/pumice systems for water treatment. Journal of Environmental Management, Volume 121, pp. 133-141.

Bilardi, S., Calabrò, P. S. and Moraci, N., 2014. Simultaneous removal of CuII, NiII and ZnII by a granular mixture of zero-valent iron and pumice in column systems. Desalination and Water Treatment.

Birke, V., Burmeier, H., Jefferis, S., Gaboriau, H., Touzé, S., and Chartier, R., 2007. Permeable Reactive Barriers (PRBs) in Europe: potentials and expectations. Italian Journal of Engineering Geology and Environment, Special Issue 1. P 1-8.

Blowes, D. et al., 2000. Treatment of inorganic contaminants using permeable reactive barriers. J. Contam. Hydrol., 45(1–2), p. 123–137.

Bolzicco, J., Carrera, J., Ayora, C., Ceron, J. C., Fernandez, I., 2001 - Comportamiento y evolución de una barrera geoquímica experimental río agrio - Aznalcollar – España.

Bowden, L. I., Jarvis, A., Orme, P., Moustafa, M., Younger P. L., 2005. - Construction of a novel Permeable Reactive Barrier (PRB) at Shilbottle, Northumberland, UK: engineering design considerations and preliminary performance assessment - 9th International Mine Water Congress.

Bronstein, K., 2005. Permeable Reactive Barriers for Inorganic and Radionuclide Contamination prepared by Bronstein, K., Network of Environmental Management Studies Fellow for U.S. Environmental Protection Agency Office of Solid Waste and Emergency Response Office of Superfund Remediation and Technology Innovation Washington, DC www.epa.gov http://www.clu-in.org

Calabrò, P. S., Moraci, N., Suraci, P., 2012. Estimate of the optimum weight ratio in Zero-Valent Iron/Pumice granular mixtures used in permeable reactive barriers for the remediation of nickel contaminated groundwater. Journal of Hazardous Materials 207–208 (2012) 111–116

Caré, S., Nguyen, Q.T., L'Hostis, V. et al. (2008) Mechanical properties of the rust layer induced by impressed current method in reinforced mortar. Cement and Concrete Research 38(8–9): 1079–1091.

Caré, S., Crane, R., Calabrò, P. S., Ghauch, A., Temgoua, E. and Noubactep, C., 2013. Modeling the Permeability Loss of Metallic Iron Water Filtration Systems. Clean – Soil, Air, Water, 41(3), p. 275–282.

Carey, M.A., Fretwell, B.A., Mosley, N.G., Smith, J.W.N., 2002. Guidance on the Use of Permeable Reactive Barriers for Remediating Contaminated Groundwater. National Groundwater and Contaminated Land Centre Report NC/01/51, UK Environment Agency, Bristol. 140pp.

Chen, Y., Li, J., Lei, C., Shim, H., 2011. Interactions between BTEX, TPH, and TCE during their bio-removal from the artificially contaminated water. In: Bionature 2011: The Second International Conference on Bioenvironment, Biodiversity and Renewable Energies, Venice, Italy, pp. 33–37.

Council Directive 91/676/EEC of 12 December 1991 concerning the protection of waters against pollution caused by nitrates from agricultural sources**.** Official Journal of European Union OJ L 375 , 31.12.1991 p. 1 – 8 (Nitrates Directive)

Courcelles, 2007 – Etude du comportement physico-chimique des filtres de barrières perméables réactives : modélisation et expérimentation à l'échelle pilote – Thèse soutenue le 22 janvier 2007.

Courcelles B., Modaressi Farahmand-Razavi A., Gouvenot, D., Esnault-Filet, A., (2008). "Testing and Modeling the Hydraulic Permeability Evolution of Permeable Reactive

Barriers Clogged by Colloids". The 12th International Conference of International Association for Computer Methods and Advances in Geomechanics (IACMAG). October, Goa, India.

Cundy, B., Hopkinson, L. and Whitby, R., 2008. Use of iron-based technologies in contaminated land and groundwater remediation: a review.. Science of the Total Environment, 400(1-3), pp. 42-51.

Crank, J., 1975. The Mathematics of Diffusion. Brunel University Uxbridge Clarendon Press Oxford, pp: 414.

Crittenden, J.C., Reddy, P.S., Arora, H. et al., 1991. Predicting GAC performance with rapid small-scale column tests. AmericanWater Works Association 83(1): 77–87.

Day, S. R., O'Hannesin, S. F. and L. Marsden, 1999, Geotechnical techniques for the construction of reactive barriers. Journal of Hazardous Materials, 67 (3), pp.285-297.

Directive 2000/60/EC of the European Parliament and of the Council establishing a framework for the Community action in the field of water policy. Official Journal of European Union OJ L 327, 22.12.2000, p. 1–73 (Water Framework Directive).

Directive 2006/118/EC of the European Parliament and of the Council on the protection of groundwater against pollution and deterioration. Official Journal of European Union OJ L. 372, 27.12.2006, p 19-31. (Groundwater Directive)

Directive 2008/1/EC of the European Parliament and of the Council of 15 January 2008 concerning integrated pollution prevention and control. Official Journal of European Union OJ L 24, 29.1.2008, p. 8–29. (Integrated Pollution Prevention and Control Directive)

Directive 2008/98/EC of the European Parliament and of the Council of 19 November 2008 on waste and repealing certain Directives. Official Journal of European Union OJ L 312, 22.11.2008, p. 3–30 (EU Waste Framework Directive).

Directive 2008/105/EC of the European Parliament and of the Council of 16 December 2008 on environmental quality standards in the field of water policy, Official Journal of European Union OJ L 348, 24.12.2008, p. 84–97 (Environmental Quality Standards of European Commission)

Di Molfetta A., Sethi R., 2005. "Barriere Reattive Permeabili". Bonifica di siti contaminati. Caratterizzazione e tecnologie di risanamento. McGraw-Hill, ed. The McGraw-Hill Companies, S.r.l. Publishing Group Italia, 26, pp. 562 - 605.

Di Molfetta A., Sethi R., 2012. Ingegneria degli acquiferi. Springer-Verlag, pp:415.

EPRI, 2006. Groundwater Remediation of Inorganic Constituents at Coal Combustion Product Management Sites - Overview of Technologies, Focusing on Permeable Reactive Barriers, Final Report, Ladwig, K.

Esposito, L. and Guadagno, L. F., 1998. Some special geotechnical properties of pumice deposits. Bull Eng Geol Env, p. 57 : 41–50.

Estabragh, A.R., Pereshkafti, M.R.S. , Javadi A.A., 2013. Comparison Between Analytical and Numerical Methods in Evaluating the Pollution Transport in Porous Media. Geotech Geol Eng, 31:93–101

Fetter, C. W., 1999. Contaminant Hydrogeology. Second edition. Waveland Press, Inc.

Fick, A., 1855. On liquid diffusion. Philos. Mag. J. Sci., 10:31–39.

Fisher, R.V. and Schmincke, H.U., 1984. Pyroclastic rocks. Springer Berlin Heidelberg New York Tokyo pp 1-472

FRTR, 2002. Evaluation of Permeable Reactive Barrier Performance, Federal Remediation Technologies Roundtable

Gavaskar, A. R., 1999. Design and construction techniques for permeable reactive barriers. Journal of Hazardous Materials, 68 (1-2), pp:41-71.

Geranio, L., 2007. Review of Zero Valent Iron and Apatite as reactive materials for Permeable Reactive Barrier. Department of Environmental Sciences, ETH Zurich, Zurich, Switzerland.

Gibert, O., Rötting, T., de Pablo, J., Cortina, L.C., Bolzicco, J., Carrera, J. and Ayora C., 2004. Metal retention mechanisms for the Aznalcóllar permeable reactive barrier (SW Spain).

Gillham, R. W., and O'Hannesim, S. F. (1992). Metal-catalyzed abiotic degradation of halogenated organic compounds. In "Modern Trends in Hydrogeology" 1992 IAH Conference, Chicago, IL.

Giroud, J., 2010. Development of criteria for geotextile and granular filters.. Guarujá: Brazil, International Geosynthetics Society, Jupiter, Fla., p. 45–64.

Gu, B., Phelps, T. J., Liang L. et al., 1999. Biogeochemical dynamics in zero-valent iron columns: implications for permeable reactive barriers. Environmental Science Technology 33(13): 2170–2177.

Gui, L., Yang, Y., Jeen, S. W. et al., 2009. Reduction of chromate by granular iron in the presence of dissolved CaCO3. Applied Geochemistry 24: 677–686.

Henderson, A.D., Demond, A.H., 2007. Long-term performance of zero-valent iron permeable reactive barriers: a critical review. Environ. Eng. Sci. 24 (4), 401–423.

Henderson, A.D. and Demond, A.H., 2011. Impact of solids formation and gas production on the permeability of ZVI PRBs. Journal of Environmental Engineering 137(8): 689–696.

Hedin, R. S., Watzlaf, G. R. and Nairn, R. W., 1994. Passive treatment of acid mine drainage with limestone. Journal Environmental Quality, 23, 1338-1345.

Herbert, R. B., 1996. Metal retention by iron oxide precipitation from acidic ground water in Dalarna. Sweden. Appl. Geochem., Volume 11, pp. 229-235.

Hohl. H., Sigg. L.. & Stumrn. W., 1980. Characterisation of surface chemical properties of oxides in natural waters. in Partieulates in water**.** Kavanaugh. M.C., & Leckie. J. (Eds.), pp. 1-31. American Chernical Society. Advanoes in Chemistry Series No. 189.

ITRC 2005, Technical/Regulatory Guidelines. Permeable Reactive Barriers: Lessons Learned/New Directions

Jeen, S.W., Mayer, K.U., Gillham, R.W. et al. ,2007. Reactive transport modeling of trichloroethene treatment with declining reactivity of iron. Environmental Science and Technology 41(4): 1432–1438.

Jeen, S.-W., Blowes, D.W., Gillham, R.W., 2008. Performance evaluation of granular iron for removing hexavalent chromium under different geochemical conditions. J. Contam. Hydrol. 95 (1–2), 76–91.

Kamolpornwijit, W., Liang, L., West, O.R., Moline, G.R., Sullivan, A.B., 2003. Preferential flow path development and its influence on long-term PRB performance: column study. J. Contam. Hydrol. 66 (3–4), 161–178.

Kantar, C. 2007 Heterogeneous processes affecting metal ion transport in the presence of organic ligands: Reactive transport modeling. Eart-Science Reviews 81(2007): 175-198.

Kedzi, A., 1696. Increase of protective capacity of flood control, Budapest, Hungary.: Department of Geotechnics, Technical University..

Kenney, T. and Lau, D., 1985. Internal stability of granular filters. Canadian Geotechnical Journal, p. 22(2): 215–225.

Kinniburgh, DG., Syers, J.K., & Jackson, M. L. 1975. Specific adsorption of trace amounts of calcium and strontium by hydrous oxides of iron and aluminium. Soil Science Society of AmenCa Pmeedings, 39, pp. 464-470.

Korte, N.E., 2001. Zero-Valent Iron Permeable Reactive Barriers: A Review of Performance. Environmental Sciences Division Publication No. 5056, U.S. Department of Energy, Washington DC.

Kouznetsova, I., Bayer, P., Ebert, M., Finkel, M., 2007. Modelling the long-term performance of zero-valent iron using a spatio-temporal approach for iron aging. J. Contam. Hydrol. 90 (1–2), 58–80.

Langmuir, I., 1915. Chemical reactions at low temperatures. J. Amer. Chem. Soc., 37:1139, 1915.

Langmuir, I., 1918. The adsorption of gases on plane surfaces of glass, mica and platinum. J. Amer. Chem. Soc., 40:1361–1403.

Laplace, P., 1806. Supplement to the tenth edition. Méchanique céleste 10

Lee C. Fergusson, 2009. Commercialisation of Environmental Technologies Derived From Alumina Refinery Residues: A Ten-Year Case History of Virotec. Provided to the Commonwealth Scientific and Industrial Research Organisation (CSIRO) as part of Project ATF-06-3: “Management of Bauxite Residues”, Department of Resources, Energy and Tourism (DRET)

Li, L. and Benson, C., 2010. Evaluation of five strategies to limit the impact of fouling in permeable reactive barriers. J. Hazard. Mater., 181(1-3), p. 170–180.

Li, X.–Q., Zhang W. X., 2007. Sequestration of Metal Cations with Zerovalent Iron Nanoparticles: A Study with High Resolution X–Ray Photoelectron Spectroscopy (HRXPS), Journal of Physical Chemistry, 111(19), 6939–6946.

Liang, L., Korte, N., Gu, B., Puls, R., Reeter, C., 2000. Geochemical and microbial reactions affecting the long-term performance of in situ ‘‘iron barriers’’. Adv. Environ. Res. 4 (4), 273–286.

Mayer, K.U. 1999. A numerical model for multicomponent reactive transport in variably saturated porous media. Ph.D. dissertation, University of Waterloo, Waterloo, Ontario, Canada.

Mayer, K.U., Frind, E.O. and D.W. Blowes. 2002. Multicomponent reactive transport modeling in variably saturated porous media using a generalized formulation for kinetically controlled reactions. *Water Resources Research* 38, no. 6: 1174.

Meggyes, T. 2005. Construction methods of permeable reactive barriers. Long-Term Performance of Permeable Reactive Barriers. Elsevier, Amsterdam, pp. 27-52.

Mountjoy, K.J., and Blowes, D.W., 2002. Installation of a full-scale permeable reactive barrier for the treatment of metal-contaminated groundwater. In: Proceedings of the Third International Conference on Remediation of Chlorinated and Recalcitrant Compounds, Monterey. CA. May 20-23. Battelle Press, Columbus, Ohio, Paper 2A-21

Moraci, N., 2010. Geotextile filter: design, characterization and factors affecting clogging and blinding limit states. Theme lecture. Guarujá, Brazil, s.n., p. 413–435.

Moraci, N. and Calabrò, P. S., 2010. Heavy metals removal and hydraulic performance in zero-valent iron/pumice permeable reactive barriers. Journal of Environmental Management, Volume 91, pp. 2336-2341.

Moraci, N., Calabrò, P. S., Suraci P., 2011. Long-Term Efficiency of Zero-Valent Iron - Pumice Granular Mixtures for the Removal of Copper or nickel From Groundwater. Soils and Rocks, São Paulo, 34(2): 129-137, May-August, 2011.

Moraci, N., Ielo, D. and Mandaglio, M. C., 2012a. A new theoretical method to evaluate the upper limit of the retention ratio for the design of geotextile filters in contact with broadly granularsoils.. Geotextiles and Geomembranes, p. 35: 50–60.

Moraci, N., Mandaglio, M. C. and Ielo, D., 2012b. A new theoretical method to evaluate the internal stability of granular soils.. Canadian Geotechnical Journal, p. 49(1): 45–58..

Moraci, N., Bilardi, S. and Calabrò, P. S., 2014. Critical aspects related to Fe0 and Fe0/pumice PRB design. Environmental Geotechnics, p. DOI: 0.1680/envgeo.13.00120.

Morrison et al., 2001 ; S. Morrison, Metzler, D. R., Carpenter, C. E. 2001. Uranium precipitation in a Permeable Reactive Barrier by progressive irreversible dissolution of zerovalent iron. Environmental Science and Technology, 35: 385-390.

Naidu, R. and Birke V., 2015. Permeable Reactive Barrier. Sustainable Groundwater Remediation. CRC Press, Taylor&Francis Group, Boca Raton, FL.

Naftz, D. L., Morrison, S. j., Davis, J. A. and Fuller, C. C., 2002. Handbook of Groundwater Remediation using Permeable Reactive Barriers. Applications to Radionuclides, Trace Metals and Nutrients. s.l.:Elsevier Science (USA).

Noubactep, C., 2007. Processes of Contaminant Removal in ‘‘Fe_0–H_2O’’Systems Revisited. The Importance of Co-Precipitation, Open Environ. J. 2007, 1, 9–13.

Noubactep, C., 2008. A critical review on the mechanism of contaminant removal in Fe^0eH_2O systems.. Environmental Technologies, 29(8), pp. 909-920.

Noubactep, C., 2009. An analysis of the evolution of reactive species in Fe^0/H_2O systems.. Journal of Hazardous Materials , 168(2-3), pp. 1626-1631.

Noubactep, C. and Schöner, 2009. A Fe0-based alloys for environmental remediation: thinking outside the box.. Journal of Hazardous Materials, 165(1-3), pp. 1210-1214.

Noubactep, C. 2010a. The Fundamental Mechanism of Aqueous Contaminant Removal by Metallic Iron, Water SA, 36, 663–670.

Noubactep, C., 2010b. The Suitability of Metallic Iron for Environmental Remediation, Environ. Prog. Sustainable Energy, 29, 286–291.

Noubactep, C., 2011. Aqueous Contaminant Removal by Metallic Iron: Is the Paradigm Shifting?, Water SA, 37, 419–426.

O, J. S., Jeen, S.-W., Gillham, R.W. et al., 2009. Effect of initial corrosion rate on long-term performance of iron reactive barriers: column experiments and numerical simulation. Journal of Contaminant Hydrology 103(3–4): 145–156.

O'Hannesin, S. and Gillham, R., 1998. Long-Term Performance of an in Situ ''Iron Wall'' for Remediation of VOCs. Ground Water, Volume 36, p. 164–170.

Panagos, P., Van Liedekerke, M., Yigini, Y. and Montanarella, L., 2013. Contaminated Sites in Europe: Review of the Current Situation Based on Data Collected through a European Network. Journal of Environmental and Public Health, p: 1-11.

Parks, G.A. and de Bruyn, P.L. 1962. The zero point of charge of oxides.Jouma/ of Physical Chemistry, 66, pp. 967-972.

Pearson, F. H., and McDonnel, A. J. 1975. Limestone barriers to neutralize acidic streams. Journal Environmental Engineering Division, EE3, pp. 425-441.

PEREBAR, 2000. Long-term Performance of Permeable Reactive Barriers used for the Remediation of Contaminated Groundwater. 5th Framework Programme Research and Technological Development Project. Literature Review: Reactive Materials and Attenuation Processes for Permeable Reactive Barriers by National Technical University of Athens. Project Contract Number: EVK1-CT-1999-00035

Perkins, T.K. and Johnson, O.C., 1963. A review of diffusion and dispersion in porous media. Society of Petroleum Engineers Journal 3: 70-84.

Plumb, O.A. and Whitaker, S., 1990. Diffusion, dispersion and adsorption in porous media: Small scale averaging and local volume averaging. In: Dynamics of Fluids in Hierarchial Porous Media, (ed.) J.H. Cushman, Academic, London.

Powell, R.M., Blowes, D.W., Gillham, R.W., Schultz, D., Sivavec, T., Puls, R.W., Vogan, J.L., Powell, P.D., Landis, R., 1998. Permeable Reactive Barrier Technologies for Contaminant Remediation. Report EPA/600/R-98/125, U. S. Environmental Protection Agency, Washington, DC, 51pp.

Puls, R.W., Paul, C.J., Powell R.M. 1999. The application of in situ permeable reactive (zero–valent iron) barrier technology for the remediation of chromate–contaminated groundwater: a field test, Applied Geochemistry, 14, 989–1000.

Puls, R.W., Blowes, D.W., Gillham, R.W., 1999. Long-term performance monitoring for a permeable reactive barrier at the U.S. Coast Guard Support Center, Elizabeth City, North Carolina. J. Hazard. Mater. 68 (5), 109–124.

Puls, R.W., Korte, N., Gavaskar, A., and Reeter, Ch., 2000. Long-term performance of permeable reactive barriers: an update on a U.S. multi-agency initiative." Contaminated Soil 2000, Proceedings of the Seventh International FZK/TNO Conference on Contaminated Soil 18-22 September 2000, Leipzig, Germany, 591-594.

Puls, R.W., 2006. Long-term performance of permeable reactive barriers: lessons learned on design, contaminant treatment, longevity, performance monitoring and cost – an overview. In: Twardowska, I. et al. (Eds.), Soil and Water Pollution Monitoring. Protection and Remediation, Springer, Dordrecht, The Netherlands, pp. 221–229.

Raii, M., 2012. Formulation, caractérisation et mise en oeuvre des barrières perméables réactives à base de phosphate de calcium, utilisation pour la fixation de polluants. Thèse soutenue le 12 décembre 2012.

Rangsivek, R. and Jekel, M., 2005. Removal of dissolved metals by zero-valent iron (ZVI): kinetics, equilibria, processes and implications for stormwater runoff treatment. Water Research, Volume 39, pp. 4153-4163.

Reardon, E. J. 1995. Anaerobic corrosion of granular iron: measurement and interpretation of hydrogen evolution rates. Environmental Science & Technology 29, no. 12: 2936-2945.

Reardon, E. J. 2005. Zero valent Irons: Styles of Corrosion and Inorganic Control on Hydrogen Pressure Buildup Environ. Sci. Technol., 39, 7311-7317.

Reardon, E. J., 2014. Capture and storage of hydrogen gas by zero-valent iron. Journal of Contaminant Hydrology 157 (2014) 117–124

RECORD, 2004. S. Touze, R. Chartier, H. Gaboriau – BRGM, Orléans. Etat de l'art sur les Barrières Perméables Réactives (BPR) Réalisation, expériences, critères décisionnels et perspectives. 02-0330/1A RECORD RAPPORT FINAL mai 2004.

RECORD, 2010. Colombano, S. and Archambault, A.- BRGM. Barrieres Permeables Reactives (BPR): Retours d'expériences, perspectives d'application et enjeux de recherche pour le traitement des pollutions métalliques. Actualisation de l'état de l'art RECORD 2004. 08-0331/1A RECORD RAPPORT FINAL octobre 2010.

Rigano G., 2007. Studio dell'efficienza di barriere permeabili reattive per la bonifica di acquiferi contaminati da metalli pesanti. Ph. D. Thesis in Geotechnical Engineering at the Mediterranean University of Reggio Calabria.

Rochmes, M., 2000. Erste Erfahrungen mit Reaktiven Wänden und Adsorberwänden in Deutschland. Boden und Altlasten Symposium 2000, Franzius, V., Lühr, H.-P., and Bachmann, G., eds., Berlin, 225-245.

Rubin, J., 1983. Transport of reacting solutes in porous media: Relationship between mathematical nature of problem formation and chemical nature reactions. Water Resources Research 19, 5, pp:1231-52.

Ruhl, A., U¨nal, N. and Jekel, M., 2012. Evaluation of Two-Component Fe(0) Fixed Bed Filters with Porous Materials for Reductive Dechlorination. Chem. Eng. J., Volume 209, p. 401–406.

Rumar, R. R. and Mitchell, J. K., 1995. Assessment of Barrier Containment Technologies", s.l.: s.n.

Saltelli,A., Tarantola, S. and Chan, K.. 1999, A quantitative, model independent method for global sensitivity analysis of model output, Technometrics, 41, 39–56

Sarr, D., 2001. Zero-Valent-Iron Permeable Reactive Barriers - How Long will they Last?. Remediation, Spring 2001, John Wiley & Sons, Inc., 2001, 1-18.

Scesi, L. P., 1997. Il rilevamento geologico-tecnico. Geologia applicata 1. Seconda edizione aggiornata. Città Studi.

Schulthess, C.P., & Huang, C.P. 1990. Adsorption of heavy metals by silicon and aluminium oxide surfaces on clay minenls. Soil Science Society of Amenca Journal, 54, pp. 679-688.

Sherard, J., 1979. Sinkholes in dams of coarse, broadly graded soils.. New Delhi, India, s.n., p. 25–35.

Scherer, M. M. S., Richter, S., Valentine, R. L., and Alvarez, P. J. J., 2000. Chemistry and microbiology of reactive barriers for in situ groundwater cleanup. Crit. Rev. Environ. Sci. Technol., 30(3), 363-411.

Simon, F.-G., Meggyes, T., Tünnermeier, T., Czurda, K., and Roehl, E. K., 2002. Long-Term Behaviour of Permeable Reactive Barriers Used for the Remediation of Contaminated Groundwater. ICEM´01 Proceedings of the 8th International

Conference on Radioactive Waste Management and Environmental Remediation, Bruges, Belgium, Sep. 30th-Oct. 4th, 2001 (Eds.: Taboas, A., VanBrabant, R., and Benda, G.). New York, The American Society of Mechanical Engineers, ISBN 0-7918-3590-1.

Skinner, S.J., Schutte, C.F., 2006. The feasibility of a permeable reactive barrier to treat acidic sulphate- and nitrate-contaminated groundwater. Water SA 32 (2), 129–136.
Suponik, T., Blanco, M. 2014. Removal of heavy metals from groundwater affected by acid mine drainage. Physicochem. Probl.Miner. Process. 50(1), 2014, 359−372

Suraci P., 2011. Studio sperimentale dell'efficienza di barriere permeabili reattive per la bonifica di acque di falda contaminate da metalli pesanti. Ph. D. Thesis in Geotechnical Engineering at the Mediterranean University of Reggio Calabria.

S. Tarantola, S., Gatelli, D., Mara, T.A, 2006. Random balance designs for the estimation of first order global sensitivity indices. Reliability Engineering and System Safety 91 (2006) 717–727.

Tratnyek, P.G., 2002. Keeping up with all that literature: the ironrefs database turns 500. Ground Water Monit. R. 22 (3), 92–94.

USEPA, 1998. Permeable reactive barrier technologies for contaminant remediation.
USEPA, 2002. Field Applications of In Situ Remediation Technologies: Permeable Reactive Barriers. U.S. Environmental Protection Agency, Office of Solid Waste and Emergency Response, Washington, DC.

Van Genuchten, M. T., 1981 Non equilibrium transport parameters from miscible displacement experiments. Research report no. 119 Unites States Department of Agriculture Science and Education Administration. U.S. Salinity Laboratory Riverside, California.

Van Liedekerke, M., Prokop G., Rabl-Berger S., Kibblewhite M., Louwagie G., 2014. Progress in the management of Contaminated Sites in Europe, Reference Report by the Joint Research Centre of European Commission, JRC85913, EUR 26376 EN.

Vidic, R. D., 2001. Permeable reactive barriers: case study review. GWRTAC E-Series Technology Evaluation Report TE-01-01, Ground-Water Remediation Technologies Analysis Center, Pittsburgh, PA.

Vodyanitskii, Y. N., 2010. The role of iron in the fixation of heavy metals and metalloids in soils: a review of publications.. Eurasian Soil Sci., Volume 43, pp. 519-532.

Wang, X. S. and Qin, Y., 2007. Relationships between heavy metals and iron oxides, fulvic acids, particle size fractions in urban roadside soils.. Environ. Geol., Volume 52, pp. 63-69.

Warner, S.D., Sorel, D., 2002. Chlorinated solvent and DNAPL remediation. In: Henry, S.M., Warner, S.D. (Eds.), American Chemical Society, Washington, DC.

Washburn, E. W., 1921. Note on a method of determining the distribution of pore sizes in a porous material. Proc. Nat. Acad. Sci., 7, 115.

Weber, W.J. and Smith, E.H., 1987. Simulation and design models for adsorption processes. Env. Sci. Technol. 21, 1040–1050.

Weiß, H., Daus, B., and Teutsch, G., 1999. SAFIRA 2. Statusbericht; Modellstandort, Mobile Testeinheit, Pilotanlage. UFZ-Bericht Nr. 17 (UFZ report #17), ISSN 0948-9452, Leipzig, Germany.

Whitham, A. G., and Sparks, R. S. J., 1986. Pumice. Bulletin of Volcanology, 48:209-223.

Wilkin, R.T., Puls, R.W., Sewell, G.W., 2000. Long-term Performance of Permeable Reactive Barriers Using Zero-valent Iron: An Evaluation at Two Sites. U.S. Environmental Protection Agency, Washington, DC. 19pp.

Wilkin, R.T., Puls, R.W., 2003. Capstone Report on the Application, Monitoring, and Performance of Permeable Reactive Barriers for Ground-Water Remediation: Volume 1 Performance Evaluations at Two Sites. Report EPA/600/R-03/045a, U.S. Environmental Protection Agency, National Risk Management Research Laboratory, Cincinnati, OH, 135pp.

Wienberg, R., 1997. Vollständige, stoffspezifische Bilanzen des Schadstoffumsatzes beim Einsatz reaktiver Wände. Sanierung von Altlasten mittels durchströmter Reinigungswände, Vorträge und Diskussionsbeiträge des Fachgespäches am 27.10.1997 im Umweltbundesamt in Berlin, Umweltbundesamt, ed., Berlin, Germany, 112-119.

Young, T., 1805. An essay on the cohesion of fluids. Phil. Trans. , pp 65.

Yoon, S. W.-S., Gavaskar, A., Sass, B., Gupta, N., Janosy, R., Drescher. E., Cumming, L., and Hicks, J., 2000. Innovative construction and performance monitoring of a permeable reactive barrier at Dover Air Force Base. Chemical Oxidation and Reactive Barriers: Remediation of Chlorinated and Recalcitrant Compounds. The Second International Conference on Remediation of Chlorinated and Recalcitrant Compounds, Monterey, California, May 22-25, 2000, C2-6, Battelle Press, 409-416.

Zhao Y, Haiyang R, Hong D *et al.* (2011) Composition and expansion coefficient of rust based on X-ray diffraction and thermal analysis. *Corrosion Science* **53(5)**: 1646–1658.

Zolla, V., Freyria, F.S., Sethi, R., Di Molfetta, A., 2009. Hydrogeochemical and biological processes affecting the long-term performance of an iron-based permeable reactive barrier. J. Environ. Qual. 38 (3), 897–908.

Web sites:

https://aquarehab.vito.be/home/Pages/home.aspx

http://basol.developpement-durable.gouv.fr

http://www.eea.europa.eu/data-and-maps/indicators/progress-in-management-of-contaminated-sites-3/assessment

http://www.perebar.bam.de/

http://www.rtdf.org/PUBLIC/permbarr/

http://www.rubin-online.de/

http://www.theadvocateproject.eu/